Mem. Grad. Sch. Fish. Sci. Hokkaido Univ.

Comparative Anatomy, Phylogeny and Cladistic Classification of the Order Orectolobiformes (Chondrichthyes, Elasmobranchii)[1)]

Tomoaki GOTO[2),3)]

Contents

[1)] The present work was submitted as a partial fulfillment of the requirements for the degree of Doctor (Fisheries Science) to Hokkaido University, Japan in 1997.

[2)] *Laboratory of Marine Biodiversity (Systematic Ichthyology), Graduate School of Fisheries Sciences, Hokkaido University, 3-1-1, Minato-cho, Hakodate, Hokkaido 041-8611, Japan*

[3)] Present address: Iwate Fisheries Technology Center, 3-75-3 Heita, Kamaishi, Iwate 026-0001, Japan

Abstract

Phylogenetic relationships of the order Orectolobiformes were analyzed cladistically on the basis of comparative morphology of external features, skeleton, musculature, and sensory system. The order Orectolobiformes is a monophyletic lineage united by two synapomorphies: foramen for the ophthalmicus profundus fused with that for the ophthalmicus superficialis, and prominent inner process present on ceratobranchial. A comparison of 22 orectolobiform fishes resulted in six most parsimonious cladograms reconstructed on the basis of 136 characters. The order Orectolobiformes is additionally supported by 17 apomorphies. *Parascyllium* and *Cirrhoscyllium* constitute a monophyletic group within Orectolobiformes supported by 41 apomorphies forming the suborder Parascylloidei and the family Parascylliidae. The other clade is supported by 24 apomorphies forming the suborder Orectoloboidei, and is divided into four succeeding clades. *Brachaelurus* is supported by eight apomorphies to be ranked in the family Brachaeluridae. *Orectolobus, Sutorectus* and *Eucrossorhinus* are supported by 16 apomorphies to be ranked in the family Orectolobidae, and synonymized in the genus *Orectolobus* based on the relationships. *Hemiscyllium* and *Chiloscyllium* form the family Hemiscylliidae supported by 13 apomorphies. *Stegostoma, Ginglymostoma* and *Rhincodon* are supported by 23 apomorphies and are ranked in the family Rhincodontidae including two incertae genera of *Pseudoginglymostoma* and *Nebrius*. Evolution of reproduction mode is proposed on the basis of the interrelationships. The common ancestor of Orectolobiformes had extended oviparity, and the ancestor of Orectoloboidei succeedingly acquired retained oviparity. Yolksac viviparity occurred in ancestors of the orectolobid-brachaelurid and *Rhincodon-Ginglymostoma* lineages, respectively, and extended oviparity was acquired secondarily in the ancestor of Hemiscylliidae.

Key words: Phylogeny, Orectolobiformes, cladistic, classification, reproduction mode

I. Introduction

The order Orectolobiformes contains approximately 14 genera and 31 species distributed in pantropical waters. Species included in this order are generally characterized by having a mouth entirely anterior to eyes, an oronasal groove between outer and inner nasal apertures and mouth, and a barbel on mesial margin of nostril. Most species are distributed on coral reefs of the western Pacific and the Indian Ocean, whereas the whale shark, *Rhincodon*, occurs in epipelagic waters of the world, and the nurse shark, *Ginglymostoma*, is distributed in the western Pacific and the Atlantic Ocean. While the habit of most species is similarly benthic in shallow waters, they exhibit greatly varied body size and shape. The smallest parascylliid genus *Cirrhoscyllium* attains only 40 cm in total length, whereas the largest *Rhincodon* grows to more than 10 m. The shape also varies greatly from well depressed in *Orectolobus* and *Eucrossorhinus* to slender and cylindrical in *Parascyllium, Cirrhoscyllium, Hemiscyllium* and *Chiloscyllium*, and some species characteristically have various shaped barbels or dermal appendages on the head or body. Furthermore, species of this order are well adapted to epipelagic or coral reef habitats by various features of life history, mode of reproduction, locomotion, or feeding behavior in addition to divergences of the size and shape.

Orectolobiform sharks were originally recognized as three isolated families, Rhinodontoidae, Crossorhinoidae and Ginglymostomatoidae, and three subfamilies of the family Scylliorhinoidae by Gill (1862). Regan (1906) provided the family Orectolobidae for all of them, which are equivalent to the Recent Orectolobiformes. Regan (1908) subsequently defined this group as the family Orectolobidae by the removal of *Rhincodon*, and he suggested that *Rhincodon* is closely related to the lamniform genus *Cetorhinus* on the basis of similarities of the symmetrical caudal fin. His idea in 1908 was supported in the subsequent systematic works published before 1970 (Garman, 1913; White, 1937; Bigelow and Schroeder, 1948). Applegate

(1972) designated the order Orectolobiformes for the previous Orectolobidae with the addition of *Rhincodon* as a distinct taxonomic unit, and he recognized three new suborders, Rhincodontoidei, Orectoloboidei and Parascylloidei, within this order. He originally mentioned that the suborder Parascylloidei composed of *Parascyllium* and *Cirrhoscyllium* is distinct from other orectolobiforms. However, his ranking was basically equivalent to the previous works because he distinguished *Rhincodon* as to be a different suborder from other orectolobiforms without any interpretations of the interrelationships among them. Recently, Dingerkus (1986) and Compagno (1988) proposed a quite different ranking from the previous hypotheses relative to the taxonomic position of *Rhincodon* to be a higher taxon within the order on the basis of the interrelationships. In particular, Dingerkus (1986) additionally proposed the family Rhincodontidae as a monophyletic group containing *Rhincodon, Stegostoma, Ginglymostoma, Nebrius* and *Pseudoginglymostoma*. However, taxonomy is still controversial because both relationships are quite different topologies. On the other hand, Holmgren (1941) and Applegate (1972) suggested that some orectolobiforms are closer to other elasmobranch families such as Squatinidae or Lamnidae, and Maisey (1985) hypothesized possible paraphyletic relationships, but they provided no comments on the taxonomic reconstruction.

The purpose of this study is to test monophyly of the order Orectolobiformes using cladistic methodology, to reconstruct interrelationships of the component taxa, and to establish a classification reflecting the reconstructed genealogical relationships.

II. Materials and methods

Materials examined for anatomical observation are listed below. Abbreviations follow Leviton et al. (1985) except for OA, Osaka Aquarium, Osaka, Japan. Body sizes are expressed in total length (TL).

Orectolobiformes. *Parascyllium variolatum* : 1 specimen, WAM P2852.001, 498 mm TL, female. *P. collare* : 1 specimen, AMS I30409.002, 354 mm TL, female. *P. ferrugineum* : 1 specimen, HUMZ 131588, 695 mm TL, male. *P.* sp. : 1 specimen, CSIRO CA H2360.01, 555 mm TL, female. *Cirrhoscyllium japonicum* : 2 specimens, HUMZ 40045, 431 mm TL, female ; HUMZ 40057, 442 mm TL, female. *C. expolitum* : 1 specimen, USNM 74603 (holotype), 330 mm TL, female (X-ray only). *C. formosanum*, 11 specimens, TFRI 103576-103586 (paratypes), 344-377 mm TL, including eight males and three females (X-ray only). *Orectolobus maculatus* : 1 specimen, WAM P28414.001, 232 mm TL, male. *O. ornatus* : 1 specimen, AMS I14236, 258 mm TL, female. *O. japonicus* : 3 specimens, HUMZ 114394, 221 mm TL, female ; HUMZ 116361, 240 mm TL, male ; HUMZ 113410, 353 mm TL, male. *O. wardi* : 1 specimen, HUMZ 117705, 355 mm TL, female. *O. dasypogon* : 1 specimen, CSIRO CA 4051, 402 mm TL, female. *O. tentaculatus* : 1 specimen : WAM P11938.001, 182 mm TL, female. *Brachaelurus waddi* : 1 specimen, AMS I20095033, 277 mm TL, female. *Brachaelurus colculoghi* : 1 specimen, QM I 27500, 481 mm TL, male (X-ray only). *Chiloscyllium plagiosum* : 2 specimens, HUMZ 37689, 735 mm TL, female ; NSMT (unregistered), 391 mm TL, male. *C. punctatum* : 1 specimen, HUMZ 6139, 719 mm TL, female. *C. hasselti* : 3 specimens, HUMZ 109476, 720 mm TL, male ; HUMZ (unregistered), 605 mm TL, female ; CAS 133856, 204 mm TL, female (external view of cartilaginous region only ; already cleared and stained specimen by Dingerkus). *C. indicum* : 2 specimens, MCZ 54, 387 mm TL, male ; CAS 48269, 265 mm, male (external view of cartilaginous region only ; already cleared and stained by Dingerkus). *Hemiscyllium ocellatum* : 2 specimens, BMNH 1911.4.1, 304.5 mm TL, male ; HUMZ 119336, 388 mm TL, female. *H. freycineti* : 1 specimen, CAS SU26798, 194 mm TL, male. *H. trispeculare* : 1 specimen, NTM S10603.008, 295 mm TL, female. *Rhincodon typus* : 1 specimen, OA 00212, 4810 mm TL, male. *Stegostoma varium* : 2 specimens, HUMZ 50031, 1682 mm TL, male ; HUMZ 78593, 1661 mm TL, male. *Ginglymostoma cirratum* : 2 specimens, ZMUC P0629, 348 mm TL, female ; HUMZ 138648, 174 mm TL, male.

Heterodontiformes. *Heterodontus japonicus* : 1 specimen, HUMZ 111039, 301 mm TL, female. *H. francisci* : 1 specimen, HUMZ 119337, 301 mm TL, male. *H. portusjacksoni* : 1 specimen, 467 mm TL, male. *H. zebra* : 1 specimen, HUMZ 37666, 440 mm TL, female.

Carcharhiniformes. *Scyliorhinus torazame* : 1 specimen, HUMZ 63580, 464 mm TL, female. *Cephaloscyllium umbratile* : 1 specimen, HUMZ 39979, 522 mm TL, female. *Galeus eastmani* : 1 specimen, HUMZ 118482, 278.5 mm TL, female. *Apristurus fedorovi* : 1 specimen, HUMZ 123842, 484 mm TL, female. *Schroederichthys bivius* : 1 specimen, HUMZ 91812, 550 mm TL, female. *Halaelurus buergeri* : 1 specimen, HUMZ 111844, 263 mm TL, female. *Proscyllium habereri* : 1 specimen, HUMZ 49378, 538 mm TL, female. *Gollum attenuata* : 1 specimen, HUMZ 65456, 1020 mm TL, female. *Triakis semifasciata* : 1 specimen, HUMZ 119338, 297 mm TL, female. *Mustelus manazo* : 1 specimen, HUMZ (unregistered), 807 mm TL, male. *Hemitriakis japanica* : 1 specimen, HUMZ

105878, 667 mm TL, male. *Carcharhinus melanopterus*: 1 specimen, HUMZ 119332, 525 mm TL, male. *C. brevipinna*: 1 specimen, OA 00212, 490 mm TL, male.

Lamniformes. *Mitsukurina owstoni*: 1 specimen, HUMZ 116282, 2030 mm TL, male. *Alopias pelagicus*: 1 specimen HUMZ 74420, 1710 mm TL, female. *Pseudocarcharias kamoharai*: 2 specimens, HUMZ 94348, 1051 mm TL, male; HUMZ 117843, 1006 mm TL, male. *Lamna nasus*: 1 specimen, HUMZ 97333, 875 mm TL, male.

Squalea. *Chlamydoselachus anguineus*: 1 specimen, MSM 1548, 1175 mm TL, male. *Heptranchias perlo*: 1 specimen, 835 mm TL, male. *Notorynchus cepedianus*: 1 specimen, HUMZ 6749, 740 mm TL, female. *Hexanchus griseus*: 1 specimen, HUMZ 95104, 698 mm TL, male. *Centroscyllium fabricii*: 1 specimen, HUMZ 112179, 290 mm TL, male. *Squalus acanthias*: 1 specimen, HUMZ 107285, 339 mm TL, female. *Dalatias licha*: 1 specimen, HUMZ 74585, 460 mm TL, female.

Osteological and myological examinations were made on specimens stained with Alcian Blue 8G and Alizarin Red-S. Illustrations were made by using a camera lucida (Nikon AMZ-10 and Wild M-8). Tooth morphology was observed and photographs taken by SEM (Hitachi S-2300). Terminology follows Edgeworth (1935) and Shirai (1992a) for osteology and myology, Norris and Hughes (1920) for cranial nerves and Daniel (1934) and Holmgren and Pehrson (1949) for head sensory canal system and ampullae of Lorenzini.

Phylogenetic analyses were made using cladistic methodology summarized by Wiley (1981), Eldredge and Cracraft (1980) and Wiley et al. (1991) under the concept of Hennig (1966). Characters were obtained from external and internal morphologies, including features of the skeleton, myology and sensory canal system. Continuous quantitative characters, e.g., number of teeth on jaws or proportion of mouth width, were not included in the present analyses because of the difficulty in estimating the range consistent within the taxon, and the degrees represented by these characters. Order was attempted for multistate characters when a possible transformation can be assumed to reduce the morphological changes based on the Wagner parsimony (Farris, 1970). Other multistate characters were used as unordered on the basis of the Fitch parsimony (Fitch, 1971). Determination of character polarity was based on the outgroup comparison method (Watrous and Wheeler, 1981; Maddison et al., 1984). In order to determine the monophyletic ingroup and the outgroup relationships, I adopted the two step procedure proposed by Maddison et al. (1984), in which a larger clade including all Orectolobiformes was attempted *a priori* to reconstruct ingroup-outgroup relationships in the first step, and interrelationships within the ingroup were determined in the next step. Most parsimonious cladograms were reconstructed by the branch and bound algorithm of the software PAUP ver. 3.0s (Swofford, 1991) by using the ACCTRAN option.

III. Ingroup and outgroup definition

This chapter provides the ingroup-outgroup relationships in order to determine the character polarity within OTU (Operational Taxonomic Unit) of the second step. Here, I reconstruct interrelationships of a large monophyletic group including all orectolobiforms and closely related taxa, adding some original characters to those discussed by previous authors, and I estimate the monophyly of orectolobiforms from this result.

1. Background on monophyly of orectolobiforms and the systematic position

Monophyly of orectolobiforms has been argued phylogenetically, and the following hypotheses were proposed. Gill (1862) categorized these sharks into four separate families: Rhincodontoidae, Ginglymostomatoidae, Crossorhinoidae and Scylliorhinoidae. He supposed that Crossorhinoidae is closely related to *Squatina* based on the depressed body and terminal mouth, and that subfamilies of the family Scylliorhinoidae containing Parascylliinae, Chiloscylliinae and Stegostomatinae are closely related to some carcharhiniform taxa, e.g., *Scylliorhinus* (=recent *Scyliorhinus*), *Cephaloscyllium* and *Halaelurus*. Regan (1908) proposed that *Rhincodon* is closer to *Cetorhinus* than to any other orectolobiform sharks based on the symmetrical caudal fin, and the subsequent authors followed his idea (Garman, 1913; White, 1930, 1937). Holmgren (1941), on the basis of morphological similarities of the neurocranium, mentioned the two different evolutionary scenarios with *Orectolobus* closely related to *Squatina* and *Chiloscyllium* closely related to *Heterodontus*. Applegate (1972) suggested that ginglymostomatids are probably closer to some lamniforms than to any other orectolobiform taxa, but he provided no reasons for this hypothesis. Maisey (1985) suggested the possibility of a paraphyletic orectolobiforms, because they share some "primitive" characters appearing during the early ontogenetic stages. Recently, Dingerkus (1986) and Compagno (1988) proposed that orectolobiforms form a monophyletic group sharing some "apomorphic" characters. However, their results remain problematic because they did not represent the consistent synapomorphies shared by all orectolobiforms based on the objec-

tive "cladistic" analysis.

Orectolobiform sharks have been traditionally included in a higher "galeoid" taxon that Regan (1906) originally proposed as the division Galeoidei to three shark groups comprising orectolobiforms, lamniforms and carcharhiniforms (Regan, 1908 ; Garman, 1913 ; White, 1937 ; Bigelow and Schroeder, 1948 ; Schaeffer, 1967). Among authors who accepted the galeoids, the sister group of the orectolobiforms has been suggested to be either lamniforms (Garman, 1913 ; White, 1937) or carcharhiniforms (Regan, 1906). Maisey (1984a) and Shirai (1992a) cladistically suggested that galeoids are monophyletic and orectolobiforms form a sister group to the clade composed of carcharhiniforms and lamniforms. On the other hand, Compagno (1973) included *Heterodontus* in galeoids and designated the superorder Galeomorphii, further suggesting that orectolobiforms are likely to be closer to *Heterodontus* than to carcharhiniforms and/or lamniforms. Subsequently, he suggested monophyly of his Galeomorphii and claimed the possibility of sister relationships of orectolobiforms and *Heterodontus* based on the hypothesized synapomorphies from some cranial and myological characters (Compagno, 1977, 1988). However, taxa closely related to orectolobiforms remain uncertain, because no consistent synapomorphies have been proposed to support the interrelationships of orectolobiforms with any other elasmobranchs. Therefore, I estimate interrelationships of all living elasmobranchs as the ingroup of the first step in order to determine the systematic position and monophyly of orectolobiforms in the following paragraphs.

2. Comments on monophyly of living elasmobranchs

Phylogeny of elasmobranchs including extinct and extant taxa has been proposed by a number of authors (e.g., Regan, 1906 ; White, 1937 ; Moy-Thomas, 1938 ; Holmgren, 1941 ; Schaeffer, 1967 ; Compagno, 1973, 1977 ; Schaeffer and Williams, 1977 ; Maisey, 1984a, b ; Gaudin, 1991 ; Shirai, 1992a, 1996 ; Carvalho, 1996). White (1937) suggested that most living sharks have been derived from the Mesozoic genus *Hybodus*, except for *Chlamydoselachus* and hexanchoids that have been placed in the direct descendants from cladodontids or primitive amphistylic sharks (Patterson, 1967 ; Glickman, 1967 ; Moy-Thomas and Miles, 1971). On the other hand, *Heterodontus* was thought to be a direct descendant of *Hybodus* but subsequent studies of the cranial morphology rejected this idea (Brough, 1935 ; Moy-Thomas, 1938 ; Maisey, 1982). Compagno (1973, 1977) suggested an evolutionary scenario that living elasmobranchs were probably derived into four groups, i.e., Squalomorphii, Squatinomorphii, Batoidea and Galeomorphii, from the ctenacanth-hybodont transition in parallel. However, he inferred the relationships without comparison based on the strict cladistic concept and never placed the systematic relationships between the living and the Mesozoic taxa. Recently, all living elasmobranchs has been suggested as a monophyletic group to form the sister group of hybodonts when the extinct genus *Palaeospinax* is included (Schaeffer and Williams, 1977 ; Young, 1982 ; Maisey, 1984a, b ; Gaudin, 1991). According to Maisey (1984a), living elasmobranchs under the cladistic concept represent a single clade sharing 15 synapomorphies (his character number 4–18) when two Mesozoic extinct genera, *Palaeospinax* and *Synechodus*, are included. Maisey (1985) noted the most parsimonious assemblage that *Synechodus* is a sister taxon of the clade composed of *Heterodontus, Chiloscyllium* and *Scyliorhinus*. Because Maisey (1977) revealed that *Palaeospinax* has the well developed orbital articulation, which is one of the synapomorphies of Squalea supposed by Shirai (1992a), the phylogenetic position of *Palaeospinax* is either close to or included in Squalea rather than to any galeomorph taxa. Moreover, no one has suggested that orectolobiform sharks are closely related to *Synechodus* or *Palaeospinax*. Therefore, I treat living elasmobranchs as a monophyletic taxon to be the ingroup of the first step, and exclude both *Palaeospinax* and *Synechodus* from the analysis because there is insufficient evidence for comparison with living taxa. In addition, I follow Shirai (1992a) on the monophyly and interrelationships within Squalea *a priori* because his result is well supported by a number of consistent synapomorphies based on the strict cladistic concept.

Concerning outgroups, living elasmobranchs are recently thought to be the sister group of the hybodonts containing *Hybodus, Egertonodus, Acrodus*, Lissodus, Paleobates*, Polyacrodus*, Asteracanthus* and *Bdellodus** which form a single clade (Maisey, 1982, 1986 ; Gaudin, 1991). Moreover, the clade composed of living elasmobranchs and hybodonts forms the sister taxon of xenacanths containing *Xenacanthus, Tamiobatis*, "*Cladodus*"* and Cleveland "*Ctenacanthus*"* which form a single clade (Schaeffer, 1981). Therefore, I used hybodonts and xenacanths as outgroups in the first step. Since taxa with an asterisk are poorly preserved, I cannot obtain characters from them. The following character analysis in the first step is based on the putative cladogram including the ingroup and outgroups as shown in Fig. 1.

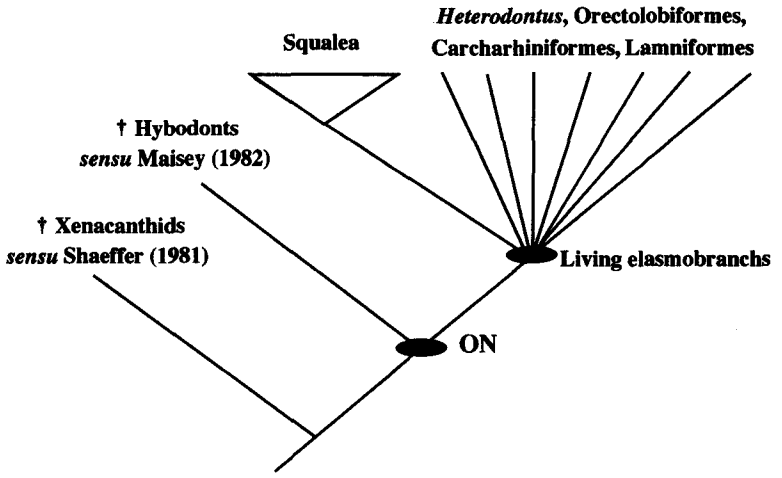

Fig. 1. Cladogram of higher elasmobranch taxa (modified from Shirai, 1992). ON : Outgroup node for inference of living elasmobranch phylogeny.

3. Character analysis for first step

In the first step, the following 34 apomorphic characters are accepted for resolution of interrelationships of living elasmobranchs on the basis of comparisons with outgroups. Character states on the basal node of Squalea are given as the hypothetical state based on the downward pass of the character optimization (Wiley et al., 1991) to the cladogram proposed by Shirai (1992a). The terms "Galea" and "galeoid" used in this chapter correspond to Galea *sensu* Shirai (1996) and Galeoidei *sensu* Regan (1906), respectively.

1. Pharyngobranchial blade present. Shirai (1992a) regarded lack of the pharyngobranchial blade as one of the synapomorphies of Squalea (his character 10) because *Tristychius* and some species of *Hybodus* share this blade. On the other hand, Carvalho and Maisey (1996) reported some species of *Hybodus* and *Xenacanthus* apparently have no blade on the pharyngobranchial. Shirai (1996) reviewed the polarity of this character again and regarded that this blade should be derived among living elasmobranchs as his character 35. Thus, the presence of the blade is assumed to be apomorphic followed Shirai (1996).

2. Orbital articulation present. Converted from character 43 of Shirai (1992a) considered a synapomorphy of Squalea.

3. Basitrabecular process present. Converted from character 44 of Shirai (1992a) and character 11 of Shirai (1996) considered a synapomorphy of Squalea.

4. Basal angle present. Converted from character 47 of Shirai (1992a) considered a synapomorphy of Squalea.

5. Pectoral propterygium not supporting radials. Converted from character 141 of Shirai (1992a) and character 63 of Shirai (1996) considered a synapomorphy of Squalea.

6. Lateral sensory canal completely closed. Converted from character 4 of Shirai (1992a) and character 101 of Shirai (1996).

7. Hyomandibular facet immediately behind orbit. Converted from character 1 of Shirai (1992a) and character 17 of Shirai (1996). In Squalea, the hyomandibular facet is located on the posterior region of otic capsule distant from orbit, whereas it is located on the anterior part of otic capsule immediately behind orbit in Galea (Holmgren, 1941 ; Compagno, 1988, 1990 ; Shirai, 1992a). Since outgroups share the former condition (Zangerl and Williams, 1975 ; Schaeffer, 1981 ; Maisey, 1982), the facet immediately behind orbit is assumed to be apomorphic.

8. Otic capsule short. Among elasmobranchs, the length of the otic capsule can be classified into two categories according to Compagno (1973, 1988). In most squaleans except rajiforms, it is greatly elongated, forming a broad floor at the lateral surface, whereas it is remarkably short in rajiforms and Galea. In outgroups, *Xenacanthus* and hybodontids have an extremely elongated otic capsule (Brough, 1935 ; Schaeffer, 1981 ; Maisey, 1982, 1986, 1987). Therefore, the short otic capsule is assumed to be apomorphic.

9. Proximal region of nasal capsule long and curved ventrally. Converted from character 2 of Shirai (1992a) and character 5 of Shirai (1996). In most taxa, the proximal region of the nasal capsule is short, whereas it is greatly elongated and ventrally curved to form the cylindrical orbito-nasal process in all orectolobiforms and *Heterodontus*. Among the outgroups, the nasal capsule is poorly preserved, but the remnant shows the capsule short, not curved ventrally in some *Hybodus* and

Xenacanthus (Schaeffer, 1981 ; Maisey 1982, 1986). Therefore, the long and ventrally curved orbito-nasal process is assumed to be apomorphic.

10. Ventral marginal cartilage of clasper well expanded dorsally. Converted from character 6 of Shirai (1992a) and character 69 of Shirai (1996). In galeoid taxa, the ventral marginal cartilage of clasper is well expanded dorsally, whereas *Hybodus* of outgroups, *Heterodontus* and squaleans do not have an expanded ventral marginal cartilage (Huber, 1901 ; White, 1937 ; Maisey, 1982). Therefore, the expanded ventral marginal cartilage is assumed to be apomorphic.

11. Basal cartilage of dorsal fin composed of isolated slender rods. Converted from character 7 of Shirai (1992a) and character 81 of Shirai (1996). In most galeoid taxa, the basal cartilage of the dorsal fin is segmented into isolated slender rods (Goodrich, 1909 ; White, 1937 ; Holmgren, 1941 ; Schaeffer, 1967). In most squalean taxa, *Heterodontus* and outgroups, it forms a single or a few large plates (Brown, 1900 ; White, 1937 ; Moy-Thomas, 1938 ; Holmgren, 1941 ; Schaeffer, 1981 ; Maisey, 1982, 1986 ; Shirai, 1992a). Therefore, the isolated slender basal cartilage is assumed to be apomorphic.

12. Dorsal fin spine absent. Converted from character 49 of Carvalho (1996). Among living elasmobranchs, some squalean taxa and *Heterodontus* have a large fin spine on the anterior margin of the dorsal fin (Holmgren, 1941 ; Shirai, 1992a). Outgroups have a large spine similar morphologically to that of the Recent taxa (Brough, 1935 ; Moy-Thomas, 1936 ; Maisey, 1978, 1979, 1982, 1986). Therefore, lack of the fin spine is assumed to be apomorphic.

13. Basal cartilage of anal fin composed of isolated cartilaginous pieces. Converted from character 8 of Shirai (1992a) and character 85 of Shirai (1996). In most galeoid taxa, the basal cartilage of the anal fin is segmented into isolated small cartilaginous pieces (White, 1937 ; Holmgren, 1941). In most squaleans with an anal fin, *Heterodontus*, and outgroups, it forms a single or a few large plates (Holmgren, 1941 ; Maisey, 1982 ; Shirai, 1992a). Therefore, the isolated basal cartilage is assumed to be apomorphic.

14. Foramen for ophthalmicus superficialis isolated (ospf : Fig. 2). Converted from character 9 of Shirai (1996) and character 7 of Carvalho (1996). All galeoid taxa have an isolated foramen for the ophthalmicus superficialis V-VII (Fig. 2B-D ; Holmgren, 1941 ; Maisey, 1985). In all Squalea, *Heterodontus* and *Hybodus*, this nerve branch passes through the main foramen for the trigeminal and facial nerves, although *Xenacanthus* has no foramina for the trigeminal and facial nerves except for the hyomandibular branch (Fig. 2A ; Holmgren, 1941 ; Schaeffer, 1981 ; Shirai, 1992a). Therefore, the isolated foramen for the ophthalmicus superficialis is assumed to be apomorphic.

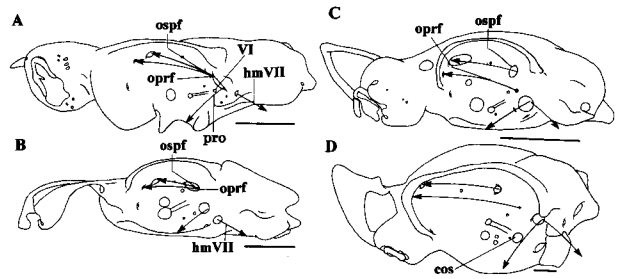

Fig. 2. Lateral views of neurocrania showing distributions of trigeminal and facial nerves. (A) *Centroscyllium fabricii* (HUMZ 112179) ; (B) *Eucrossorhinus dasypogon* (CSIRO CA 4051) ; (C) *Triakis semifasciata* (HUMZ 119338) ; (D) *Alopias pelagicus* (HUMZ 74420). Scales indicate 10 mm.

15. Foramen for ophthalmicus profundus isolated or fused with that for ophthalmicus superficialis (oprf : Fig. 2). Among living elasmobranchs, the foramen for the ophthalmicus profundus V nerve is classified into the following three categories : it is fused with the main foramen for the trigeminal and facial nerves in Squalea and *Heterodontus* (Fig. 2A) ; fused with that for the ophthalmicus superficialis in orectolobiforms (Fig. 2B) ; isolated in carcharhiniforms and lamniforms (Fig. 2C-D). Among the outgroups, *Hybodus* represents the first state (Maisey, 1982 ; 1985). Therefore, the latter two states are assumed to be apomorphic, respectively.

16. Foramen for hyomandibularis VII fused with the main foramen for trigeminal and facial nerves (hmVII : Fig. 2). In most squalean taxa, *Heterodontus* and several galeoid taxa, the foramen for the hyomandibularis VII is isolated from the main foramen for the trigeminal and facial nerves (Fig. 2A-B), whereas both foramina fused in most galeoids (Fig. 2C-D). Since outgroups share the former state (Schaeffer, 1981 ; Maisey, 1982, 1985), the latter state is assumed to be apomorphic.

17. Foramen for abducens nerve fused with foramen for trigeminal and facial nerves (VI : Fig. 2). In most living elasmobranchs, the abducens VI nerve passes through the foramen for the trigeminal and facial nerves (Fig. 2B-D ; Shirai, 1992a), whereas most squaleans, some lamniforms, and some orectolobiforms have an isolated foramen for the abducens VI nerve (Fig. 2A). Since outgroups have an isolated foramen for the abducens VI nerve, the fused condition is assumed to be apomorphic.

18. Canal for orbital sinus present (cos : Fig. 2). In some lamniforms, e.g., *Alopias* and *Pseudocarcharias*, a canal for the orbital sinus is present ventral to the

eyestalk (Fig. 2D). Since no such canal appears in any outgroup taxa, the presence of this canal is assumed to be apomorphic.

19. Internasal space narrow, with high internasal septum. In most galean taxa, the internasal space is narrow, with a thin and high internasal septum (Holmgren, 1941). In most squalean taxa, it is broad and trough shaped, forming a somewhat thickened region medially (Holmgren, 1941 ; Shirai, 1992a). According to Holmgren (1940), the latter condition is ontogenetically different from the former, and is formed below the precerebral fossa. Since the states of outgroups correspond to the latter principally (Schaeffer, 1981 ; Maisey, 1982, 1986), the narrow interspace with an internasal septum is assumed to be apomorphic.

20. Medial rostral rod greatly elongated anteriorly. In galeoid taxa except *Rhincodon*, the medial rostral rod is thin and greatly elongated anteriorly from the anterior margin of the basal plate. In Squalea, there is a broad expansion with a large concavity, precerebral fossa, on the dorsal margin, and Holmgren (1940) suggested that the expansion is not homologous with the rostrum of galeoids because of the ontogenetic differences. In *Heterodontus*, there is no such appendage. Since outgroups have no rostral rod, the elongated medial rostral rod is assumed to be apomorphic.

21. Lateral rostral rod present. All carcharhiniforms and lamniforms have the lateral rostral rod (Compagno, 1988, 1990), whereas all other taxa including outgroups do not have such a rod. Therefore, presence of the lateral rostral rod is assumed to be apomorphic.

22. Supraorbital crest absent. In most living elasmobranchs, there is a supraorbital crest expanding over the orbit, whereas some taxa of galeoids have no such expansion (Jordan and Fowler, 1903 ; Nakaya, 1975 ; Compagno, 1988, 1990a). Since outgroups have this crest, lack of the crest is assumed to be apomorphic.

23. Supraorbital blade present. Among the ingroup, only some orectolobiforms have a large, bifurcated overhang over the orbit (supraorbital blade : see description in Chapter IV). Since outgroups do not have such an overhang, its presence is assumed to be apomorphic.

24. Eyestalk. In most living taxa, the eyestalk is present, whereas it is absent in *Oxynotus*, scyliorhinids and proscylliids (Schaeffer, 1981). Among the outgroups, there is a remnant of it in *Xenacanthus, Tamiobatis* and *Cladodus* but there is no evidence of its presence in *Hybodus* (Stensiö, 1937 ; Schaeffer, 1981). Although Gardiner (1984a, b), Schaeffer (1981) and Young (1982) made interpretations for the polarity of the eyestalk among the placoderms, teleosts, holocephalans and elasmobranchs, these assumptions are still incongruent. Thus, I tentatively treated this character as equivocal in this analysis.

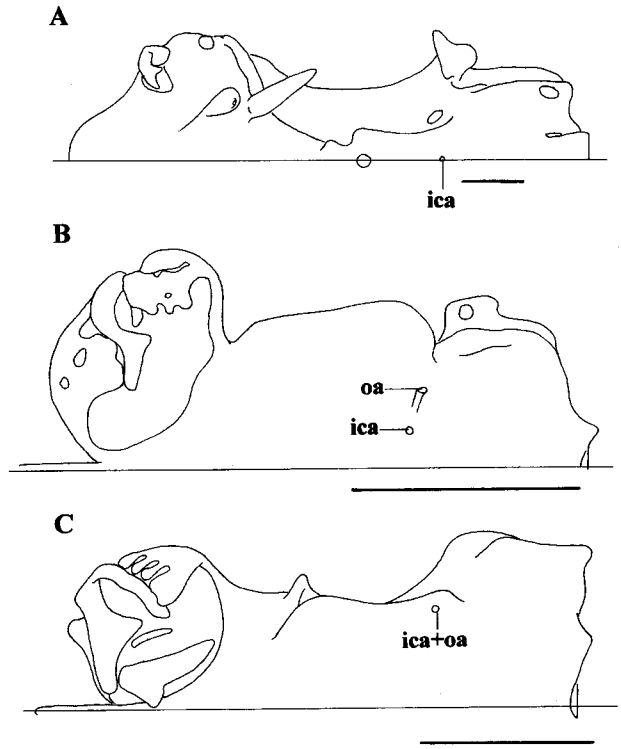

Fig. 3. Ventral views of neurocrania. (A) *Heptranchias perlo* (HUMZ 123503) ; (B) *Halaelurus buergeri* (HUMZ 111844) ; (C) *Brachaelurus waddi* (AMS I20095033). Scales indicate 10 mm.

25. Foramen for internal carotid artery paired or fused with that for orbital artery (ica : Fig. 3). Among living elasmobranchs, the foramen for the internal carotid artery is classified into three categories : single in some scyliorhinids, *Heterodontus, Stegostoma* and most squalean taxa (Fig. 3A) ; paired in most galeoid taxa (Fig. 3B) ; fused with the foramen for the orbital artery in some orectolobiforms (Fig. 3C ; Compagno, 1988). Since outgroups have a single foramen (Stensiö, 1937 ; Schaeffer, 1981 ; Maisey, 1982, 1987), the latter two states are assumed to be apomorphic, respectively.

26. Foramen for orbital artery absent (oa : Fig. 3). In most living taxa, the foramen for the orbital artery is present (Fig. 3B-C), whereas it is absent in some orectolobiforms and some squalean taxa (Fig. 3A ; Shirai, 1992a). Since outgroups have this foramen (Schaeffer, 1981 ; Maisey, 1982), lack of this foramen is assumed to be apomorphic.

27. Ventral foramen for vagus X nerve present. In some lamniforms, e.g., *Alopias, Pseudocarcharias* and *Lamna*, the vagus X nerve is branched, one of which passes through the foramen opening on the ventral

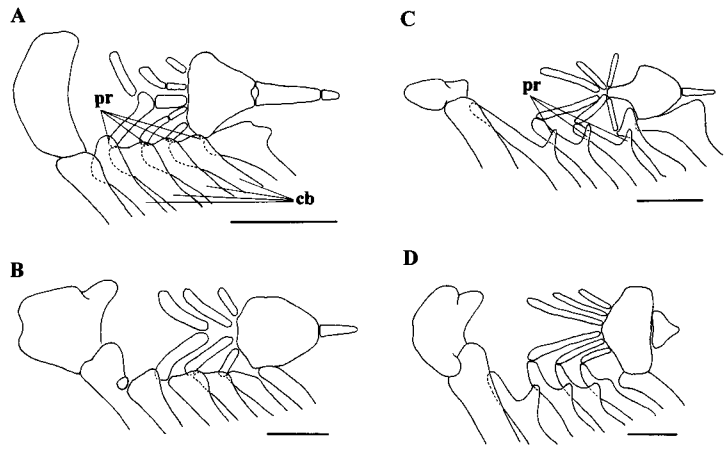

Fig. 4. Ventral views of hypobranchial skeletons. (A) *Centroscyllium fabricii* (HUMZ 112179); (B) *Schroederichthys bivius* (HUMZ 91812); (C) *Cirrhoscyllium japonicum* (HUMZ 40057); (D) *Orectolobus wardi* (HUMZ 117705). Scales indicate 10 mm.

surface of the basal plate. Since no foramen appears in outgroups, the presence of this foramen is assumed to be apomorphic.

28. Marginal quadrate expansion absent. Among living taxa, the dorsal margin of the palatoquadrate has an overhanging, marginal quadrate expansion, to form a concavity for the adductor mandibulae in *Chlamydoselachus*, hexanchoids and lamniforms, whereas it is absent in the remaining taxa. Among the outgroups, such overhanging is seen in *Hybodus, Asteracanthus* and *Xenacanthus* (Woodward, 1886; Koken, 1907; Peyer, 1946; Schaeffer, 1981). Therefore, lack of this expansion is assumed to be apomorphic.

29. Prominent inner process of ceratobranchial (pr: Fig. 4). Among living taxa, the inner process of the ceratobranchial is blunt and located on the proximal region, and is connected posteriorly with the succeeding hypobranchial and ceratobranchial via a ligament (Fig. 4A-B). In orectolobiforms except *Rhincodon*, it is prominent, located on the medial margin of the ceratobranchial in the anterior three arches (Fig. 4C-D). Among outgroups, only some branchial arches of hybodonts are found, but there is an evidence that a weakly expanded inner process is present at the proximal region of the ceratobranchial (Maisey, 1982). Therefore, the prominent inner process is assumed to be apomorphic.

30. Suprascapular cartilage present. Among living taxa, the suprascapular cartilage is present in some orectolobiforms and *Chlamydoselachus*, whereas it is absent in the remaining taxa (Garman, 1885; Braus, 1902; Shirai, 1992a). Among the outgroups, it is preserved only in *Hybodus cassangensis* of hybodonts (Maisey, 1982) and *Pleuracanthus sessilis* of xenacanths (Jaekel, 1906), but it is absent in other hybodont and xenacanthid taxa (Moy-Thomas, 1936, 1938; Maisey, 1982). The presence of this cartilage is assumed to be apomorphic because an additional information indicates it is lacking in *Cladoselache* (Schaeffer, 1967).

31. Some pectoral basal cartilages fused. Most living taxa have the tribasal pectoral basal cartilages composed of isolated propterygium, mesopterygium and metapterygium, whereas these cartilages are partly fused into two or less cartilaginous plates (Mivert, 1879; Balfour, 1881; Miller, 1952; Dingerkus, 1986; Shirai, 1992a). Among the outgroups, xenacanths have elongated and greatly segmented basal cartilages unlike those of the Recent taxa (Schaeffer, 1966; Schaeffer and Williams, 1977), but *Ctenacanthus* and hybodonts have a completely isolated tribasal cartilages (Moy-Thomas, 1938; Schaeffer and Williams, 1977; Maisey, 1985). Therefore, the fused basal cartilages are assumed to be apomorphic. Although Shirai (1996) treated as two separate characters based on the fused condition among propterygium, mesopterygium and metapterygium (his character 60 and 61), I attempted a single character to such conditions *a priori* because it is difficult to estimate homology of cartilaginous elements from the fused condition.

32. Neural arch not calcified. Most squaleans and some galeoids do not have calcified neural arches, whereas those of most galeoid and *Heterodontus* are well calcified. Since outgroups have well calcified neural arches (Maisey, 1982), the uncalcified neural arch is assumed to be apomorphic.

33. Hemal arch formation extending well forward. Converted from character 78 of Shirai (1996). Among living taxa, hemal arches are completely closed in most precaudal tail vertebrae in most taxa, whereas *Chlamydoselachus*, carcharhiniforms and most orectolobiforms have opened hemal arches in the anterior precaudal tail vertebrae. According to Shirai (1992a),

the hybodont *Orthacanthus* corresponds to the latter condition. Therefore, the forward extension of the hemal arch formation is assumed to be apomorphic.

34. Vertebral ribs present. In most living taxa, vertebral ribs are present, inserting in the horizontal myoseptum between epaxial and hypaxial body muscles, whereas these are absent in some lamniforms. *Hybodonts* has well developed vertebral ribs that are likely to be placed on the mesial wall of the body cavity (Maisey, 1982). According to Rosen et al. (1981) and Maisey (1982), the former are termed "dorsal ribs", and the latter "pleural ribs." Rosen et al. (1981) pointed out that both ribs are not homologous, and the dorsal ribs are not primitive. Therefore, the presence of the vertebral ribs is assumed to be apomorphic.

4. Reconstruction of cladogram

On the basis of the character analysis, 34 characters including 32 binary and 2 unordered multistate characters were available for the first step (Table 1). Depending upon the data matrix for 25 shark genera and a clade containing the Squalea, 54 most parsimonious trees (length=70, CI=0.600, RI=0.774) were provided by the

Table 1. Character states and coding for first step.

Character	Coding	Status
1	Pharyngobranchial blade absent (0)/present (1)	Binary
2	Orbital articulation abent (0)/present (1)	Binary
3	Basitrabecular process absent (0)/present (1)	Binary
4	Basal angle absent (0)/present (1)	Binary
5	Pectoral propterygium supporting radials (0)/no radials (1)	Binary
6	Lateral sensory canal partly opened (0)/completely closed (1)	Binary
7	Hyomandibular facet separate from orbit (0)/immediately behind orbit (1)	Binary
8	Otic capsule long (0)/short (1)	Binary
9	Inter-orbito nasal region short (0)/elongated and ventrally curved (1)	Binary
10	Ventral marginal cartilage not expanded (0)/well expanded (1)	Binary
11	Basal cartilage of dorsal fin hardly segmented (0)/composed of isolated slender rods (1)	Binary
12	Dorsal fin spine present (0)/absent (1)	Binary
13	Basal cartilage of anal fin hardly segmented (0)/composed of isolated cartilaginous pieces (1)	Binary
14	Foramen for ophthalmicus superficialis fused with main foramen for trigeminal and facial nerves (0)/isolated (1)	Binary
15	Foramen for ophthalmicus profundus fused with main foramen for trigeminal and facial nerves (0)/isolated (1)/fused with foramen for ophthalmicus superficialis (2)	Unordered
16	Foramen for hyomandibularis VII isolated (0)/fused with main foramen for trigeminal and facial nerves (1)	Binary
17	Foramen for abducens nerve isolated (0)/fused with that for trigeminal and facial nerves (1)	Binary
18	Canal for orbital sinus absent (0)/present (1)	Binary
19	Internasal space broad, with no septum (0)/narrow, with internasal septum (1)	Binary
20	Medial rostral rod not elongated (0)/greatly elongated anteriorly	Binary
21	Lateral rostral rod absent (0)/present (1)	Binary
22	Supraorbital crest present (0)/absent (1)	Binary
23	Supraorbital blade absent (0)/present (1)	Binary
24	Eyestalk absent (0)/present (1)	Binary
25	Foramen for internal carotid artery single (0)/paired (1)/fused with that for orbital artery (2)	Unordered
26	Foramen for orbital artery present (0)/absent	Binary
27	Ventral foramen for vagus nerve absent (0)/present (1)	Binary
28	Overhanging of palatoquadrate present (0)/ansent (1)	Binary
29	Inner process blunt, located on the proximal region of ceratobranchial (0)/prominent, located on the medial region of ceratobranchial (1)	Binary
30	Suprascapular cartilage absent (0)/present (1)	Binary
31	Pectoral basal cartilages three (0)/fused into two or less cartilages (1)	Binary
32	Neural arch calcified (0)/not calcified (1)	Binary
33	Hemal arch formation not extending forward in tail region (0)/well extending forward (1)	Binary
34	Vertebral ribs absent (0)/present (1)	Binary

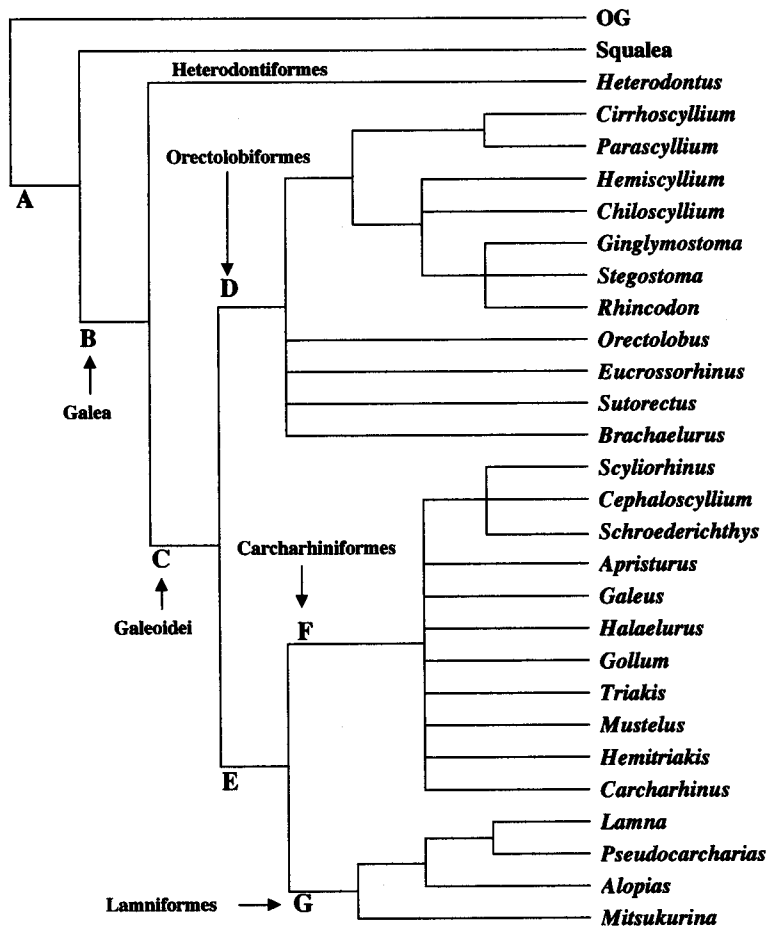

Fig. 5. Strict consensus tree of 54 most parsimonious cladograms of the living elasmobranchs.

branch and bound algorithm under the ACCTRAN option of PAUP ver. 3.0. These cladograms agree in the principal relationships, with unresolved polytomous relationships within carcharhiniforms, and the strict consensus tree is shown in Fig. 5, with assignments of apomorphies. The letter "r" following the number means reversal.

Clade B containing all members of Galea *sensu* Shirai (1996) forms a monophyletic group defined by six apomorphies 6-1, 7-1, 8-1, 9-1, 19-1 and 28-1. This clade forms a sister group of Squalea. Clade C containing all members of Galeoidei *sensu* Regan (1906) forms a monophyletic group defined by seven apomorphies 10-1, 11-1, 13-1, 14-1, 15-1, 20-1 and 25-1. Clade D containing all members of Orectolobiformes *sensu* Applegate (1972) forms a monophyletic group defined by two apomorphies 15-2 and 29-1. Clade E containing all members of Carcharhiniformes and Lamniformes *sensu* Compagno (1973) forms a monophyletic group defined by two apomorphies 9-0 (r) and 21-1. Clade F containing all members of Carcharhiniformes *sensu* Compagno (1973) forms a monophyletic group defined by only one apomorphy 16-1. However, no consistent topologies appear within this clade except for a clade composed of *Scyliorhinus, Cephaloscyllium* and *Schroederichthys*, which lacks any synapomorphies. Clade G containing all members of Lamniformes *sensu* Compagno (1973) forms a monophyletic group defined by the following three apomorphies 28-0 (r), 32-1 and 33-1. Relationships of the component genera are resolved as follows: the clade, except *Mitsukurina*, is supported by three apomorphies 18-1, 28-1 and 34-0 (r); *Lamna* and *Pseudocarcharias* are a sister group defined by two apomorphies 17-0 and 25-0.

5. Discussion

Orectolobiformes *sensu* Applegate (1972) comprises a monophyletic group sharing two synapomorphies (Fig. 5). The present results differ from those of some previous authors who suggested that these taxa are unlikely to be a natural group (e.g., Garman, 1913; White, 1937; Applegate, 1972; Maisey, 1985). Compagno (1973, 1977, 1988) consistently asserted the possibility of sister relationships between *Heterodontus* and orectolobiforms based on the similarities including the elongated eth-

moidal region and pectoral mesopterygium, the vertical suborbitalis, and the adductor mandibulae divided into three subdivisions. However, *Heterodontus* is initially derived from the galean clade in the present results, with no apparent relationships with orectolobiforms, corresponding to those of Shirai (1992a, 1996) and Carvalho (1996). Because cranial similarities shared by both taxa are equivalent to features of the early stages during the development (De Beer, 1937; Holmgren, 1940), Maisey (1985) pointed out that the similarities presumably occurred in parallel caused by extended timing of differentiation by paedomorphosis in ontogeny. Galeoids, which have been mentioned as comprising a natural taxon (Regan, 1906; White, 1937; Bigelow and Schroeder, 1948; Maisey, 1984a; Shirai, 1992a, 1996; Carvalho, 1996), are redefined as a single clade in this analysis. Orectolobiforms are a sister group of the clade composed of carcharhiniforms and lamniforms although some of them were previously said to be close to either group of lamniforms or carcharhiniforms (Regan, 1908; Garman, 1913; White, 1930, 1937; Applegate, 1972; Maisey, 1985).

Interrelationships reconstructed from the first step are still provisional because these are based on restricted morphological evidences and the relationships within the carcharhiniforms are unresolved. However, this result is plausible because it is almost equal to the previous cladistic hypotheses by Maisey (1984a), Shirai (1992a, 1996) and Carvalho (1996), and is consistent with occurrences of the fossils. Thus, I treat all orectolobiforms defined by Applegate (1972) as a monophyletic ingroup, and accept the relationships (Fig. 5) derived from the strict consensus method as the outgroup-relationships for the second-step analysis.

IV. General description and morphological differences

1. Neurocranium (Figs. 6–17).

1–1. Ethmoidal region

General description

In orectolobiforms, the ethmoidal region is extended anteriorly and curved ventrally, to form a large, broad, groove-like fossa for the palatoquadrate. The nasal capsule (nc) is large, globular or rain-drop shaped, surrounding the olfactory organ to form a large nasal chamber. The ventral surface has a large, unchondrified area, in which the nasal apertures open. The proximal region (orbito-nasal process: onp), that encloses the olfactory peduncle, is projected anteriorly and more or less curved ventrally, with a large groove (etg) for the palatoquadrate on the ventral surface. The interspace between both capsules is either narrow and high or broad and depressed. In the former, there is a thin, vertically high, oval internasal septum (ins) lying along the midline. There are some nasal cartilages around the nasal apertures. The outer nasal cartilage (onc) is a ring-like cartilage with an expansion supporting the anterior nasal flap mesially. The inner nasal cartilage (inc) is present or absent. If present, it is a small plate with a groove for the infraorbital sensory canal, articulated with the posteromesial margin of the outer nasal cartilage. The efferent opening of the orbito-nasal vein (onv) is present. The medial rostral rod (rm) is depressed and arched dorsally to marginate the ventral profile of the snout. It extends anteriorly from the anterior edge of the basal plate and is more or less expanded distally. The prefrontal fontanelle (pff) is large, covered with a fibrous membrane and opens at the anterodorsal wall of the cranial cavity just posterior to the inter-nasal region.

Morphological differences

1. Nasal capsule (nc). In most orectolobiforms, the surface of the nasal capsule is completely closed dorsally, with no fenestrae or, if fenestrae are present, they are small, rounded and restricted in the area near the rim (Figs. 6–10, 13–15). In *Parascyllium* and *Cirrhoscyllium*, there are large, slit-like fenestrae (fsn) on the surface (Figs. 11, 12).

2. Rim of nasal capsule (nc). In most orectolobiforms, the rim of the nasal capsule is nearly straight or undulated (Figs. 9–15). In *Chiloscyllium, Hemiscyllium* and *Brachaelurus*, it is fringed by a number of long, brush-like processes (Figs. 6–8).

3. Outer nasal cartilage (onc). In most orectolobiforms, the outer nasal cartilage opens posteriorly and is completely isolated from the nasal capsule (Fig. 16C-E). In *Parascyllium* and *Cirrhoscyllium*, it has a thin cartilaginous fringe supporting the anterior nasal flap that is fused with the nasal capsule anteromesially (Fig. 16A-B). In *Rhincodon*, it is completely circular, and fused with the nasal capsule anteromesially and laterally (Fig. 16F).

4. Inner nasal cartilage (inc). In most orectolobiforms, the inner nasal cartilage is present (Fig. 16C, E); whereas, *Parascyllium* except *P. ferrugineum, Cirrhoscyllium, Ginglymostoma* and *Rhincodon* do not have this cartilage (Fig. 16A, B, F). *Parascyllium ferrugineum* has a small, comb-like cartilaginous piece in the same position (inc?; Fig. 16B), but it is doubtful that this cartilage is homologous with the inner nasal cartilage because there is no association with the infraorbital sensory canal.

5. Extra cartilages of nasal cartilages (enc). In

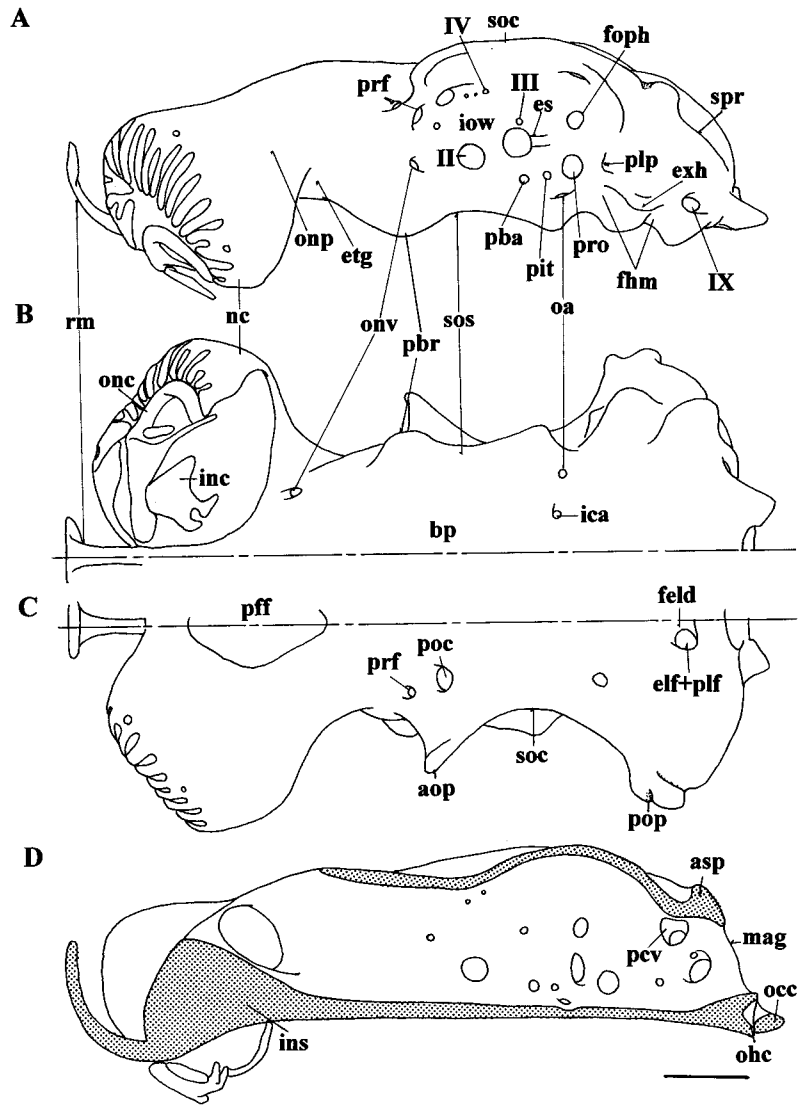

Fig. 6. Neurocranium of *Chiloscyllium plagiosum* (HUMZ 37689) in lateral (A), ventral (B), dorsal (C) and median (D) views. Scale indicates 10 mm.

Orectolobus, Sutorectus and *Eucrossorhinus*, one extra cartilage is present (Fig. 16D). In *Brachaelurus*, there are two small extra cartilages in the nasal cartilages (Fig. 16E). They are small and thin, and articulated with the expansion of the outer nasal cartilage.

6. Internasal space. In most orectolobiforms, the internasal space is very narrow, with an inter-nasal septum (ins : Figs. 6-8, 15-17). In *Orectolobus, Sutorectus, Eucrossorhinus, Ginglymostoma* and *Rhincodon*, the nasal capsule is widely separated from the opposite one by a broad and depressed interspace, without a septum (Figs. 9, 10, 14, 15).

7. Orbito-nasal process (onp). While all orectolobiform members share an elongated and ventrally curved orbito-nasal process, it is classified into the following three categories. In *Chiloscyllium, Hemiscyllium, Brachaelurus, Stegostoma, Ginglymostoma* and *Rhincodon*, the process is stout and cylindrical shaped, extending anterolaterally from the space between the rostrum and the anterior end of the orbit, and almost entirely enclosing the olfactory peduncle (Figs. 6-8, 13-15). The ventral opening of the nasal chamber is rather small and rounded, and is located anterior to the groove of the process. In *Orectolobus, Sutorectus* and *Eucrossorhinus*, the process is divided into two large, depressed plates that extend anteriorly above the olfactory peduncle (Figs. 9, 10). A distinct nasal chamber is not formed in this region, and the olfactory peduncle is covered only with a fibrous membrane ventrally. In *Parascyllium* and *Cirrhoscyllium*, the process is reduced laterally, enclosing the olfactory peduncle mesially and dorsally (Figs. 11, 12). The ventral opening of the nasal chamber is large, expanded laterally and posteriorly below the groove.

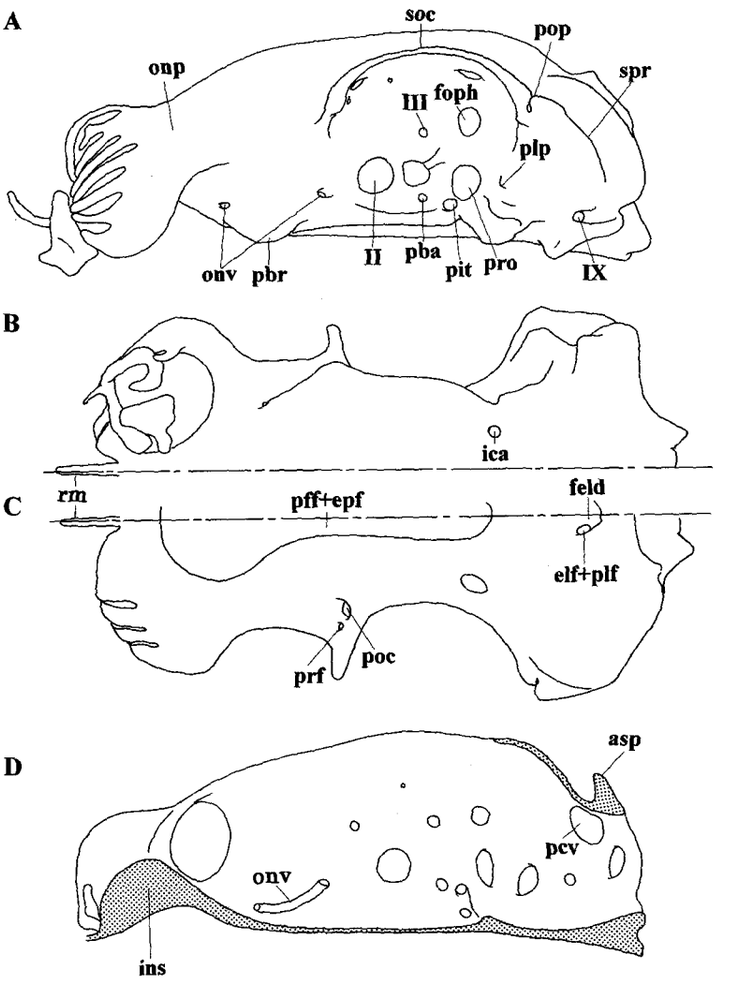

Fig. 7. Neurocranium of *Hemiscyllium freycineti* (CAS SU26798) in lateral (A), ventral (B), dorsal (C) and median (D) views. Scale indicates 10 mm.

8. Fenestra on orbito-nasal process (fed). There is an unchondrified fenestra (fed: Compagno, 1988) on the orbito-nasal process in *Parascyllium, Cirrhoscyllium, Brachaelurus* and *Ginglymostoma*. In the former two genera, it is very large, occupying most of the dorsal region (Figs. 11, 12). In the latter two genera, it is small and oval shaped, and located on the dorsolateral region just anterior to the opening of the profundus canal (Figs. 8, 14).

9. Efferent opening for orbito-nasal vein (onv). In most orectolobiforms, the efferent opening for the orbito-nasal vein opens on the posterior wall of the nasal chamber (Figs. 8-12). In *Chiloscyllium, Hemiscyllium, Stegostoma* and *Ginglymostoma*, it opens on the ventral surface of the orbito-nasal process (Figs. 6, 7, 13, 14).

10. Shape of rostral rod (rm). In most orectolobiforms, the rostral rod is thin and feeble, projecting well anteriorly, with a large expansion on its tip in *Stegostoma* (Fig. 13); with a weak or no expansion in the remaining taxa (Figs. 6-12, 14). In *Rhincodon*, it is greatly broadened and shortened, barely distinguished from the nasal capsule by a triangular concavity (Fig. 15).

11. Precerebral fossa. The precerebral fossa is recognized as a concavity formed on the medial region immediately anterior to the prefrontal fontanelle (Holmgren, 1941; Shirai, 1992a). Among orectolobiforms, *Orectolobus, Sutorectus, Eucrossorhinus* and *Rhincodon* have a broad, flattened space anterior to this fontanelle (Figs. 9, 10, 15). According to Holmgren (1940), how-

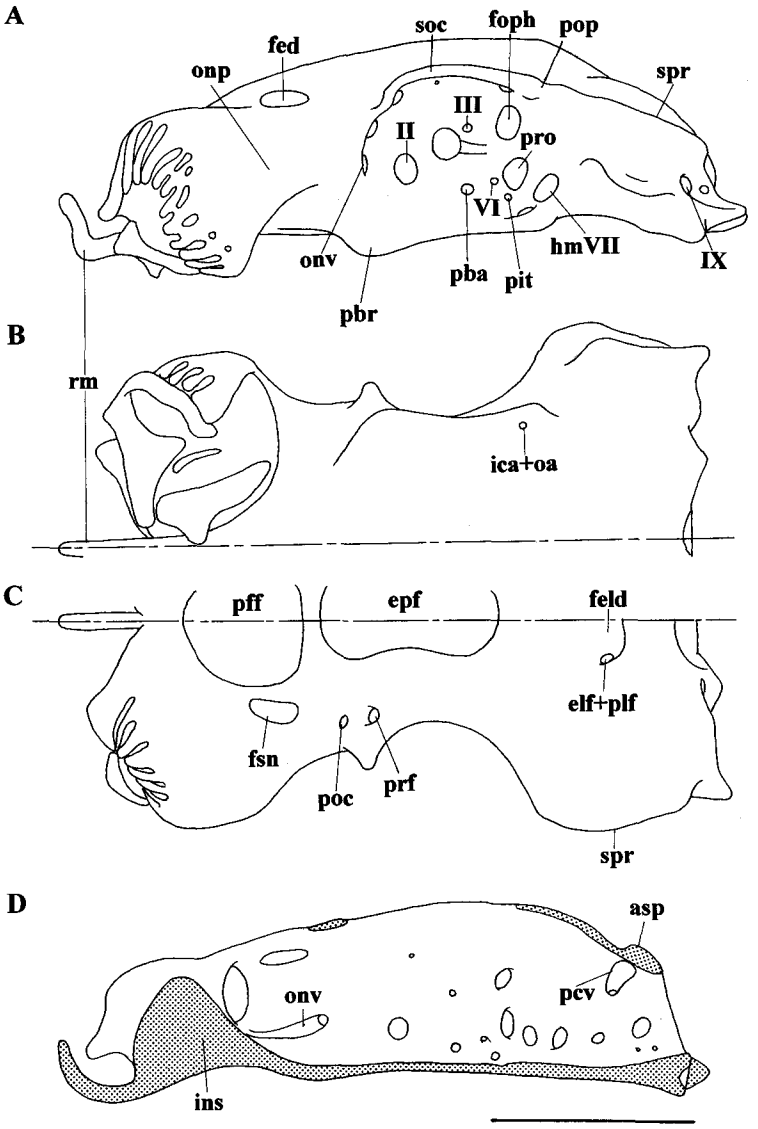

Fig. 8. Neurocranium of *Brachaelurus waddi* (AMS I20095033) in lateral (A), ventral (B), dorsal (C) and median (D) views. Scale indicates 10 mm.

ever, this fossa is represented as a floor formed on the lateral extension of the suprarostral part of the rostrum in *Squalus*, and this part is not homologous with the rostrum of galeoids. Thus, the floor seen in orectolobiforms should not be homologous with the precerebral fossa, and the precerebral fossa is absent in orectolobiforms.

1-2. Orbital region

General description

The epiphyseal foramen (epf) is present or absent on the dorsal surface of this region. The supraorbital crest (soc) is a ridge-like expansion fringing the dorsal margin of the interorbital wall. It is distinguished by the longitudinal groove and preorbital canal located on the base. The antorbital process (aop) projects laterally, forming an anterior corner of the supraorbital crest. The postorbital process (pop) bluntly projects laterally at the posterior end of the supraorbital crest. The preorbital canal (poc) penetrated by the ramus ophthalmicus superficialis V and VII pierces the base of the supraorbital crest. The profundus canal (prf), penetrated by the ramus ophthalmicus profundus V, is small and pierces the base of the antorbital process anterior to the preorbital canal. The interorbital wall (iow) is a large, oval floor with a number of foramina for cranial nerves and blood vessels. The preorbital wall is reduced, forming a gentle slope towards the orbito-nasal process, with an afferent opening of the orbito-nasal vein (onv) on the anterior margin. The eyestalk (es) is relatively stout, with a rounded disc carrying the eyeball. It originates from the posterior region of the interorbital

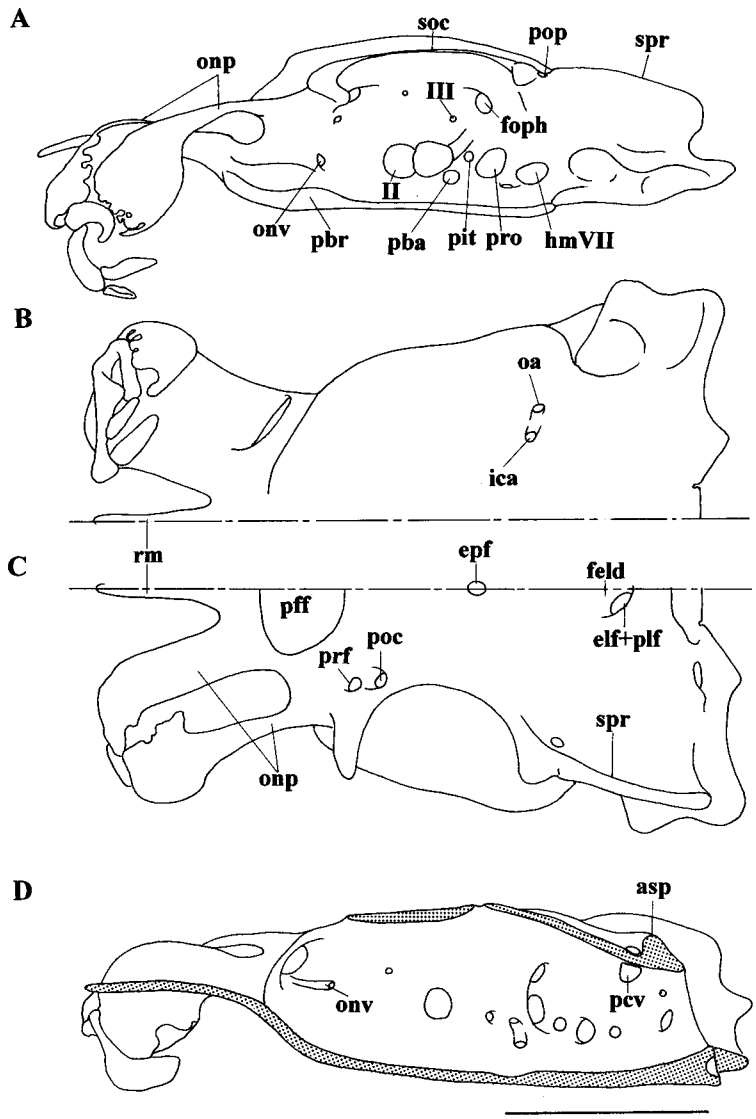

Fig. 9. Neurocranium of *Orectolobus ornatus* (AMS I14236) in lateral (A), ventral (B), dorsal (C) and median (D) views. Scale indicates 10 mm.

wall. The foramen opticum (II), in which the optic nerve passes, is large, perforating the center of this wall. The foramen for the oculomotor nerve (III) is small, located above the eyestalk. The foramen for the trochlear nerve (IV) is extremely small, perforating near the dorsal margin of this wall. The foramen for the trigeminal and facial nerves is divided into two foramina. The foramen for the ophthalmicus superficialis V and VII and ophthalmicus profundus V (foph) is large, located on the posterodorsal region of this wall. The foramen for the remaining twigs (pro), i.e., buccalis, mandibularis, maxillaris and hyomandibularis branches, is large, located on the posteroventral region posterior to the eyestalk. The abducens nerve (VI) passes through the foramen for the trigeminal and facial nerves or through its own foramen. The foramen for the pseudobranchial artery (pba) is small, located below the eyestalk. The foramen for the pituitary vein (pit) is small, opening posterior to the foramen for the pseudobranchial artery. The ventral margin of the interorbital wall is entirely fringed by a large, flattened suborbital shelf (sos). There is a prominent palatobasal ridge (pbr), which articulates with the palatoquadrate via a ligament, at the anterior extremity of the suborbital shelf. The foramen for the orbital artery (oa) is small, piercing the posterior region of the suborbital shelf vertically. The basal plate (bp) is broad and flat. The foramen for the internal carotid artery (ica) penetrates the basal plate toward the cranial cavity.

Morphological differences

1. Relationship between epiphyseal foramen (epf) and prefrontal fontanelle (pff). Among orectolobiforms, the epiphyseal foramen is categorized into the fol-

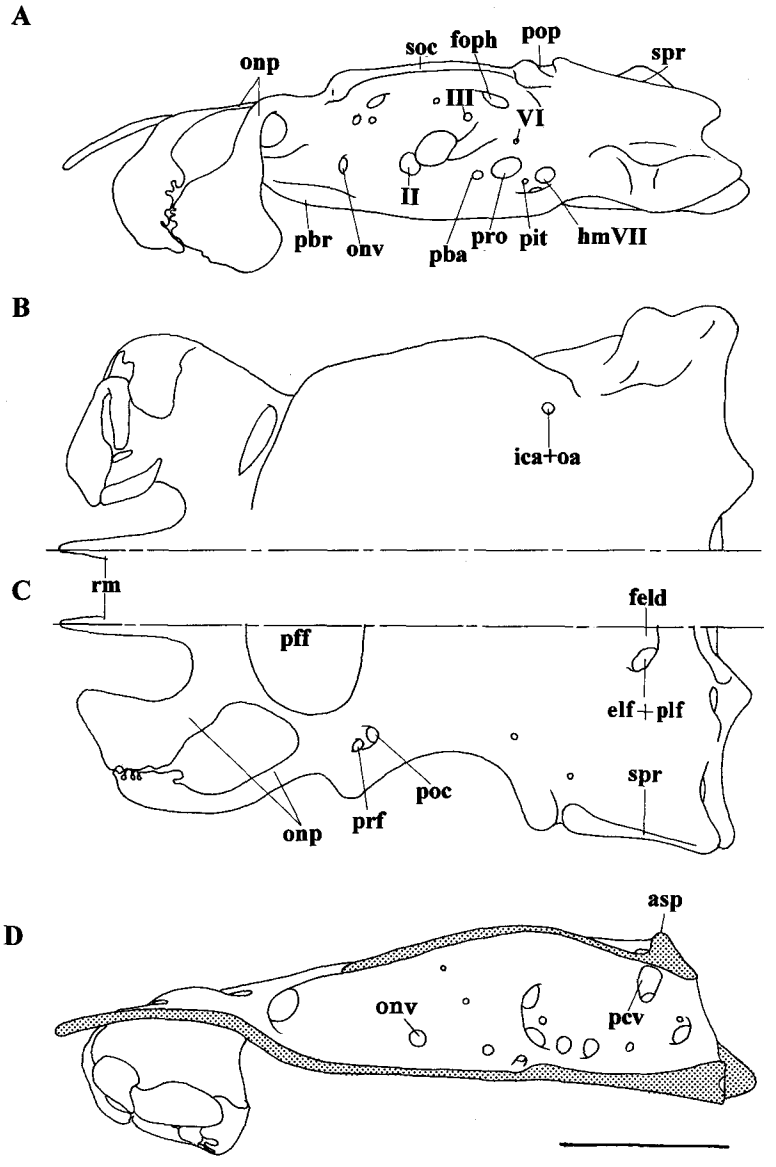

Fig. 10. Neurocranium of *Orectolobus wardi* (HUMZ 117705) in lateral (A), ventral (B), dorsal (C) and median (D) views. Scale indicates 10 mm.

lowing states depending upon the association with the prefrontal fontanelle. In *Chiloscyllium* except *C. indicum, Orectolobus wardi, Eucrossorhinus* and *Stegostoma*, it is apparently absent (Figs. 6, 10, 13). In *C. indicum, Brachaelurus, Orectolobus* except *O. wardi* and *Sutorectus*, it is large and rounded, well separated from the prefrontal fontanelle (Figs. 8, 9). In *Hemiscyllium, Ginglymostoma* and *Rhincodon*, it is fused with the prefrontal fontanelle, forming a single, large fenestra extending to the posterior area of the orbital region immediately anterior to the endolymphatic fossa (pff+epf: Figs. 7, 14, 15). In *Parascyllium* and *Cirrhoscyllium*, it is fused with the prefrontal fontanelle, extending to the supraotic region (pff+epf: Figs. 11, 12).

2. Supraorbital crest (soc). In most orectolobiforms, the supraorbital crest is present (Figs. 6–10, 13–15), but it is lacking in *Parascyllium* and *Cirrhoscyllium* (Figs. 11, 12).

3. Supraorbital blade (sbl). In *Stegostoma, Ginglymostoma* and *Rhincodon*, there is a supraorbital blade (sbl) expanding laterally over the dorsal margin of the orbit lateral to the preorbital and profundus canals (Figs. 13–15). It is large and depressed, with an anteroposteriorly bifurcated expansion at the distal margin covering over eyeball. The anterior expansion is long, slender, and weakly arched ventrally, and the posterior is short, depressed, and expanded laterally, with a vertical groove through which passes the infraorbital sensory canal on the distal margin. Homology of this blade has been controversial. Luther (1909a) treated it as the complex composed of the antorbital process, supraorbital crest and postorbital process in *Stegostoma*.

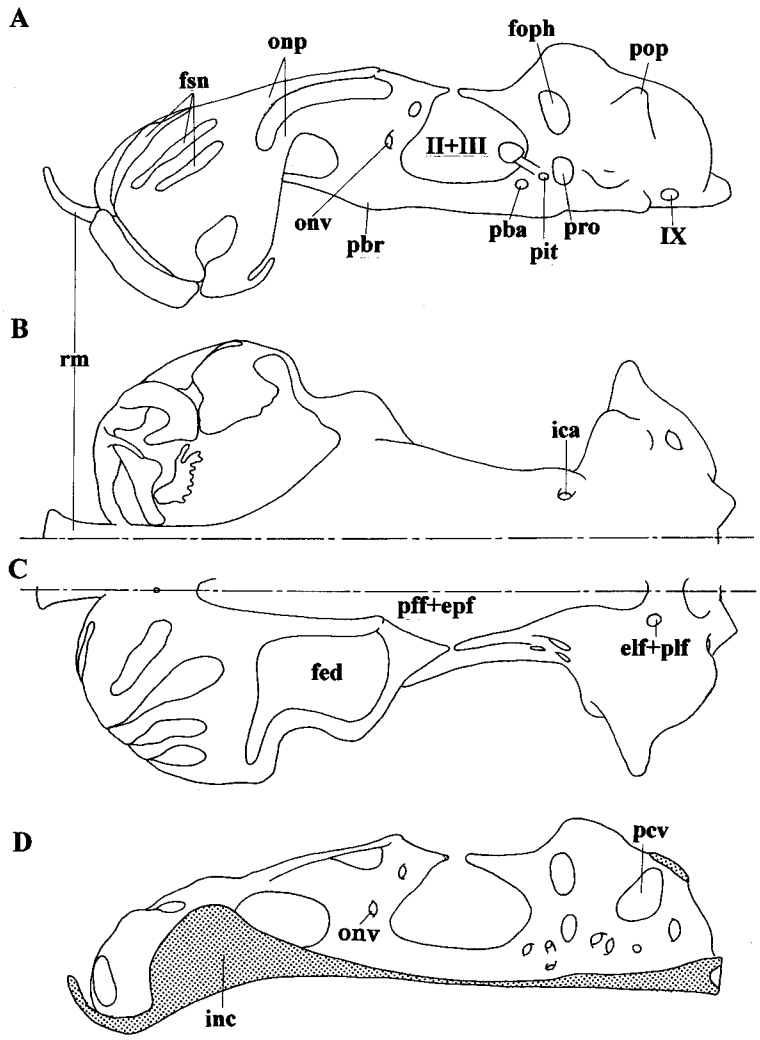

Fig. 11. Neurocranium of *Parascyllium ferrugineum* (HUMZ 131588) in lateral (A), ventral (B), dorsal (C) and median (D) views. Scale indicates 10 mm.

Denison (1936) regarded the large, square-shaped process covering the posterior region of the orbit as the postorbital process in *Rhincodon*; however, he showed only the posterior half of the proximal region of this process because most of the distal region was apparently damaged. Dingerkus (1986) also recognized it as the postorbital process but provided no certain reasons for doing so. Compagno (1988) pointed out that it is an expansion modified from the supraorbital crest. According to Compagno (1988), the antorbital process is generally recognized as an expansion penetrated by the ophthalmicus profundus V nerve. Holmgren (1940) showed that the preorbital canal is ontogenetically formed on the anterior region of the supraorbital crest in *Scyliorhinus*. Moreover, the postorbital process is usually associated with the infraorbital canal of the head sensory canal by the groove distally (Nakaya, 1975; Compagno, 1988). Thus, the supraorbital blade should be homologous with the reduced antorbital process, and greatly modified supraorbital crest and postorbital process.

4. Shape of postorbital process (pop). In most orectolobiforms, the postorbital process is blunt, with a vertical groove through which passes the infraorbital sensory canal (Figs. 6-10, 13-15). In *Parascyllium* and *Cirrhoscyllium*, it is pointed, without a groove on it (Figs. 11, 12).

5. Preorbital (poc) and profundus (prf) canals. Most orectolobiforms have preorbital and profundus canals (Figs. 6-10, 13-15); while, *Parascyllium* and *Cirrhoscyllium* lack both canals (Figs. 11, 12). In *Ginglymostoma* and *Rhincodon*, the preorbital canal is greatly enlarged, forming a rounded, oval-shaped vertical fenestra (Figs. 14, 15).

6. Foramina for optic (II) and oculomotor (III) nerves. In most orectolobiforms, the foramina for the

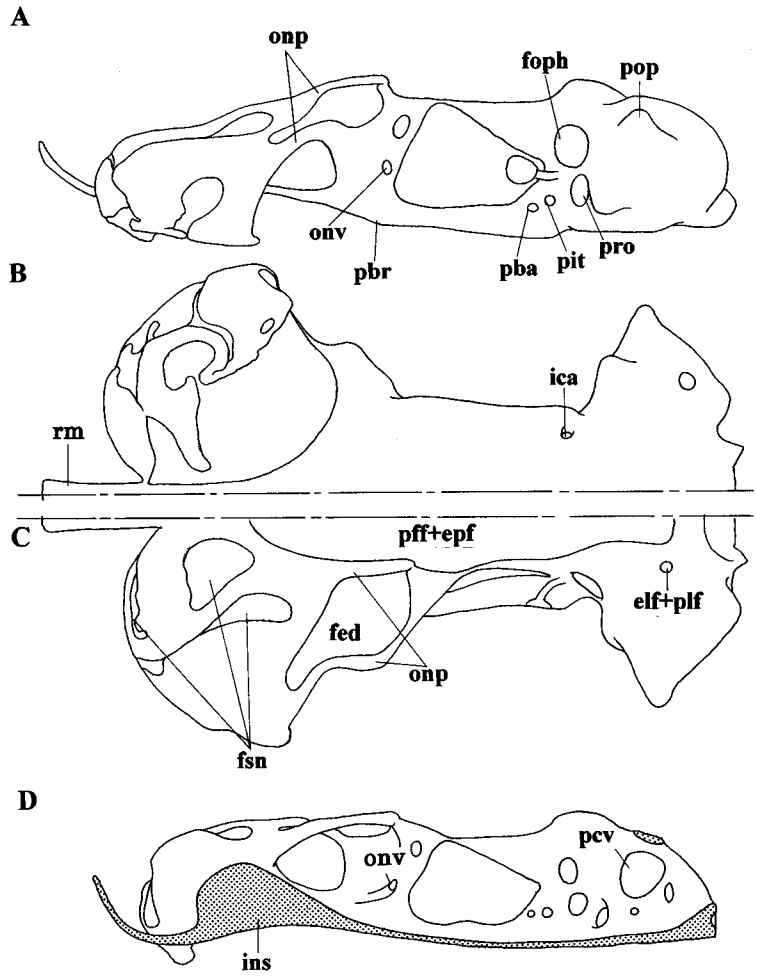

Fig. 12. Neurocranium of *Cirrhoscyllium japonicum* (HUMZ 40057) in lateral (A), ventral (B), dorsal (C) and median (D) views. Scale indicates 10 mm.

optic and oculomotor nerves are separated (Figs. 6-10). In *Parascyllium, Cirrhoscyllium, Stegostoma, Ginglymostoma* and *Rhincodon*, both foramina are fused into a single, large fenestra (II+III ; Figs. 11-15).

7. Foramen for hyomandibularis VII nerve (hmVII). In most orectolobiforms, the hyomandibularis branch of the facial nerve penetrates the main foramen for the trigeminal and facial nerves (pro ; Figs. 6, 7, 11-15). In *Brachaelurus, Orectolobus, Sutorectus* and *Eucrossorhinus*, this branch passes through the isolated foramen (foramen for hyomandibularis : hmVII) located posterior to the main foramen (Figs. 8-10).

8. Foramen for abducens nerve (VI). In most orectolobiforms, the abducens nerve passes through the main foramen for the trigeminal and facial nerves (pro ; Figs. 6, 7, 9, 11-14). In *Brachaelurus* and *Orectolobus wardi*, an isolated foramen penetrated by this nerve is present (VI ; Figs. 8, 10). In *Rhincodon*, this nerve passes through the foramen for the ophthalmicus branches (foph ; Fig. 15).

9. Foramina for pseudobranchial artery (pba) and pituitary vein (pit). In most orectolobiforms, the foramina for the pseudobranchial artery and pituitary vein are separated (Figs. 6-12). In *Stegostoma, Ginglymostoma* and *Rhincodon*, both foramina are fused into a single fenestra located just ventral to the eyestalk (pba+pit ; Figs. 13-15).

10. Palatobasal ridge (pbr). In most orectolobiforms, the palatobasal ridge is a thickened part of the suborbital shelf (Figs. 6-12, 14, 15). In *Stegostoma*, it is projected anteriorly, forming a prominent articular condyle for the palatoquadrate (Fig. 13).

11. Foramen for orbital artery (oa). Most

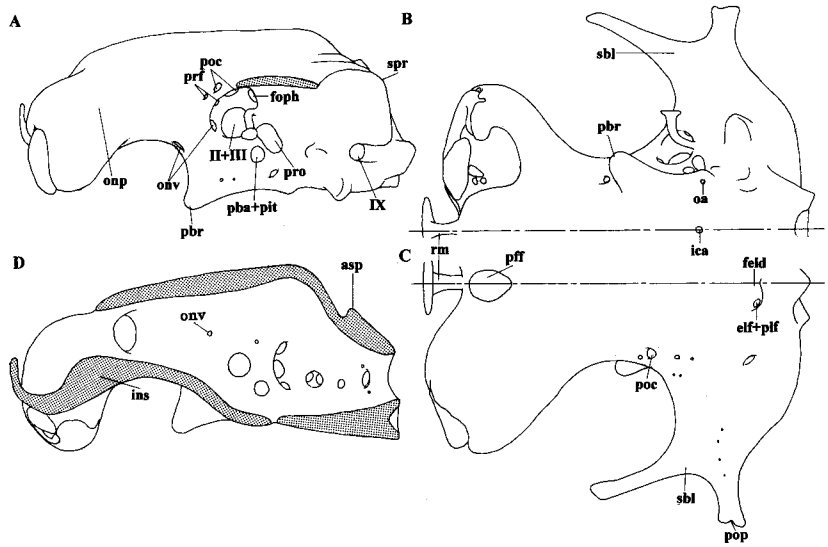

Fig. 13. Neurocranium of *Stegostoma varium* (HUMZ 78593) in lateral (A), ventral (B), dorsal (C) and median (D) views. Scale indicates 10 mm.

orectolobiforms have a foramen for the orbital artery piercing the suborbital shelf (Figs. 6, 8–10, 13–15). In *Hemiscyllium freycineti*, *Parascyllium* and *Cirrhoscyllium*, it is absent, and the artery passes over the posterior edge of the suborbital shelf (Figs. 7, 11, 12).

12. Foramen for internal carotid artery (ica). The foramen for the internal carotid artery is classified into the following three categories. It is divided into a pair of foramina in most orectolobiforms (Figs. 6, 7, 9, 11, 12, 14, 15), and fused into a single foramen on the midline in *Stegostoma* (Fig. 13). It is absent, and the artery passes through the foramen for the orbital artery in *Brachaelurus* and *Orectolobus wardi* (ica+oa; Figs. 8, 10).

1–3. Otic and occipital regions

General description

In orectolobiforms, the otic and occipital regions are generally short, and dome-shaped. The endolymphatic fossa (feld) consists of a single, rounded concavity located on the midspace of the supraotic region. The posterior margin of the fossa is abruptly expanded dorsally, forming an ascending process (asp). There are a small endolymphatic fenestra (elf) and a large perilymphatic fenestra (plf) piercing the lateral margin of the fossa. The sphenopterotic ridge (spr) varies greatly in the extent of its development. The lateral surface of the otic capsule forms a vertical, flat floor lying between the sphenopterotic ridge and hyomandibular facet. The hyomandibular facet (fhm) is large, fringed by a prominent, triangular expansion (exh) dorsally. It is divided into two concavities: the anterior one is deep, located immediately posterior to the foramen for the trigeminal and facial nerves (pro); the posterior one is shallow, located posteroventral to the anterior. The foramen for the glossopharyngeal nerve (IX) is large, opening posterior to the hyomandibular facet. The ventral surface of the otic region is flat, forming the posterior part of the basal plate. The posterior wall of the neurocranium is broadly convex, dome-like in dorsal profile. The foramen magnum (mag) is large and ovoid, and opens at the medial part of this wall. The occipital hemicentrum (ohc) is buried in the posterior tip of the basal plate, and articulates with the first vertebral centrum. The occipital condyle (occ) is large, projected posteriorly, with an oblique, oval-shaped face tightly articulated with the first basiventral process. The foramen for the vagus nerve (X) is large, opening at this wall lateral to the occipital centrum.

Morphological differences

1. Endolymphatic fossa (feld). In most orectolobiforms, the endolymphatic fossa is present as a prominent concavity (Figs. 6–10, 13–15). In *Parascyllium* and *Cirrhoscyllium*, no such concavity occurs on this region (Figs. 11, 12).

2. Endolymphatic (elf) and perilymphatic (plf) fenestrae. *Ginglymostoma* has separate endolymphatic and perilymphatic fenestrae (Fig. 14), whereas both fenestrae are fused into a single, large foramen in the remaining taxa (elf+plf; Figs. 6–13, 15).

3. Ascending process of endolymphatic fossa (asp). In most orectolobiforms, the ascending process of the endolymphatic fossa is recognized as a thickened section projected dorsally (Figs. 6–10, 13–15). In *Parascyllium* and *Cirrhoscyllium*, it is absent (Figs. 11, 12).

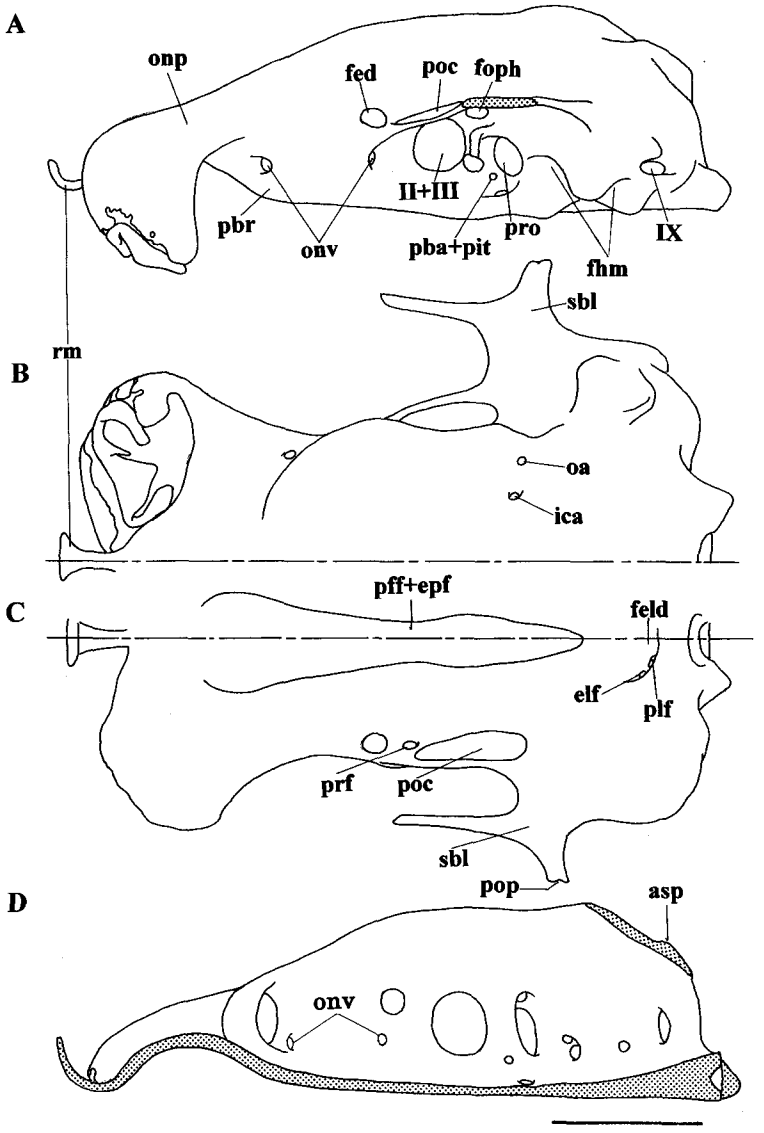

Fig. 14. Neurocranium of *Ginglymostoma cirratum* (ZMUC P0629) in lateral (A), ventral (B), dorsal (C) and median (D) views. Scale indicates 10 mm.

4. Sphenopterotic ridge (spr). In *Brachaelurus, Orectolobus, Sutorectus, Eucrossorhinus* and *Rhincodon*, the sphenopterotic ridge is well expanded dorsally, forming a vertical wall providing an insertion of the epaxial body muscle medially, with a blunt posteriorly projected process (Figs. 8–10, 15). In *Chiloscyllium, Hemiscyllium* and *Stegostoma*, it is not expanded dorsally, forming a distinct ridge broadly covered with the epaxial body muscle, with no prominent process (Figs. 6, 7, 13). In *Parascyllium, Cirrhoscyllium* and *Ginglymostoma*, it is either a considerably weak ridge or entirely absent, and is broadly covered with the epaxial (Figs. 11, 12, 14).

5. Projection for levator palatoquadrati (plp). In *Chiloscyllium* and *Hemiscyllium*, there is a weak but distinct projection on the anterior margin of the otic capsule (Figs. 6, 7). That is the attachment site for the origin of the levator palatoquadrati muscle.

6. Expansion of glossopharyngeal nerve (IX). In most orectolobiforms, the foramen for the glossopharyngeal nerve is fringed by a prominent expansion ventrally (Fig. 17B). In *Parascyllium, Cirrhoscyllium* and *Rhincodon*, there is no such expansion (Fig. 17A).

7. Posterior canal vacuity (pcv). In most orectolobiforms except *Stegostoma, Ginglymostoma* and *Rhincodon*, there is a round, unchondrified fenestra covered with fibrous membrane on the mesial surface of the auditory capsule that forms a bottom corner of the endolymphatic duct (Figs. 6–12). DeBeer (1937) termed the fenestra of *Scyliorhinus* as the posterior canal vacuity, and the fenestra shared by orectolobiforms is equivalent to the posterior canal vacuity based on the position and shape.

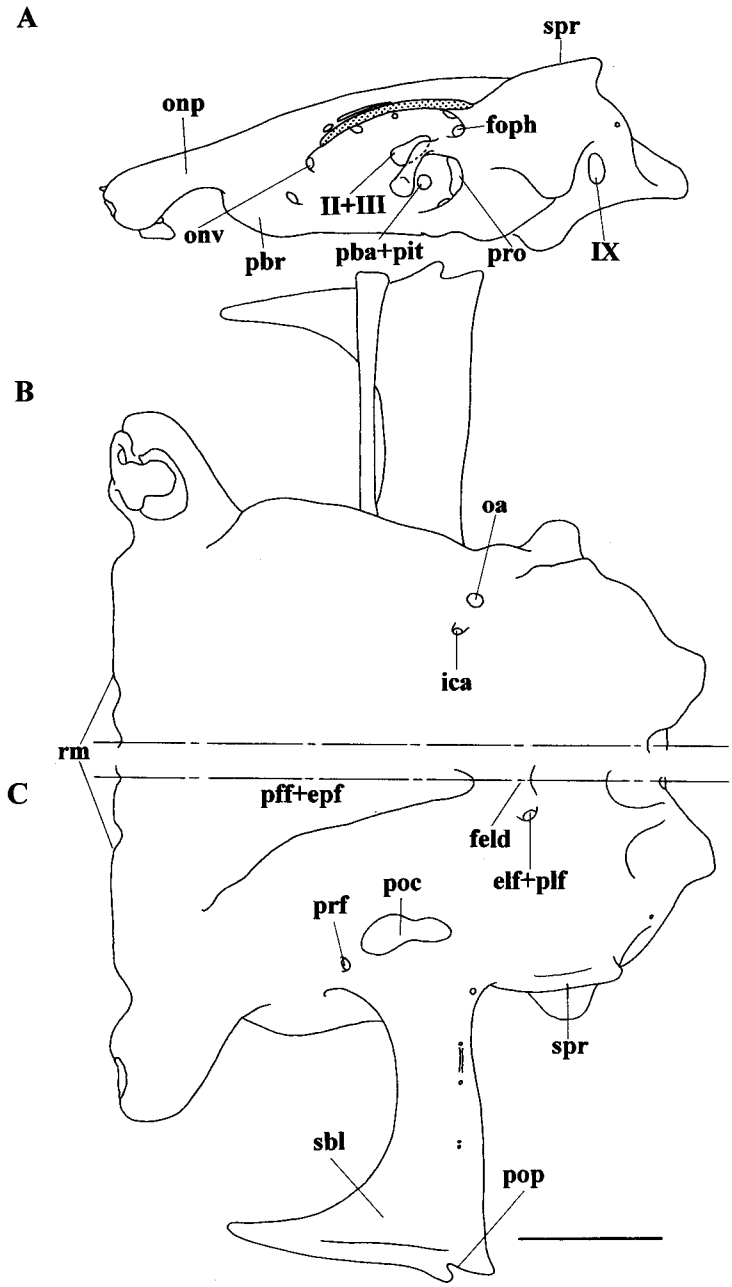

Fig. 15. Neurocranium of *Rhincodon typus* (OA 00212) in lateral (A), ventral (B) and dorsal (C) views. Scale indicates 100 mm.

2. Visceral arch

2-1. Mandibular arch

***General description* (*Fig. 18*)**

The mandibular arch of orectolobiforms is large and stout, greatly extending forward to the ethmoidal region. It consists of palatoquadrate, mandibula and labial cartilages. The palatoquadrate (pq) is massive, with a broad dental band on the ventral margin of the anterior half. The anterior tip is tightly articulated with its antimere at the symphysis. The lingual surface has a prominent, ridge-like process, the ethmo-palatine process (epp ; after Maisey, 1980), covered with a massive ligament (*leth*) for the articulation with the palatobasal ridge of the neurocranium. The labial surface is weakly convex, with a small ridge (rgp) providing the insertion of the adductor mandibulae. The posterior end is bluntly pointed, with a facet composed of the weak palatoquadrate concavity (pc) and ovoid-shaped condyle (pcd) on the ventral margin. The mandibula (md) is large and depressed, with a broad dental band on the dorsal margin of the anterior half. The anterior tip is tightly articulated with its antimere at the symphysis. The labial surface is weakly convex in the anterior

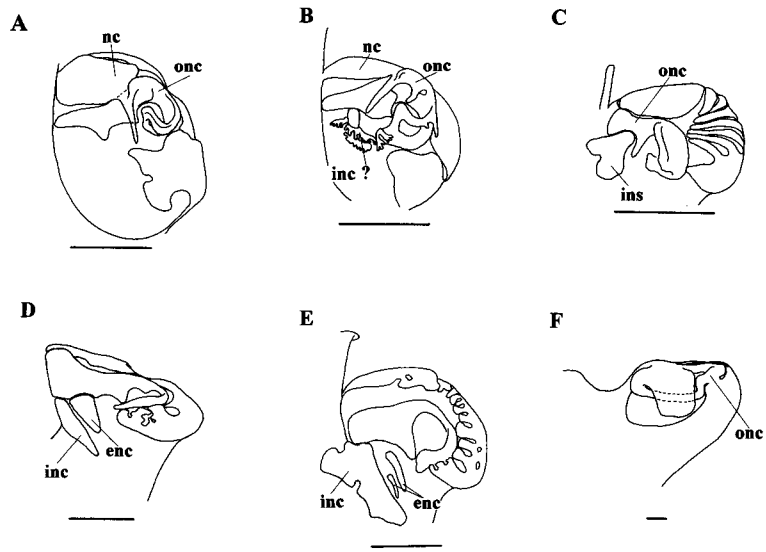

Fig. 16. Ventral views of nasal capsules showing nasal cartilages. (A) *Parascyllium collare* (AMS I30409002); (B) *P. ferrugineum* (HUMZ 131588); (C) *Chiloscyllium indicum* (MCZ 54); (D) *Eucrossorhinus dasypogon* (CSIRO CA 4051); (E) *Brachaelurus waddi* (AMS I20095033); (F) *Rhincodon typus* (OA 00212). Scales indicate 5 mm in A, C and E, and 10 mm in B, D and F.

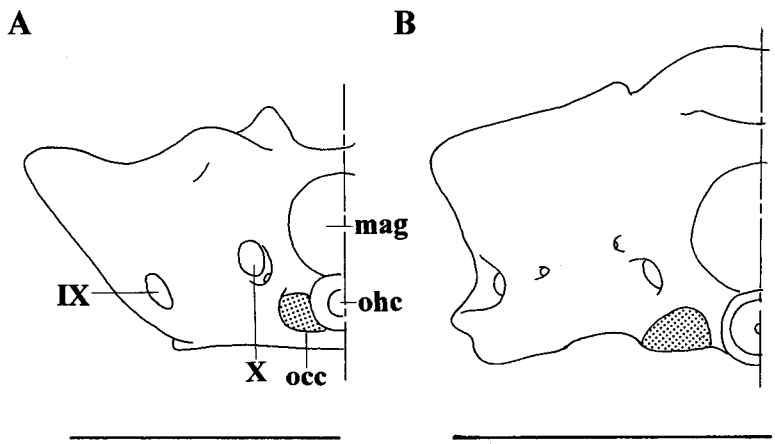

Fig. 17. Posterior views of neurocrania. (A) *Cirrhoscyllium japonicum* (HUMZ 40057); (B) *Brachaelurus waddi* (AMS I20095033). Scales indicate 10 mm.

region, and slightly concave in the posterior region. The posterior margin is more or less expanded labially, forming a ridge which provides the insertion of the adductor mandibulae, with a prominent articular fossa (maf) and a ridge-like condyle (mc) articulated with the condyle (pcd) and concavity (pc) of the palatoquadrate, respectively, on the dorsal surface. The lingual surface has a large mandibular knob (mk), which articulates with the hyomandibula via several ligaments (*ljs*). The ligamentum mandibulo-palatoquadrati (*lmp*) is long and strong, connecting the lingual surfaces of the mandibula and palatoquadrate just anterior to the articulation of both cartilages. A prominent ligament (*lcm*), which originates from the lateral edge of the basal plate immediately ventral to the hyomandibular facet, inserts onto the posteroventral region of the lingual surface of the mandibula. The dental band in both jaws consists of two or more naked functional tooth rows and the following replacement series covered with epithelium. Morphological differentiation among teeth in various positions of the jaws is absent or, if present, rather weak to approximate homodonty. Each tooth is generally small, principally comprising a bifurcated root and a crown. The crown is flat and reef-like, with a labially expanded apron; a single, conical medial cusp; and a pair of small lateral cusps. The labial cartilages are composed of anterior and posterior upper cartilages, and a lower one. The anterior upper labial cartilage (alc) is

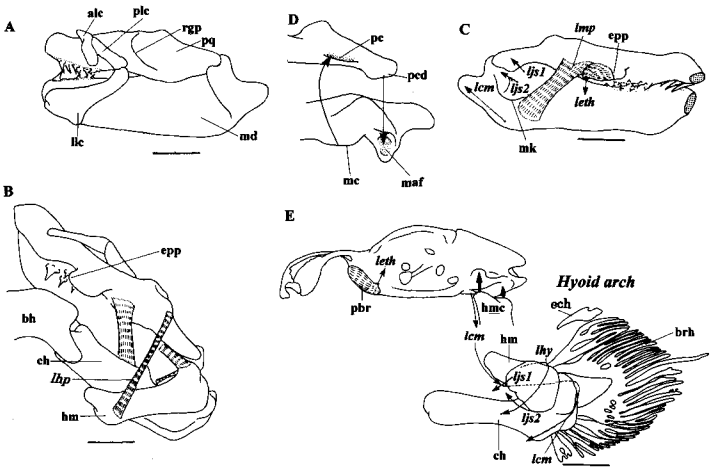

Fig. 18. Mandibular and hyoid arches of *Eucrossorhinus dasypogon* (CSIRO CA 4051) showing labial (A), dorsal (B) and lingual (C) views, articulation between both jaws (D), and association of hyoid arch with neurocranium (E). Scales indicate 10 mm.

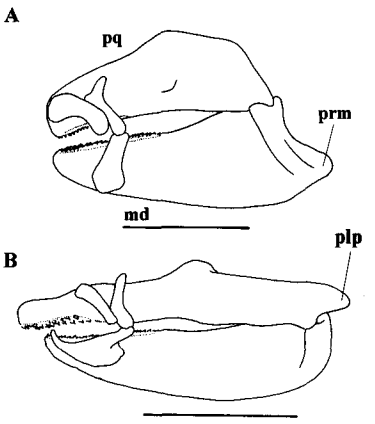

Fig. 19. Labial views of mandibular arches. (A) *Brachaelurus waddi* (AMS I20095033); (B) *Parascyllium collare* (AMS I30409002). Scales indicate 10 mm.

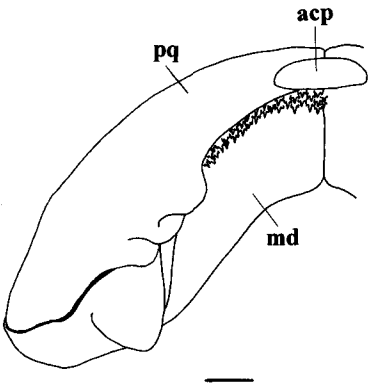

Fig. 20. Dorsal view of mandibular arch in *Stegostoma varium* (HUMZ 78593). Scale indicate 10 mm.

slender and weakly arched ventrally, and articulates with the palatoquadrate at the anteromesial region. The posterior upper labial cartilage (plc) is elongated, somewhat bending dorsally at the center, and tightly attached with the anterior upper one at the ventral margin of the bending corner. The lower cartilage (llc) is large and depressed, articulated with the posterior upper one distally, and broadly attached with the mandibula mesially.

Morphological differences

1. Post-palatoquadrate process (plp). In *Parascyllium* and *Cirrhoscyllium*, there is a prominent post-palatoquadrate process posterior to the articular facet of the palatoquadrate (Fig. 19B). It provides the insertions of some constrictor muscles.

2. Process of mandibula (prm). In *Brachaelurus, Orectolobus, Eucrossorhinus, Sutorectus, Ginglymostoma* and *Rhincodon*, the posterior end of the mandibula is expanded posteriorly, forming a prominent triangular process (Fig. 19A). In *Chiloscyllium, Hemiscyllium, Parascyllium, Cirrhoscyllium* and *Stegostoma*, there is no such expansion (Fig. 19B).

3. Accessory cartilage of palatoquadrate (acp). Only in *Stegostoma*, there is a single, ovoid-shaped accessory cartilage just dorsal to the symphysis of the palatoquadrate (Fig. 20).

4. Accessory cartilage on symphysis of mandibula (acs). In *Parascyllium, Cirrhoscyllium, Orectolobus, Sutorectus* and *Eucrossorhinus*, there is a small, globular-shaped accessory cartilage immediately posterior to the symphysis of the mandibula (Fig. 21B-C). In *Rhincodon*, this cartilage is large and disc-shaped, and is buried in the rounded fenestra formed at the symphyseal region of the mandibula (Fig. 21D).

5. Accessory cartilage on mandibula (acm). *Parascyllium* and *Cirrhoscyllium* have a small, oval-shaped accessory cartilage on the ventral margin of the

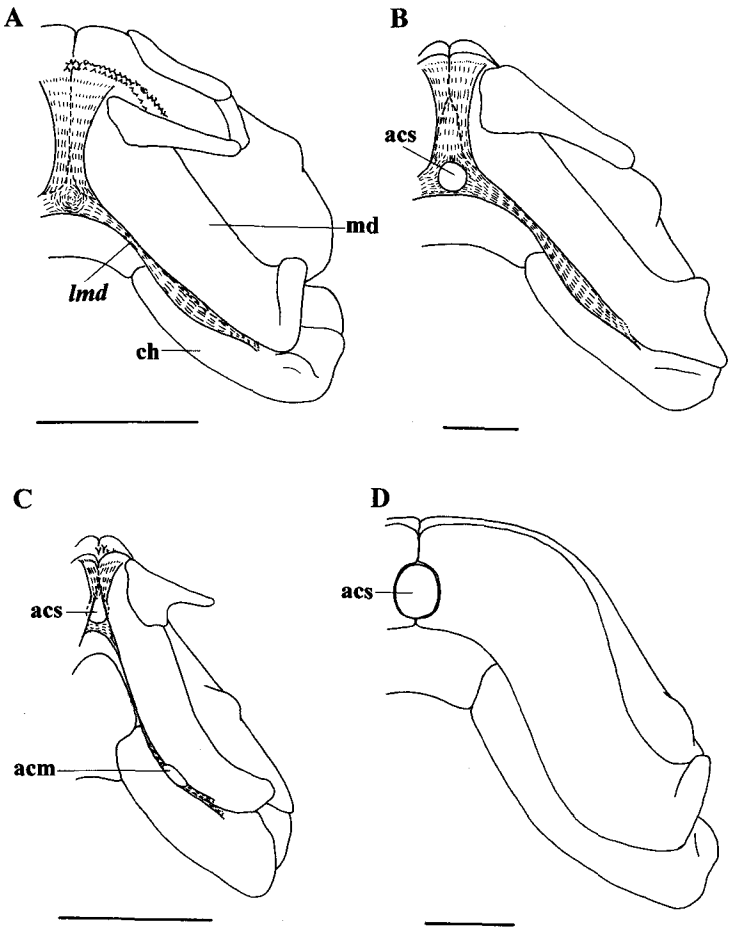

Fig. 21. Ventral views of mandibular arches. (A) *Chiloscyllium indicum* (MCZ 54); (B) *Eucrossorhinus dasypogon* (CSIRO CA 4051); (C) *Parascyllium collare* (AMS I30409002); *Rhincodon typus* (OA 00212). Scales indicate 10 mm in A-C, and 100 mm in D.

mandibula (Fig. 21C). In the remaining taxa, a massive, fusiform connective tissue is located in the same position as this cartilage, and is connected by a prominent ligament (*lmd*) extending from the symphyseal region of the mandibula to the posterior regions of the mandibula and ceratohyal (Fig. 21A).

6. Ligamentum cranio-palatoquadrati (*lcp*). In *Chiloscyllium, Hemiscyllium* and *Brachaelurus*, the ligamentum cranio-palatoquadrati is present (Fig. 22A). It originates from the expansion above the hyomandibular facet, passes through the posterior wall of the spiracular cleft, and inserts on the dorsal margin of the palatoquadrate.

7. Ethmoidal articulation. All orectolobiforms have direct articulation of the palatoquadrate with the palatobasal ridge of the neurocranium as the hyostylic jaw articulation (Maisey, 1980). Among them, this articulation can be classified into the following three categories. In most orectolobiforms, this articulation is rather tight, via a remarkably massive and flexible ligament; the ethmopalatine process is prominent, located on the lingual surface of the palatoquadrate; and the palatobasal ridge is thickened (Fig. 22A). In *Parascyllium* and *Cirrhoscyllium*, this articulation is loose, maintained by only a thin ligament (*leth*); the ethmopalatine process (epp) is low, located on the dorsomesial margin of the palatoquadrate; and the palatobasal ridge is weak, forming a flattened slope (Fig. 22B). In *Stegostoma*, it is almost similar to the second category but remarkably firm; the ethmopalatine process is well pronounced, with a concaved facet on its head; and the palatobasal ridge projects anteriorly, forming an articular condyle (Fig. 22C).

8. Tooth arrangements. In orectolobiforms, two categories are found in the relationship between adjacent teeth along the series among the independent dentition, overlapping dentition, alternate overlap, imbricate dentition and mixed dentition recognized by Strasburg (1963), Springer (1966), and Compagno (1988). The other orectolobiform members are essentially categorized as having imbricated dentition (Fig. 23A). *Orectolobus, Eucrossorhinus* and *Sutorectus* have independent denti-

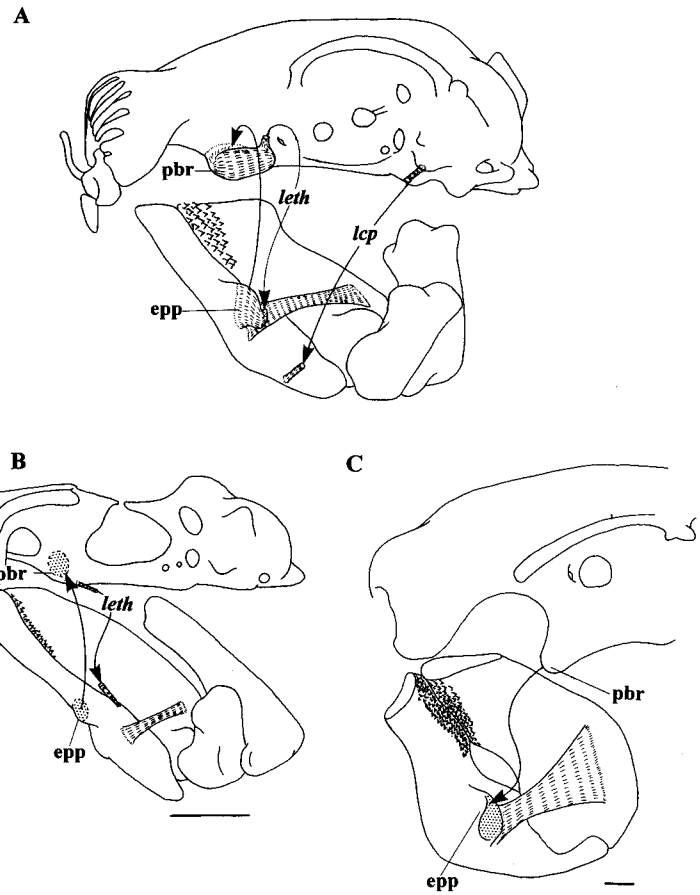

Fig. 22. Jaw-neurocranium articulation in three orectolobiforms. (A) *Hemiscyllium trispeculare* (S10603-008); *Parascyllium collare* (AMS I30409002); *Stegostoma varium* (HUMZ 78593). Scales indicate 10 mm.

tion, in which the adjacent tooth bases are separate and do not overlap each other (Fig. 23B). In this category, the mesial edge of each tooth lingually overlaps posterior to the lateral end of the mesially adjacent tooth, and the distal edge overlaps anterior to the mesial end of the distally adjacent tooth. Although Compagno (1984) described the tooth arrangement of *Ginglymostoma* as not imbricated, it indicates more or less imbricated condition in the present materials.

9. Tooth morphology. Orectolobiform tooth morphology varies greatly within individuals (e.g., heterodonty associated with position, sex, development) and also among taxa, but the following categories are consistent among taxa (Figs. 24, 25). In *Chiloscyllium* and *Hemiscyllium*, the lateral cusps are extremely short, and inclined mesiodistally (Fig. 24B). In *Parascyllium, Cirrhoscyllium, Brachaelurus* and *Stegostoma*, prominent erected lateral cusps (lcp) are present (Fig. 24A). *Ginglymostoma* has prominent lateral cusps, with two additional rudimentary cusps on the mesiodistal ends in some teeth (Fig. 24C). In *Orectolobus, Eucrossorhinus* and *Sutorectus*, most teeth have no lateral cusps, but inconspicuous lateral cusps are present on several teeth in the distal region (Fig. 24D, E). *Rhincodon* has no lateral cusps on any teeth (Fig. 24F). In most orectolobiforms, the medial cusp has sharp cutting edges (ced) on both sides (Fig. 25A). In *Brachaelurus, Chiloscyllium* and *Hemiscyllium*, the cutting edge is indistinct (Fig. 25B). In most orectolobiforms, the apron of the crown (apr) is broadly expanded labially. In *Brachaelurus*, it is more prominent, forming a stout process with abrupt concavities on the mesiodistal margins (Fig. 24A). In *Orectolobus, Eucrossorhinus* and *Sutorectus*, it is pointed, narrow, and greatly elongated labially (Fig. 24D, E).

10. Number of labial cartilages. Although Wu (1994) noted that *Hemiscyllium* and *Orectolobus* have four labial cartilages, all orectolobiform members examined in the present study have only three elements. Wu's judgement of a fourth labial cartilage may be based on the mistaken interpretation of the bending corner of the posterior upper labial cartilage as an isolated part. Thus, I treat the labial cartilages as containing three elements.

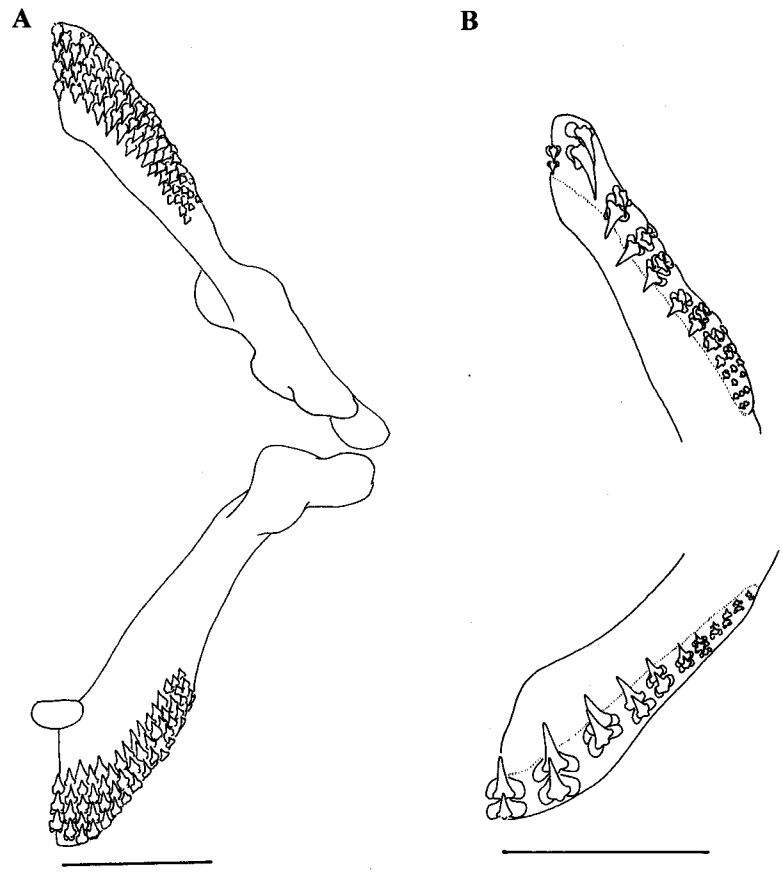

Fig. 23. Tooth arrangement on upper (above) and lower (below) jaws. (A) *Parascyllium ferrugineum* (HUMZ 131588); (B) *Orectolobus maculatus* (WAM P28414-001). Scales indicate 10 mm.

2-2. Hyoid arch

***General description* (*Fig. 18*)**

The hyoid arch of orectolobiforms is short and rather stout, consisting of the hyomandibula, ceratohyal, basihyal and prespiracular cartilage. There are branchial rays and extrabranchial cartilages supporting the anterior hemibranch of the first branchial chamber. The hyomandibula (hm) is short and robust, with two prominent, rounded processes forming articular condyles (hmc) for the cranio-hyomandibular articulation; the distal end is thick and globular-shaped, articulating with the mandibular knob at the anteroventral surface via a ligamentous complex (*ljs1-2*). The ceratohyal (ch) is long and broadly arched; the proximal end is simple or weakly concave, forming an articular condyle for the basihyal; the distal end is thick, globular-shaped, with a large articular fossa articulated with the hyomandibula via a long ligament (*lhy*). There is a prominent ridge providing an insertion of the constrictor hyoideus ventralis on the external surface of this cartilage. The basihyal (bh) is large and depressed; the posterior margin is broadly concave, and the posterolateral edge is deeply concave, forming a facet for the ceratohyal. The branchial rays (brh) are composed of a number of large, comb-like plates and elongated, rod-like plates, both of which articulate with the ceratohyal and/or hyomandibula. The extrabranchial cartilage (ech) is flattened, and located on the dorsolateral margin of the anterior hemibranch of the first branchial chamber. The prespiracular cartilage is composed of a small and thin cartilaginous plate located on the anterior wall of the spiracular cleft.

Morphological differences

1. Pharyngohyal (phy). In *Ginglymostoma* and *Stegostoma*, the posterior condyle of the hyomandibula is segmented, and completely divided into a single, rounded cartilage (Fig. 26A). Luther (1909a) recognized this cartilage of *Stegostoma* as pharyngohyal. In this study, this cartilage of *Ginglymostoma* is estimated homologous with the pharyngohyal of *Stegostoma*.

2. Ligamentum hyomandibulo-palatoquadrati (*lhp*). Orectolobiforms, except *Brachaelurus, Hemiscyllium* and *Chiloscyllium*, have a ligamentum hyomandibulo-palatoquadrati (*lhp*; Fig. 18).

3. Formation of branchial rays (brh). In most orectolobiforms, the largest two branchial rays, which articulate with the hyomandibula and ceratohyal, respec-

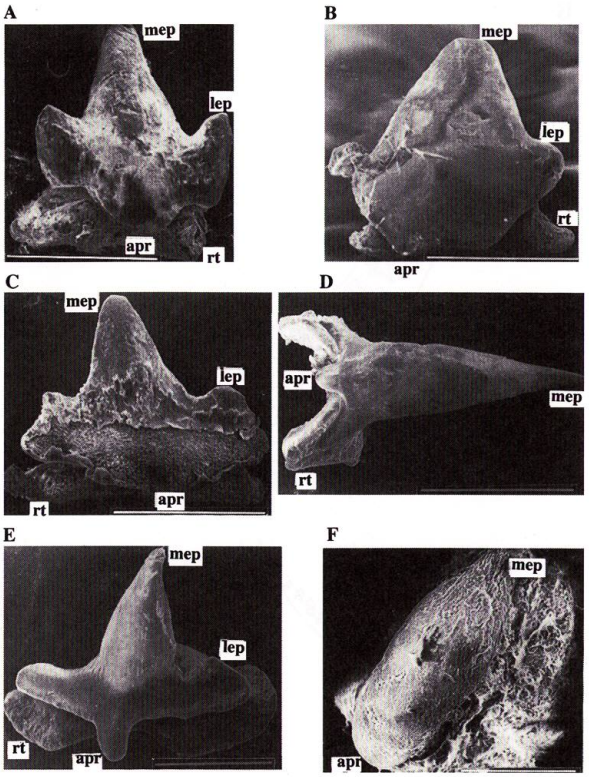

Fig. 24. Labial views of teeth near symphysis (A-D, F) and distal region (E). (A) *Brachaelurus waddi* (AMS I20095033); (B) *Chiloscyllium indicum* (MCZ 54); (C) *Ginglymostoma cirratum* (ZMUC P0629); (D-E) *Eucrossorhinus dasypogon* (CSIRO CA 4051); (F) *Rhincodon typus* (OA 00212). Scales indicate 500 μm in A-C and E-F, and 2 mm in D.

tively, are fused distally to form a completely continuous arch (Fig. 26A). In *Parascyllium* and *Cirrhoscyllium*, both cartilages are separate (Fig. 26B).

4. Extrabranchial cartilage on hyoid arch (ech). In *Eucrossorhinus* and *Ginglymostoma*, the extrabranchial cartilage is small and triangular, and completely isolated from the branchial rays (Figs. 18, 26A). In other orectolobiforms, it is fused with the distal end of some radials, forming a variously shaped expansion (Fig. 26B).

5. Prespiracular cartilage. In most orectolobiforms, the prespiracular cartilage is present, whereas it is absent in *Parascyllium* and *Cirrhoscyllium*.

2-3. Branchial arches

General description (*Fig. 27*)

The branchial arches of orectolobiforms contain five paired components forming four interbranchial septa and the last anterior hemibranch. According to Shirai (1992b), branchial arches 1-5 are identified as arches α, β1, β2, γ and δ, respectively, in order to compare with the taxa that have six or seven arches on the basis of the repeated structures in the β arches, and I follow his identification for comparison with the outgroups. Each consists of a pharyngobranchial, an epibranchial, ceratobranchial, a hypobranchial, and a basibranchial principally, and branchial rays and extrabranchials are inserted into each interbranchial septum. The pharyngobranchial (ph) is depressed and elongated posteromesially, with a triangular-shaped pharyngobranchial blade (pbb) on the posterolateral margin, and tightly attached with the vertebral centrum at the distal tip. The epibranchial (eb) is rather short and stout, with a depressed expansion (exe) connected with the anteriorly adjacent arch via a ligament, and a fenestra for the twigs of the branchial nerves on the external surface; the anteromesial end articulates with the pharyngobranchial. The last two pharyngobranchials and the last epibranchial are fused into a large, proximally bifurcated gill pickax (gpx). The ceratobranchial (cb) is greatly elongated, with a variously developed inner process (pr) on the medial margin in the first four arches; the distal end articulates with the epibranchial, and the anteromesial extremity articulates with the posterolateral end of the basihyal in arch α; with the hypobranchial in arches β and γ; with the basibranchial in arch δ. The hypobranchial (hb) is present in arches β and γ. It is rather feeble, extending anterolaterally, and articulated with the basibranchial mesially. The basibranchial (bb) is generally composed of a single, large cardiobranchial. The accessory cartilage (acc) is small and feeble, and articulated with the posterior end of the basibranchial. The branchial ray (br) is slender and elongated radially, usually articulated with both the epibranchial and the ceratobranchial in the anterior four arches, whereas it is remarkably small and oval-shaped, and articulated with the ceratobranchial in the last arch. The number of rays is generally four or more in the anterior four arches; one or a few in the last arch. The extrabranchial cartilage consists of dorsal and ventral elements marginating the interbranchial septa in the first four arches. The dorsal extrabranchial cartilage (exd) is slender, with a depressed, variously shaped expansion on the mesial end. The ventral extrabranchial cartilage (exv) is rather elongated and more or less expanding mesially.

Morphological differences

1. Gill pickax (gpx). In *Rhincodon*, the gill pickax is fused with epibranchial γ, and is weakly divided by an indistinct vestige (Fig. 28C).

2. Pre-epibranchial cartilage (pec). In *Orectolobus, Eucrossorhinus* and *Sutorectus*, there is an isolated and disc-shaped pre-epibranchial cartilage at the anterior end of the epibranchial α-β that replaces the expansion (exe) seen in other taxa (Fig. 28B).

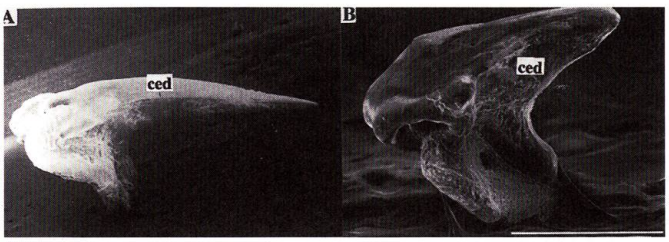

Fig. 25. Medial views of teeth near symphysis. (A) *Eucrossorhinus dasypogon* (CSIRO CA4051) ; (B) *Chiloscyllium indicum* (MCZ 54).

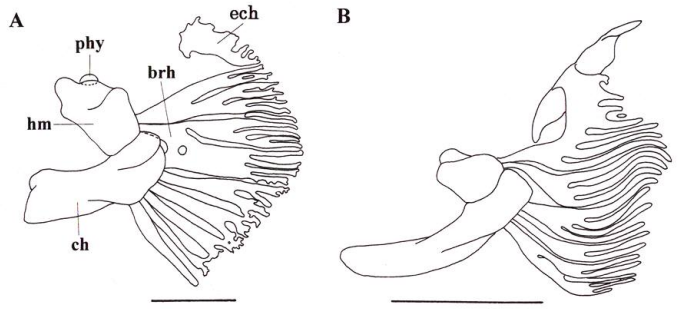

Fig. 26. External views of left hyoid arches. (A) *Ginglymostoma cirratum* (ZMUC P0629) ; (B) *Parascyllium collare* (AMS I30409002). Scales indicate 10 mm.

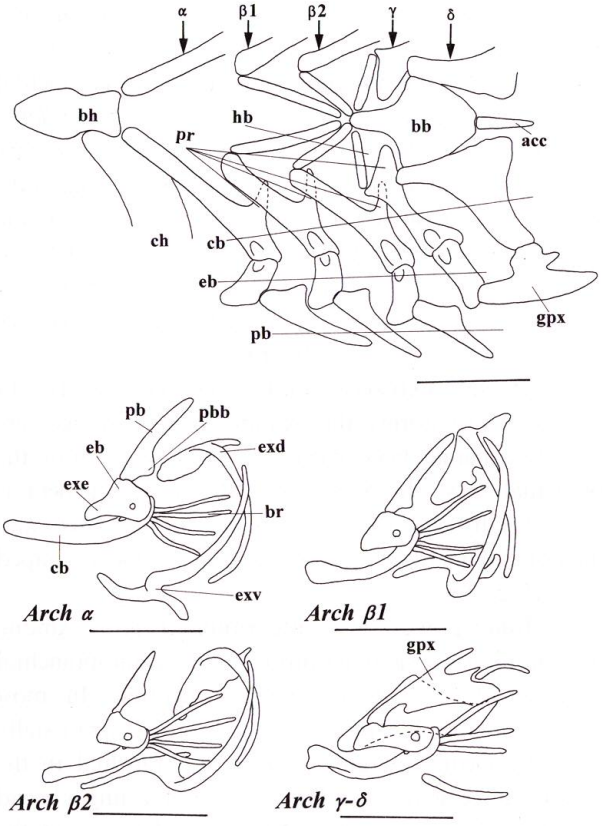

Fig. 27. Branchial arches of *Cirrhoscyllium japonicum* (HUMZ 40057) in dorsal view with entire elements unfolded (above), and in external view of each arch. Scales indicate 10 mm.

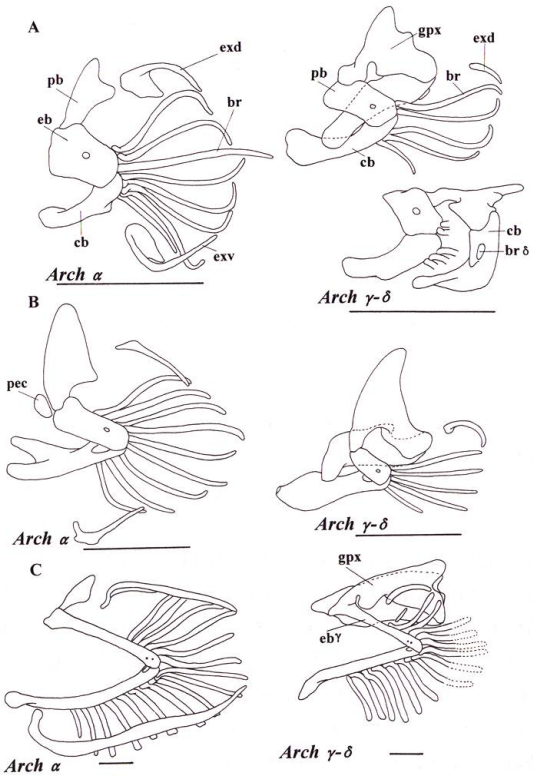

Fig. 28. External views of branchial arch α (left) and γ-δ (right). (A) *Chiloscyllium indicum* (MCZ 54) ; (B) *Orectolobus ornatus* (AMS I14236) ; (C) *Rhincodon typus* (OA 00212). Scales indicate 10 mm in A-B, and 100 mm in C.

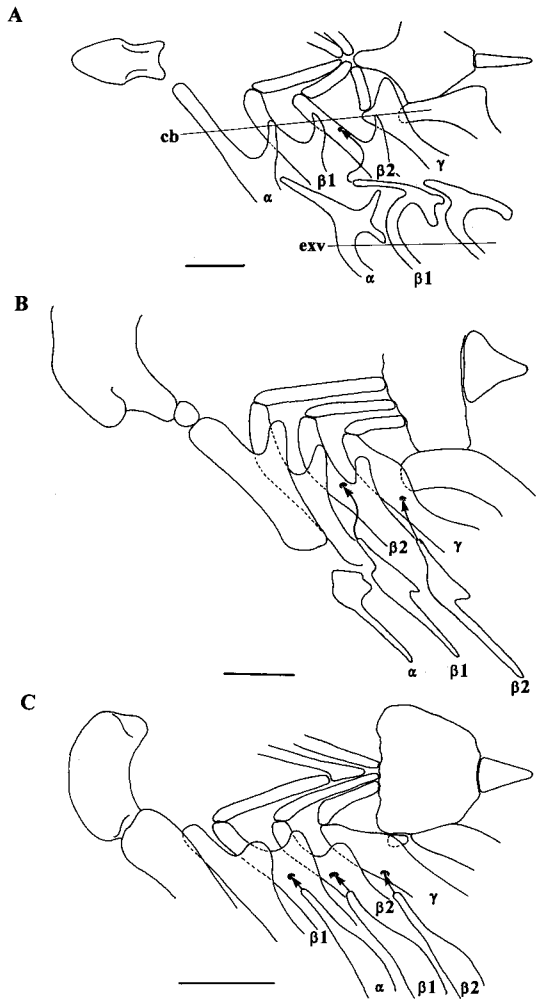

Fig. 29. Associations of extrabranchials with ceratobranchials in ventral view. (A) *Cirrhoscyllium japonicum* (HUMZ 40057); (B) *Eucrossorhinus dasypogon* (CSIRO CA 4051); (C) *Ginglymostoma cirratum* (ZMUC P0629). Scales indicate 10 mm.

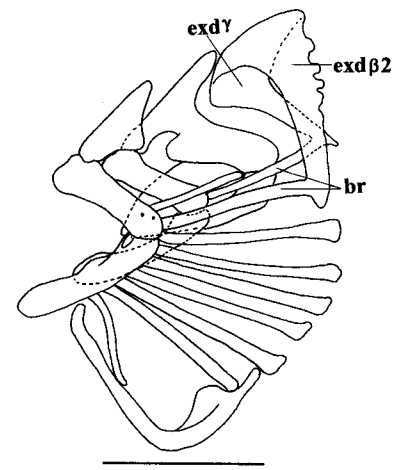

Fig. 30. External views of last three arches showing associations of dorsal extrabranchial $\beta 2$-γ and branchial rays in *Stegostoma varium* (HUMZ 78593). Scale indicates 10 mm.

3. Branchial rays (br). In *Parascyllium* and *Cirrhoscyllium*, the branchial rays of the anterior four arches articulate only with the ceratobranchial (Fig. 27). In most orectolobiforms, the rays articulate with both epibranchial and ceratobranchial (Fig. 28).

4. Branchial ray δ (brδ). In *Chiloscyllium, Hemiscyllium, Brachaelurus, Ginglymostoma* and *Stegostoma*, one or a few branchial rays are present on the ceratobranchial δ (Fig. 28A), whereas *Orectolobus, Sutorectus, Eucrossorhinus, Parascyllium, Cirrhoscyllium* and *Rhincodon* have no cartilaginous components on the ceratobranchial (Fig. 28B-C).

5. Ventral extrabranchial cartilage γ (exvγ). In most orectolobiforms, there is no extrabranchial cartilage on the ventral margin of the last interbranchial septum (Fig. 28), whereas *Parascyllium* and *Cirrhoscyllium* have a short, simple, and rod-shaped extrabranchial cartilage γ (Fig. 27).

6. Association of ventral extrabranchial cartilage (exv) with ceratobranchial (cb). Among orectolobiforms, the following three categories are found in the relationship between the ventral extrabranchial cartilage and ceratobranchial. In *Parascyllium* and *Cirrhoscyllium*, the ventral extrabranchial cartilage $\beta 1$ articulates with the ventral margin of the ceratobranchial $\beta 2$ at the mesial tip (Fig. 29A). In *Chiloscyllium, Hemiscyllium, Brachaelurus, Orectolobus, Eucrossorhinus* and *Sutorectus*, the ventral extrabranchial cartilages $\beta 1$-2 articulate with the ventral margins of the ceratobranchials $\beta 2$ and γ, respectively (Fig. 29B). In *Stegostoma, Ginglymostoma* and *Rhincodon*, the ventral extrabranchial cartilages α-$\beta 2$ articulate with the ceratobranchials $\beta 1$-γ, respectively (Fig. 29C).

7. Dorsal extrabranchial cartilages (exd). In most orectolobiforms, the extrabranchial cartilages are entirely separate from each other and also from the branchial rays. In *Stegostoma*, the dorsal element is fused distally with the branchial rays in each arch, and the last two are fused dorsally, forming a large, U-shaped plate (Fig. 30).

8. Inner process of ceratobranchial (pr). Among orectolobiforms, the inner process of the ceratobranchial is classified into the following categories. In most orectolobiforms, it is prominent, well projecting mesially from the medial margin of the ceratobranchial in the anterior three arches; and rather small, forming a broad expansion located on near the proximal region in the arch γ (Fig. 31A-B). In *Parascyllium* and *Cirrhoscyllium*, it forms a large, triangular-shaped plate well projecting mesially from the proximal region of ceratobranchial in the arch γ (Fig. 27). In *Rhincodon*, all

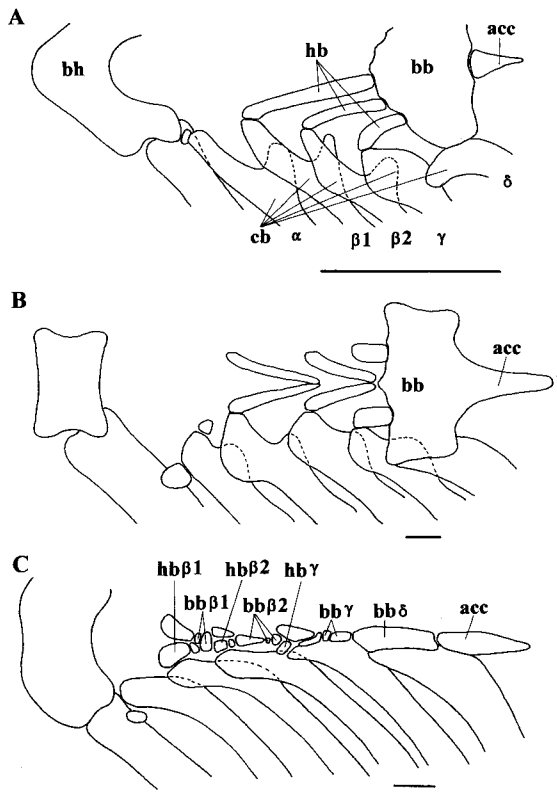

Fig. 31. Dorsal views of hypobranchial skeletons. (A) *Sutorectus tentaculatus* (WAM PI1938.001) ; (B) *Stegostoma varium* (HUMZ 78593) ; (C) *Rhincodon typus* (OA 00212). Scales indicate 10 mm in A-B, and 100 mm in C.

inner processes are greatly reduced, and slightly convex at the mesial margin of the proximal regions (Fig. 31C).

9. Shape of hypobranchial (hb). In most orectolobiforms, the hypobranchial is long and thin (Fig. 31A-B). In *Rhincodon*, it is extremely short, forming a small, irregular-shaped cartilaginous piece somewhat expanded distally (Fig. 31C).

10. Relationship between basibranchial (bb) and hypobranchial (hb). Among orectolobiforms, the relationship between basibranchial and hypobranchial is classified into the following categories. In most orectolobiforms, the basibranchial consists of a single cardiobranchial articulated with all hypobranchials in *Orectolobus, Eucrossorhinus* and *Sutorectus* (Fig. 31A) ; articulated with only hypobranchials β2-γ in the remaining taxa (Fig. 31B). In *Rhincodon*, it is segmented into isolated small cartilaginous pieces corresponding to each respective hypobranchial in arches β-γ, and an longitudinally elongated cardiobranchial in arch δ (Fig. 31C).

11. Accessory cartilage of basibranchial (acc). In most orectolobiforms, the accessory cartilage is isolated from the cardiobranchial (Fig. 31A, C). In *Chiloscyllium, Hemiscyllium, Brachaelurus* and *Stegostoma*, it is fused with the cardiobranchial forming a posteriorly directed projection (Fig. 31B).

3. Shoulder girdle and pectoral fin

General description (Figs. 32-34)

The shoulder girdle of orectolobiforms consists of a single, U-shaped seamless scapulo-coracoid cartilage. The scapular (sc) is cylindrical, extending vertically or inclining posteriorly. The suprascapular cartilage (ssc) is present or absent. If present, it is small and oval, and articulates with the head of the scapular. The coracoid (cor) is depressed and extends transversely. The medial region of the coracoid is usually expanded anteriorly to form an apron (apc) supporting the ventral wall of the pericardial cavity. The articular condyle (pcc) for the pectoral basals is oval and strongly convex, and located on the lateral end of the coracoid. The fossa for the depressor pectoralis (exp) is formed anteroventral to the articular condyle. The process for the levator pectoralis (pcp) is prominent and conical, and located behind the articular condyle. A canal for the pectoral nerves and the brachial artery (cpn) opens anteriorly below the articular condyle, and posteriorly above the process for the levator pectoralis. The pectoral fin skeleton is composed of basal cartilages and numerous radials. The basal cartilages basically consist of the propterygium, mesopterygium and metapterygium. The propterygium (prp) is rather short and depressed, bearing a few small and plate-like radials. The mesopterygium (msp) is the largest, and well expanded distally. The metapterygium (mtp) is elongated, forming a roundly expanded distal end, with or without a small metapterygial axis (mtx) on its distal tip. The pectoral radials (rdc) are segmented into elongated proximal and rather shortened medial and distal elements basically.

Morphological differences

1. Suprascapular cartilage (ssc). The suprascapular cartilage is found in *Chiloscyllium, Hemiscyllium, Ginglymostoma, Stegostoma* and *Rhincodon*, whereas it is absent in the remaining genera (Fig. 32).

2. Apron of coracoid (apc). In most orectolobiforms, the anterior margin of the coracoid is depressed and more or less expanded anteriorly to form an apron (Fig. 32B-C). In *Orectolobus, Eucrossorhinus* and *Sutorectus*, the dorsal surface of this cartilage is somewhat depressed, but no such expansion appears (Fig. 32A). In *Rhincodon* and *Ginglymostoma*, there is a greatly expanded apron with a rounded fenestra on the medial region (fco ; Fig. 32B).

3. Foramen for brachial artery (fbr). In *Chiloscyllium* and *Hemiscyllium*, the foramen for the brachial

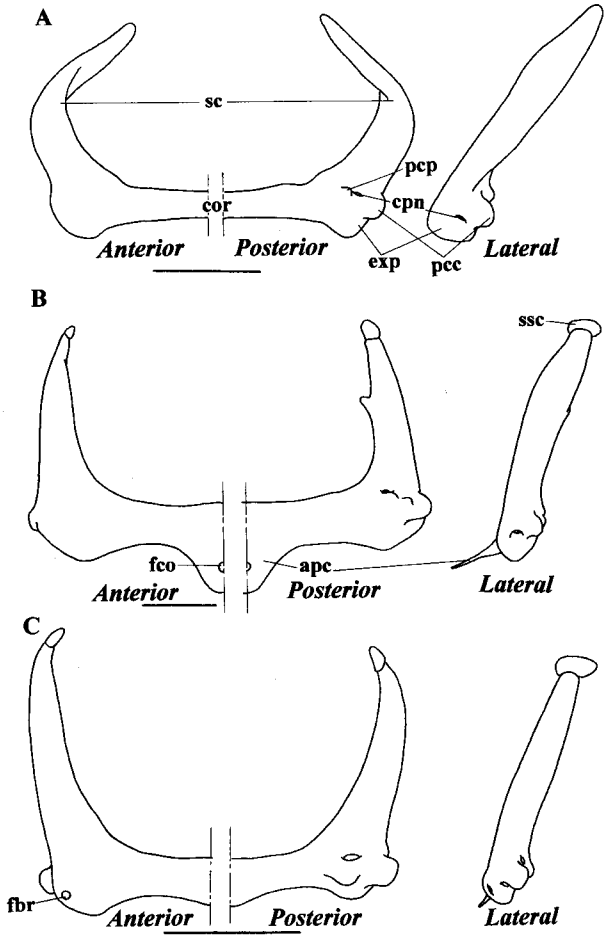

Fig. 32. Pectoral girdle in anterior (left), posterior (middle) and lateral (right) views. (A) *Eucrossorhinus dasypogon* (CSIRO CA 4051); (B) *Ginglymostoma cirratum* (ZMUC P0629); (C) *Hemiscyllium ocellatum* (HUMZ 119336). Scales indicate 10 mm.

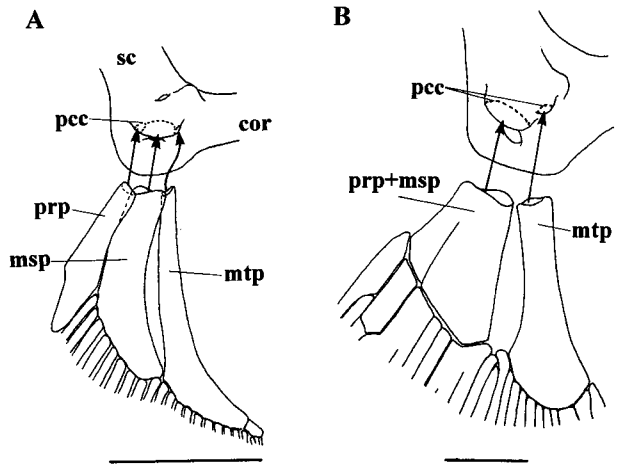

Fig. 33. Articulations of pectoral basal cartilages with pectoral girdle. (A) *Eucrossorhinus dasypogon* (CSIRO CA 4051); (B) *Ginglymostoma cirratum* (ZMUC P0629). Scales indicate 10 mm.

artery penetrates the fossa for the depressor pectoralis muscle longitudinally (Fig. 32C).

4. Articular condyle of coracoid (pcc). Among orectolobiforms, the number of articular condyles is classified into two categories. In most orectolobiforms, there is a single condyle articulating with all basal cartilages (Fig. 33A). In *Ginglymostoma, Stegostoma* and *Rhincodon*, there are two condyles: the anterior condyle is large and oval, and articulates with the propterygium and mesopterygium; the posterior is small and blunt, and articulates with the metapterygium (Fig. 33B).

5. Pectoral basal cartilages. Among orectolobiforms, the pectoral basal cartilages are classified into the following categories. In *Orectolobus, Eucrossorhinus, Brachaelurus* and *Chiloscyllium* except *C. indicum*, the propterygium, mesopterygium and metapterygium are divided into three isolated cartilages, i.e., propterygium (prp), mesopterygium (msp) and metapterygium (mtp) (Fig. 34A-B). In *Sutorectus, C. indicum, Hemiscyllium, Ginglymostoma, Stegostoma* and *Rhincodon*, the propterygium and mesopterygium are apparently fused into a single cartilage, but both components are clearly distinguished by a distinct fissure located at their distal regions (Fig. 34C-E). In *Parascyllium* and *Cirrhoscyllium*, there are two cartilages: the anterior cartilage is large and broadly arched posteriorly, with no fissure at its distal region; the posterior one is rather elongated, forming a rounded expansion at the distal end (Fig. 34F). Compagno (1988) pointed out that these two cartilages should be equivalent to the mesopterygium and metapterygium, respectively, and the propterygium is considered lost. Recently, Shirai (1992a) considered as ambiguous this interpretation of whether it is the mesopterygium or is a fused cartilage of the propterygium and mesopterygium. The present study follows Shirai's treatment for this character as ambiguous (?) because of lack of the consistent identification of this element.

6. Metapterygium (mtp). In most orectolobiforms, the metapterygium articulates with the posterior surface of the articular condyle of the coracoid. In *Sutorectus*, it has no association with the coracoid, and articulates with the proximal region of the mesopterygium (Fig. 34C).

7. Development of metapterygial axis (mtx). In most orectolobiforms, the metapterygial axis is indistinguishable from the adjacent branchial rays (Fig. 34B, D-F). In *Orectolobus* except *O. maculatus, Eucrossorhinus, Sutorectus* and *Rhincodon*, there is a short cartilage somewhat stouter than the adjacent radials on the distal tip of the metapterygium. It articulates with

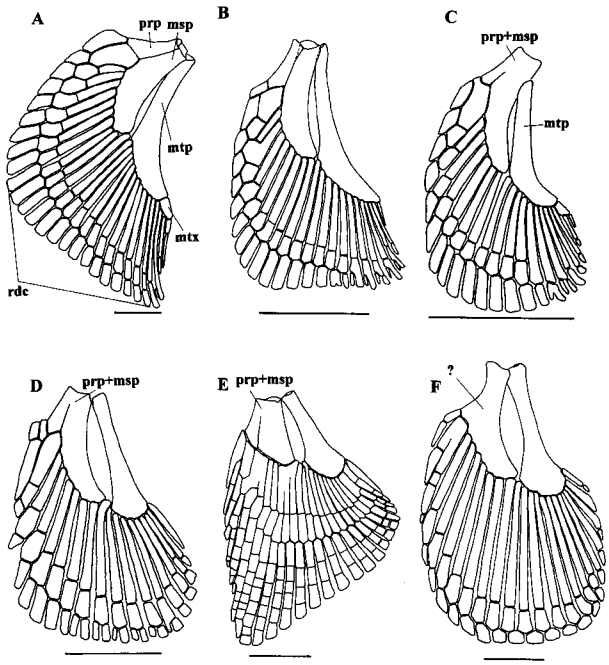

Fig. 34. Dorsal views of pectoral fin skeletons. (A) *Eucrossorhinus dasypogon* (CSIRO CA 4051); (B) *Orectolobus maculatus* (WAM P28414-001); (C) *Sutorectus tentaculatus* (WAM PI1938.001); (D) *Chiloscyllium indicum* (MCZ 54); (E) *Ginglymostoma cirratum* (ZMUC P0629); (F) *Parascyllium ferrugineum* (HUMZ 131588). Scales indicate 10 mm.

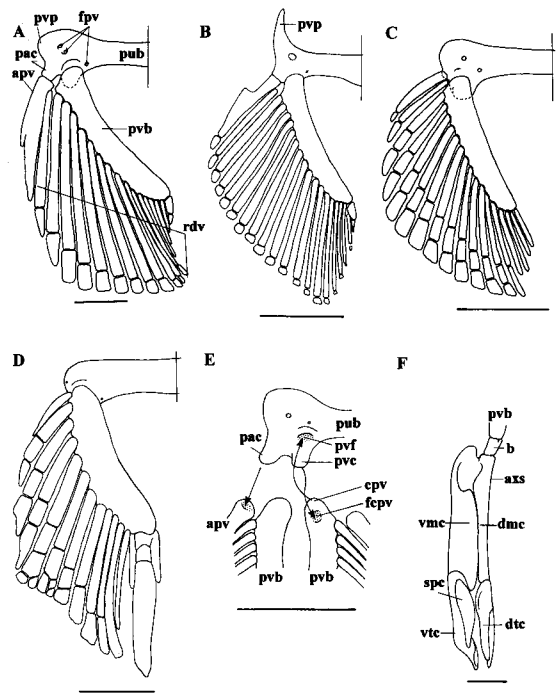

Fig. 35. Pelvic girdle and associated skeletons in ventral view (A-D), articulation of pelvic fin skeleton with pelvic girdle (E) and dorsal view of clasper skeleton (F). (A) *Chiloscyllium punctatum* (HUMZ 6139); (B) *Parascyllium collare* (AMS 130409002); *Ginglymostoma cirratum* (ZMUC P0629); *Hemiscyllium ocellatum* (HUMZ 119336); (F) *Chiloscyllium hasselti* (HUMZ 109476). Scales indicate 10 mm.

two or more rows of radials on its lateral and distal margins (Fig. 34A, C).

8. Number of pectoral radials (rdc). In most orectolobiforms, the pectoral radials are principally composed of three components (Fig. 34A-D, F). In *Ginglymostoma, Rhincodon* and *Stegostoma*, the distal radials are segmented into numerous (up to 10) cartilaginous pieces (Fig. 34E).

9. Extension of pectoral radials (rdc). In most orectolobiforms, the pectoral radials are short, with long ceratotrichia distally, aplesodic style. In *Rhincodon*, these are greatly extending distally towards near the fin margin, plesodic style. In *Ginglymostoma* and *Stegostoma*, these are elongated but not extending to the fin margin, which represents the intermediate condition between both styles.

4. Pelvic girdle and fin, and clasper

General description (Fig. 35)

The puboischiadic bar (pub) is simple and somewhat depressed, with a depressed floor, on which several foramina for the pelvic nerves (fpv) open ventrally, on the lateral end. The anterolateral margin of the floor is more or less expanded, representing the prepelvic process (pvp), with an articular condyle (pvc) and a facet (pvf) for the pelvic basipterygium on the posterior margin. The posterolateral margin of the floor is more or less projected posterolaterally, forming a granulated condyle (pac) for the anterior pelvic basal. The pelvic basipterygium (pvb) is stout, broadly arched mesially, with numerous pelvic radials on its lateral margin. The proximal end has a granulated condyle (cpv) and a shallow facet (fcpv), which articulate with the articular condyle and facet of the puboischiadic bar, respectively. The pelvic radials (rdv) are basically divided into an elongated, slender proximal element and a short, square-shaped distal element. The anteriormost radial is somewhat larger than the adjacent radials, and articulates directly with the puboischiadic bar, termed the anterior pelvic basal (apv). In males, the basipterygium supports the clasper cartilages at the posterior end. The clasper cartilages of orectolobiforms consist of the joint cartilage, stem cartilage, dorsal and ventral terminal cartilages, spur, and hook. The joint cartilages (b) are composed of one or two small segments, with no beta cartilage. The stem cartilage (axs) is extremely large, and broadly covering the ventral margin of clasper. The mesial and lateral margins of the stem are well expanded dorsally, forming dorsal marginal (dmc) and

ventral marginal (vmc) cartilages. The dorsal terminal cartilage (dtc) is slender and tapering distally, and originates from the distal tip of the dorsal marginal cartilage. The ventral terminal cartilage (vtc) is somewhat depressed and tapering distally, and originates from the distal tip of the ventral marginal cartilage. The spur (spc) is small and tapering distally, and articulates with the ventral terminal cartilage.

Morphological differences

1. Prepelvic process (pvp). In most orectolobiforms, the prepelvic process is reduced, and rounded or bluntly pointed (Fig. 35A, C-D). In *Parascyllium* and *Cirrhoscyllium*, it is projected well anteriorly and is strongly pointed distally (Fig. 35B).

2. Anterior pelvic basal (apv). Most orectolobiforms have a single anterior pelvic basal. It is slender and simple in *Ginglymostoma* and *Stegostoma* (Fig. 35C); somewhat stout and distally subdivided into a few branches in *Chiloscyllium* and *Hemiscyllium* (Fig. 35A); and depressed and more or less expanded distally in *Parascyllium, Cirrhoscyllium, Orectolobus, Sutorectus, Eucrossorhinus* and *Brachaelurus* (Fig. 35B). *Rhincodon* has neither the anterior pelvic basal nor its articular condyle on the puboischiadic bar (Fig. 35D).

3. Number of pelvic radials. In most orectolobiforms, the pelvic radials consist of two elements (Fig. 35A-B). In *Ginglymostoma, Stegostoma* and *Rhincodon*, these are segmented into three elements (Fig. 35C-D).

5. Dorsal and anal fins

General description (Fig. 36)

Dorsal and anal fins of orectolobiforms are basically supported by the set composed of a basal cartilage and two radials, arranged longitudinally. In the dorsal fin (Fig. 40A-B), the basal cartilage (bd) is slender and elongated, lying on the midline between the epaxial body muscles. It originates from the completely separated region from the head of the neural arch. The distal end is more or less expanded, with a small facet for the proximal radial on the dorsal margin. The radial (rd) consists of a slender, elongated proximal element and a short, distally tapering distal one. In the anal fin (Fig. 40C), the basal cartilage (ba) is reduced compared with that of the dorsal fin. It is short, rounded, and occurring on the distal region of the midline between the hypaxial body muscles. The radial (rd) consists of two elements similar to those of the dorsal fin, but are feeble compared with those of the dorsal fin.

Morphological differences

1. Basal cartilages of dorsal fin (bd). Among orectolobiforms examined here, the following five variations are found in the basal cartilages of the dorsal fin. 1) All cartilages are simple and completely separate in *Eucrossorhinus*, and the second dorsal fin of one specimen (HUMZ 37689) of *Chiloscyllium plagiosum* examined in the present study (Fig. 36B). 2) Anteriorly, some cartilages are fused, with several anteriormost radials in *Orectolobus, Sutorectus* and *Brachaelurus* (Fig. 37A). 3) Posteriorly, some cartilages are fused,

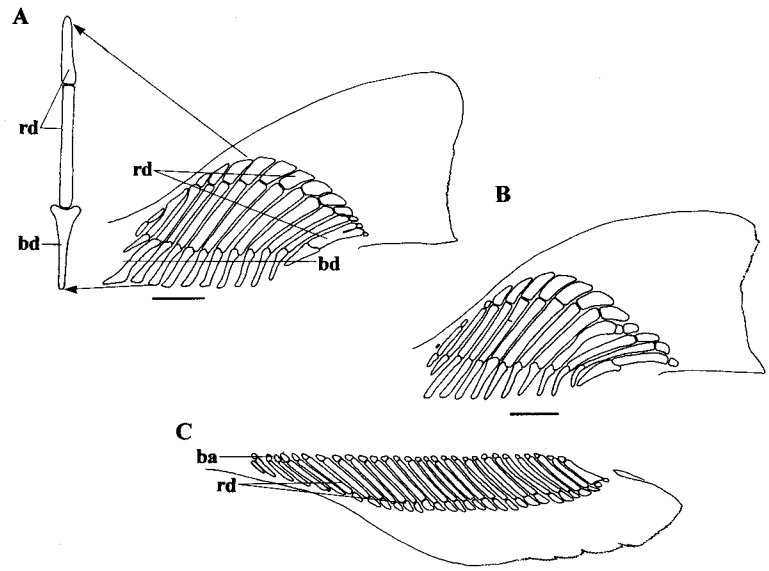

Fig. 36. Endoskeletons of dorsal and anal fins in *Chiloscyllium plagiosum* (HUMZ 37689). (A) Lateral view of first dorsal fin and anterior view of fourth set; (B) lateral view of second dorsal fin; (C) lateral view of anal fin. Scales indicate 10 mm.

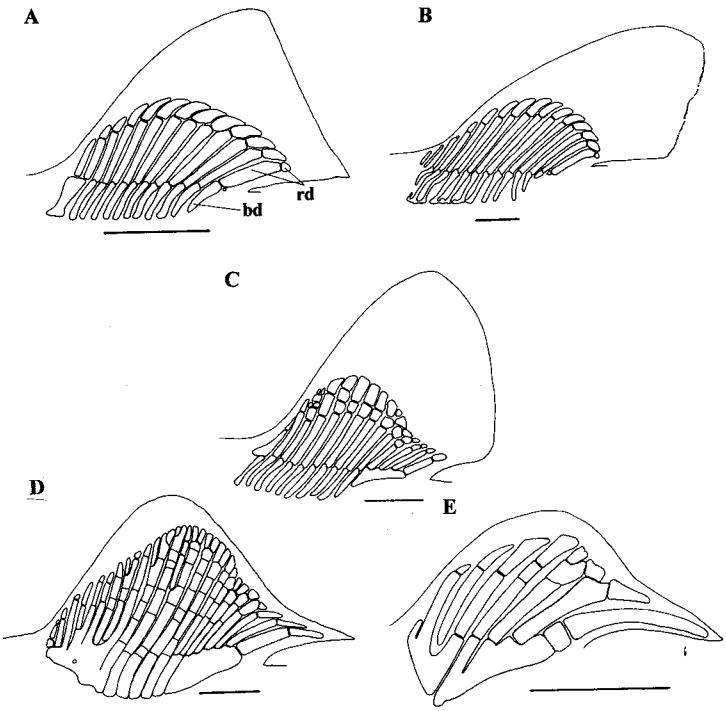

Fig. 37. Endoskeletons of dorsal fin. (A) First dorsal fin of *Orectolobus japonicus* (HUMZ 116361); (B) first dorsal fin of *Parascyllium ferrugineum* (HUMZ 131588); (C) first dorsal fin of *Ginglymostoma cirratum* (ZMUC P0629); (D) first dorsal and (E) second dorsal fins of *Rhincodon typus* (OA 00212). Scales indicate 10 mm in A-C, and 100 mm in D and E.

with several posteriormost radials in most examined individuals of *Chiloscyllium*, and *Hemiscyllium, Ginglymostoma* and *Stegostoma* (Figs. 36A, 37C). 4) Some approximate cartilages are fused only at the proximal ends in *Parascyllium* and *Cirrhoscyllium* (Fig. 37B). 5) Many cartilages are fused into a large cartilaginous plate in *Rhincodon* (Fig. 37D-E).

2. Number of dorsal fin radials (rd). The radial set of most orectolobiforms consists of two cartilages in both dorsal fins (Figs. 36A-B, 37A-B), whereas it is divided into three or more segments in *Ginglymostoma, Stegostoma* and *Rhincodon* (Fig. 37C-E).

3. Basal cartilages of anal fin (ba). In most orectolobiforms, the basal cartilages are composed of small, rounded, cartilaginous pieces (Figs. 36C, 38A-B). In *Rhincodon*, these are fused into a large, single cartilaginous plate carrying all radials (Fig. 38C).

4. Number of anal fin radials (rd). The radial set of most orectolobiforms consists of two cartilages in the anal fin (Figs. 36C, 38A), whereas it is divided into three segments in *Ginglymostoma, Stegostoma* and *Rhincodon* (Fig. 38B-C).

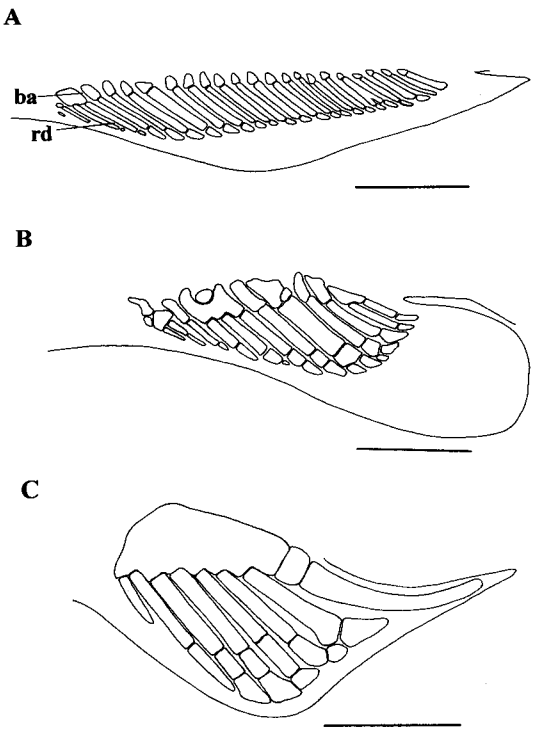

Fig. 38. Endoskeletons of anal fin. (A) *Cirrhoscyllium japonicum* (HUMZ 40057); (B) *Ginglymostoma cirratum* (ZMUC P0629); (C) *Rhincodon typus* (OA 00212). Scales indicate 10 mm in A and C, and 100 mm in C.

6. Vertebrae and caudal fin

General description (Figs. 39, 40)

Vertebrae are principally divided into abdominal

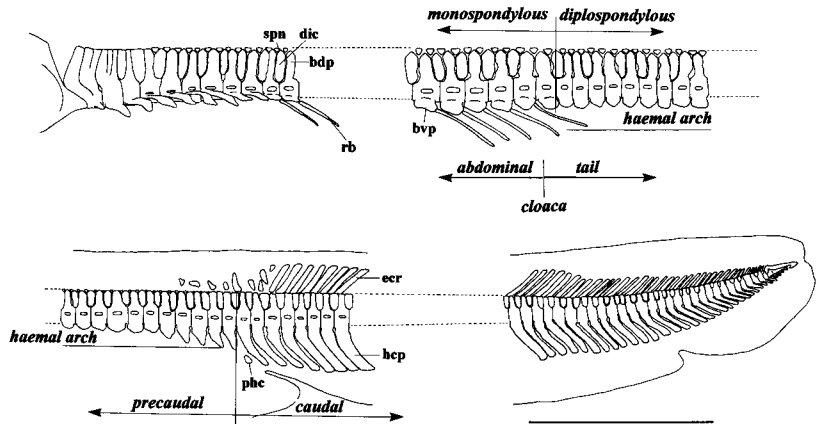

Fig. 39. Vertebrae and caudal skeleton in *Hemiscyllium freycineti* (CAS I26798). Scale indicates 10 mm.

vertebrae (*abdominal*) anterior to the cloaca, with no hemal arch; precaudal tail vertebrae (*tail, precaudal*) from the cloaca to the origin of the lower caudal fin, with incomplete hemal arch except for the posteriormost a few vertebrae in general, and caudal vertebrae (*caudal*) located in the dorsal lobe of the caudal fin entirely. The first two portions are differently divided into monospondylous (*monospondylous*) vertebrae, lying only one condyle in a single myotome, with a pair of vertebral ribs, and diplospondylous vertebrae (*diplospondylous*), lying two condyles in a single myotome, without vertebral ribs in general. The neural arch is composed of the basidorsal process, dorsal intercalary plate and supraneural. The basidorsal process (bdp) is calcified or chondrified, and expands dorsally to fuse with the antimere at the dorsal end. The dorsal intercalary plate (dic) is calcified or chondrified, and inserted between immediate basidorsals. The supraneural (spn) is extremely small and oval-shaped, and articulated with the head of the intermediate region between the basidorsal and intercalary plates in the precaudal and in some anterior caudal vertebrae. The vertebral centrum is cylindrical, and subdivided into the notochordal sheath and intermedialia. The notochordal sheath (nsh) composed of a double cone and an outer zone. The double cone (dbc) is calcified, forming a concentric inner wall surrounding the remains of the notochord. The outer zone (ozc) is a thick layer surrounding the double cone, with or without secondary calcified lamellae (scl) extending radially from the rim of the double cone. The intermedialia (imd) is thin, calcified superficially, and inconspicuously bordered by the membrana elastica externa (mee). The basiventral process (bvp) is chondrified, expanding laterally to support the dorsal wall of the body cavity in the abdominal region; expanding ventrally to form a complete or incomplete hemal arch in the tail. The vertebral rib (rb) is thin and elongated, and articulated with the basiventral process in most monospondylous vertebrae. In the posterior region, it is inserted into the horizontal septum formed between the epaxial and hypaxial body muscles. The epichordal radial (ecr) is small and feeble, lying on the dorsal rim of the neural arch in the upper caudal lobe. The basiventral process is fused to form a complete hemal arch, and extends ventrally as a large, compressed hypochordal process (hcp). In some anterior caudal vertebrae, the hypochordal processes are separated from the basiventral process, forming prehypochordal cartilages (phc).

Morphological differences

1. Neural arch. In most orectolobiforms, the neural arch is composed of completely segmented basidorsal process (bdp), dorsal intercalary plate (dic) and supraneural (spn) (Fig. 41A-C). In *Rhincodon*, the basidorsal process and dorsal intercalary plate are partly fused, entirely forming a large, seamless neural arch (Fig. 41D).

2. Calcification of neural arch. In most orectolobiforms, the neural arch, basidorsal process and dorsal intercalary plate are well calcified in adults. In *Rhincodon* and *Stegostoma*, these remain chondrified even in adults.

3. Secondary calcification pattern. Among orectolobiforms, the following four categories are found, depending upon the classification by Ridewood (1921). In most taxa, eight calcified lamellae are primarily extending radially from the rim of the double cone. In *Chiloscyllium, Hemiscyllium, Stegostoma* and *Ginglymostoma*, these calcified lamellae extend to the membrane elastica externa (mee) (Figs. 40, 41C). In *Orectolobus, Sutorectus, Eucrossorhinus* and *Brachaelurus*, they are not extending to the membrana elastica externa (Fig. 41A). In *Parascyllium* and *Cirrhoscyllium*, no calcification area is present into the outer zone (Fig. 41B). In *Rhincodon*, the chondrified basidorsal and basiventral insert deeply into the outer zone to the

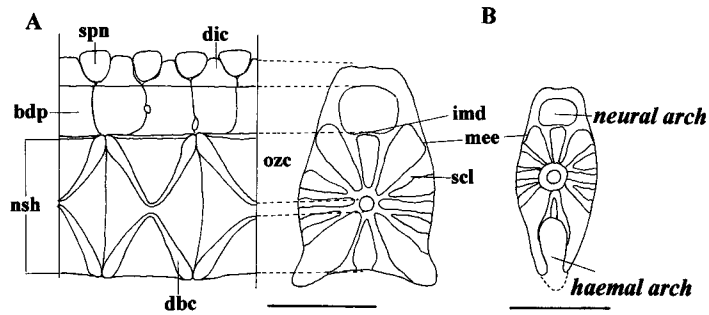

Fig. 40. Sections of vertebrae in *Chiloscyllium plagiosum* (HUMZ 37689). (A) Vertical (left) and transverse (right) section of abdominal vertebra; (B) transverse section of precaudal tail vertebra. Scales indicate 10 mm.

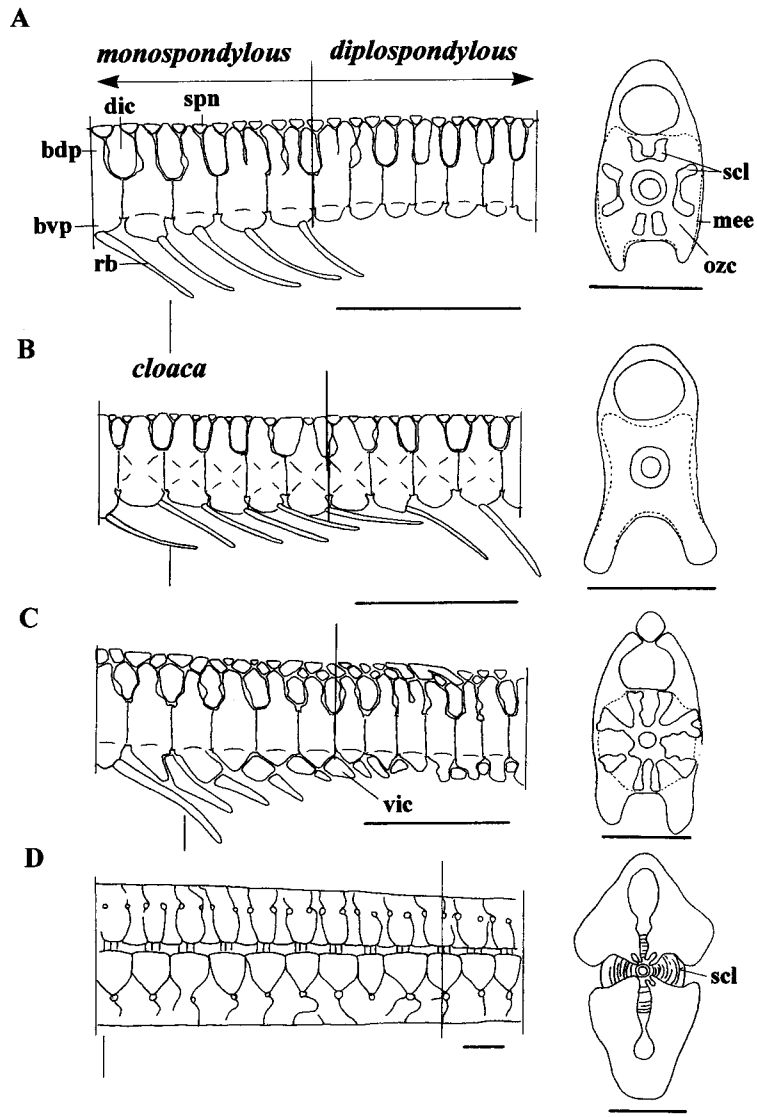

Fig. 41. Lateral views of vertebrae near cloaca (left) and transverse section of vertebral centrum showing secondary calcification pattern (right). (A) *Brachaelurus waddi* (AMS I20095033); (B) *Cirrhoscyllium japonicum* (HUMZ 40057); (C) *Ginglymostoma cirratum* (ZMUC P0629); (D) *Rhincodon typus* (OA 00212). Scales indicate 10 mm in A-C, and 100 mm in D.

double cone, and a number of thin concentric calcified layers are placed in the outer zone (Fig. 41D), and are equivalent to the concentric type in *Cetorhinus* (Ridewood, 1921).

4. Ventral intercalary plate (vic). The ventral intercalary plate is found only in *Ginglymostoma, Stegostoma* and *Rhincodon* (Fig. 41C-D). Among these taxa, it is partly fused with the basiventral process, forming a large, weakly segmented cartilaginous process in *Rhincodon* (Fig. 41D).

5. Hemal arch formation. Most orectolobiforms have the ventrally opened hemal arches in most precaudal tail vertebrae (Figs. 39, 40, 41A). In *Rhincodon*, the tail vertebrae consist of those with completely closed hemal arches (Fig. 41D). *Parascyllium, Cirrhoscyllium* and *Stegostoma* have hemal arches partly closed via a thin cartilaginous bar extending along the midline in some vertebrae anterior to the origin of the caudal vertebrae (Fig. 42B).

6. Vertebral ribs on diplospondylous vertebrae (rb). Most orectolobiforms have no vertebral ribs on diplospondylous vertebrae (Fig. 41A). In *Parascyllium, Cirrhoscyllium, Orectolobus, Sutorectus* and *Eucrossorhinus*, a few to more than 10 additional vertebral ribs are present on some anterior diplospondylous vertebrae (Fig. 41B). Each rib on the diplospondylous vertebra articulates with one basiventral process against two vertebrae.

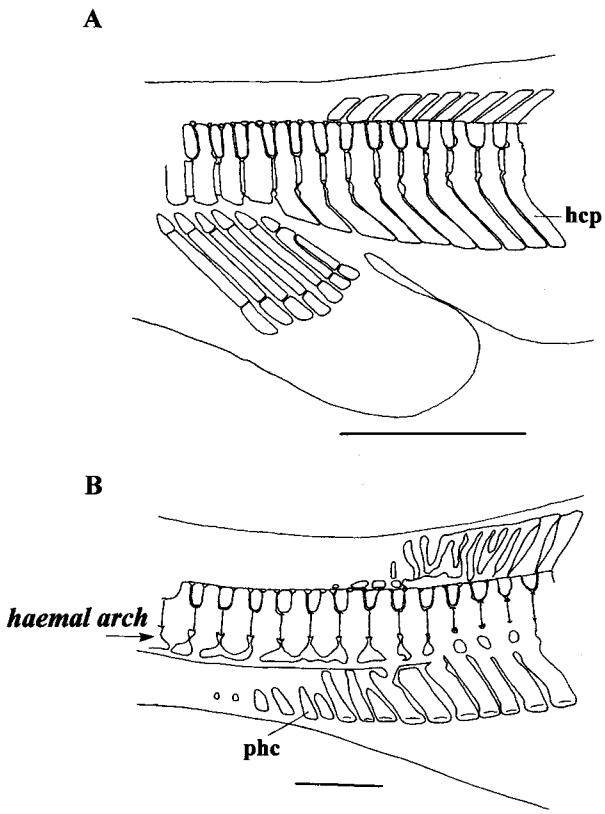

Fig. 42. Lateral views of anterior parts of caudal fins. (A) *Orectolobus ornatus* (AMS I14236); (B) *Parascyllium ferrugineum* (HUMZ 131588). Scales indicate 10 m.

7. Prehypochordal cartilage (phc). In *Hemiscyllium freycineti, Parascyllium* and *Cirrhoscyllium*, one or some prehypochordal cartilages (phc) are present (Figs. 39, 42B).

8. Hypochordal process (hcp). In most orectolobiforms, the hypochordal process is almost equal in size and shape in the anterior region, and is gradually reduced posteriorly in size, without segments entirely (Figs. 39, 42). In *Rhincodon*, some hypochordal processes are greatly elongated and segmented to broadly support the lower caudal lobe (Goto and Nishida, 2001).

7. Musculature on neurocranium

7-1. Oculomotor musculature

General description (Fig. 43)

The oculomotor musculature basically consists of two obliquus and four rectus muscles. The obliquus superior (oqs) is innervated by the trochlear nerve IV, originates from the anterior region of the orbit, and inserts onto the dorsal surface of the eyeball. The obliquus inferior (oqi) is innervated by the oculomotor nerve III, originates from the anterior region of the orbit, and inserts onto the ventral surface of the eyeball. The rectus inferior (rif) originates from the interorbital wall posterior to the eyestalk, and inserts onto the ventral surface of the eyeball. The rectus superior (rsp) originates from the interorbital wall anterior to that of the rectus inferior, and inserts onto the dorsal surface of the eyeball. The rectus internus (rit) originates from the interorbital wall above that of the rectus superior, and inserts onto the anterior surface of the eyeball. The rectus externus (rex) originates from the interorbital wall posterior to that of the rectus internus, and inserts onto the posterior surface of the eyeball. The rectus muscles except the rectus externus, which is supplied by the abducens nerve VI, are innervated by the oculomotor nerve III.

Morphological differences

1. Origins of obliquus muscles. In most orectolobiforms, the obliquus superior and inferior are well separated, and originate from the interorbital wall (Fig. 43). In *Ginglymostoma, Stegostoma* and *Rhincodon*, these muscles originate closely from the anterior tip of the supraorbital blade (Fig. 44). Among them, the following two types are included: both muscles not crossed in *Ginglymostoma* (Fig. 44A); both crossed, i.e., the obliquus superior originating just anterior to the

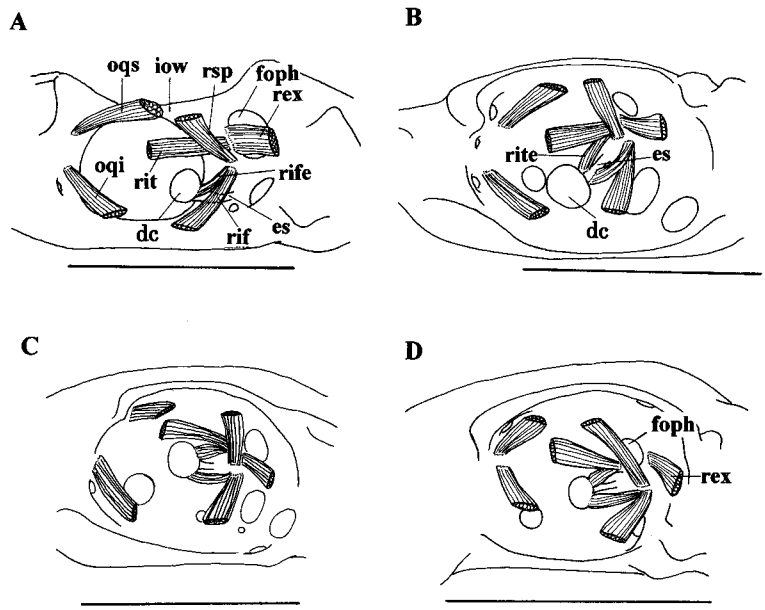

Fig. 43. Lateral views showing oculomotor musculature in four orectolobiforms. (A) *Parascyllium collare* (AMS I30409002); (B) *Orectolobus ornatus* (AMS I14236); (C) *Brachaelurus waddi* (AMS I20095033); (D) *Hemiscyllium trispeculare* (SI 0603.008). Scales indicate 10 mm.

other in *Stegostoma* and *Rhincodon* (Fig. 44B).

2. Origins of rectus muscles. In most orectolobiforms, the rectus muscles originate individually from the interorbital wall (Fig. 43). In *Ginglymostoma* and *Stegostoma*, these originate in a single muscle bundle, and are divided into each bundle distally (Fig. 44A). In *Rhincodon*, these originate in a single, greatly elongated tendon, and are divided into each muscle bundle distally (Fig. 44B).

3. Origin of rectus externus (rex). In most orectolobiforms, the rectus externus originates from the interspace between the eyestalk and the foramen for the ophthalmicus nerve branches (Fig. 43A-C). In *Hemiscyllium* and *Chiloscyllium*, it originates from just posterior to that foramen (Fig. 43D).

4. Extra bundle of rectus inferior (rife). In all orectolobiforms, there is an extra bundle of the rectus inferior that is classified into the following categories depending on its origin and insertion. It originates from the interorbital wall close to the rectus inferior in most orectolobiforms (Figs. 43, 44A); from the interorbital wall and additionally from the tendon for all the rectus muscles in *Rhincodon* (Fig. 44B). The insertion of this muscle is the posterodorsal rim of the disc on eyestalk in *Parascyllium, Cirrhoscyllium, Brachaelurus, Hemiscyllium* and *Chiloscyllium* (Fig. 43A, C-D); and the stem of the eyestalk in *Orectolobus, Sutorectus, Eucrossorhinus, Ginglymostoma, Stegostoma* and *Rhincodon* (Figs. 43B, 44).

5. Extra bundle of rectus internus (rite). In the orectolobiforms except *Parascyllium* and *Cirrhoscyllium*, there is an extra bundle of the rectus internus located symmetrically against the extra bundle of the rectus inferior (Figs. 43, 44). It is classified into the same categories with the extra bundle of the rectus inferior.

7-2. Musculature in parietal fossa

***General description* (*Fig. 45*)**

There is only the muscle parietalis (par) in the endolymphatic fossa. It usually originates from the fascia of the epaxial body muscle near the lateral rim of the fossa, and inserts onto the endolymphatic duct.

Morphological differences

1. Muscle parietalis (par). The muscle parietalis is known in most orectolobiform taxa, whereas there is no such element in *Parascyllium* and *Cirrhoscyllium*.

2. Extra bundle of muscle parietalis (pare). In most orectolobiforms, the muscle parietalis is composed of a single, small muscle bundle (Fig. 45A). In *Stegostoma*, there is an extra bundle of the muscle parietalis that originates from the anterolateral surface of the endolymphatic fossa and inserts on the anterior corner of the endolymphatic duct (Fig. 45B).

8. Musculature of visceral arches

8-1. Musculature on mandibular arch

***General description* (*Figs. 46-49*)**

In orectolobiforms, the musculature associated with the mandibular arch consists of the adductor mandibulae, suborbitalis, constrictor dorsalis, spiracularis,

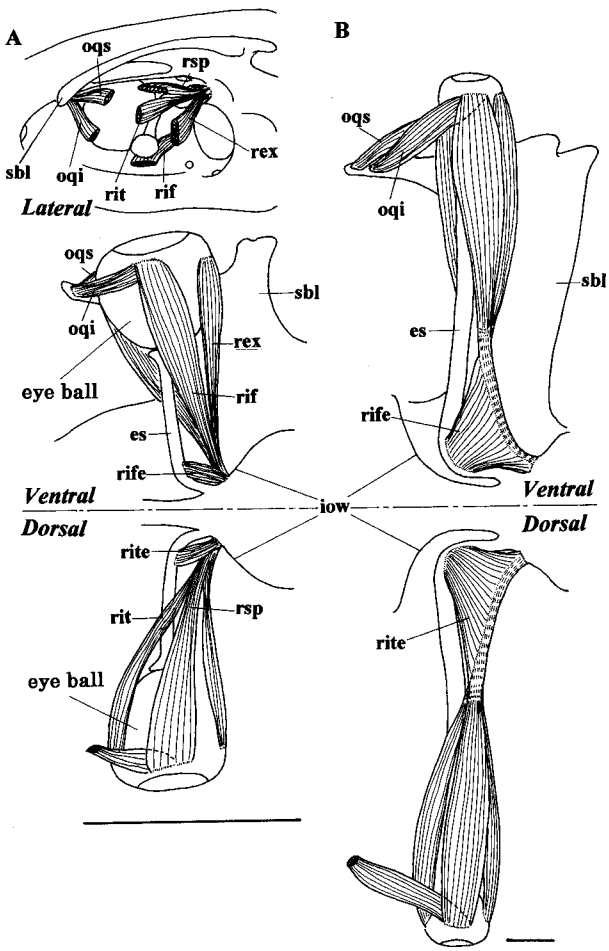

Fig. 44. Oculomotor musculature in two orectolobiforms. (A) Lateral (above), ventral (middle) and dorsal (below) views in *Ginglymostoma cirratum* (ZMUC P0629); (B) ventral (above) and dorsal (below) views in *Rhincodon typus* (OA 00212). Scales indicate 10 mm in A, and 100 mm in B.

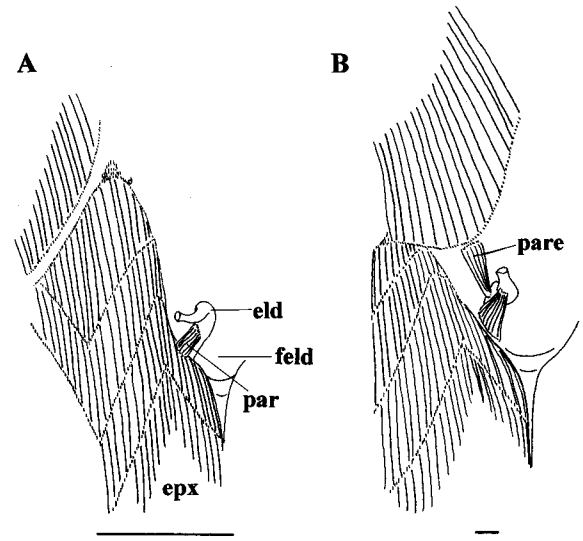

Fig. 45. Dorsal view of parietal fossa. (A) *Brachaelurus waddi* (AMS I20095033); (B) *Stegostoma varium* (HUMZ 78595). Scales indicate 10 mm.

and intermandibularis. The adductor mandibulae (am) is massive and very complicated, connecting posterior halves of the mandibula and palatoquadrate labially. It is divided into four subdivisions, which are termed as adductor mandibulae I to IV here, via weak aponeurotic septa. The adductor mandibulae I (amI) is small, triangular-shaped, occupying the anteroventral edge of this muscle complex. It originates from the mandibula, and inserts on the suborbitalis. The adductor mandibulae II (amII) is large and vertical, occupying the anterior half of this muscle complex. The adductor mandibulae III (amIII) is the largest bundle, and lying obliquely from the posteroventral region of the mandibula to the labial and dorsal surfaces of the palatoquadrate. The adductor mandibulae IV (amIV) is small, covering the posterodorsal surface of the adductor mandibulae III. It is divided from the posteromesial region of the adductor mandibulae III, and inserts onto the subcutaneous tissue covering the superficial region of the muscle complex. The suborbitalis (sob) is greatly massive, fan-shaped, and lying vertically. It originates from the ethmoidal and sometimes also from the orbital regions, and inserts on the adductor mandibulae I or the mandibula. The constrictor dorsalis connects the mandibular arch with the orbital or otic region of the neurocranium. It is divided into two large isolated muscle bundles, i.e., levator palatoquadrati and constrictor dorsalis I (after Compagno, 1988). The levator palatoquadrati (lpq) originates from the posterior region of the orbit or the anterolateral surface of the otic capsule, and inserts on the lingual surface of the palatoquadrate. The constrictor dorsalis I (codI) originates from the lateral surface of the otic capsule, and inserts on the dorsal margin of the palatoquadrate. The spiracularis (spm) is feeble, elongated, and surrounds the anterior wall of the spiracular cleft over the prespiracular cartilage. It originates from the lateral surface of the otic capsule above the hyomandibular facet, and inserts on the lingual surface of the palatoquadrate above the articulated region with the mandibula in main; and on the posterior wall of the spiracular cleft in part. The intermandibularis (im) is thin and broad, broadly covering the ventral surface of the pharynx between the mandibulae. It originates from the subcutaneous tissue covering the genio-coracoideus in the posterior region, and inserts on the ventral edge of the mandibula.

Morphological differences

1. Rostromandibularis (rmd). In *Parascyllium* and *Cirrhoscyllium*, there is a large longitudinal muscle bundle, the rostromandibularis after Compagno (1988),

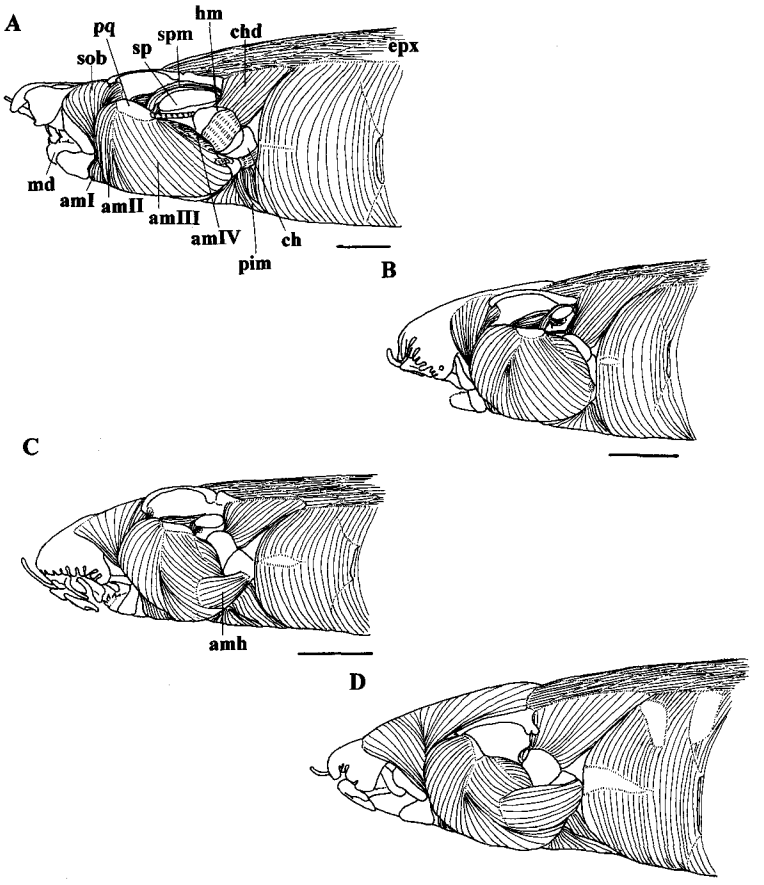

Fig. 46. Lateral view of superficial musculature on head. (A) *Orectolobus wardi* (HUMZ 117705); (B) *Brachaelurus waddi* (AMS I20095033); (C) *Chiloscyllium indicum* (MCZ 54); (D) *Ginglymostoma cirratum* (ZMUC P0629). Scales indicate 10 mm.

on the most superficial region of the mandibular arch (Fig. 47). It is large, triangular-shaped, and covering the adductor mandibulae superficially. It originates from the post-palatoquadrate process of the palatoquadrate and the posterior margin of the mandibula, and inserts on the lateral edge of the rostrum via a long tendon passing under the nasal capsule.

2. Levator palpebrae anterodorsalis (lpa). In *Parascyllium* and *Cirrhoscyllium*, there is a vertical muscle bundle, the levator palpebrae anterodorsalis after Compagno (1988), just in front of the eye (Fig. 47). It originates from the fascia of the suborbitalis, and inserts on the anterior tip of the subcutaneous tissue composed of the upper eye lid.

3. Adductor mandibulae hyoideus (amh). In *Parascyllium, Cirrhoscyllium, Orectolobus, Sutorectus, Eucrossorhinus* and *Brachaelurus*, the adductor mandibulae has no association with the hyoid arch (Figs. 46A-B, 47). In *Chiloscyllium, Hemiscyllium, Ginglymostoma, Stegostoma* and *Rhincodon*, the adductor mandibulae hyoideus (corresponding to the adductor mandibulae γ; Luther, 1909a, b), which is divided from the posterior

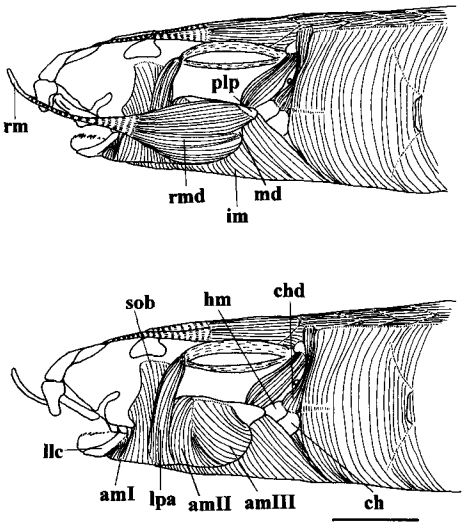

Fig. 47. Lateral views of superficial musculature (above) and musculature after removed rostromandibularis (below) in *Parascyllium collare* (AMS I30409002). Scale indicates 10 mm.

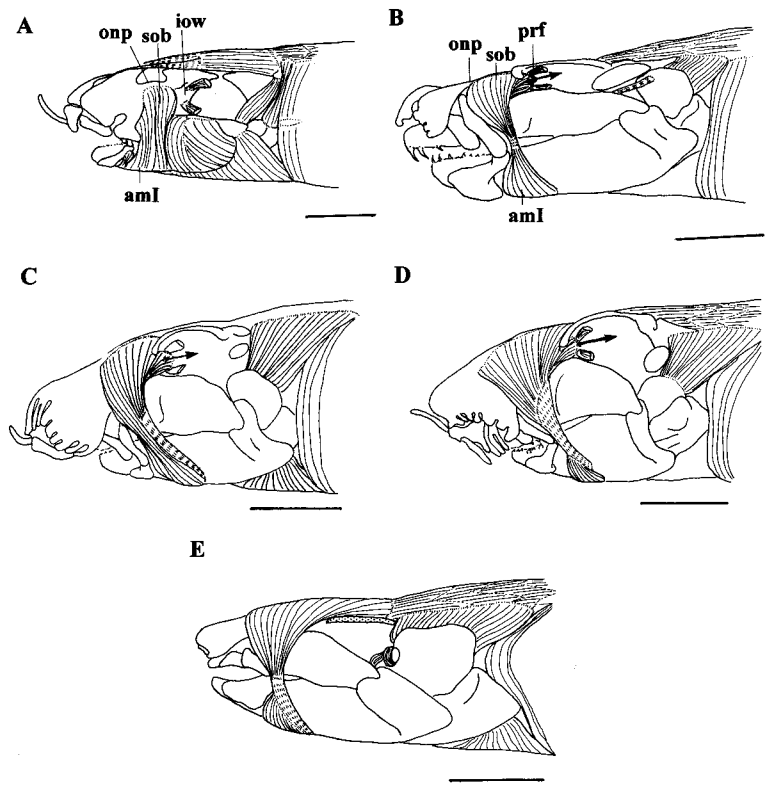

Fig. 48. Suborbitalis in lateral views of five orectolobiforms. (A) *Parascyllium collare* (AMS I30409002); (B) *Orectolobus ornatus* (AMS I14236); (C) *Brachaelurus waddi* (AMS I20095033); (D) *Chiloscyllium indicum* (MCZ 54); (E) *Rhincodon typus* (OA00212). Scales indicate 10 mm in A-D, and 100 mm in E.

region of adductor mandibulae III and inserted on the ceratohyal, is preesnt (Fig. 46C-D).

4. Adductor mandibulae IV (amIV). In most orectolobiforms, there is a distinct bundle of the adductor mandibulae IV, whereas no such bundle is found in *Parascyllium* and *Cirrhoscyllium* (Figs. 46, 47).

5. Origin of suborbitalis (sob). In *Parascyllium* and *Cirrhoscyllium*, the suborbitalis originates from the lateral margin of the orbito-nasal process, with no association with the orbit (Fig. 48A). In *Orectolobus, Sutorectus* and *Eucrossorhinus*, it originates from the lateral margin of the orbito-nasal process and from the anterior part of the interorbital wall, and covers the fenestra of the profundus canal (Figs. 48B, 49A). In *Brachaelurus*, it originates from the dorsolateral margin of the orbito-nasal process and from the anterior part of the interorbital wall covering the fenestra of the profundus canal (Figs. 48C, 49B). In *Chiloscyllium* and *Hemiscyllium*, it originates from the dorsal surfaces of the orbito-nasal process and the orbital region, and from the anterior region of the interorbital wall entirely anterior to the fenestra of the profundus canal (Figs. 48D, 49C). In *Ginglymostoma, Stegostoma* and *Rhincodon*, it originates from the dorsal surfaces of the orbito-nasal process and from the orbital region, with no association with the interorbital wall (Figs. 48E, 49). In the latter five genera, the origin extends immediately anterior to the anterior terminal of the epaxial body muscle (Figs. 49C, 50).

6. Extra bundle of suborbitalis (esob). In *Ginglymostoma*, there is an extra bundle of the suborbitalis (Fig. 50) divided from the suborbitalis. It passes over the palatoquadrate and inserts onto the palatobasal ridge and the anterior expansion of the supraorbital blade.

7. Insertion of suborbitalis (sob). The insertion of the suborbitalis is classified into four categories. It is entirely continuous from the adductor mandibulae I via a muscle bundle in *Parascyllium* and *Cirrhoscyllium* (Fig. 48A), and entirely continuous via a short tendon in *Orectolobus, Eucrossorhinus* and *Sutorectus* (Fig. 48B). It is almost continuous from the adductor mandibulae I via a muscle bundle, and partly inserts on the mandibula via a tendon in *Brachaelurus* (Fig. 48C); and entirely inserts on the mandibula via a long tendon in *Chiloscyllium, Hemiscyllium, Stegostoma, Ginglymostoma* and *Rhincodon* (Fig. 48D-E).

8. Origin of levator palatoquadrati (lpq). In *Parascyllium* and *Cirrhoscyllium*, the levator palatoquadrati originates in a muscle bundle from the ventral margin of the interorbital wall ventral to the foramen opticum (Fig. 51). It originates from the anterior edge of the

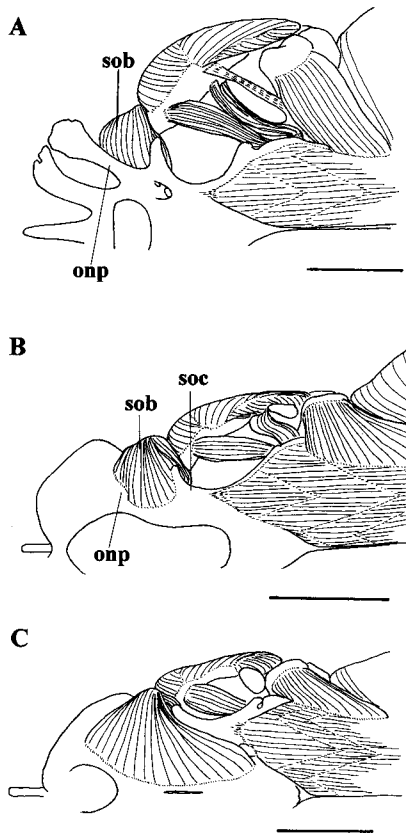

Fig. 49. Suborbitalis in dorsal views of three orectolobiforms. (A) *Orectolobus ornatus* (AMS I14236); (B) *Brachaelurus waddi* (AMS I20095033); (C) *Chiloscyllium indicum* (MCZ 54). Scales indicate 10 mm.

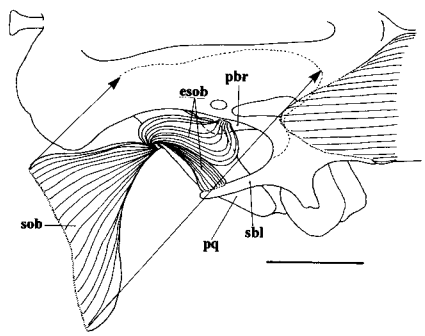

Fig. 50. Suborbitalis of *Ginglymostoma cirratum* (ZMUC P0629) in dorsal view. Scale indicates 10 mm.

otic capsule via a short tendon in *Chiloscyllium* and *Hemiscyllium* (Fig. 52), and originates in a thick muscle bundle in the remaining taxa (Figs. 53, 54).

9. Insertion of levator palatoquadrati (lpq). In most orectolobiforms, the levator palatoquadrati inserts on the lingual surface of the palatoquadrate just posterior to the ligamentum mandibulo-palatoquadrati (Figs. 52-54). In *Parascyllium* and *Cirrhoscyllium*, it is subdivided into two sections: one inserts on the lingual

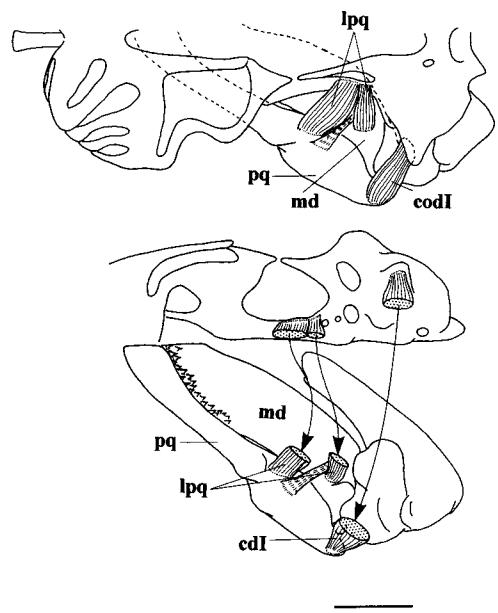

Fig. 51. Musculature associated with mandibular arch of *Parascyllium ferrugineum* (HUMZ 131588) in dorsal view (above); in lateral view of neurocranium and dorsal view of mandibular arch (below). Scale indicates 10 mm.

surfaces of the palatoquadrate just anterior to the ligamentum mandibulo-palatoquadrati, and the other inserts on the mandibula posterior to this ligament (Fig. 51).

10. Constrictor dorsalis I (cdI). Among orectolobiforms, the constrictor dorsalis I is classified into the following four states. It is composed entirely of a single muscle bundle throughout its length from origin to insertion in *Parascyllium* and *Cirrhoscyllium* (Fig. 51). It is composed of a single bundle with a short tendon at the proximal end in *Orectolobus, Sutorectus, Eucrossorhinus* and *Brachaelurus* (Fig. 53), and a single bundle with a short tendon at the distal end in *Ginglymostoma, Stegostoma* and *Rhincodon* (Fig. 54). It is divided into two separate bundles, one with a tendon proximally and the other with a tendon distally in *Chiloscyllium* and *Hemiscyllium* (Fig. 52).

11. Insertion of constrictor dorsalis I (cdI). In most orectolobiforms, the constrictor dorsalis I (cdI) inserts on the dorsal margin of the center of the palatoquadrate (Figs. 52-54). In *Parascyllium* and *Cirrhoscyllium*, it inserts on the posterodorsal margin of the post-palatoquadrate process on the palatoquadrate (Fig. 51).

12. Spiracularis (spm). In most orectolobiforms, there is a variously developed spiracularis muscle; whereas it is absent in *Parascyllium* and *Cirrhoscyllium* (Figs. 51-54).

13. Subdivision of spiracularis (smsp). In most

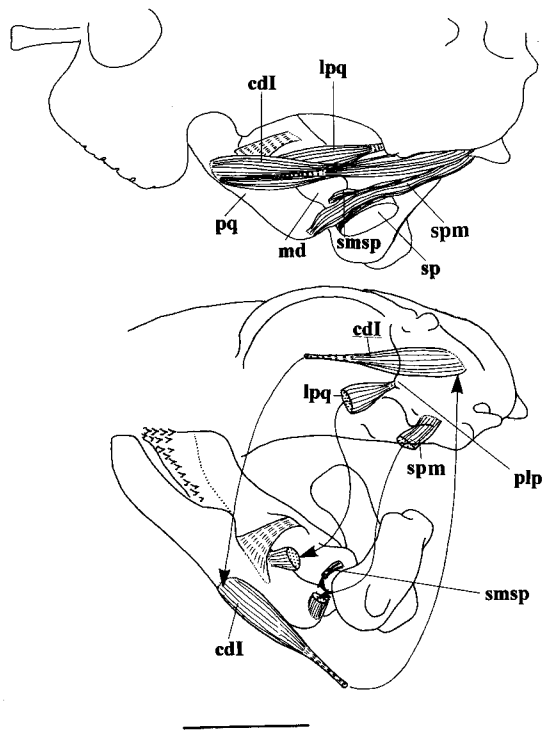

Fig. 52. Musculature associated with mandibular arch of *Chiloscyllium plagiosum* (HUMZ 37689) in dorsal view (above); in lateral view of neurocranium and dorsal view of mandibular arch (below). Scale indicates 10 mm.

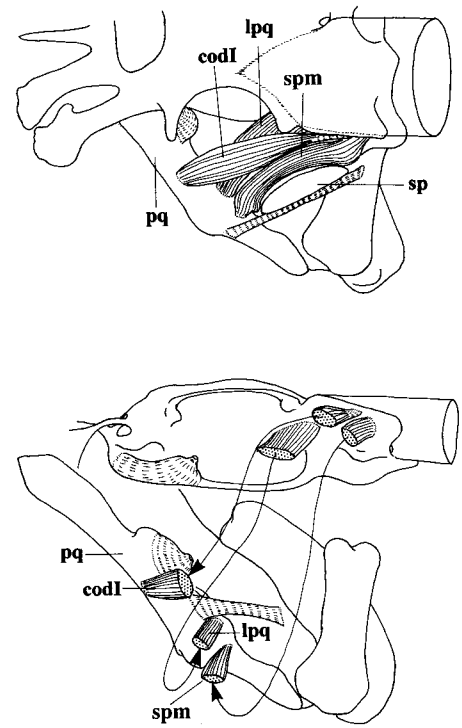

Fig. 53. Musculature associated with mandibular arch of *Orectolobus ornatus* (AMS 114236) in dorsal view (above); in lateral view of neurocranium and dorsal view of mandibular arch (below). Scale indicates 10 mm.

taxa having the spiracularis, this muscle inserts only on the palatoquadrate. There is a small subdivision branched from the spiracularis and inserted on the mandibular knob of the mandibula in *Chiloscyllium* (Fig. 52).

14. Intermandibularis (im). In *Parascyllium* and *Cirrhoscyllium*, the intermandibularis is composed of a single muscle sheet with a long insertion at the posteroventral margin of the mandibula (Fig. 55A). In the remaining taxa, it is clearly divided into the large anterior sheet (aim) inserted on the ventral margin of mandibula, and the thin posterior sheet (pim) inserted on the posterior edge of the mandibula (Fig. 55B).

15. Insertion of intermandibularis (im). In most orectolobiforms, the intermandibularis inserts mainly on the ventral margin of the mandibula and in part on the fascia of the adductor mandibulae (Fig. 55B). In *Parascyllium* and *Cirrhoscyllium*, it additionally inserts onto the ventral surface of the post-palatoquadrate process (Fig. 55A).

8-2. Musculature on hyoid arch

***General description* (*Figs. 46, 47, 55*)**

In orectolobiforms, the musculature associated with the hyoid arch consists of the constrictor hyoideus dorsalis and the constrictor hyoideus ventralis. The constrictor hyoideus dorsalis (chd) is massive, and completely divided from the posteriorly adjacent constrictor branchiales superficiales. It originates from the dorsolateral margin of the otic capsule and the fascia of the epaxial body muscle, and inserts on the hyomandibula. The constrictor hyoideus ventralis (chv) is moderate, fan-shaped, and broadly continuous from the posteriorly adjacent constrictor branchiales superficiales and from the intermandibularis. It originates from the subcutaneous tissue over lying the genio-coracoideus, and inserts on the ceratohyal.

Morphological difference

1. Insertion of constrictor hyoideus dorsalis (chd). In most orectolobiforms, the constrictor hyoideus dorsalis inserts only on the hyomandibula (Fig. 46), whereas in *Parascyllium* and *Cirrhoscyllium* it inserts additionally on the ceratohyal (Fig. 47).

8-3. Musculature on hypobranchial region

***General description* (Figs. 56, 57)**

In orectolobiforms, the musculature associated with the hypobranchial region consists of the genio-

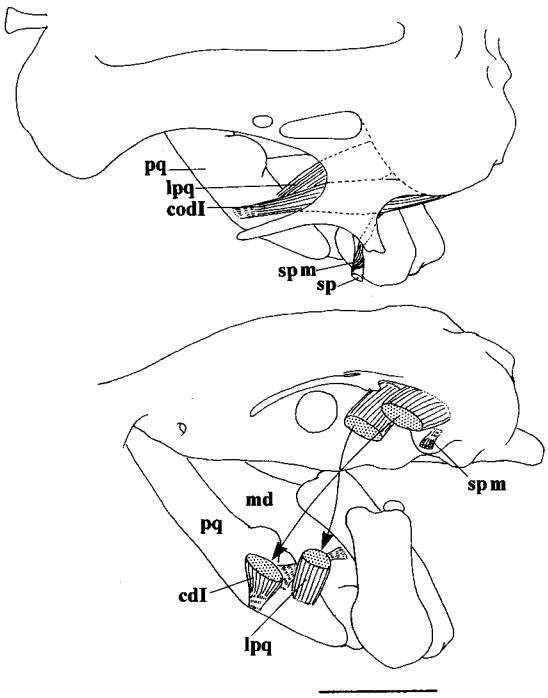

Fig. 54. Musculature associated with mandibular arch of *Ginglymostoma cirratum* (ZMUC P0629) in dorsal view (above); in lateral view of neurocranium and dorsal view of mandibular arch (below). Scale indicates 10 mm.

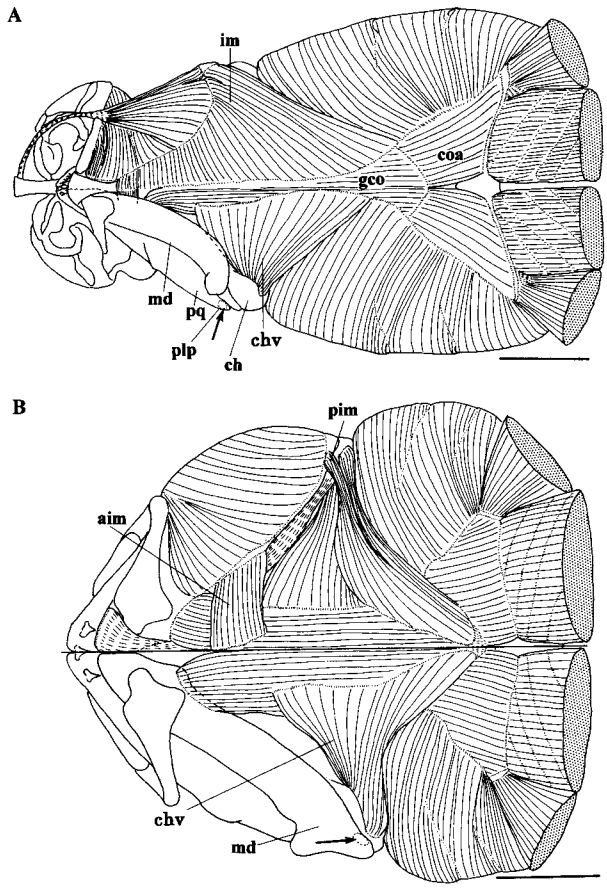

Fig. 55. Pharyngeal musculature associated with mandibular (above) and hyoid (below) arches. (A) *Parascyllium collare* (AMS I30409002); (B) *Orectolobus ornatus* (AMS I14236). Arrows indicate insertion of intermandibularis. Scales indicate 10 mm.

coracoideus, rectus cervicis and coraco-branchiales. The genio-coracoideus (gco) is a single, massive bundle arising from the fascia of the rectus cervicis, pericardial membrane, or coracoid, and inserts onto the posteromesial region of the mandibula near the symphysis. The rectus cervicis consists of the coraco-arcualis and coraco-hyoideus, which are clearly bordered by an aponeurotic septum. The coraco-arcualis (coa) is paired and massive, and originates from the anteroventral margin of the coracoid. The coraco-hyoideus (coh) is mesially fused, originates from the anterior terminal of the coraco-arcualis and from the pericardial membrane, and inserts on the ventral surface of the basihyal. The coraco-branchialis α (cobα) is isolated from the adjacent bundles, originates from the dorsomesial fascia of the rectus cervicis, and inserts on the posterolateral edge of the basihyal and/or on the isolated cartilaginous piece located between the basihyal and ceratobranchial α. The coraco-branchiales β1-δ (cobβ1-δ) are well developed, and each bundle is incompletely separated proximally. Each originates from the pericardial membrane and the anterolateral surface of the coracoid above that of the rectus-cervicis, and inserts on the hypobranchial and/or the ceratobranchial in the arch β-γ; and on the ventral surfaces of the basibranchial and ceratobranchial in the arch δ.

Morphological differences

1. Origin of genio-coracoideus (gco). In orectolobiforms, the origin of the genio-coracoideus is classified into the following three categories. In *Parascyllium, Cirrhoscyllium, Hemiscyllium, Chiloscyllium* and *Rhincodon*, it originates from the fascia of the coraco-hyoideus and from the aponeurotic septum located on its origin (Fig. 56A). In *Orectolobus, Sutorectus* and *Eucrossorhinus*, it originates from the ventral fascia of the coraco-arcualis apparently behind the aponeurotic septum (Fig. 56B). In *Brachaelurus, Ginglymostoma* and *Stegostoma*, it originates not only from the fascia of the coraco-arcualis but also from the symphyseal region of the coracoid (Fig. 56C).

2. Insertion of genio-coracoideus (gco). In most orectolobiforms, the genio-coracoideus inserts on the ventral surface of the mandibula, whereas it inserts on the lingual surface in *Parascyllium* and *Cirrhoscyllium* (Fig. 56).

3. Origin of coraco-arcualis (coa). In most orectolobiforms, the coraco-arcualis originates from the

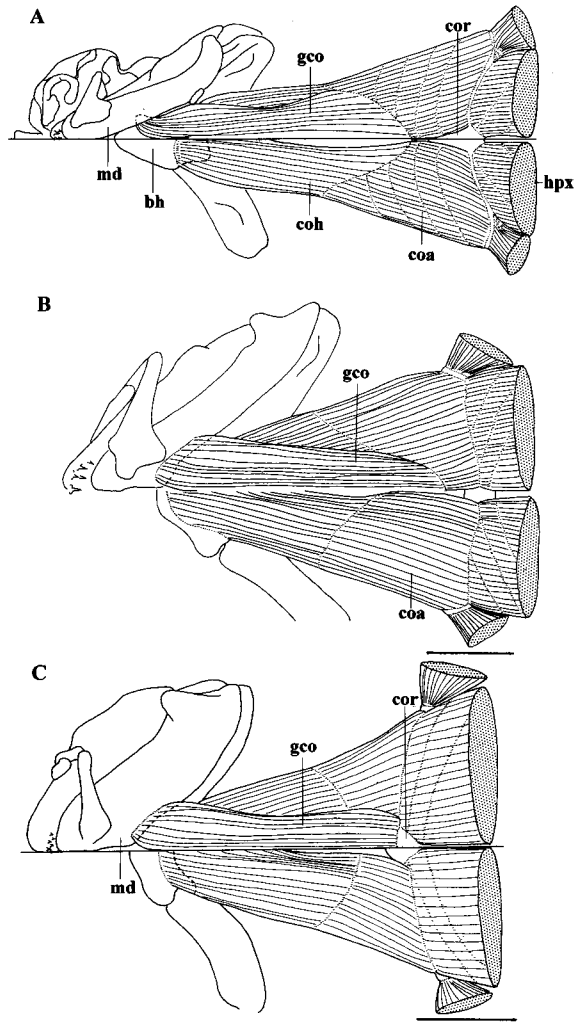

Fig. 56. Hypobranchial musculature showing genio-coracoideus (above) and rectus-cervicis (below) in ventral view. (A) *Parascyllium collare* (AMS I30409002); (B) *Orectolobus ornatus* (AMS I14236); (C) *Brachaelurus waddi* (AMS I20095033). Scales indicate 10 mm.

ventral surface of the coracoid and from the anterior extremity of the hypaxial body muscle via an aponeurotic septum (Fig. 56B-C). In *Parascyllium* and *Cirrhoscyllium*, it entirely inserts on the coracoid, and is isolated from the hypaxial body muscle (Fig. 56A).

4. Coraco-branchialis γ. In most orectolobiforms, the coraco-branchiales β-γ are incompletely isolated proximally, and insert on both ceratobranchial and hypobranchial in all arches (Figs. 57, 58B-C). In *Parascyllium* and *Cirrhoscyllium*, the coraco-branchialis γ is completely isolated from the adjacent bundles as an elongated muscle bundle, and inserts on the inner process of the ceratobranchial γ (Fig. 58A).

5. Origins of coraco-branchialis (cob). In most orectolobiforms, the coraco-branchiales series is more or less associated with either coracoid or pericardial membrane (Figs. 57, 58A, C). In *Rhincodon*, this series is

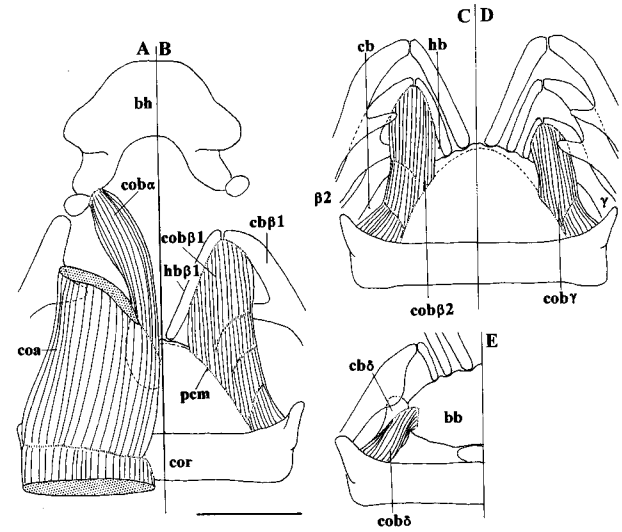

Fig. 57. Coraco-branchiales of *Orectolobus wardi* (HUMZ 117705) in ventral view, showing coraco-branchialis α (A); coraco-branchialis β1 (B); coraco-branchialis β2 (C); coraco-branchialis γ (D); coraco-branchialis δ (E). Scale indicates 10 mm.

very reduced, and the coraco-branchialis β is originated from the fascia of rectus cervicis and from the pericardial membrane, with no association with the coracoid nor the pericardial membrane (Fig. 58B).

6. Insertion of coraco-branchialis. In *Parascyllium* and *Cirrhoscyllium*, a part of coraco-branchialis γ has a branch inserting on the ventral extrabranchial cartilage γ (Fig. 58A). In *Ginglymostoma*, the coraco-branchial β2 inserts on the ventral extrabranchial cartilage β2 (Fig. 58C).

8-4. Musculature on epibranchial region

General description (Fig. 59)

In orectolobiforms, musculature associated with the epibranchial region consists of the subspinalis and interpharyngobranchialis. The subspinalis (ssp) is simple and thin, originates from the basal plate of the neurocranium between the hyomandibular fossa and the occipital condyle, and inserts on the dorsal surface of the pharyngobranchial α. The interpharyngobranchialis (ipb) is simple and thin, originates from the posterior edge of the pharyngobranchial blade, and inserts on the dorsal surface of the posteriorly adjacent pharyngobranchial.

Morphological differences

1. Subspinalis (ssp). In most orectolobiforms, the subspinalis is present (Fig. 59A-C), whereas no muscle bundle is found in *Brachaelurus* (Fig. 59D).

2. Interpharyngobranchialis (ipb). Four states are found in the interpharyngobranchialis. There are three

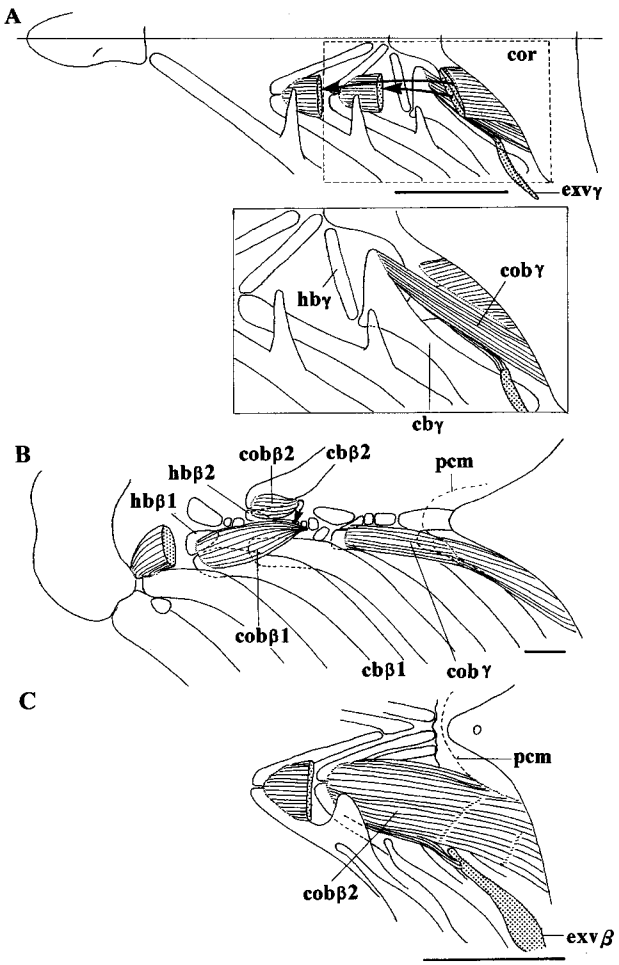

Fig. 58. Coraco-branchiales of three orectolobiforms in ventral view. (A) *Cirrhoscyllium japonicum* (HUMZ 40057); (B) *Rhincodon typus* (OA00212); (C) *Ginglymostoma cirratum* (ZMUC P0629). Scales indicate 10 mm in A and C, and 100 mm in B.

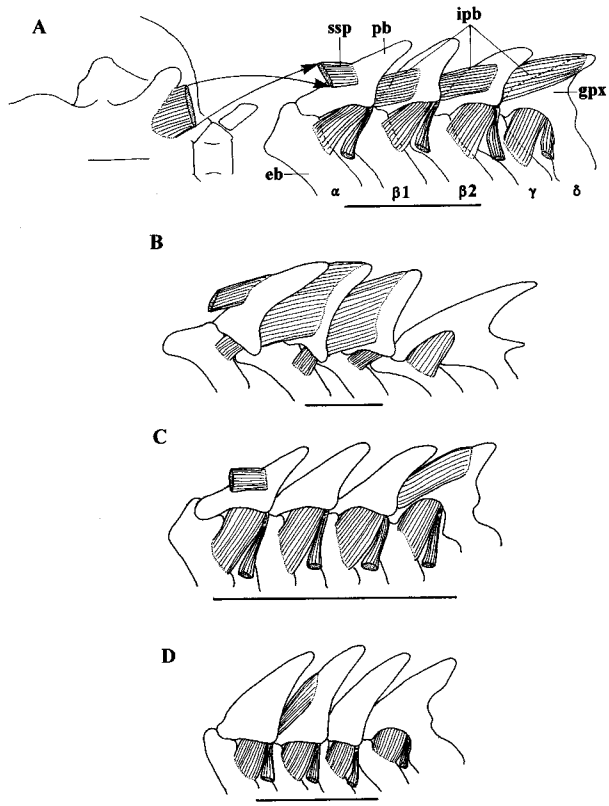

Fig. 59. Musculature associated with pharyngobranchials in external view. (A) *Chiloscyllium indicum* (MCZ 54); (B) *Parascyllium ferrugineum* (HUMZ 131588); (C) *Hemiscyllium freycineti* (CAS I26798); (D) *Brachaelurus waddi* (AMS I20095033). Scales indicate 10 mm.

bundles between the anterior four arches in *Chiloscyllium, Stegostoma, Ginglymostoma* and *Rhincodon* (Fig. 59A). The third bundle between arches $\beta 2$-γ is absent in *Parascyllium, Cirrhoscyllium, Orectolobus, Sutorectus* and *Eucrossorhinus* (Fig. 59B). The first and second bundles between arches α-$\beta 1$ and between $\beta 1$-$\beta 2$ are absent in *Hemiscyllium* (Fig. 59C). The second and third bundles between arches $\beta 1$-$\beta 2$ and between $\beta 2$-γ are absent in *Brachaelurus* (Fig. 59D).

8-5. Musculature on branchial arch

General description (Figs. 60, 61)

In orectolobiforms, musculature on the branchial arches consists of the constrictor branchiales superficiales, interbranchialis, cucullaris, arcualis dorsalis and adductor arcuum branchialium. The constrictor branchiales superficiales (cbs) are composed of five thin muscle sheets. The anteriormost sheet covers the anterior hemibranch of the hyoid arch over the branchial rays; the succeeding sheets cover external margins of the interbranchial septa distal to the extrabranchials. These originate dorsally from the fasciae of the epaxial and cucullaris and from the scapular; ventrally from the seam of connective tissue, that covers the ventral region of the throat and coracoid. The interbranchialis (ibr) is an extremely thin muscle sheet covering vertically the anterior surface of the interbranchial septum over the branchial rays in the anterior four arches: the dorsal and ventral extremities of most part insert on the extrabranchials; the mesial part is a feeble bundle that originates from the ceratobranchial and inserts in the interspace between the coraco-branchiales. The distal margin of this muscle is continuous from the constrictor branchiales superficialis at the external gill opening. The arcualis dorsalis (acd) is simple and rather small, connected the lateral margin of the pharyngobranchial blade with the epibranchial in the anterior three arches; and connected the concavity located on the lateral margin of the gill pickax with epibranchial γ. The adductor arcuum branchialium (aab) is simple and extremely small, connecting the mesial corner formed

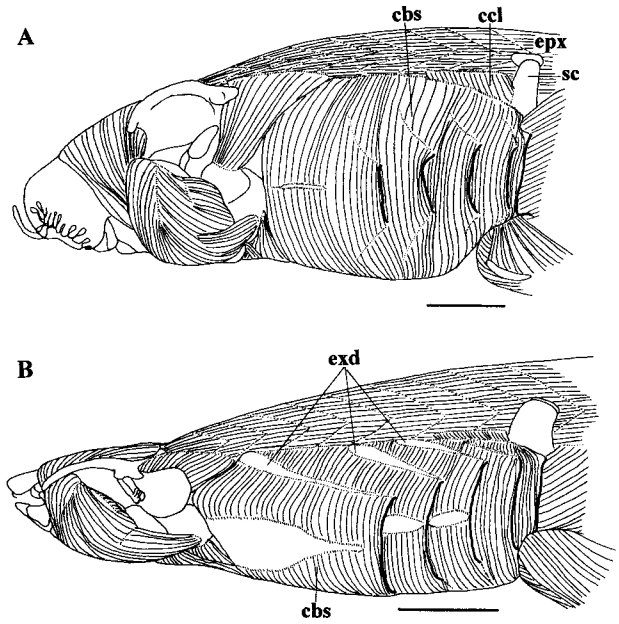

Fig. 60. Superficial musculature on branchial arches in lateral view. (A) *Chiloscyllium plagiosum* (unregistered specimen of NSMT); (B) *Rhincodon typus* (OA00212). Scales indicate 10 mm in A and 100 mm in B.

between the epibranchial and ceratobranchial in all arches. The cucullaris (ccl) is large, fan-shaped, distributed between the epaxial body muscle and constrictor branchiales superficiales. It originates from the fascia of the epaxial, and inserts on the dorsolateral surface of the gill pickax and the anterior surface of the scapular.

Morphological differences

1. Development of constrictor branchiales superficiales (cbs). In most orectolobiforms, the constrictor branchiales superficiales entirely cover the branchial arches over the extrabranchials (Fig. 60A). In *Ginglymostoma, Stegostoma* and *Rhincodon*, these are reduced, and the external regions of the extrabranchials are exposed externally (Fig. 60B).

2. Development of interbranchialis (ibr). In most orectolobiforms, the interbranchialis entirely covers the anterior hemibranch of each interbranchial septum over the branchial rays (Fig. 61A-B). In *Ginglymostoma, Stegostoma* and *Rhincodon*, it is reduced, merely connecting the neighboring branchial rays and extrabranchials, with the exposed region on the rays (Fig. 61C).

3. Subdivision of interbranchialis (ibm). Orectolobiforms, except *Parascyllium* and *Cirrhoscyllium*, have a small subdivision of the interbranchialis lying on the mesial region of the interbranchial septum (Fig. 61B-C). It originates from the tip of the pharyngobranchial blade and the subcutaneous tissue continuous from the blade, and it is entirely composed of muscle fibers in *Orectolobus, Sutorectus, Eucrossorhinus* and *Brachaelurus* (Fig. 61B); in the remaining taxa two muscle bundles are clearly divided via a tendon near the corner between the epibranchial and the ceratobranchial (Fig. 61C).

4. Association of branchial arch with hypaxial. In most orectolobiforms, the branchial arches have no association with the hypaxial (Fig. 62A). In *Parascyllium* and *Cirrhoscyllium*, a part of the hypaxial inserts onto the lateral surfaces of the gill pickax and ceratobranchial δ via a ligamentous membrane over the scapular (Fig. 62B).

9. Musculature associated with pectoral fin

General description (Figs. 63, 64)

In orectolobiforms, musculature associated with the pectoral fin consists of the levator and depressor muscles. The levator pectoralis is divided into one superficial and two deep layers on the basis of the origin and insertion. The levator pectoralis superficialis (lps) is large, thick, and fan-shaped, originates from the lateral edge of the scapular, and inserts on the dorsal surface of the fin. The levator pectoralis inferior (lpi) is rather short and completely separated from the other levator muscles. It originates from the process for the levator pectoralis, and inserts on the pectoral basal cartilages. The levator pectoralis distalis (lpd) is thin, fan-shaped, and continuous from the superficial layer dorsally. It originates from the distal margins of the pectoral basal cartilages and partly from the proximal radials, and inserts on the dorsal surface of the fin. The depressor pectoralis (dpc) is massive and fan-shaped, originates from the fossa on the lateral edge of the coracoid, and inserts on the ventral surface of the fin.

Morphological differences

1. Insertion of levator pectoralis inferior (lpi). The levator pectoralis inferior inserts on the mesopterygium in *Parascyllium, Cirrhoscyllium, Chiloscyllium, Stegostoma* and *Rhincodon* (Fig. 64A); on the propterygium and mesopterygium in *Orectolobus, Sutorectus* and *Eucrossorhinus* (Fig. 64B); on the propterygium, mesopterygium and metapterygium in *Brachaelurus* (Fig. 64C); and not only on the mesopterygium but also on the proximal ends of some proximal radials in *Hemiscyllium* and *Ginglymostoma* (Fig. 64D).

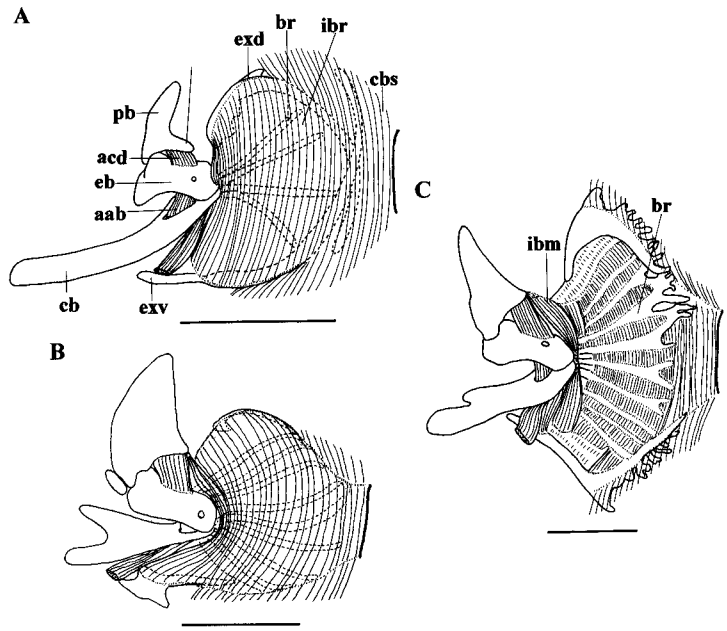

Fig. 61. Musculature on branchial arch in arch α of *Parascyllium collare* (AMS I30409002) (A); arch α of *Orectolobus maculatus* (WAM P28414.001) (B); arch $\beta 1$ of *Ginglymostoma cirratum* (ZMUC P0629). Scales indicate 10 mm.

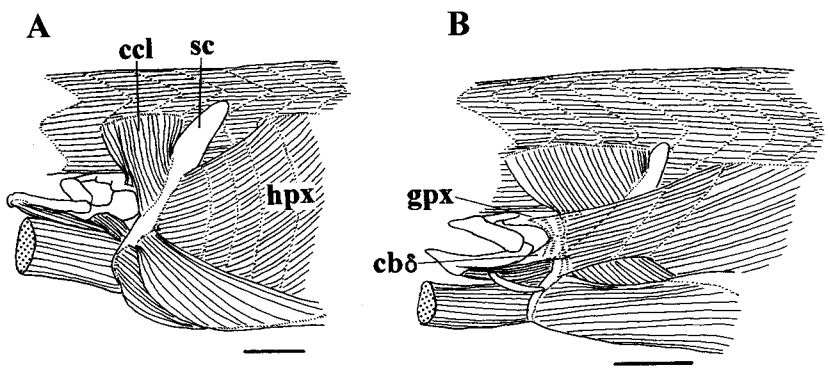

Fig. 62. Association of branchial arches with hypaxial body muscle in lateral view. (A) *Orectolobus wardi* (HUMZ 117705); (B) *Cirrhoscyllium japonicum* (HUMZ 40057). Scales indicate 10 mm.

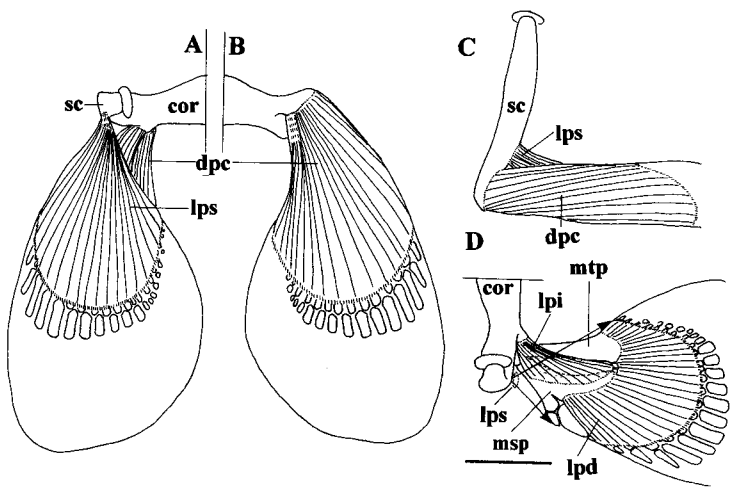

Fig. 63. Musculature associated with pectoral fin of *Hemiscyllium ocellatum* (HUMZ 119336) in dorsal (A), ventral (B) and lateral (C) views, and in dorsal view of inferior musculature (D). Scale indicates 10 mm.

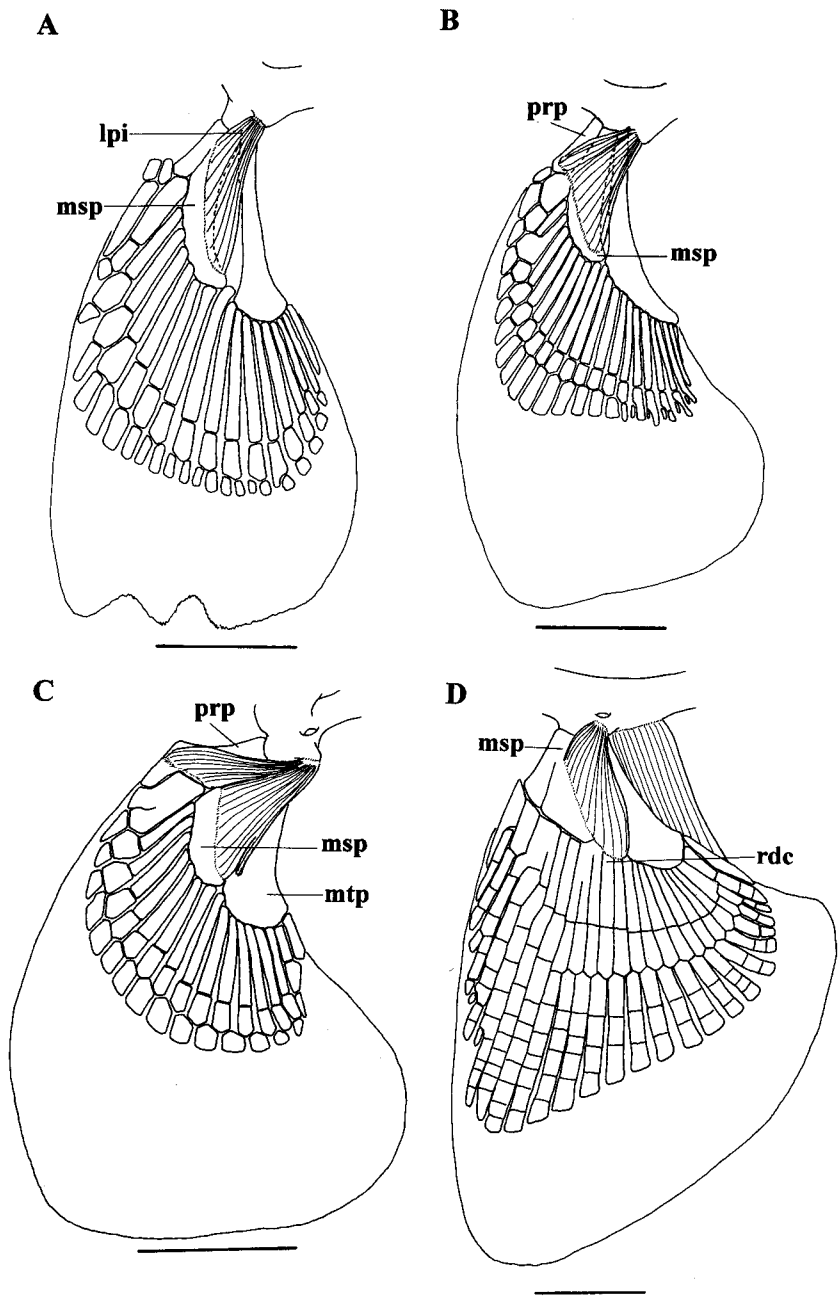

Fig. 64. Levator pectoralis inferior in dorsal view. (A) *Chiloscyllium indicum* (MCZ 54); (B) *Orectolobus maculatus* (WAM P28414.001); (C) *Brachaelurus waddi* (AMS I20095033); (D) *Ginglymostoma cirratum* (ZMUC P0629). Scales indicate 10 mm.

10. Musculature associated with pelvic fin and clasper

***General description* (*Figs. 65, 66*)**

In orectolobiforms, musculature associated with the pelvic girdle and fins consists of the levator, depressor and adductor pelvicus. In males, there are flexor and several muscle complexes associated with the clasper. The levator pelvicus (lpv) is a thin muscle sheet, originating from the fascia of the hypaxial body muscle, and inserting on the dorsal surfaces of the pelvic basipterygium and radials. The depressor pelvicus (dpv) inserts on the anterolateral edge and ventral surface of the fin; the anterolateral layer is rather massive, originating from the ventral surface of the puboischiadic bar, and the posterolateral one is thin, running along the radials and originating from the ventral surface of the pelvic basipterygium. The adductor pelvicus (adv) is fan-shaped, originating from the ventral and posterior surfaces of the puboischiadic bar and from the

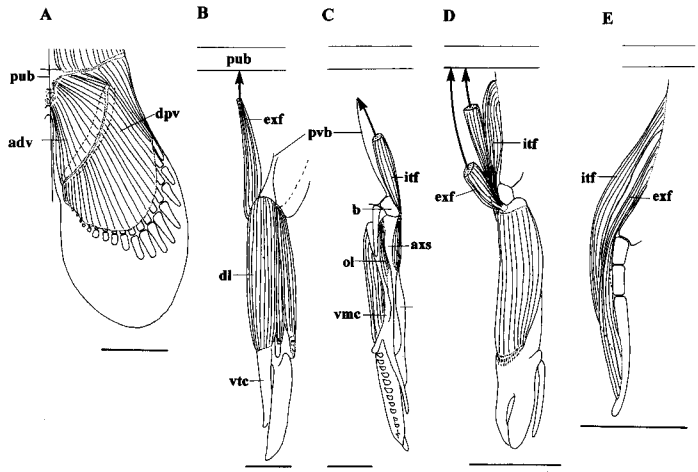

Fig. 65. Musculature associated with pelvic fin in *Hemiscyllium ocellatum* (HUMZ 119336) and clasper musculature (A-E) : ventral (B) and dorsal (C) views in *Parascyllium ferrugineum* (HUMZ 131588) ; ventral view in *Chiloscyllium hasselti* (HUMZ 109476) (D) ; ventral view in *Orectolobus maculatus* (WAM P28414.001) (E). Scales indicate 10 mm.

ligamentous membrane continuous from the opposite bundle anterior to the cloaca, and inserting on the ventral surface of the pelvic basipterygium. The clasper muscles consist of the flexor externus, flexor internus, dilitator and outer-lip muscle. The flexor externus (exf) is lying along the mesial margin of the adductor pelvicus. It originates from the posterior margin of the puboischiadic bar, and inserts on the proximal region of the ventral marginal cartilage. The flexor internus (itf) originates from the mesial margin of the pelvic basipterygium, and inserts on the mesial and dorsal surfaces of the axial cartilage. The dilitator (dl) is massive, originates from the proximal margin of the ventral marginal cartilage, and inserts on the ventral terminal cartilage. The outer-lip muscle (ol) is small and feeble, connecting the axial cartilage with the dorsal margin of the ventral marginal cartilage.

Morphological differences

1. Origin of flexor internus (itf). In most orectolobiforms examined here, the flexor internus originates from the mesial margin of the pelvic basipterygium (Fig. 65B, E). In *Chiloscyllium indicum* and *C. hasselti*, it is proximally divided into two sub-bundles originating from the puboischiadic bar and from the pelvic basipterygium (Fig. 65D).

2. Origin of flexor externus (exf). In most orectolobiforms examined here, the flexor externusthis originates from the puboischiadic bar (Fig. 65C-D). In the species of *Orectolobus* examined, it originates from the mesial margin of the pelvic basipterygium (Fig. 65E).

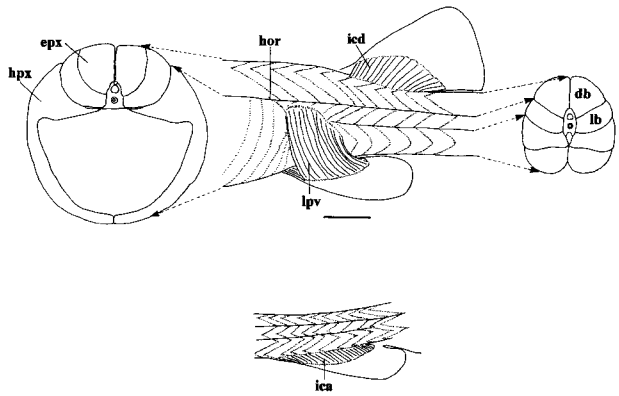

Fig. 66. Body musculature and first dorsal and anal fin muscles in *Orectolobus japonicus* (HUMZ 116361). Scale indicates 10 mm.

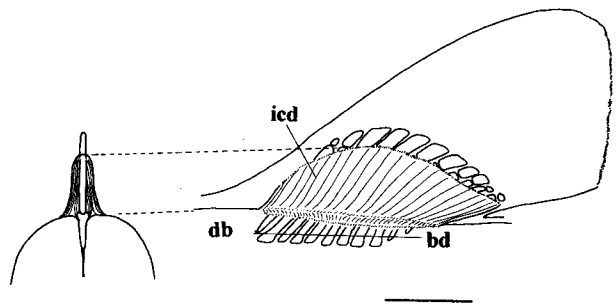

Fig. 67. Musculature associated with first dorsal fin in *Chiloscyllium plagiosum* (unregistered specimen of NSMT). Scale indicates 10 mm.

11. Musculature associated with dorsal and anal fins

General description (Figs. 66-68)

Musculature associated with the dorsal and anal fins consists of an inclinator muscle. The inclinator dor-

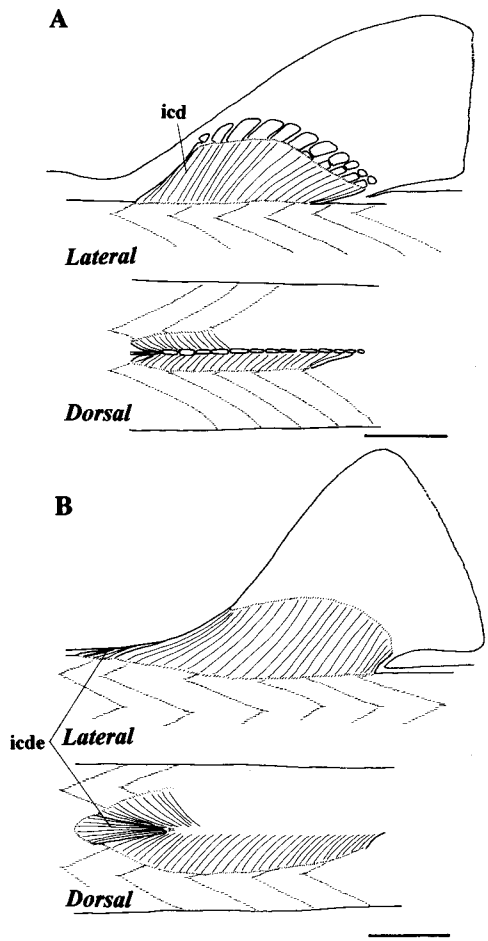

Fig. 68. Musculature associated with dorsal fin in lateral (above) and dorsal views (below). (A) *Chiloscyllium plagiosum* (unregistered specimen of NSMT); (B) *Parascyllium variolatum* (WAM P2852.001). Scales indicate 10 mm.

salis (icd) runs vertically and covers the proximal half of the dorsal fin. It originates from the edges of the distal regions of the basal cartilages mesially and from the fascia of the dorsal bundle superficially, and inserts on the lateral surface of the fin. The inclinator analis (ican) is rather small, and covers the proximal half of the anal fin. It originates from the basal cartilages mesially, and from the fascia of the hypaxial body muscle superficially, and inserts on the lateral surface of the fin.

Morphological difference

1. Extra bundle of inclinator dorsalis (icde). *Parascyllium* and *Cirrhoscyllium* have a single extra bundle located on the anterior margin of the dorsal fin (Fig. 78B). It originates from the fascia of the dorsal bundle near the midline, and inserts on the anterior edge of the dorsal fin.

12. Musculature of body and caudal fin

***General description* (*Figs. 66, 69*)**

The body muscles are massive, covering the trunk, tail and caudal fin entirely. They are divided vertically into the following three bundles by the aponeurotic septa. The dorsal (db) and lateral (lb) bundles occupy the area dorsolateral to the vertebrae above the basiventral process. In the trunk and caudal regions, both bundles are indistinct, forming a single, longitudinal bundle termed the epaxial (epx), whereas in the precaudal tail region, both bundles are rather distinctly divided over the neural arches. The ventral bundle is composed of a single bundle (hypaxial: hpx) occupying the area ventrolateral to the vertebrae, and wholly distinguished from the epaxial by the horizontal myoseptum (hor) over the basiventral process. In the trunk region, this bundle forms a thin muscle sheet enclosing the body cavity from the coracoid and the scapular to the puboischiadic bar. In the tail region and caudal fin, it forms a longitudinal bundle running along the body axis. There is a flexor caudalis (fxc) along the ventral margin of the body muscles. It originates from the fascia of the hypaxial, and inserts on the lateral surfaces of the hypochordal processes.

Morphological differences

1. Rostronuchal (rnc) and ethmonuchal (enm) muscles. In most orectolobiforms, the epaxial originates from the posterodorsal surface of the neurocranium from the orbital to occipital regions. In *Parascyllium* and *Cirrhoscyllium*, the anterior tip of this muscle extends well anteriorly, and is divided into the rostronuchal and ethmonuchal muscles (Fig. 70; after Compagno, 1988). The former is thin, forming a long tendon, and inserting onto the dorsal margin of the rostrum. The latter is rather short, inserting onto the mesial stay of the orbito-nasal process via a tendon.

2. Flexor caudalis (fxc). The anterior end of the flexor caudalis generally begins behind the origin of the lower caudal lobe, and does not extend to the anal fin, even if the anal fin is close to the caudal fin (Fig. 69A). In *Hemiscyllium* and *Chiloscyllium*, this muscle extends forward over the origin of the lower caudal lobe, to attain the position at above the anal basal cartilages (Fig. 69B).

13. Head sensory canal system

***General description* (*Fig. 71*)**

The head sensory canal system consists of the supratemporal, supraorbital, infraorbital, hyomandibular and mandibular canals. The supratemporal canal (stc)

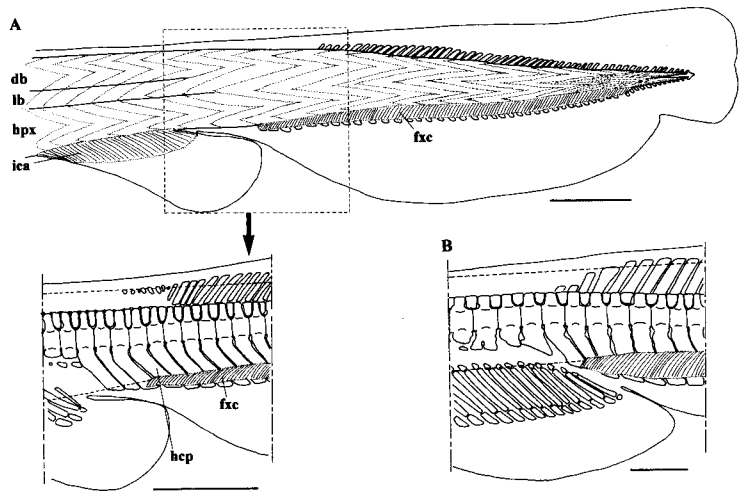

Fig. 69. Musculature associated with caudal fin. (A) *Brachaelurus waddi* (AMS I20095033); (B) *Chiloscyllium punctatum* (HUMZ 6139). Scales indicate 10 mm.

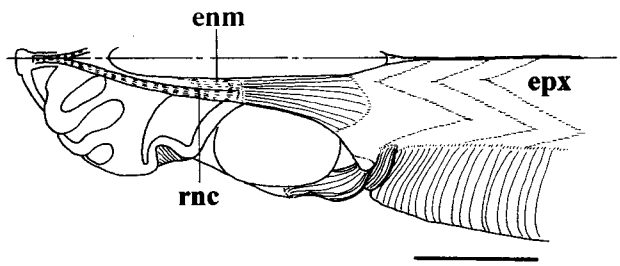

Fig. 70. Dorsal view of head showing the anterior terminal of epaxial in *Parascyllium collare* (AMS I30409002). Scale indicates 10 mm.

is short and feeble. It is branched from the lateral line at the supraotic region, and runs transversely over the parietal fossa. The supraorbital canal (socn) extends forward from the lateral line, passes above the base of the supraorbital crest, and undulates greatly over the nasal capsule. It is curved posteriorly near the snout tip, and passes through the lateral edge of the nostril to fuse with the infraorbital canal above the mouth corner. The infraorbital canal (ioc) originates from the supraorbital canal at the supraotic region, and passes ventrally beside the postorbital process through the interspace between the eye and spiracle. It runs across the dorsal margin of the oronasal groove, and extends anteriorly on the ventral surface of the pre-oral snout to fuse with the supraorbital canal at its anterior tip and with the opposite one at the symphyseal region. The hyomandibular canal (hyc) runs posteriorly from the supraorbital canal to the area in front of the first gill opening. The mandibular canal (mdc) runs on the lower jaw below the mouth gape toward the symphyseal region.

Morphological differences

1. Relationship between supraorbital canal (socn) and postorbital process (pop). In most orectolobiforms, the supraorbital canal passes through the vertical groove formed on the postorbital process of the neurocranium (Fig. 71B-C). In *Parascyllium* and *Cirrhoscyllium*, it has no association with this process, and passes immediately behind it (Fig. 71A).

2. Relationship between hyomandibular (hyc) and mandibular (mdc) canals. In *Orectolobus, Sutorectus, Eucrossorhinus* and *Brachaelurus*, the mandibular canal is separated from the hyomandibular canal (Fig. 71B). In *Parascyllium, Cirrhoscyllium, Hemiscyllium, Chiloscyllium, Ginglymostoma, Stegostoma* and *Rhincodon*, both canals are continuous below the eye (Fig. 71A, C).

3. Mandibular canal (mdc). In most orectolobiforms, the mandibular canal is continuous at the symphyseal region (Fig. 71B-C). In *Parascyllium, Cirrhoscyllium* and *Hemiscyllium*, it is separate, opening to the outside as the terminal apertures (Fig. 71A).

14. Distribution of ampullae of Lorenzini

General description (Fig. 72)

The ampullae of Lorenzini consist of the clusters of ampullae innervated by the afferent branches of the trigeminal or facial nerves, with numerous tubules occupied by jelly-like substance and with apertures opening to the outside. They are classified into the superficial ophthalmic, deep ophthalmic, buccal, hyoid, and mandibular groups. The superficial ophthalmic group (soa), innervated by the ramus ophthalmicus superficialis V and VII nerves, is located above the rostrum, and is divided into three subgroups of tubules. The rostral subgroup (soa1) opens on the ventral surface of snout, the second subgroup (soa2) extends laterally and opens in the space anterior to the eye, and the

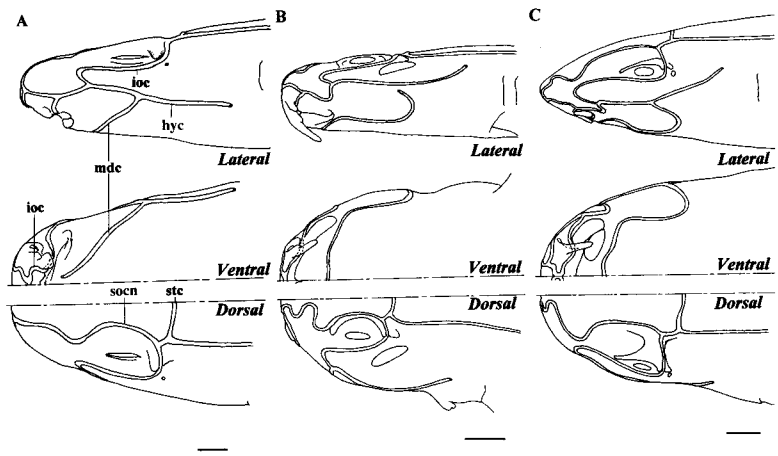

Fig. 71. Head sensory canal system in lateral (above), ventral (middle) and dorsal (below) views. (A) *Parascyllium ferrugineum* (HUMZ 131588); *Orectolobus ornatus* (AMS I14236); (C) *Ginglymostoma cirratum* (ZMUC P0629). Scales indicate 10 mm.

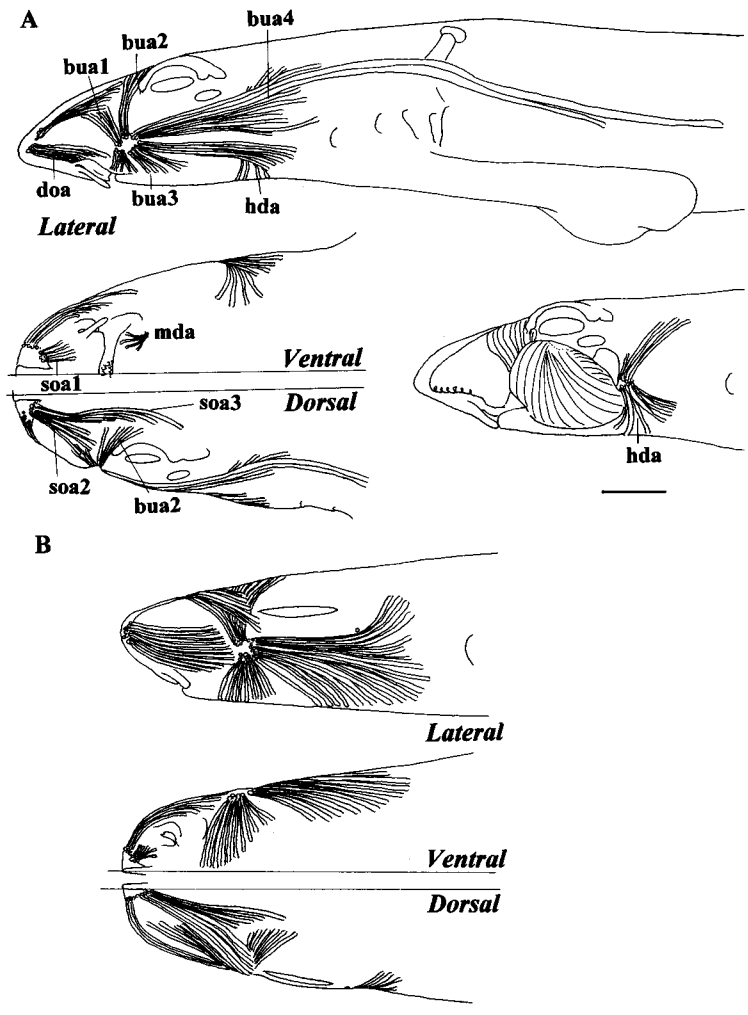

Fig. 72. Distributions of ampullae of Lorenzini in lateral (above), ventral (middle) and dorsal (below) views. (A) *Chiloscyllium indicum* (MCZ 54); (B) *Parascyllium ferrugineum* (HUMZ 131588). Scales indicate 10 mm.

posterior subgroup (soa3) extends posteriorly and opens on the dorsal surface of the orbit along the supraorbital canal. The deep ophthalmic group (doa) is located in the interspace between the nasal apertures and rostrum, extends to the lateral area to the nasal capsule, and opens in the interspace between eye and mouth. The buccal group (bua), innervated by the ramus buccalis VII nerve, is large, located in the interspace between the nasal capsule and the antorbital process, and is divided into four subgroups of tubules. The first buccal group (bua1) extends dorsally and opens on the dorsal surface of the nasal capsule along the supraorbital sensory canal. The second buccal group (bua2) extends dorsally and opens above the orbit along the supraorbital sensory canal. The third buccal group (bua3) is dispersed ventroposteriorly and opens below the infraorbital and hyomandibular sensory canals. The fourth buccal group (bua4) extends posteriorly and opens above the hyomandibular sensory canal. The hyoid group (hda), innervated by the ramus hyomandibularis VII nerve, is located behind the mandibular arch and is divided into two subgroups : one subgroup opens behind the spiracle and the other opens on the ventral surface of the pharyngeal region. The mandibular group (mda) located on the ventral margin of the mandibula is extremely reduced.

Morphological differences

1. Hyoid group of ampullae of Lorenzini (hda). In most orectolobiforms, the hyoid group of the ampullae of Lorenzini is present (Fig. 72A), whereas no ampullae are present on the hyoid in *Parascyllium* and *Cirrhoscyllium* (Fig. 72B).

2. Tubules of buccal group of ampullae of Lorenzini (bua). In most orectolobiforms, all tubules of the buccal group of the ampullae of Lorenzini that extend posteriorly (bua4) open externally in front of the first gill opening (Fig. 72B). In *Hemiscyllium* and *Chiloscyllium*, some tubules of this group greatly extend posteriorly over the pectoral girdle, with their apertures opening at the posterior region of the trunk (Fig. 72A).

15. External morphology

General morphology

All orectolobiforms share the following morphological features: body fusiform, cylindrical, or depressed; nostril close to mouth, oronasal groove present between nostril and mouth; nasal barbel present on the mesial margin of nostril (Fig. 73); mouth nearly straight, terminal or subterminal, entirely anterior to eye; eye rather narrow, spindle-shaped, lateral or dorsolateral on head; spiracle present; external gill openings five, at least last two above base of pectoral fin; dorsal fins with no spine, located on the posterior half of

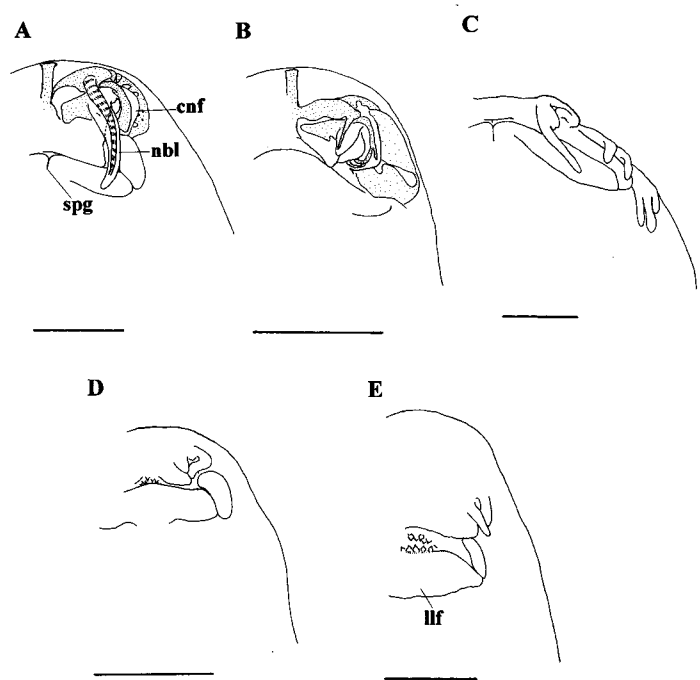

Fig. 73. Ventral views of heads showing nasal barbels with internal components (A-B) and external features only (C-E). (A) *Brachaelurus waddi* (AMS I20095033); (B) *Parascyllium collare* (AMS I30409002); (C) *Orectolobus ornatus* (AMS I14236); (D) *Hemiscyllium trispeculare* (SI 0603.008); (E) *Chiloscyllium indicum* (MCZ 54). Scales indicate 10 mm.

body ; anal fin present.

Morphological differences

For external morphology, I describe only distinct differences among taxa examined here, not such relative differences as those in proportions or coloration, which are sometimes variable among individuals.

1. Nasal barbel (nbl). In most orectolobiforms, the nasal barbel is simple, with no branch or cartilaginous support (Fig. 73A). *Parascyllium* and *Cirrhoscyllium* have an unbranched nasal barbel supported by a thin cartilaginous bar extending from the nasal capsule (Fig. 73B). In *Orectolobus* except *O. wardi* and *Eucrossorhinus*, the nasal barbel is bifurcated, with a few of small branches, but it has no cartilaginous support (Fig. 73C).

2. Circumnarial fold (cnf). In most orectolobiforms, the circumnarial fold surrounds the outer margins of the incurrent and excurrent apertures (Fig. 73B). In *Ginglymostoma, Stegostoma* and *Rhincodon*, no such appendages are present.

3. Symphyseal groove (spg). In *Brachaelurus, Orectolobus, Eucrossorhinus* and *Sutorectus*, there is a distinct groove, the symphyseal groove (Compagno, 1988), on the medial region of the lower jaw (Fig. 73A, C).

4. Lower labial furrow (llf). In most orectolobiforms, the lower labial furrow represents a thick and oval-shaped fold located on the mouth corner. In *Hemiscyllium*, it is considerably enlarged, forming a paired thin dermal fold (Fig. 73D). In *Chiloscyllium*, it is more developed, forming a single, thin dermal fold entirely across the lower jaw (Fig. 73E).

5. Subocular pocket. There is a weak groove called subocular pocket on the lower margin of the eye in *Cirrhoscyllium, Parascyllium, Orectolobus, Sutorectus, Eucrossorhinus* and *Brachaelurus*.

6. Dermal lobe on head (dlb). *Orectolobus, Sutorectus* and *Eucrossorhinus* have variously-shaped dermal lobes on the lateral margin of the head along the mouth gape and below the spiracle. In *O. wardi* and *Sutorectus*, the dermal lobes are rudimentary, simple, and not branched, located on the upper jaw and below the eye (Fig. 74A). In the remaining species of *Orectolobus*, at least some of the dermal lobes are branched, high in number, and located on the upper jaw and below the eye (Fig. 74B). In *Eucrossorhinus*, these are highly branched and considerably increased in numbers, and located not only on the upper, but also on the lower jaw (Fig. 74C). Each lobe is constructed by dermis, and innervated at only the proximal region by the extremely thin branches of the facial nerve V (Goto et al., 1992).

7. Throat barbel. In *Cirrhoscyllium*, paired barbels are present on the throat. Each is composed of dermis supported by two cartilaginous stems and innervated by a branch of the ramus hyomandibularis VII nerve (Goto et al., 1992).

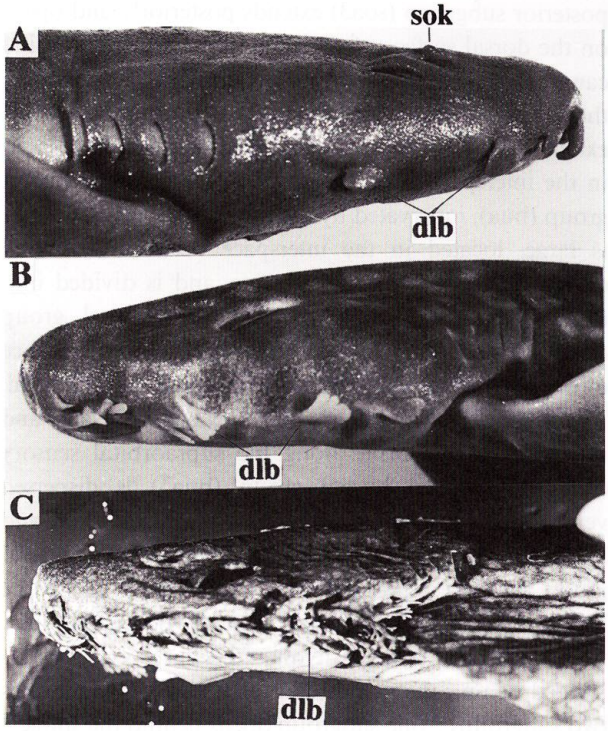

Fig. 74. Lateral views of heads of three orectolobiforms. (A) *Orectolobus wardi* (HUMZ 117705) ; (B) *O. japonicus* (HUMZ 114394) ; (C) *Eucrossorhinus dasypogon* (CSIRO CA4051).

8. Dorsal spiracular caecum (dsc). The dorsal spiracular caecum (dsc) is a mesially closed duct branched from the spiracular cleft, and extending over the hyomandibula toward the anterolateral rim of the otic capsule in most orectolobiforms (Fig. 75A). In *Ginglymostoma, Stegostoma* and *Rhincodon*, it is extremely thin and shortened, not extending to the otic capsule (Fig. 75B). In *Parascyllium* and *Cirrhoscyllium*, no such duct is found.

9. Supraocular knob (sok). In *Orectolobus* except *O. japonicus* and *O. ornatus, Sutorectus* and *Eucrossorhinus*, one or two granulated supraocular knobs (sok) are present on the dorsal margin of the eye (Fig. 74).

10. Last interbranchial septum. In most orectolobiforms, the last interbranchial septum has gill filaments on both sides, forming a holobranch, whereas in *Parascyllium* and *Cirrhoscyllium*, it has no filaments on the posterior side, representing a hemibranch.

11. Dermal ridges on back and lateral surface of body. There are various dermal ridges on the dorsum or lateral surfaces of the body in *Chiloscyllium, Hemiscyllium, Stegostoma* and *Rhincodon*. In the former two genera, except *C. indicum* and *C. plagiosum*, a single,

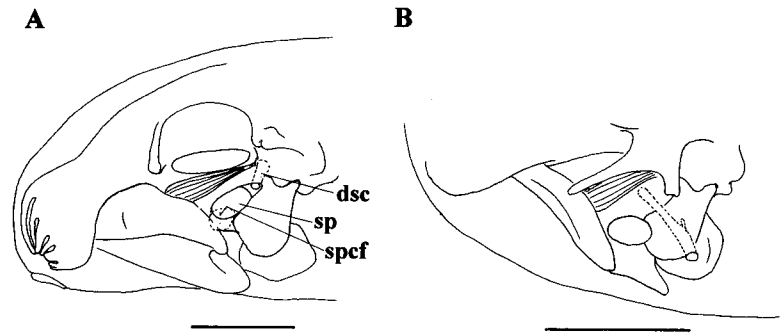

Fig. 75. Dorsolateral view of head showing left spiracle and associated organs. (A) *Hemiscyllium ocellatum* (HUMZ 1193366); (B) *Ginglymostoma cirratum* (ZMUC P0629). Scales indicate 10 mm.

distinct longitudinal ridge (interdorsal ridge) is present between the dorsal fins. *C. indicum* and *C. plagiosum* have not only the interdorsal ridge but also a pair of weak lateral ridges. In *Stegostoma* and *Rhincodon*, there are five thin ridges on the interdorsal region and lateral surface.

12. Position of anal fin. In *Orectolobus, Sutorectus, Eucrossorhinus, Brachaelurus* and *Stegostoma*, the anal fin is located immediately anterior to the origin of the lower caudal lobe with no interspace. In *Chiloscyllium* and *Hemiscyllium*, it is posteriorly shifted, overlapping the lower caudal lobe. In *Ginglymostoma*, it is weakly separate by a short distance from the origin of the lower caudal lobe. In *Parascyllium, Cirrhoscyllium* and *Rhincodon*, it is widely separated from the lower caudal lobe.

13. Precaudal notch. In *Rhincodon*, the distinct precaudal notch is present only on the origin of the upper caudal lobe.

14. Caudal fin. In most orectolobiforms, the caudal fin has no distinct lower caudal lobe, whereas *Rhincodon* has a large and pointed lower caudal lobe.

V. Character analysis for second step

In this chapter, the character analysis for the second step is examined in order to estimate the ON state, depending upon the distribution of the character states among the outgroup taxa. I attempted a topology proposed by Shirai (1992a) within Squalea, and the unresolved polytomous clade within the carcharhiniforms *a priori* for the character-state reconstruction among the outgroups. The number and title put on the head of each character is equivalent to that in the Chapter IV "General description and morphological differences," respectively.

1-1-1. Nasal capsule. Two states are recognized in the nasal capsule as (a) completely closed ; (b) having slit-like fenestrae. Since all outgroups share state (a), the alternate state (b) is estimated to be apomorphic. Coding : 0=(a) ; 1=(b)/status : binary (*Character 1*).

1-1-2. Rim of nasal capsule. Two states are recognized in the rim of the nasal capsule as (a) nearly straight or undulated ; (b) with brush-like processes. Since all outgroups share state (a), the alternate state (b) is estimated to be apomorphic. Coding : 0=(a) ; 1=(b)/status : binary (*Character 2*).

1-1-3. Outer nasal cartilage (A). Two states are recognized in the outer nasal cartilage as (a) isolated from nasal capsule ; (b) fused with nasal capsule. Most outgroup taxa have state (a), whereas *Heterodontus*, except *H. francisci*, and *Apristurus, Gollum, Mitsukurina* and *Alopias* share state (b). This fusion in the species of *Heterodontus* is, however, located at the posterolateral margin of the outer nasal cartilage that is quite different from those of orectolobiforms. Therefore, state (b) is estimated to be apomorphic. Coding : 0=(a) ; 1=(b)/status : binary (*Character 3*).

1-1-3. Outer nasal cartilage (B). Two states are recognized in the outer nasal cartilage as (a) opened posteriorly ; (b) circular. Since outgroups except some species of *Heterodontus* share state (a), the alternate state (b) is an autapomorphy for *Rhincodon*.

1-1-4. Inner nasal cartilage. Two states are recognized in the inner nasal cartilage as (a) absent ; (b) present. Since all outgroups share state (a), state (b) is estimated to be apomorphic. The condition of *Parascyllium ferrugineum* shown as "inc ?" (Fig. 21B) is assigned as "?." Coding : 0=(a) ; 1=(b)/status : binary (*Character 4*).

1-1-5. Extra cartilages of nasal cartilages. Two states are recognized in the extra cartilage of nasal cartilage as (a) absent ; (b) present. Since all outgroups share state (a), the alternate state (b) is estimated to be apomorphic. Coding : 0=(a) ; 1=(b)/status : binary (*Character 5*).

1-1-6. Internasal space. Two states are recognized in the internasal septum as (a) present ; (b) absent. According to the first step (Ch. 17), all galean taxa share state (a). Therefore, state (b) is estimated to be apomor-

phic. Coding: 0=(a); 1=(b)/status: binary (*Character 6*).

1-1-7. Orbito-nasal process. Three states are recognized in the orbito-nasal process as (a) cylindrical, with enclosed olfactory peduncle; (b) laterally reduced; (c) divided into two plates. Since all outgroups share state (a), states (b) and (c) are apomorphic, respectively. Coding: 0=(a); 1=(b); 2=(c)/status: unordered (*Character 7*).

1-1-8. Fenestra on orbito-nasal process. Two states are recognized in the fenestra on the orbito-nasal process as (a) absent; (b) present. Since all outgroups share state (a), the alternate state (b) is estimated to be apomorphic. Coding: 0=(a); 1=(b)/status: binary (*Character 8*).

1-1-9. Efferent opening for orbito-nasal vein. Two states are recognized in the orbito-nasal vein as (a) opening in nasal chamber; (b) opening at orbito-nasal process. Among outgroups examined, *Heterodontus, Mitsukurina* and carcharhiniforms, except *Carcharhinus*, share state (a), and the remains share state (b). Therefore, ON state is assigned as equivocal. Coding: 0=(a); 1=(b)/status: binary (*Character 9*).

1-1-10. Shape of rostral rod. Two states are recognized in the shape of rostral rod as (a) thin and well projecting forward; (b) greatly broad and short. Since state (a) is put on the ON in the first step, state (b) is an autapomorphy for *Rhincodon*.

1-2-1. Relationship between epiphyseal foramen and prefrontal fontanelle. Three states are recognized in the epiphyseal foramen as (a) absent; (b) isolated from prefrontal fontanelle; (c) fused with prefrontal fontanelle. Since all outgroups examined share state (a) except for some squalean taxa (Shirai, 1992a), states (b) and (c) are estimated to be apomorphic, respectively. Coding: 0=(a); 1=(b); 2=(c)/status: unordered (*Character 10*).

1-2-2. Supraorbital region (A). Two states are recognized in the supraorbital crest as (a) absent; (b) present. Since outgroups except some carcharhiniforms e.g., *Apristurus, Galeus* and *Halaelurus*, and lamniform *Mitsukurina* share state (b), the alternate state (a) is estimated to be apomorphic. Coding: 0=(b); 1=(a)/status: binary (*Character 11*).

1-2-2. Supraorbital region (B). Two states are recognized in the supraorbital region as (a) completely closed; (b) interrupted. Since all outgroups share state (a), the alternate state (b) is estimated to be apomorphic. Coding: 0=(a); 1=(b)/status: binary (*Character 12*).

1-2-3. Supraorbital blade. Two states are recognized in the supraorbital blade as (a) absent; (b) present. As shown in the first step (Ch. 21), the ON state is assigned as state (a). Coding: 0=(a); 1=(b)/status: binary (*Character 13*).

1-2-4. Shape of postorbital process. Two states are recognized in the shape of the postorbital process as (a) pointed; (b) with a vertical groove. Most outgroups share state (a), while state (b) appears in some carcharhiniforms. Therefore, state (b) is estimated to be apomorphic. Coding: 0=(a); 1=(b)/status: binary (*Character 14*).

1-2-5. Preorbital and profundus canals (A). Two states are recognized in the preorbital canal as (a) present; (b) absent. Since outgroups except some carcharhiniforms and *Mitsukurina* share state (a), the alternate state (b) is estimated to be apomorphic. Coding: 0=(a); 1=(b)/status: binary (*Character 15*).

1-2-5. Preorbital and profundus canals (B). Two states are recognized in the preorbital canal as (a) small and extending anterodorsally; (b) large and vertical. Since all outgroups having preorbital canal share state (a), the alternate state (b) is estimated to be apomorphic. Coding: 0=(a); 1=(b)/status: binary (*Character 16*).

1-2-5. Preorbital and profundus canals (C). Two states are recognized in the profundus canal as (a) present; (b) absent. Since all outgroups share state (a), the alternate state (b) is estimated to be apomorphic. Coding: 0=(a); 1=(b)/status: binary (*Character 17*).

1-2-6. Foramina for optic and oculomotor nerves. Two states are recognized in the foramina for optic and oculomotor nerves as (a) separated; (b) fused. Since all outgroups share state (a), the alternate state (b) is estimated to be apomorphic. Coding: 0=(a); 1=(b)/status: binary (*Character 18*).

1-2-7. Foramen for hyomandibularis VII nerve. Two states are recognized in the foramen for hyomandibularis VII nerve as (a) fused with the main foramen for the trigeminal and facial nerves; (b) isolated. According to the first step (Ch. 15), the ON state is assigned as state (b). Coding: 0=(b); 1=(a)/status: binary (*Character 19*).

1-2-8. Foramen for abducens VI nerve. Three states are recognized in the foramen for abducens VI nerve as (a) fused with the main foramen for the trigeminal and facial nerves; (b) isolated; (c) fused with that for the ophthalmicus nerves. According to the first step (Ch. 16), the ON state is assigned as state (a). Therefore, states (b) and (c) are apomorphic, respectively, and state (c) is an autapomorphy for *Rhincodon*. Coding: 0=(a), (c); 1=(b)/status: binary (*Character* 20).

1-2-9. Foramina for pseudobranchial artery and pituitary vein. Two states are recognized in the fora-

mina for the pseudobranchial artery and pituitary vein as (a) separate; (b) fused. Since all outgroups share state (a), the alternate state (b) is estimated to be apomorphic. Coding: 0=(a); 1=(b)/status: binary (*Character 21*).

1-2-10. Palatobasal ridge. Two states are recognized in the palatobasal ridge as (a) thickened; (b) projected anteriorly. Among outgroups, all galeans share state (a). Therefore, state (b) is estimated to be an autapomorphy for *Stegostoma*.

1-2-11. Foramen for orbital artery. Two states are recognized in the foramen for orbital artery as (a) present; (b) absent. According to the first step, the ON state is assigned as state (a). Coding: 0=(a); 1=(b)/status: binary (*Character 22*).

1-2-12. Foramen for internal carotid artery. Three states are recognized in the foramen for internal carotid artery as (a) paired; (b) single; (c) fused with foramen for orbital artery. According to the first step, the ON state is assigned as state (a). Coding: 0=(a); 1=(b); 2=(c)/status: unordered (*Character 23*).

1-3-1. Endolymphatic fossa. Two states are recognized in the endolymphatic fossa as (a) present; (b) absent. Since all outgroups share state (a), the alternate state (b) is estimated to be apomorphic. Coding: 0=(a); 1=(b)/status: binary (*Character 24*).

1-3-2. Foramina for endolymphatic and perilymphatic ducts. Two states are recognized in the foramina for endolymphatic and perilymphatic ducts as (a) separated; (b) fused. Since outgroups, except some squaleans, share state (a) (Shirai, 1992a), the alternate state (b) is an autapomorphy for *Ginglymostoma*.

1-3-3. Ascending process of endolymphatic fossa. Two states are recognized in the ascending process of endolymphatic fossa as (a) present; (b) absent. Since outgroups share state (a) except for some carcharhiniforms, the alternate state (b) is estimated to be apomorphic. Coding: 0=(a); 1=(b)/status: binary (*Character 25*).

1-3-4. Sphenopterotic ridge. Two states are recognized in the sphenopterotic ridge as (a) absent or weak to be broadly covered with epaxial body muscle; (b) high, with a prominent process. Among outgroups, all galean taxa share state (a), while some squaleans have the similar condition to state (b) (Shirai, 1992a). Therefore, state (b) is estimated to be apomorphic. Coding: 0=(a); 1=(b)/status: binary (*Character 26*).

1-3-5. Projection for levator palatoquadrati. Two states are recognized in the projection for levator palatoquadrati as (a) absent; (b) present. Since all outgroups share state (a), the alternate state (b) is estimated to be apomorphic. Coding: 0=(a); 1=(b)/status: binary (*Character 27*).

1-3-6. Foramen for glossopharyngeal nerve. Two states are recognized in the foramen for glossopharyngeal nerve IX as (a) having no expansion; (b) fringed by an expansion. Since outgroups except most carcharhiniforms (e.g., *Halaelurus, Triakis* and *Carcharhinus*) share state (a), the alternate state (b) is estimated to be apomorphic. Coding: 0=(a); 1=(b)/status: binary (*Character 28*).

1-3-7. Posterior canal vacuity. Two states are recognized in the posterior canal vacuity as (a) absent; (b) present. Since all outgroups except *Scyliorhinus, Cephaloscyllium* and *Schroederichthys* share state (a), the alternate state (b) is estimated to be apomorphic. Coding: 0=(a); 1=(b)/status: binary (*Character 29*).

2-1-1. Post-palatoquadrate process. Two states are recognized in the post-palatoquadrate process as (a) absent; (b) present. Since all outgroups share state (a), the alternate state (b) is estimated to be apomorphic. Coding: 0=(a); 1=(b)/status: binary (*Character 30*).

2-1-2. Process of mandibula. Two states are recognized in the process of mandibula as (a) absent; (b) present. Since all outgroups share state (a), the alternate state (b) is estimated to be apomorphic. Coding: 0=(a); 1=(b)/status: binary (*Character 31*).

2-1-3. Accessory cartilage of palatoquadrate. Two states are recognized in the accessory cartilage of palatoquadrate as (a) absent; (b) present. Since all outgroups share state (a), the alternate state (b) is estimated to be an autapomorphy for *Stegostoma*.

2-1-4. Accessory cartilage on symphysis of mandibula. Three states are recognized in the accessory cartilage on symphyseal region of mandibula as (a) absent; (b) located behind the symphysis; (c) buried in rounded fenestra of mandibula. Since outgroups except some squaleans, e.g., *Centroscymnus, Scymnodon* and *Zameus* (according to Shirai, 1992a), share state (a), both states (b) and (c) are estimated to be apomorphic, respectively. Coding: 0=(a); 1=(b); 2=(c)/status: unordered (*Character 32*).

2-1-5. Accessory cartilage on mandibula. Two states are recognized in the accessory cartilage on mandibula as (a) absent; (b) present. Since all outgroups share state (a), the alternate state (b) is estimated to be apomorphic. Coding: 0=(a); 1=(b)/status: binary (*Character 33*).

2-1-6. Ligamentum cranio-palatoquadrati. Two states are recognized in the ligamentum cranio-palatoquadrati as (a) absent; (b) present. Since all outgroups share state (a), the alternate state (b) is estimated to be apomorphic. Coding: 0=(a); 1=(b)/

status: binary (*Character 34*).

2-1-7. Ethmoidal articulation. Three states are recognized in the ethmoidal articulation as (a) loose, via a thin and long ligament; (b) prominent, via a massive and flexible ligament; (c) tight. Among outgroups, all members which have the ethmoidal articulation represent state (b). Therefore, both states (a) and (c) are estimated to be apomorphic, respectively. Coding: 0=(b); 1=(a); 2=(c)/status: unordered (*Character 35*).

2-1-8. Tooth arrangements. Two states are recognized in the tooth arrangement as (a) imbricated overlap; (b) independent. Among outgroups, state (a) appears in the lower jaw of previous "squaloids" and a carcharhiniform *Hemipristis*, and state (b) is restricted in the lamniforms and a carcharhiniform *Pseudotriakis* (Compagno, 1988). Since any other members are categorized in the other "alternate overlap," the ON state is assigned as "?." Coding: 0=(a); 1=(b)/status: binary (*Character 36*).

2-1-9. Tooth morphology (A). Three states are recognized in the apron of tooth crown as (a) broadly expanded; (b) prominent, forming a stout process; (c) narrowly extended labially. Since outgroups, except some squalean species which have states (b) or (c), share state (a), states (b) and (c) are thus estimated to be apomorphic, respectively. Coding: 0=(a); 1=(b); 2=(c)/status: unordered (*Character 37*).

2-1-9. Tooth morphology (B). Two states are recognized in the lateral cusps of tooth crown as (a) absent in any teeth; (b) present at least in some teeth. Outgroups share state (b) except for some higher taxa of carcharhiniforms, lamniforms and squaleans. Therefore, state (a) is estimated to be an autapomorphy for *Rhincodon*.

2-2-1. Pharyngohyal. Two states are recognized in the pharyngohyal as (a) absent; (b) present. Since outgroups, except a few triakids (Luther, 1909a), share state (a), the alternate state (b) is estimated to be apomorphic. Coding: 0=(a); 1=(b)/status: binary (*Character 38*).

2-2-2. Ligamentum hyomandibulo-palatoquadrati. Two states are recognized in the ligamentum hyomandibulo-palatoquadrati as (a) absent; (b) present. Since all outgroups share state (b), the alternate state (a) is estimated to be apomorphic. Coding: 0=(b); 1=(a)/status: binary (*Character 39*).

2-2-3. Formation of branchial rays. Two states are recognized in the branchial rays articulating with hyomandibula and ceratohyal as (a) fused; (b) separated. Since outgroups, except *Halaelurus*, share state (b), the alternate state (a) is estimated to be apomorphic. Coding: 0=(b); 1=(a)/status: binary (*Character 40*).

2-2-4. Extrabranchial cartilage on hyoid arch. Two states are recognized in the extrabranchial cartilage on hyoid arch as (a) absent or fused with branchial rays; (b) isolated. Among outgroups, most squaleans, *Schroederichthys* and *Scyliorhinus* share state (b), whereas *Chlamydoselachus, Heterodontus*, lamniforms and most carcharhiniforms represent state (a). Thus, the ON state is assigned as state (a). Coding: 0=(a); 1=(b)/status: binary (*Character 41*).

2-2-5. Prespiracular cartilage. Two states are recognized in the prespiracular cartilage as (a) absent; (b) present. Among outgroups, lamniforms and hexanchoids share state (a), whereas the remaining taxa share state (b). Although in *Chlamydoselachus* it is ambiguous either (a) or (b) (Fürbringer, 1904; Allis, 1923; Shirai, 1992a), the ON state is assigned as state (b). Coding: 0=(b); 1=(a)/status: binary (*Character 42*).

2-3-1. Gill pickax. Two states are recognized in the gill pickax as (a) composed of pharyngobranchial γ-δ and epibranchial δ; (b) fused with epibranchial γ. Since outgroups, except for *Isistius* (see Shirai, 1992b), share state (a), the alternate state (b) is estimated to be an autapomorphy for *Rhincodon*.

2-3-2. Pre-epibranchial cartilage. Two states are recognized in the pre-epibranchial cartilage as (a) absent; (b) present. Since all outgroups share state (a), the alternate state (b) is estimated to be apomorphic. Coding: 0=(a); 1=(b)/status: binary (*Character 43*).

2-3-3. Branchial rays. Two states are recognized in the branchial rays as (a) articulating with both epibranchial and ceratobranchial; (b) articulating with only ceratobranchial. Since all outgroups share state (a), the alternate state (b) is estimated to be apomorphic. Coding: 0=(a); 1=(b)/status: binary (*Character 44*).

2-3-4. Branchial ray δ. Two states are recognized in the branchial ray δ as (a) absent; (b) present. Since outgroups, except *Lamna*, share state (b), the alternate state (a) is estimated to be apomorphic. Coding: 0=(b); 1=(a)/status: binary (*Character 45*).

2-3-5. Ventral extrabranchial cartilage γ. Two states are recognized in the ventral extrabranchial cartilage γ as (a) absent; (b) present. Since outgroups, except *Scyliorhinus* and *Cephaloscyllium*, share state (b), the alternate state (a) is estimated to be apomorphic. Coding: 0=(b); 1=(a)/status: binary (*Character 46*).

2-3-6. Association of ventral extrabranchial cartilage with ceratobranchial. Three states are recog-

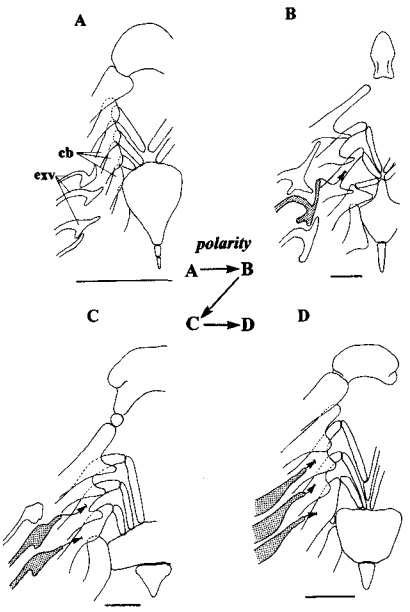

Fig. 76. Variations in the relationship between ventral extrabranchial cartilages and ceratobranchials and the possible polarity. (A) *Galeus eastmani* (HUMZ 118482); (B) *Cirrhoscyllium japonicum* (HUMZ 40057); (C) *Eucrossorhinus dasypogon* (CSIRO CA 4051); (D) *Ginglymostoma cirratum* (ZMUC P0629). Scales indicate 10 mm.

nized in the articulation of ventral extrabranchial cartilage with ceratobranchial as (a) present in arch $\beta 2$ (Fig. 76B); (b) present in arches $\beta 2$ and γ (Fig. 76C); (c) present in arches $\beta 1$-γ (Fig. 76D). A possible order (a)-(b)-(c) is attempted (Fig. 76). Since all outgroups with no articulation of the extrabranchial with the ceratobranchial in any arches (Fig. 76A), the ON state is assigned as an additional state (d) and a possible polarity is attempted (Fig. 76). Coding: 0=(d); 1=(a); 2=(b); 3=(c)/status: ordered (*Character 47*).

2-3-7. Dorsal extrabranchial cartilages. Two states are recognized in the last two dorsal extrabranchial cartilages as (a) separate; (b) fused. Since all outgroups share state (a), the alternate state (b) is estimated to be an autapomorphy for *Stegostoma*.

2-3-8. Inner process of ceratobranchial. Three states are recognized in the inner process of ceratobranchial for arch γ as (a) small and broadly expanded; (b) large and triangular-shaped; (c) hardly expanded. According to the first step, the ON state is assigned as state (a). Coding: 0=(a); 1=(b); 2=(c)/status: unordered (*Character 48*).

2-3-9. Shape of hypobranchial. Two states are recognized in the shape of hypobranchial as (a) long and thin; (b) small and triangular-shaped. Since all outgroups share state (a), the alternate state (b) is estimated to be an autapomorphy for *Rhincodon*.

2-3-10. Relationship between basibranchial and hypobranchial. Three states are recognized in the basibranchial as (a) composed of a single cartilage articulating with hypobranchials $\beta 2$-γ; (b) composed of a single cartilage articulating with all hypobranchials; (c) divided into four cartilaginous pieces. Among outgroups, some squalean taxa, *Heterodontus*, carcharhiniforms and lamniforms share state (a). Therefore, the ON state is assigned as state (a). Coding: 0=(a); 1=(b); 2=(c)/status: unordered (*Character 49*).

2-3-11. Accessory cartilage of basibranchial. Two states are recognized in the accessory cartilage of basibranchial as (a) isolated; (b) fused with basibranchial. Since outgroups, except *Chlamydoselachus* and hexanchoid taxa, share state (a), the alternate state (b) is estimated to be apomorphic. Coding: 0=(a); 1=(b)/status: binary (*Character 50*).

3. Process for levator pectoralis. The process for levator pectoralis is shared by all orectolobiforms (state a), whereas all outgroups except *Heterodontus* have no such process (state b). Therefore, state (a) is estimated to be apomorphic. Coding: 0=(b); 1=(a)/status: binary (*Character 51*).

3-1. Suprascapular cartilage. Two states are recognized in the suprascapular cartilage as (a) absent; (b) present. According to the first step (Ch. 29), the ON state is assigned as state (a). Coding: 0=(a); 1=(b)/status: binary (*Character 52*).

3-2. Apron of coracoid. Three states are recognized in the apron of coracoid as (a) expanded anteriorly, with no fenestra; (b) not expanded, with no fenestra; (c) expanded, with a fenestra. Since all outgroups share state (a), states (b) and (c) are apomorphic, respectively. Coding: 0=(a); 1=(b); 2=(c)/status: unordered (*Character 53*).

3-3. Foramen for brachial artery. Two states are recognized in the foramen for brachial artery as (a) absent; (b) present. Since all outgroups share state (a), the alternate state (b) is estimated to be apomorphic. Coding: 0=(a); 1=(b)/status: binary (*Character 54*).

3-4. Articular condyle of coracoid. Two states are recognized in the articular condyle of coracoid as (a) single (Fig. 77B); (b) divided into two (Fig. 77C). Although *Heterodontus* represents state (a), the other outgroups share more complicated condyles, which are termed glenoid fossa (glf; Fig. 77A; Maisey, 1982), different from those states of orectolobiforms. Therefore, the ON state is assigned as "?." Coding: 0=(a); 1=(b)/status: binary (*Character 55*).

3-5. Pectoral basal cartilages. Three states are recognized in the propterygium as (a) isolated; (b) fused with mesopterygium; (c) ambiguous, either "absent" or "fused." According to the first step, the ON

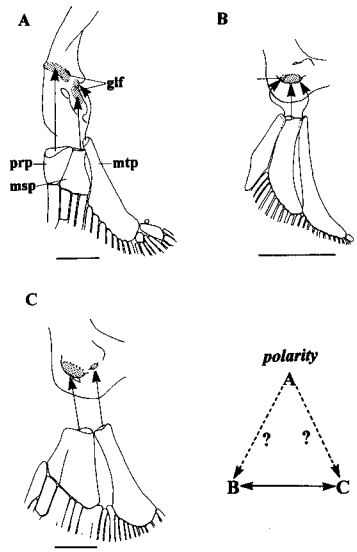

Fig. 77. Variations in the articulation of pectoral basal cartilages with coracoid and the possible polarity. (A) *Hemitriakis japanica* (HUMZ 105878); (B) *Eucrossorhinus dasypogon* (CSIRO CA 4051); (C) *Ginglymostoma cirratum* (ZMUC P0629). Scales indicate 10 mm.

state is assigned as state (a). Coding: 0=(a); 1=(b); 2=(c)/status: unordered (*Character 56*).

3-6. Metapterygium. Two states are recognized in the metapterygium as (a) articulating with articular condyle of coracoid; (b) articulating with mesopterygium. Since all outgroups share state (a), the alternate state (b) is estimated to be an autapomorphy for *Sutorectus*.

3-7. Development of metapterygial axis. Two states are recognized in the metapterygial axis as (a) absent; (b) present. Among outgroups, squaleans, *Heterodontus*, carcharhiniforms except *Schroederichthys* and *Scyliorhinus*, and lamniforms share a distinct state (b). Therefore, the alternate state (a) is estimated to be apomorphic. Coding: 0=(b); 1=(a)/status: binary (*Character 57*).

3-8. Number of pectoral radials. Two states are recognized in the number of radials in pectoral fin as (a) three; (b) more than four (up to 10). Since outgroups, except hexanchoids and *Heterodontus*, share state (a), the alternate state (b) is estimated to be apomorphic. Coding: 0=(a); 1=(b)/status: binary (*Character 58*).

3-9. Extension of pectoral radials. In this part, I cannot divide into the consistent states though previous authors used this character as informative for estimation of elasmobranch phylogeny in various taxa including fossils (e.g., Moy-Thomas, 1938; Compagno, 1988, 1990).

4-1. Prepelvic process. Two states are recognized in the prepelvic process as (a) rounded or bluntly pointed; (b) greatly projected anteriorly. Since outgroups except some scyliorhinids share state (a), the alternate state (b) is estimated to be apomorphic. Coding: 0=(a); 1=(b)/status: binary (*Character 59*).

4-2. Anterior pelvic basal. Two states are recognized in the anterior pelvic basal as (a) absent; (b) present. Since all outgroups share state (b), the alternate state (a) is estimated to be an autapomorphy for *Rhincodon*.

4-3. Number of pelvic radials. Two states are recognized in the number of radials in pelvic fin as (a) two; (b) three. Among outgroups, hexanchoids, *Chlamydoselachus* and *Heterodontus* share state (b), and the remaining taxa represent state (a). Therefore, the ON state is assigned to be equivocal. Coding: 0=(a); 1=(b)/status: binary (*Character 60*).

5-1. Basal cartilage of dorsal fin. I can not categorize this character into certain consistent states among taxa because minor variations are present within individuals and species.

5-2. Number of dorsal fin radials. Two states are recognized in the number of radials in dorsal fin as (a) two; (b) three. Among outgroups, most of the squaleans and carcharhiniforms, and lamniforms share state (a), whereas hexanchoid taxa and *Heterodontus* represent state (b). Although the dorsal fins of *Hybodus*, hypothesized as the sister group of the living elasmobranchs, has been described in a number of cases, only Koken (1907) described the number of the dorsal radial as two (equal to the state a) in *H. hauffianus*. Therefore, the ON state is assigned as state (a). Coding: 0=(a); 1=(b)/status: binary (*Character 61*)

5-3. Basal cartilages of anal fin. Two states are recognized in the basal cartilage of anal fin as (a) composed of small cartilaginous pieces; (b) fused into a single plate. According to the first step, the ON state is assigned as state (a), and the alternate state (b) is estimated to be an autapomorphy for *Rhincodon*.

5-4. Number of anal fin radials. Two states are recognized in the number of radials of anal fin as (a) two; (b) three. Since outgroups having anal fin share state (a), except for *Heterodontus* which have more than three radials, the alternate state (b) is estimated to be apomorphic. Coding: 0=(a); 1=(b)/status: binary (*Character 62*).

6-1. Neural arch. Two states are recognized in the neural arch formation as (a) completely segmented; (b) partly fused. Since outgroups except *Lamna* share state (a), the alternate state (b) is estimated to be an autapomorphy for *Rhincodon*.

6-2. Calcification of neural arch. Two states are

recognized in the calcification of neural arch as (a) absent ; (b) present. According to the first step, the ON state is assigned as state (b). Coding : 0=(b) ; 1=(a)/status : binary (*Character 63*).

6-3. Secondary calcification pattern. Four states are recognized in the secondary calcification pattern as (a) cyclospondylic ; (b) extending radially to intermedialia ; (c) extending radially not to intermedialia ; (d) concentric. Among outgroups, squaleans and most carcharhiniforms share state (a), while lamniforms and *Heterodontus* represent state (b) or (c) except for *Cetorhinus* having state (d) (Ridewood, 1921). Therefore, the ON state is assigned to be equivocal either (a), (b) or (c). Coding : 0=(a) ; 1=(b) ; 2=(c) ; 3=(d)/status : unordered (*Character 64*).

6-4. Ventral intercalary plate. Two states are recognized in the ventral intercalary plate as (a) absent ; (b) present. Among outgroups, some species of the squaleans represent state (b) (Shirai, 1992a), but most taxa have state (a). Therefore, state (b) is estimated to be apomorphic. Coding : 0=(a) ; 1=(b)/status : binary (*Character 65*).

6-5. Hemal arch formation. Three states are recognized in the hemal arch as (a) almost opened in precaudal diplospondylous vertebrae ; (b) partly closed by a thin cartilaginous bar ; (c) almost closed. According to the first step, the ON state is assigned as state (a). Coding : 0=(a) ; 1=(b) ; 2=(c)/status : unordered (*Character 66*).

6-6. Vertebral ribs on diplospondylous vertebrae. Two states are recognized in the ribs on the diplospondylous vertebrae as (a) absent ; (b) present. Since outgroups share state (a) except some scyliorhinid taxa, the alternate state (b) is estimated to be apomorphic. Coding : 0=(a) ; 1=(b)/status : binary (*Character 67*).

6-7. Prehypochordal cartilage. Two states are recognized in the prehypochordal cartilage as (a) absent ; (b) present. Among outgroups, state (b) is seen in some squalean taxa (Shirai, 1992a) and also in some scyliorhinids, while the remaining taxa share state (a). Therefore, state (b) is estimated to be apomorphic. Coding : 0=(a) ; 1=(b)/status : binary (*Character 68*).

6-8. Hypochordal process. Two states are recognized in the hypochordal process as (a) short ; (b) greatly elongated and segmented. The states of all outgroups are equal to state (a) though some taxa have the segmented cartilages on the basiventral processes near the lower caudal origin. Therefore, state (b) is regarded to be an autapomorphy for *Rhincodon*.

7-1. Extra bundle of rectus inferior. Orectolobiforms share the extra bundle of the rectus inferior associated with eyestalk (state a). While, it is absent in all outgroups (state b). Therefore, state (a) is estimated to be apomorphic. Coding : 0=(b) ; 1=(a)/status : binary (*Character 69*).

7-1-1. Origins of obliquus muscles (A). Two states are recognized in the obliquus muscles as (a) originating from interorbital wall ; (b) originating from supraorbital blade. Since all outgroups share state (a), the alternate state (b) is estimated to be apomorphic. Coding : 0=(a) ; 1=(b)/status : binary (*Character 70*).

7-1-1. Origins of obliquus muscles (B). Two states are additionally recognized in the obliquus muscles as (a) not crossed throughout from origin to insertion ; (b) crossed proximally. Among outgroups, *Heterodontus* except *H. francisci*, *Carcharhinus* and lamniforms share state (b), and the remaining taxa have the alternate state (a). Therefore, the ON state is assigned to be equivocal. Coding : 0=(a) ; 1=(b)/status : binary (*Character 71*).

7-1-2. Origins of rectus muscles. Two states are recognized in the rectus muscles as (a) originating in individuals ; (b) originating in a single muscle bundle ; (c) originating in a single tendon. A possible order (a)-(b)-(c) is attempted. Since outgroups except *Mitsukurina* share state (a), states (b) and (c) are apomorphic. Coding : 0=(a) ; 1=(b) ; 2=(c)/status : ordered (*Character 72*).

7-1-3. Origin of rectus externus. Two states are recognized in the origin of rectus externus as (a) anterior to foramen for ophthalmicus superficialis and profundus ; (b) posterior to the foramen. Since all outgroups share state (a), the alternate state (b) is estimated to be apomorphic. Coding : 0=(a) ; 1=(b)/status : binary (*Character 73*).

7-1-4. Extra bundle of rectus inferior (A). Three states are recognized in the origin of extra bundle of rectus inferior as (a) from interorbital wall ; (b) associated with tendon for rectus muscles. Since any states are absent in all the outgroups, the ON state is assigned as "?." Coding : 0=(a) ; 1=(b)/status : binary (*Character 74*).

7-1-4. Extra bundle of rectus inferior (B). Two states are recognized in the extra bundle of rectus inferior as (a) inserting on disc of eyestalk ; (b) inserting on stem of eyestalk. Since any states are absent in all outgroups, the ON state is assigned as "?." Coding : 0=(a) ; 1=(b)/status : binary (*Character 75*).

7-1-5. Extra bundle of rectus internus (A). Two states are recognized in the extra bundle of rectus internus as (a) absent ; (b) present. Since all outgroups share state (a), the alternate state (b) is estimated to be apomorphic. Coding : 0=(a) ; 1=(b)/status : binary (*Character 76*).

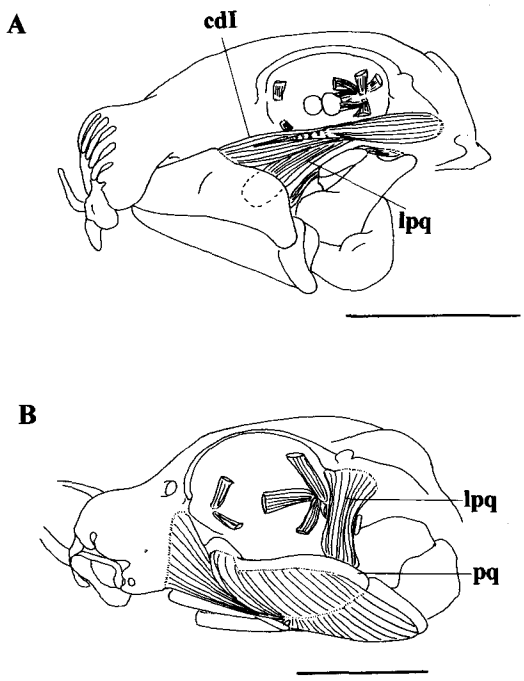

Fig. 78. Comparison of the constrictor dorsalis between *Hemiscyllium trispeculare* (SI0603.008) (A) and *Triakis semifasciata* (HUMZ 119338) (B). Scales indicate 10 mm.

7-1-5. Extra bundle of rectus internus (B). Two states are recognized in the origin of extra bundle of rectus internus as (a) on interorbital wall; (b) associated with tendon for rectus muscles. Since any states are absent in all outgroups, the ON state is assigned as "?." Coding: 0=(a); 1=(b)/status: binary (*Character 77*).

7-1-5. Extra bundle of rectus internus (C). Two states are recognized in the extra bundle of rectus internus as (a) inserting on stem of eyestalk; (b) inserting on disc of eyestalk. Since any states are absent in all outgroups, the ON state is assigned as "?." Coding: 0=(a); 1=(b)/status: binary (*Character 78*).

7-2-1. Muscle parietalis. Two states are recognized in the muscle parietalis as (a) absent; (b) present. Since outgroups except *Mitsukurina* share state (b), the alternate state (a) is estimated to be apomorphic. Coding: 0=(b); 1=(a)/status: binary (*Character 79*).

7-2-2. Extra bundle of muscle parietalis. Two states are recognized in the extra bundle of muscle parietalis as (a) absent; (b) present. Since outgroups except *Alopias* share state (a), the alternate state (b) is estimated to be an autapomorphy for *Stegostoma*.

8-1. Constrictor dorsalis (lpq, cdI: Fig. 78). Although the constrictor dorsalis consists of two muscle bundles in orectolobiforms (state a: Fig. 78A), it is only a single bundle (state b: Fig. 78B) in all outgroups. Therefore, state (a) is estimated to be apomorphic. Coding: 0=(b); 1=(a)/status: binary (*Character 80*).

8-1-1. Rostromandibularis. Two states are recognized in the rostromandibularis as (a) absent; (b) present. Since all outgroups share state (a), the alternate state (b) is estimated to be apomorphic. Coding: 0=(a); 1=(b)/status: binary (*Character 81*).

8-1-2. Levator palpebrae anterodorsalis. Two states are recognized in the levator palpebrae anterodorsalis as (a) absent; (b) present. Since all outgroups share state (a), the alternate state (b) is estimated to be apomorphic. Coding: 0=(a); 1=(b)/status: binary (*Character 82*).

8-1-3. Adductor mandibulae hyoideus. Two states are recognized in the adductor mandibulae hyoideus as (a) absent; (b) present. Since all outgroups share state (a), the alternate state (b) is estimated to be apomorphic. Coding: 0=(a); 1=(b)/status: binary (*Character 83*).

8-1-4. Adductor mandibulae IV. Two states are recognized in the adductor mandibulae IV as (a) absent; (b) present. Since all outgroups share state (a), the alternate state (b) is estimated to be apomorphic. Coding: 0=(a); 1=(b)/status: binary (*Character 84*).

8-1-5. Origin of suborbitalis (A). Two states are recognized in the suborbitalis as (a) originating from lateral margin of orbito-nasal process; (b) originating from dorsal surface of neurocranium. Since all outgroups share state (a), the alternate state (b) is estimated to be apomorphic. Coding: 0=(a); 1=(b)/status: binary (*Character 85*).

8-1-5. Origin of suborbitalis (B). Two states are recognized in the origin of suborbitalis as (a) not associated with interorbital wall (Fig. 79A); (b) associated with interorbital wall, not extending to fenestra of profundus canal (Fig. 79B); (c) associated with interorbital wall, covering the fenestra (Fig. 79C). A possible order (a)-(b)-(c) is attempted (Fig. 79). Since outgroups share state (a) except for some carcharhiniforms (e.g., *Schroederichthys* and *Hemitriakis*), states (b) and (c) are estimated to be apomorphic. Coding: 0=(a); 1=(b); 2=(c)/status: ordered (*Character 86*).

8-1-6. Extra bundle of suborbitalis. Two states are recognized in the extra bundle of suborbitalis as (a) absent; (b) present. Since all outgroups share state (a), the alternate state (b) is estimated to be an autapomorphy for *Ginglymostoma*.

8-1-7. Insertion of suborbitalis (A). Four states are recognized in the suborbitalis as (a) entirely inserting on adductor mandibulae I in a muscle bundle; (b) entirely inserting on adductor mandibulae I via a ten-

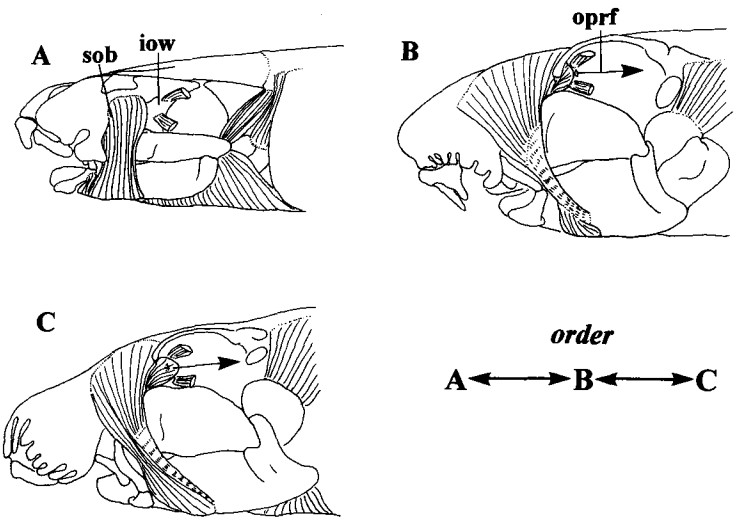

Fig. 79. Variations in the association of suborbitalis with interorbital wall and the possible order. (A) *Parascyllium collare* (AMS I30409002); (B) *Chiloscyllium indicum* (MCZ 54); (C) *Brachaelurus waddi* (AMS I20095033).

don; (c) partly inserting on mandibula via a tendon; (d) entirely inserting on mandibula via a tendon. Since all outgroups share state (a), the remaining states are estimated to be apomorphic. Coding: 0=(a); 1=(b); 2=(c); 3=(d)/status: unordered (*Character 87*).

8-1-7. Insertion of suborbitalis (B). Two states are recognized in the insertion of suborbitalis as (a) not associated with labial cartilage; (b) associated with lower labial cartilage. Since all outgroups share state (a), the alternate state (b) is estimated to be apomorphic. Coding: 0=(a); 1=(b)/status: binary (*Character 88*).

8-1-8. Origin of levator palatoquadrati (A). Two states are recognized in the levator palatoquadrati as (a) originating from otic capsule; (b) originating from interorbital wall. Since all outgroups except *Carcharhinus* share state (a), the alternate state (b) is estimated to be apomorphic. Coding: 0=(a); 1=(b)/status: binary (*Character 89*).

8-1-8. Origin of levator palatoquadrati (B). Two states are additionally recognized in the levator palatoquadrati as (a) originating in a muscle bundle; (b) originating via a tendon. Since all outgroups share state (a), the alternate state (b) is estimated to be apomorphic. Coding: 0=(a); 1=(b)/status: binary (*Character 90*).

8-1-9. Insertion of levator palatoquadrati. Two states are recognized in the levator palatoquadrati as (a) inserting on palatoquadrate; (b) inserting on both palatoquadrate and mandibula. Since all outgroups share state (a), the alternate state (b) is estimated to be apomorphic. Coding: 0=(a); 1=(b)/status: binary (*Character 91*).

8-1-10. Constrictor dorsalis I. Two states are recognized in the constrictor dorsalis I as (a) composed of a single muscle bundle; (b) composed of a single bundle with a tendon proximally; (c) composed of a single bundle with a tendon distally; (d) composed of two crossed bundles, each with a tendon. Because any states are absent in outgroups, the ON state is assigned as "?." Coding: 0=(a); 1=(b); 2=(c); 3=(d)/status: unordered (*Character 92*).

8-1-11. Insertion of constrictor dorsalis I. Two states are recognized in the constrictor dorsalis I as (a) inserting on center of palatoquadrate; (b) inserting on post-palatoquadrate process. Since all outgroups share state (a), the alternate state (b) is estimated to be apomorphic. Coding: 0=(a); 1=(b)/status: binary (*Character 93*).

8-1-12. Spiracularis. Two states are recognized in the spiracularis as (a) absent; (b) present. Among outgroups, the taxa except carcharhiniforms, *Mitsukurina* and *Lamna* share state (b). Therefore, the ON state is estimated to be equivocal. Coding: 0=(b); 1=(a)/status: binary (*Character 94*).

8-1-13. Subdivision of spiracularis. Two states are recognized in the spiracularis as (a) with no subdivision; (b) with a subdivision inserting on mandibula. All outgroups having spiracularis share state (a), but the ancestral state of the sister group cannot determined. Therefore, the ON state is assigned as "?." Coding: 0=(a); 1=(b)/status: binary (*Character 95*).

8-1-14. Intermandibularis. Two states are recognized in the intermandibularis as (a) composed of a single muscle sheet; (b) divided into two muscle sheets. Since all outgroups share state (a), the alternate state (b)

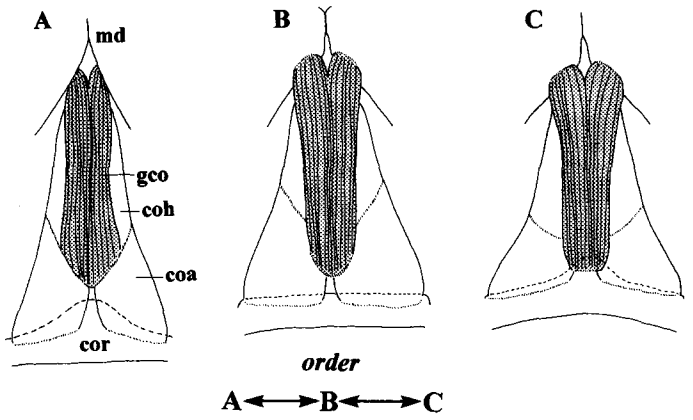

Fig. 80. Diagrams of the variations of genio-coracoideus and the possible order.

is estimated to be apomorphic. Coding: 0=(a); 1=(b)/status: binary (*Character 96*).

8-1-15. Insertion of intermandibularis. Two states are recognized in the insertion of intermandibularis as (a) not associated with palatoquadrate; (b) associated with palatoquadrate. Since all outgroups share state (a), the alternate state (b) is estimated to be apomorphic. Coding: 0=(a); 1=(b)/status: binary (*Character 97*).

8-2. Constrictor hyoideus dorsalis. In orectolobiforms, the constrictor hyoideus dorsalis is completely separated from the adjacent constrictor muscles (State a). While, outgroups except *Heterodontus* have the muscle unifying the succeeding constrictors (state b). Therefore, state (a) is estimated to be apomorphic. Coding: 0=(b); 1=(a)/status: binary (*Character 98*).

8-2-1. Insertion of constrictor hyoideus dorsalis. Two states are recognized in the insertion of constrictor hyoideus dorsalis as (a) not associated with ceratohyal; (b) associated with ceratohyal. Since outgroups except *Alopias* share state (a), the alternate state (b) is estimated to be apomorphic. Coding: 0=(a); 1=(b)/status: binary (*Character 99*).

8-3. Insertion of coracobranchialis. In orectolobiforms, the coraco-branchialis is inserting on both ceratobranchial and hypobranchial at least in arches β1-2 (state a). Among outgroups, this state is found in *Triakis*, and in arches β2-γ of *Squalus*, whereas this muscle inserts only on the hypobranchial in most outgroups; only on the ceratobranchial in some squaleans (Shirai, 1992a). Herein, the latter two states are regarded as primitive (state b), and state (a) is estimated to be apomorphic. Coding: 0=(b); 1=(a)/status: binary (*Character 100*).

8-3-1. Origin of genio-coracoideus. Three states are recognized in the genio-coracoideus as (a) originating from fascia of coraco-hyoideus (Fig. 80A); (b) originating from fascia of coraco-arcualis (Fig. 80B); (c) associated with coracoid (Fig. 80C). A possible order (a)-(b)-(c) is attempted (Fig. 80). Among outgroups, state (a) is shared by some squaleans (e.g., *Chlamydoselachus*, hexanchoid taxa, *Echinorhinus, Centropholus, Cirrhigaleus, Deania* and *Squalus*; Davidson, 1918; Allis, 1923; Smith, 1937; Shirai, 1992a) and most galeans; state (b) is shared by squaleans like *Etmopterus, Euprotomicrus* and *Squaliolus* (Shirai, 1992a) and carcharhiniform *Schroederichthys* and *Hemitriakis*; state (c) is shared by most squaleans and some carcharhiniforms like *Prionace* (Edgeworth, 1935). Thus, the ON state is assigned as state (a). Coding: 0=(a); 1=(b); 2=(c)/status: ordered (*Character 101*).

8-3-2. Insertion of genio-coracoideus. Two states are recognized in the genio-coracoideus as (a) inserting on ventral surface of mandibula; (b) inserting on lingual surface of mandibula. Since outgroups except *Heterodontus* share state (b), the alternate state (a) is estimated to be apomorphic. Coding: 0=(b); 1=(a)/status: binary (*Character 102*).

8-3-3. Origin of coraco-arcualis. Two states are recognized in the coraco-arcualis as (a) originating at anterior terminal of hypaxial; (b) not associated with hypaxial directly. Since outgroups except *Triakis, Hemitriakis* and *Carcharhinus* share state (b), the alternate state (a) is estimated to be apomorphic. Coding: 0=(b); 1=(a)/status: binary (*Character 103*).

8-3-4. Coraco-branchialis γ. Two states are recognized in the coraco-branchialis γ as (a) incompletely isolated proximally; (b) completely isolated. Since all outgroups share state (a), the alternate state (b) is estimated to be apomorphic. Coding: 0=(a); 1=(b)/status: binary (*Character 104*).

8-3-5. Origin of coraco-branchialis. Two states are recognized in the coraco-branchialis as (a) directly associated with coracoid; (b) not associated with cor-

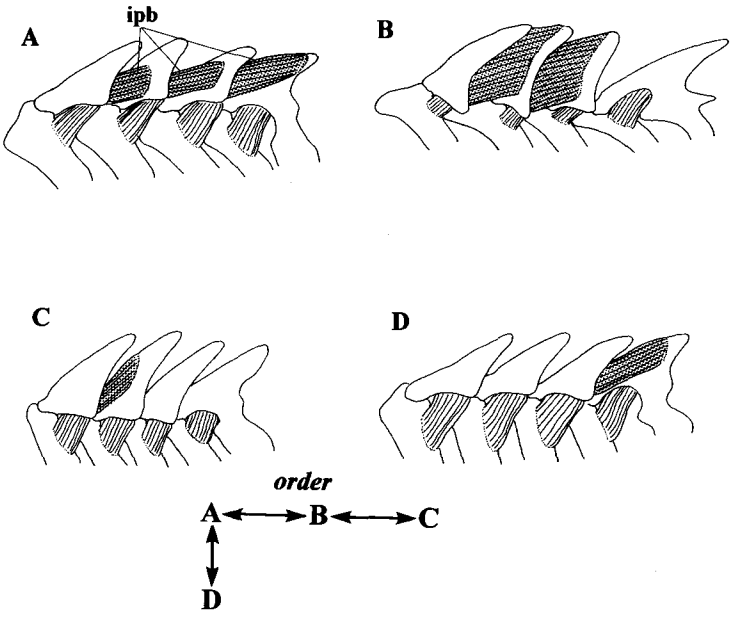

Fig. 81. Diagrams of the variations of interpharyngobranchialis and the possible order.

acoid. Since the outgroups except *Lamna* share the state (a), the alternate state (b) is estimated to be an autapomorphy for *Rhincodon*.

8-3-6. Insertion of coraco-branchialis. Four states are recognized from the insertion of coraco-branchialis as (a) not associated with ventral extrabranchial cartilages; (b) associated with ventral extrabranchial cartilage γ; (c) associated with ventral extrabranchial cartilage $\beta 2$. Since all outgroups share state (a), states (b) and (c) are estimated to be apomorphic, respectively. Among them, state (c) is an autapomorphy for *Ginglymostoma*. Coding: 0=(a) or (c); 1=(b)/status: binary (*Character 105*).

8-4-1. Subspinalis. Two states are recognized in the subspinalis as (a) absent; (b) present. Since all outgroups share state (b), the alternate state (a) is estimated to be an autapomorphy for *Brachaelurus*.

8-4-2. Interpharyngobranchialis. Four states are recognized in the interpharyngobranchialis as (a) all bundles present (Fig. 81A); (b) third bundle absent (Fig. 81B); (c) second and third bundles absent (Fig. 81C); (d) first and second bundles absent (Fig. 81D). Following two possible orders are attempted as (a)-(b)-(c) and (a)-(d) (Fig. 81), and I treat them as two isolated characters. Since all outgroups share state (a), the states (b) to (d) are estimated to be apomorphic, respectively. Coding: 0=(a); 1=(b); 2=(c)/status: ordered (*Character 106*); 0=(a); 1=(d)/status: binary (*Character 107*).

8-5-1. Development of constrictor branchiales superficialis. Two states are recognized in the constrictor branchiales superficialis as (a) entirely covering branchial arches superficially; (b) with exposed regions on extrabranchials. Since all outgroups share state (a), the alternate state (b) is estimated to be apomorphic. Coding: 0=(a); 1=(b)/status: binary (*Character 108*).

8-5-2. Development of interbranchialis. Two states are recognized in the interbranchialis as (a) entirely covering branchial rays; (b) with exposed regions on branchial rays. Since all outgroups share state (a), the alternate state (b) is estimated to be apomorphic. Coding: 0=(a); 1=(b)/status: binary (*Character 109*).

8-5-3. Subdivision of interbranchialis. Three states are recognized in the subdivision of interbranchialis as (a) absent; (b) composed of muscle fibers only; (c) divided into two bundles via a tendon. Since all outgroups share state (a), states (b) and (c) are estimated to be apomorphic, respectively. Coding: 0=(a); 1=(b); 2=(c)/status: unordered (*Character 110*).

8-5-4. Association of branchial arch with hypaxial. Two states are recognized in the association of branchial arch δ with hypaxial body muscle as (a) absent; (b) present. Since all outgroups share state (a), the alternate state (b) is estimated to be apomorphic. Coding: 0=(a); 1=(b)/status: binary (*Character 111*).

9. Levator pectoralis inferior (Fig. 82). Orectolobiforms have the levator pectoralis inferior (state a; Fig. 82B-E), while outgroups except *Heterodontus* have no such muscle bundle (state b; Fig. 82A). Therefore, the ON state is assigned as state (b). Cod-

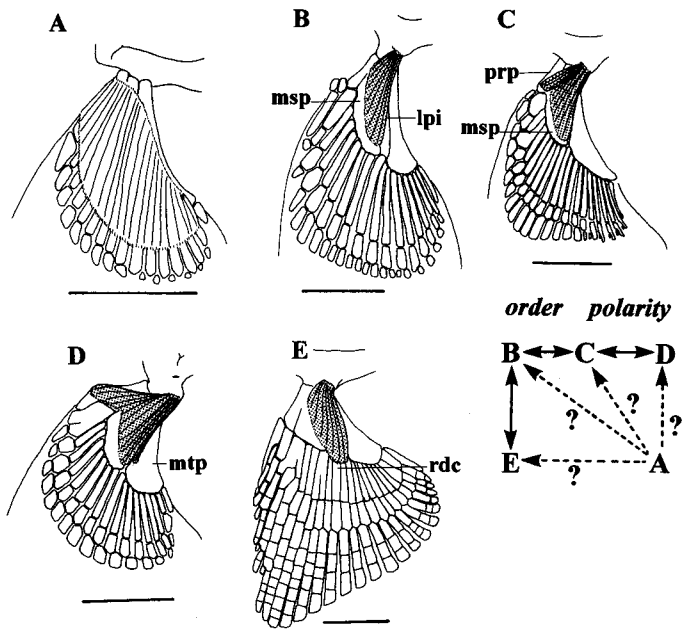

Fig. 82. Variations of levator pectoralis and fin skeletons, and the possible order and polarity. (A) *Triakis semifasciata* (HUMZ 119338); (B) *Chiloscyllium indicum* (MCZ 54); (C) *Orectolobus maculatus* (WAM P28414.001); (D) *Brachaelurus waddi* (AMS I20095033); (E) *Ginglymostoma cirratum* (ZMUC P0629). Scales indicate 10 mm.

ing: 0=(b); 1=(a)/status: binary (*Character 112*).

9-1. Insertion of levator pectoralis inferior. Four states are recognized in the levator pectoralis inferior as (a) inserting on mesopterygium only (Fig. 82B); (b) inserting on propterygium and mesopterygium (Fig. 82C); (c) inserting on all basal cartilages (Fig. 82D); (d) inserting on mesopterygium and radials (Fig. 82E). Two possible orders are attempted as (a)-(b)-(c) and (a)-(d) (Fig. 82), and I treat them as two isolated characters. Since there are no any states in outgroups (Fig. 82A), the ON states are assigned as "?." Coding: 0=(a); 1=(b); 2=(c)/status: ordered (*Character 113*); 0=(a); 1=(d)/status: binary (*Character 114*).

11. Inclinator dorsalis (Fig. 83). In orectolobiforms, the inclinator dorsalis originates from the distal regions of basal cartilages (State a; Fig. 83B), whereas it originates from the proximal regions of basal cartilages in outgroups (state b; Fig. 83A). Therefore, the ON state is assigned as state (b). Coding: 0=(b); 1=(a)/status: binary (*Character 115*).

11-1. Extra bundle of inclinator dorsalis. Two states are recognized in the extra bundle of inclinator dorsalis as (a) absent; (b) present. Since all outgroups share state (a), the alternate state (b) is estimated to be apomorphic. Coding: 0=(a); 1=(b)/status: binary (*Character 116*).

12-1. Rostronuchal and ethmonuchal muscles. Two states are recognized in the rostronuchal and ethmonuchal muscles as (a) absent; (b) present. Since all

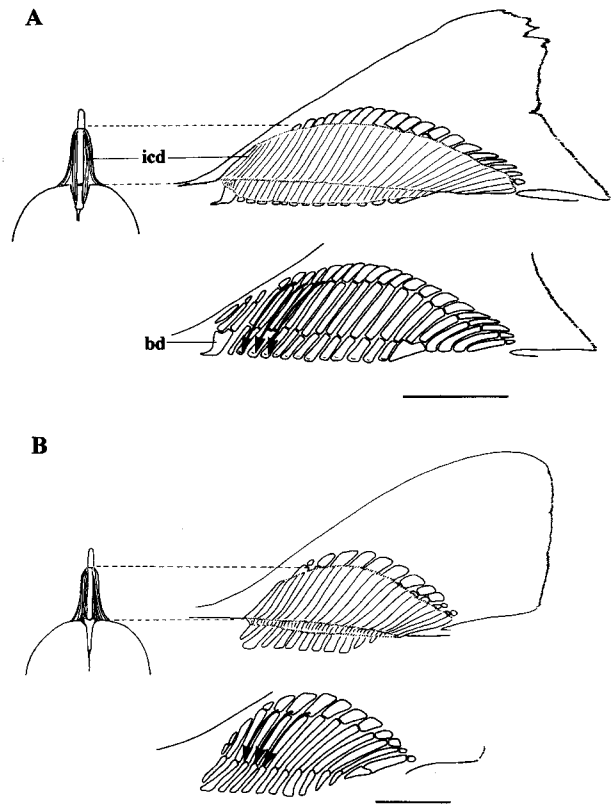

Fig. 83. Comparison of inclinator dorsalis between *Hemitriakis japanica* (HUMZ 105878) (A) and *Chiloscyllium plagiosum* (unregistered specimen of NSMT) (B). Scales indicate 10 mm.

outgroups share state (a), the alternate state (b) is estimated to be apomorphic. Coding : 0=(a) ; 1=(b)/status : binary (*Character 117*).

12-2. Flexor caudalis. Two states are recognized in the flexor caudalis as (a) not extending to origin of lower caudal lobe ; (b) extending anterior to the origin. Since outgroups except "hypnosqualean group" (Shirai, 1992a, c) share state (a), the alternate state (b) is estimated to be apomorphic. Coding : 0=(a) ; 1=(b)/status : binary (*Character 118*).

13-1. Relationship between infraorbital canal and postorbital process. Two states are recognized in the infraorbital canal as (a) passing through groove on postorbital process ; (b) passing behind the process. Since outgroups except scyliorhinids and triakids, in which it passes through the groove or fenestra on the postorbital process, share state (b), the alternate state (a) is estimated to be apomorphic. Coding : 0=(b) ; 1=(a)/status : binary (*Character 119*).

13-2. Relationship between hyomandibular and mandibular canals. Two states are recognized in the hyomandibular and mandibular canals as (a) separate ; (b) continuous. Most outgroups share state (a), whereas *Chlamydoselachus, Heterodontus*, carcharhinids like *Scoliodon* and some species of the *Carcharhinus, Mitsukurina, Carcharias* and *Alopias* represent state (b) (Allis, 1923 ; Chu and Wen, 1963). Therefore, the ON state is assigned as state (b) under the outgroup comparison. Coding : 0=(b) ; 1=(a)/status : binary (*Character 120*).

13-3. Mandibular canal. Two states are recognized in the mandibular canal as (a) continuous at symphyseal region ; (b) separate. Since outgroups except most rajiform skates and rays (Chu and Wen, 1963) share state (b), the alternate state (a) is estimated to be apomorphic. Coding : 0=(b) ; 1=(a)/status : binary (*Character 121*).

14-1. Hyoid group of ampullae of Lorenzini. Two states are recognized in the hyoid group of the ampullae of Lorenzini as (a) absent ; (b) present. Among outgroups, carcharhiniforms and lamniforms share state (a), whereas the other outgroups share state (b). Therefore, the ON state is assigned to be equivocal. Coding : 0=(a) ; 1=(b)/status : binary (*Character 122*).

14-2. Tubules of buccal group of ampullae of Lorenzini. Two states are recognized in the tubules of buccal group of ampullae of Lorenzini as (a) not extending to first gill opening ; (b) extending over pectoral girdle. Since all outgroups share state (a), the alternate state (b) is estimated to be apomorphic. Coding : 0=(a) ; 1=(b)/status : binary (*Character 123*).

15. Nasal barbel. Orectolobiforms share the nasal barbel including two states as (a) having cartilaginous support ; (b) having no cartilaginous support. While most outgroups have no barbel on the anterior nasal flap (c). Although *Cirrhigaleus, Pristiopholus*, some scyliorhinids and *Furgaleus* have the similar barbel, at least those of *Cirrhigaleus* and *Pristiopholus* are primarily different on the basis of the nerve innervation (Shirai, 1992a ; Goto et al., 1994). Therefore, the ON state is assigned as state (c). Coding : 0=(c) ; 1=(a) ; 2=(b)/status : unordered (*Character 124*).

15. Oronasal groove. Orectolobiforms share the oronasal groove (state a), whereas outgroups except *Heterodontus* and some scyliorhinids (e.g., *Atelomycterus, Haploblepharus* and *Scylliogaleus* ; Compagno, 1984) have no groove between nostril and mouth (state b). Compagno (1988) mentioned that the groove found in carcharhiniforms differs from those of orectolobiforms and *Heterodontus* morphologically. Therefore, the ON state should be assigned as state (b). Coding : 0=(b) ; 1=(a)/status : binary (*Character 125*).

15-1. Nasal barbel. Two states are recognized in the shape of the nasal barbel as (a) simple ; (b) branched. Most outgroups represent no states among them, whereas it is simple in the taxa with a barbel. However, the ON state is assigned as "?," because the ancestral state of the sister group is ambiguous. Coding : 0=(a) ; 1=(b)/status : binary (*Character 126*).

15-2. Circumnarial fold. Two states are recognized in the circumnarial fold as (a) absent ; (b) present. Since outgroups except *Heterodontus* share state (a), the alternate state (b) is estimated to be apomorphic. Coding : 0=(a) ; 1=(b)/status : binary (*Character 127*).

15-3. Symphyseal groove. Two states are recognized in the symphyseal groove as (a) absent ; (b) present. Since all outgroups share state (a), the alternate state (b) is estimated to be apomorphic. Coding : 0=(a) ; 1=(b)/status : binary (*Character 128*).

15-4. Lower labial furrow. Three states are recognized in the lower labial furrow as (a) forming a small and oval fold ; (b) forming paired, large dermal folds ; (c) forming a single, large dermal fold. A possible order (a)-(b)-(c) is attempted. Since outgroups having lower labial furrow share state (a), states (b) and (c) are estimated to be apomorphic. Coding : 0=(a) ; 1=(b) ; 2=(c)/status : ordered (*Character 129*).

15-5. Subocular pocket. Two states are recognized in the subocular pocket as (a) absent ; (b) present. Outgroups except carcharhiniforms share state (a). Compagno (1988) pointed out that the subocular pocket of orectolobiforms and carcharhiniforms seem to be derived in parallel because of the differences of the musculature support. Thus, the ON state is assigned as state (a). Coding : 0=(a) ; 1=(b)/status : binary

(*Character 130*).

15-6. Dermal lobe on head. Three states are recognized in the dermal lobe on head as (a) absent; (b) simple, not distributed on lower jaw; (c) branched, not distributed on the lower jaw; (d) greatly branched, distributed on lower jaw. A possible order (a)-(b)-(c)-(d) is attempted. Since all outgroups share state (a), the remaining states (b) to (d) are estimated to be apomorphic. Coding: 0=(a); 1=(b); 2=(c); 3=(d)/status: ordered (*Character 131*).

15-7. Throat barbel. Two states are recognized in the throat barbel as (a) absent; (b) present. Since all outgroups share state (a), the alternate state (b) is estimated to be an autapomorphy for *Cirrhoscyllium*.

15-8. Dorsal spiracular caecum. Three states are recognized in the dorsal spiracular caecum as (a) absent; (b) not extending to otic capsule; (c) extending to the capsule. Among outgroups, carcharhiniforms, *Heterodontus* and some squalean taxa (e.g., *Squalus, Squatina* and *Heptanchus*; Ridewood, 1896) share state (c), while I cannot find it within lamniform taxa. Therefore, the ON state is estimated as state (c). Coding: 0=(c); 1=(b); 2=(a)/status: unordered (*Character 132*).

15-9. Supraocular knob. Two states are recognized in the supraocular knob as (a) absent; (b) present. Since all outgroups share state (a), the alternate state (b) is estimated to be apomorphic. Coding: 0=(a); 1=(b)/status: binary (*Character 133*).

15-10. Last interbranchial septum. Two states are recognized in the last interbranchial septum as (a) with gill filaments on both sides; (b) with no gill filaments on posterior side. Since all outgroups share state (a), the alternate state (b) is estimated to be apomorphic. Coding: 0=(a); 1=(b)/status: binary (*Character 134*).

15-11. Dermal ridges on back and lateral surface of body. Two states are recognized in the dermal ridges as (a) absent; (b) present. Since outgroups except some species of *Carcharhinus* share state (a), the alternate state (b) is estimated to be apomorphic. Coding: 0=(a); 1=(b)/status: binary (*Character 135*).

15-12. Position of anal fin. Two states are recognized in the position of the anal fin as (a) separate from lower caudal lobe; (b) close to lower caudal lobe; (c) overlapping lower caudal lobe. A possible order (a)-(b)-(c) is attempted. Since outgroups, except *Chlamydoselachus, Mitsukurina* and *Apristurus*, share state (a), states (b) and (c) are estimated to be apomorphic. Coding: 0=(a); 1=(b); 2=(c)/status: ordered (*Character 136*).

15-13. Precaudal notch. Two states are recognized in the precaudal notch as (a) absent; (b) present. Since outgroups, except some lamniforms and carcharhinids, share state (a), the alternate state (b) is estimated to be an autapomorphy for *Rhincodon*.

15-14. Caudal fin. Two states are recognized in the shape of the caudal fin as (a) with no lower caudal lobe; (b) lunate. Since outgroups except some lamniforms share state (a), the alternate state (b) is estimated to be an autapomorphy for *Rhincodon*.

VI. Interrelationships within Orectolobiformes

1. Results of computer analysis

On the basis of this character analysis, 136 characters including 110 binary and 26 multistate characters (Table 2) were available without autapomorphies for the second step (Appendix 3). Among multistate characters, eight are ordered. Depending upon the data matrix for 22 orectolobiform species, six most parsimonious trees (length=229, CI=0.760, RI=0.919) were provided by the branch and bound algorithm under the ACCTRAN option of PAUP ver. 3.0. These cladograms are almost same, with differences of the topology among the species including *Orectolobus, Sutorectus* and *Eucrossorhinus*. The strict consensus tree is shown in Fig. 84.

2. Description of cladogram

The set of morphological evidence that supports each node is summarized as follows. The letter "r" added on the character number indicates a reversal.

According to the first analysis, Orectolobiformes is defined by two characters: foramen for ophthalmicus profundus V fused with that of ophthalmicus superficialis V-VII; inner process prominent located on the medial region of ceratobranchial. Based on the second step, clade A is supported by additional 17 apomorphic characters 10-2, 19-1, 29-1, 47-1, 51-1, 57-1, 69-1, 80-1, 98-1, 100-1, 106-1, 112-1, 115-1, 124-1, 125-1, 127-1 and 130-1. This clade is divided into clades B and D.

Clade B contains all species of *Parascyllium* and *Cirrhoscyllium*. It is well defined by 41 apomorphies 1-1, 3-1, 7-1, 8-1, 11-1, 15-1, 17-1, 18-1, 22-1, 24-1, 25-1, 30-1, 32-1, 33-1, 35-1, 42-1, 44-1, 45-1, 48-1, 56-2, 59-1, 66-1, 67-1, 68-1, 79-1, 81-1, 82-1, 88-1, 89-1, 91-1, 93-1, 97-1, 99-1, 104-1, 105-1, 111-1, 116-1, 117-1, 124-2, 132-1 and 134-1. This clade is divided into clades B1 and C. Clade B1 consisting of *Cirrhoscyllium* has no apomorphies. Clade C contains all species of *Parascyllium*. It is supported by an apomorphy 12-1.

Clade D contains all orectolobiform taxa excluding *Parascyllium* and *Cirrhoscyllium*. It is well defined by

Table 2. Character states and coding for second step.

Character	Coding	Status	ON state
1	Nasal capsule completely closed (0) ; having slit-like fenestrae (1)	Binary	0
2	Rim of nasal capsule nearly straight or undulated (0) ; with brush-like processes (1)	Binary	0
3	Outer nasal cartilage isolated from nasal capsule(0) ; fused with nasal capsule (1)	Binary	0
4	Inner nasal cartilage absent (0) ; present (1)	Binary	0
5	Extra cartilages of nasal cartilages absent (0) ; present (1)	Binary	0
6	Inter-nasal septum present (0) ; absent (1)	Binary	0
7	Orbito-nasal process cylindrical (0) ; laterally reduced (1) ; divided into two plates (2)	Unordered	0
8	Fenestra on orbito-nasal process absent (0) ; present (1)	Binary	0
9	Efferent opening for orbito-nasal vein in nasal chamber (0) ; at orbito-nasal process (1)	Binary	0, 1
10	Epiphyseal foramen absent (0) ; present, isolated (1) ; preesnt, fused with prefrontal fontanelle (2)	Unordered	0
11	Supraorbital crest present (0) ; absent (1)	Binary	0
12	Supraorbital region completely closed (0) ; interrupted (1)	Binary	0
13	Supraorbital blade absent (0) ; present (1)	Binary	0
14	Shape of postorbital process pointed (0) ; with a vertical groove (1)	Binary	0
15	Preorbital canal present (0) ; absent (1)	Binary	0
16	Preorbital canal small and extending anterodorsally (0) ; large and vertical (1)	Binary	0
17	Profundus canal present (0) ; absent (1)	Binary	0
18	Foramina for optic and oculomotor nerves separated (0) ; fused (1)	Binary	0
19	Foramen for hyomandibularis VII isolated (0) ; fused with main foramen for V-VII nerves (1)	Binary	0
20	Foramen for abducens VI fused with main foramen for V-VII nerves (0) ; isolated (1)	Binary	0
21	Foramina for pseudobranchial artery and pituitary vein separate (0) ; fused (1)	Binary	0
22	Foramen for orbital artery present (0) ; absent (1)	Binary	0
23	Foramen for internal carotid artery paired (0) ; single (1) ; fused with foramen for orbital artery (2)	Unordered	0
24	Endolymphatic fossa present (0) ; absent (1)	Binary	0
25	Ascending process of endolymphatic fossa present (0) ; absent (1)	Binary	0
26	Sphenopterotic ridge absent or weak (0) ; high, with a prominent process (1)	Binary	0
27	Projection for levator palatoquadrati absent (0) ; present (1)	Binary	0
28	Foramen for glossopharyngeal nerve having no expansion (0) ; fringed by an expansion (1)	Binary	0
29	Posterior canal vacuity absent (0) ; present (1)	Binary	0
30	Post-palatoquadrate process absent (0) ; present (1)	Binary	0
31	Process of mandibula absent (0) ; present (1)	Binary	0
32	Accessory cartilage on symphysis of mandibula absent (0) ; behind symphysis (1) ; buried in fenestra (2)	Unordered	0
33	Accessory cartilage on mandibula absent (0) ; present (1)	Binary	0
34	Ligamentum cranio-palatoquadrati absent (0) ; present (1)	Binary	0
35	Ethmoidal articulation prominent, via a massive and flexible ligament (0) ; loose (1) ; tight (2)	Unordered	0
36	Tooth arrangements imbricated overlap (0) ; independent (1)	Binary	?
37	Apron of tooth crown broadly expanded (0) ; prominent, forming a stout process (1) ; narrowly extended labially (2)	Unordered	0
38	Pharyngohyal absent (0) ; present (1)	Binary	0
39	Ligamentum hyomandibulo-palatoquadrati present (0) ; absent (1)	Binary	0
40	Branchial rays articulating with hyomandibula and ceratohyal separated (0) ; fused (1)	Binary	0
41	Extrabranchial cartilage on hyoid arch absent or fused with branchial rays (0) ; isolated (1)	Binary	0
42	Prespiracular cartilage present (0) ; absent (1)	Binary	0
43	Pre-epibranchial cartilage absent (0) ; present (1)	Binary	0
44	Branchial rays articulating with epibranchial and ceratobranchial (0) ; with only ceratobranchial (1)	Binary	0
45	Branchial ray δ present (0) ; absent (1)	Binary	0
46	Ventral extrabranchial cartilage γ present (0) ; absent (1)	Binary	0
47	Articulation of ventral extrabranchial cartilage with ceratobranchial absent (0) ; in arch $\beta 2$ (1) ; in arches $\beta 2$ and γ (2) ; in arches $\beta 1$-γ (3)	Ordered	0
48	Inner process of ceratobranchial for arch γ small and broadly expanded (0) ; large and triangular (1) ; hardly expanded (2)	Unordered	0

Table 2. Continued.

Character	Coding	Status	ON state
49	Basibranchial composed of a single cartilage articulating with hypobranchials β2-γ (0); a single cartilage articulating with all hypobranchials (2); divided into four cartilaginous pieces (3)	Unordered	0
50	Accessory cartilage of basibranchial isolated (0); fused with basibranchial (1)	Binary	0
51	Process for levator pectoralis absent (0); present (1)	Binary	0
52	Suprascapular cartilage absent (0); present (1)	Binary	0
53	Apron of coracoid expanded anteriorly, with no fenestra (0); not expanded, with no fenestra (1); expanded, with a fenestra (2)	Unordered	0
54	Foramen for brachial artery absent (0); present (1)	Binary	0
55	Articular condyle of coracoid single (0); divided into two (1)	Binary	?
56	Propterygium isolated (0); fused with mesopterygium (1); ambiguous, either "absent" or "fused" (2)	Unordered	0
57	Metapterygial axis present (0); absent (1)	Binary	0
58	Number of radials in pectoral fin three (0); more than four (1)	Binary	0
59	Prepelvic process rounded or bluntly pointed (0); greatly projected anteriorly (1)	Binary	0
60	Number of radials in pelvic fin two (0); three (1)	Binary	0, 1
61	Number of radials in dorsal fin two (0); three (1)	Binary	0
62	Number of radials of anal fin two (0); three (1)	Binary	0
63	Calcification of neural arch present (0); absent (1)	Binary	0
64	Secondary calcification pattern cyclospondylic (0); extending radially to intermedialia (1); extending radially not to intermedialia (2); concentric (3)	Unordered	0, 1, 2
65	Ventral intercalary plate absent (0); present (1)	Binary	0
66	Hemal arch almost opened in precaudal diplospondylous vertebrae (0); partly closed (1); almost closed (2)	Unordered	0
67	Ribs on diplospondylous vertebrae absent (0); present (1)	Binary	0
68	Prehypochordal cartilage absent (0); present (1)	Binary	0
69	Extra bundle of rectus inferior absent (0); present (1)	Binary	0
70	Obliquus muscles originating from interorbital wall (0); from supraorbital blade (1)	Binary	0
71	Obliquus muscles not crossed throughout from origin to insertion (0); crossed proximally (1)	Binary	0, 1
72	Rectus muscles originating in individuals (0); in a single muscle bundle (1); in a single tendon (2)	Ordered	0
73	Origin of rectus externus anterior (0); posterior (1) to foramen for ophthalmicus	Binary	0
74	Extra bundle of rectus inferior originating from interorbital wall (0); from tendon for rectus muscles (1)	Binary	?
75	Extra bundle of rectus inferior inserting on disc of eyestalk (0); on stem of eyestalk (1)	Binary	?
76	Extra bundle of rectus internus absent (0); present (1)	Binary	0
77	Extra bundle of rectus internus originating from interorbital wall (0); from tendon for rectus muscles (1)	Binary	?
78	Extra bundle of rectus internus inserting on stem of eyestalk (0); on disc of eyestalk (1)	Binary	?
79	Muscle parietalis present (0); absent (1)	Binary	0
80	Constrictor dorsalis consists of a single bundle (0); two muscle bundles (1)	Binary	0
81	Rostromandibularis absent (0); present (1)	Binary	0
82	Levator palpebrae anterodorsalis absent (0); present (1)	Binary	0
83	Adductor mandibulae hyoideus absent (0); present (1)	Binary	0
84	Adductor mandibulae IV absent (0); present (1)	Binary	0
85	Suborbitalis originating from orbito-nasal process (0); from dorsal surface of neurocranium (1)	Binary	0
86	Suborbitalis not associated with interorbital wall (0); associated with interorbital wall: not extending to fenestra of profundus canal (1); covering the fenestra (2)	Ordered	0
87	Suborbitalis entirely inserting on adductor mandibulae I: in a muscle bundle (0); via a tendon (1); partly inserting on mandibula via a tendon (2); entirely inserting on mandibula via a tendon (3)	Unordered	0
88	Suborbitalis not associated with labial cartilage (0); associated with lower labial cartilage (1)	Binary	0
89	Levator palatoquadrati originating from otic capsule (0); from interorbital wall (1)	Binary	0
90	Levator palatoquadrati originating in a muscle bundle (0); via a tendon (1)	Binary	0
91	Levator palatoquadrati inserting on palatoquadrate (0); on both palatoquadrate and mandibula (1)	Binary	0
92	Constrictor dorsalis I composed of a single muscle bundle (0); with a tendon proximally (1); with a tendon distally (2); two crossed bundles, each with a tendon (3)	Unordered	?
93	Constrictor dorsalis I inserting on center of palatoquadrate (0); on post-palatoquadrate process (1)	Binary	0
94	Spiracularis present (0); absent (1)	Binary	0, 1

Table 2. Continued.

Character	Coding	Status	ON state
95	Spiracularis with no subdivision (0); with subdivision inserting on mandibula (1)	Binary	?
96	Intermandibularis composed of a single muscle sheet (0); divided into two muscle sheets (1)	Binary	0
97	Intermandibularis not associated with palatoquadrate (0); associated with palatoquadrate (1)	Binary	0
98	Constrictor hyoideus dorsalis unifying succeeding constrictor muscles (0); completely separated (1)	Binary	0
99	Constrictor hyoideus dorsalis not associated with ceratohyal (0); associated with ceratohyal (1)	Binary	0
100	Coraco-branchialis inserting on either hypobranchial or ceratobranchial (0); on both cartilages (1)	Binary	0
101	Genio-coracoideus originating from coraco-hyoideus (0); from coraco-arcualis (1); from coracoid (2)	Ordered	0
102	Genio-coracoideus inserting on lingual surface of mandibula (0); ventral surface of mandibula (1)	Binary	0
103	Coraco-arcualis not associated with hypaxial (0); originating from hypaxial (1)	Binary	0
104	Coraco-branchialis γ incompletely isolated proximally (0); completely isolated (1)	Binary	0
105	Coraco-branchialis not associated with extrabranchial (0); associated with extrabranchial γ (1)	Binary	0
106	Interpharyngobranchialis with all bundles (0); without third bundle (1); without second and third bundles (2)	Ordered	0
107	Interpharyngobranchialis with all bundles (0); without first and second bundles (1)	Binary	0
108	Constrictor branchiales superficialis entirely covering branchial arches (0); with exposed regions on extrabranchials (1)	Binary	0
109	Interbranchialis entirely covering branchial rays (0); with exposed regions on branchial rays (1)	Binary	0
110	Subdivision of interbranchialis absent (0); present: muscle fibers only (1); two bundles with a tendon (2)	Unordered	0
111	Association of branchial arch δ with hypaxial body muscle absent (0); present (1)	Binary	0
112	Levator pectoralis inferior absent (0); present (1)	Binary	0
113	Levator pectoralis inferior inserting on mesopterygium (0); on propterygium and mesopterygium (1); on all basal cartilages (2)	Ordered	?
114	Levator pectoralis inferior inserting on mesopterygium (0); on mesopterygium and radials (1)	Binary	?
115	Inclinator dorsalis originating from proximal (0); distal regions of basal cartilages (1)	Binary	0
116	Extra bundle of inclinator dorsalis absent (0); present (1)	Binary	0
117	Rostronuchal and ethmonuchal muscles absent (0); present (1)	Binary	0
118	Flexor caudalis not extending to origin of lower caudal lobe (0); extending anterior to the origin (1)	Binary	0
119	Infraorbital canal passing behind the process (0); through groove on postorbital process (1)	Binary	0
120	Hyomandibular and mandibular canals continuous (0); separate (1)	Binary	0
121	Mandibular canal separate (0); continuous at symphyseal region (1)	Binary	0
122	Hyoid group of ampullae of Lorenzini absent (0); present (1)	Binary	0, 1
123	Tubules of ampullae of Lorenzini not to first gill opening (0); extending over pectoral girdle (1)	Binary	0
124	Nasal barbel absent (0); present; with caritilaginous support (1); without cartilaginous support (2)	Unordered	0
125	Oronasal groove absent (0); present (1)	Binary	0
126	Nasal barbel simple (0); branched (1)	Binary	?
127	Circumnarial fold absent (0); present (1)	Binary	0
128	Symphyseal groove absent (0); present (1)	Binary	0
129	Lower labial furrow paired, small and oval (0); paired, large (1); single, large (2)	Ordered	0
130	Subocular pocket absent (0); present (1)	Binary	0
131	Dermal lobe on head absent (0); simple, not distributed on lower jaw (1); branched, not distributed on the lower jaw (2); greatly branched, distributed on lower jaw (3)	Ordered	0
132	Dorsal spiracular caecum extending to otic capsule (0); not to otic capsule (1); absent (2)	Unordered	0
133	Supraocular knob absent (0); present (1)	Binary	0
134	Last interbranchial septum with gill filaments on both sides (0); with no gill filaments on posterior side (1)	Binary	0
135	Dermal ridges absent (0); present (1)	Binary	0
136	Anal fin and lower caudal lobe separate (0); close (1); overlapping (2)	Ordered	0

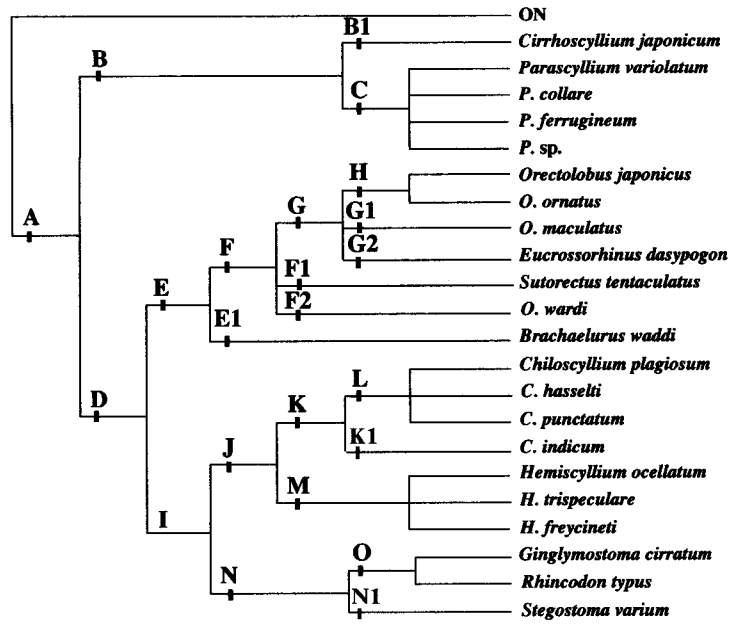

Fig. 84. Strict consensus tree of six most parsimonious cladograms of 22 orectolobiform species, with length of 229 steps and consistency index 0.760.

24 apomorphies 4-1, 14-1, 28-1, 40-1, 46-1, 47-2, 50-1, 64-1, 76-1, 84-1, 85-1, 86-1, 87-1, 92-1, 94-1, 96-1, 101-1, 102-1, 103-1, 110-1, 119-1, 121-1, 122-1 and 136-1. This clade is divided into clades E and I.

Clade E contains all species of *Brachaelurus, Orectolobus, Sutorectus* and *Eucrossorhinus*. It is well defined by 11 apomorphies 5-1, 10-1, 19-0(r), 26-1, 31-1, 37-1, 64-2, 86-2, 113-1, 120-1 and 128-1. This clade is divided into clades E1 and F. Clade E1 consisting of *Brachaelurus waddi* is supported by eight apomorphies 2-1, 8-1, 34-1, 39-1, 87-2, 101-2, 106-2 and 113-2.

Clade F contains all species of *Orectolobus, Sutorectus* and *Eucrossorhinus*. It is well defined by 16 apomorphies 6-1, 7-2, 32-1, 36-1, 37-2, 43-1, 45-1, 49-1, 50-0(r), 53-1, 67-1, 75-1, 78-1, 85-0(r), 131-1 and 133-1. This clade is divided into clades F1, F2 and G. Clade F1 consisting of *Sutorectus tentaculatus* has an apomorphy 56-1. Clade F2 consisting of *Orectolobus wardi* has no consistent apomorphies. Clade G contains *Eucrossorhinus* and *Orectolobus* excluding *O. wardi*. It is defined by two apomorphies 126-1 and 131-2. Moreover, this clade is divided into clades G1, G2 and H. Clade G1 consisting of *Orectolobus maculatus* has no consistent apomorphies. Clade G2 consisting of *Eucrossorhinus dasypogon* is supported by two apomorphies 41-1 and 131-3. Clade H contains *Orectolobus japonicus* and *O. ornatus*. It is supported by two apomorphies 57-0(r) and 133-0(r). This clade is divided into two clades consisting of *Orectolobus japonicus* and *O. ornatus* with no consistent apomorphies, respectively.

Clade I contains all species of *Chiloscyllium, Hemiscyllium, Ginglymostoma, Stegostoma* and *Rhincodon*. It is well defined by 10 apomorphies 9-1, 52-1, 56-1, 83-1, 87-3, 92-2, 106-0(r), 110-2, 130-0(r) and 135-1. This clade is divided into clades J and N.

Clade J contains all species of *Chiloscyllium* and *Hemiscyllium*. It is well defined by 13 apomorphies 2-1, 27-1, 34-1, 39-1, 54-1, 73-1, 90-1, 92-3, 101-0(r), 118-1, 123-1, 129-1 and 136-2. This clade is divided into clades K and M. Clade K contains all species of *Chiloscyllium* supported by three apomorphies 10-0(r), 95-1 and 129-2. This clade is divided into clades K1 and L. Clade K1 consisting of *Chiloscyllium indicum* has an apomorphy 10-1. Clade L containing *Chiloscyllium* except *C. indicum* represents an unresolved polytomy including *C. plagiosum, C. punctatum* and *C. hasselti*. This clade is supported by a single reversed character 56-0(r). Clade M containing all species of *Hemiscyllium* represents an unresolved polytomy. It is supported by three apomorphies 107-1, 114-1 and 121-0(r). *Hemiscyllium freycineti* has two apomorphies 22-1 and 68-1, whereas *H. ocellatum* and *H. trispeculare* have no consistent apomorphies, respectively.

Clade N contains *Ginglymostoma, Stegostoma* and *Rhincodon*. It is well defined by 23 apomorphies 18-1, 21-1, 29-0(r), 38-1, 47-3, 55-1, 58-1, 60-1, 61-1, 62-1, 63-1, 65-1, 70-1, 71-1, 72-1, 75-1, 78-1, 86-0(r), 101-2, 108-1, 109-1, 127-0(r) and 132-1, in addition to the character 13-1 corresponding to the apomorphic character 23 of the first step (see Chapter III). This clade is divided into clades N1 and O. Clade N1 consisting of

Stegostoma varium is supported by four apomorphies 10-0(r), 23-1, 35-2 and 66-1. Clade O contains *Ginglymostoma* and *Rhincodon*. It is well defined by seven apomorphies 4-0(r), 6-1, 16-1, 31-1, 50-0(r), 53-2 and 136-0(r). This clade is divided into two clades. The clade consisting of *Ginglymostoma cirratum* has six apomorphies 8-1, 41-1, 63-0(r), 71-0(r), 114-1 and 135-0(r); the clade consisting of *Rhincodon typus* has 16 apomorphies 3-1, 9-0(r), 26-1, 32-2, 36-1, 38-0(r), 45-1, 48-2, 49-2, 57-0(r), 64-3, 66-2, 72-2, 74-1, 77-1 and 101-0(r).

3. Comparison with previous hypotheses

Two hypotheses have been proposed on the interrelationships within Orectolobiformes by Dingerkus (1986) and Compagno (1988) based on "cladistic" concepts. Dingerkus (1986) originally proposed the cladogram showing close relationships of *Rhincodon* to *Stegostoma* and ginglymostomatid nurse sharks, and the sister relationships of parascylliids and a clade containing orectolobids and *Brachaelurus*. The former relationships are congruent with the hypothesis of Regan (1906) although some previous works (White 1937; Bigelow and Schroeder, 1948) supposed that *Rhincodon* has phylogenetic relationships not with the "orectolobid" carpet sharks but with some lamniforms like *Cetorhinus*. The latter relationships are different from those proposed by Applegate (1972) who suggested that parascylliids differed phylogenetically from any other orectolobiform taxa. Compagno's hypothesis in 1988 significantly differed from that of Dingerkus (1986) in its topology, excluding the polyphyletic nature of *Ginglymostoma cirratum* and *Pseudoginglymostoma brevicaudatum* and the systematic position of *Rhincodon* as a descendant of the higher orectolobiform clade.

The present study proposes the almost same topology as that of Compagno (1988). Concerning the incongruence with the Dingerkus' hypothesis shown in Fig. 85, I provide some comments on his synapomorphies. In Dingerkus (1986), the synapomorphies of Orectolobidae including *Orectolobus, Sutorectus* and *Eucrossorhinus, Brachaelurus* and parascylliids including *Parascyllium* and *Cirrhoscyllium* are based on the fifth gill opening being larger than the others (his character 5) and the dermal denticles having reduced keels on crown (his character 6). The first character is principally different between the parascylliids and the remaining taxa on the basis of internal morphology. *Parascyllium* and *Cirrhoscyllium* share the unique internal morphology associated with the fifth gill opening as:

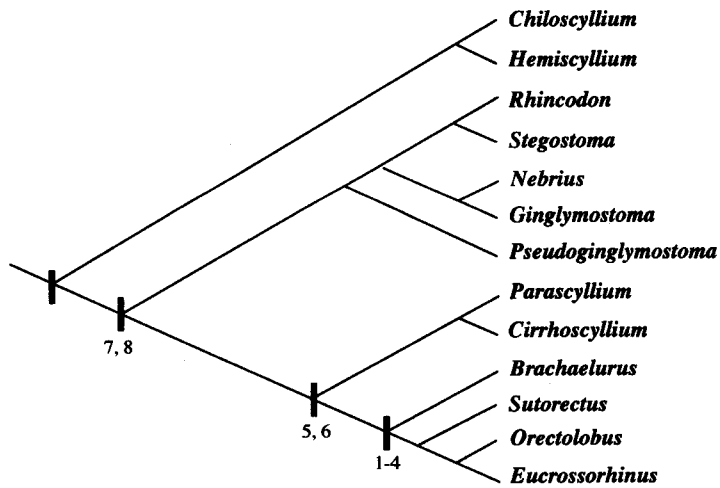

Character number / apomorphic state	
1	Symphyseal cleft present
2	Labial fold extending to near midline
3	Nasal barbel long
4	Ovoviviparous reproduction
5	Fifth gill opening larger than others
6	Dermal denticle ovoid, with reduced keels
7	Dermal denticle somewhat ovoid, with not Strongly developed keels
8	Teeth with well developed lateral cusps

Fig. 85. Interrelationships of Orectolobiformes (above) and the synapomorphies supporting the principal clades (below) proposed by Dingerkus (1986).

the last interbranchial septum with no gill filaments on the posterior side (present character 135-1); the coracobranchialis γ completely isolated from the succeeding bundles to insert on the large, triangular-shaped inner process located on the proximal region of the ceratobranchial (present characters 48-1, 105-1); coracobranchialis γ associated with ventral extrabranchial γ (present character 106-1); hypaxial body muscle associated with the epibranchial and ceratobranchial δ (present character 111-1). Therefore, the larger fifth gill opening of both genera is judged as a unique modification with drastic changes of the internal constructions. These modifications likely to be used for respiratory and/or feeding behaviors more effectively than other taxa having large fifth gill opening. The second character proposed by Dingerkus (1986) is unavailable as a synapomorphy of these taxa because some species of *Parascyllium* have dermal denticles with relatively distinct ridges (personal obs.), and the degree of ridges are known to greatly change in various regions on the body (Raschi and Tabit, 1992). Moreover, the synapomorphies linking Rhincodontidae and the "clade" shown above are also unacceptable because of the following reasons. The dermal denticle with a somewhat ovoid shape and keels not strongly developed (character 7 in Dingerkus, 1986) should be rejected because of reasons discussed above. The teeth with developed lateral cusps (character 8 in Dingerkus, 1986) should be regarded as rather primitive under the outgroup comparison (present character 38). Dingerkus (1986) linked *Rhincodon* and *Stegostoma* as a sister group based on two characters: presence of dermal ridges and low second dorsal fin. However, the former character is also shared in hemiscylliids, and is judged to be lost secondarily in *Ginglymostoma* in the present study (Character 137-0(r)). The latter is fundamentally different between both genera, because the second dorsal fin of *Stegostoma* is nearly same as the first in size, while the second dorsal fin is much smaller than the first in *Rhincodon*. Therefore, I reject the hypothesis proposed by Dingerkus (1986) because of his misinterpretation of the characters as discussed above.

4. Systematic positions of Orectolobus, Sutorectus and Eucrossorhinus

Although no hypothesis has supported the orectolobiform genera as distinct systematic units based on the cladistic concept, the present study initially provides that the genera *Orectolobus, Sutorectus* and *Eucrossorhinus* included in clade F (see Fig. 84) are systematically problematic. The genus *Eucrossorhinus* Regan, 1908 was established as a monotypic genus for *Crossorhinus dasypogon* Bleeker, 1867 in having a depressed head, smaller eyes, wider spiracles, and smaller gill openings, with four of them above the pectoral fin. The genus *Sutorectus* Whitley, 1939 was also established as a monotypic genus for *C. tentaculatus* Peters, 1864 in having a simple nasal barbel, and tubercles or papillae on the body. On the other hand, the genus *Orectolobus* Bonaparte, 1834 has been defined only by the absence of the diagnostic features of both genera as: dermal lobes

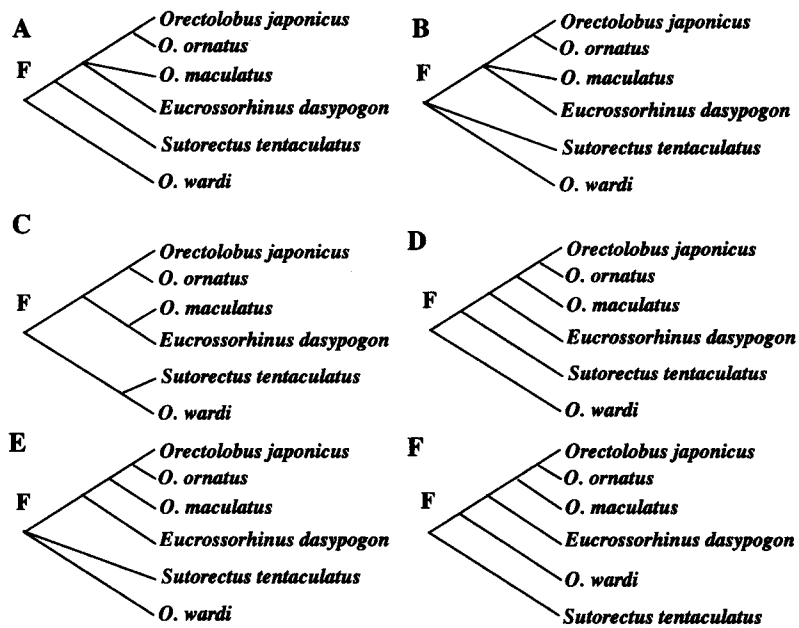

Fig. 86. Six possible cladograms of clade F including *Orectolobus, Sutorectus* and *Eucrossorhinus* provided from the most parsimonious relationships.

on lower jaw, tubercles on body, and reticular pattern of narrow dark lines. This suggests that they are not-A group (Eldredge and Cracraft, 1980). In this study, *Eucrossorhinus* is a descendant derived from clade G containing three species of *Orectolobus*, i.e., *O. japonicus, O. ornatus* and *O. maculatus*, in all trees. *Sutorectus* is derived from the root of clade F containing all orectolobid wobbegongs as one descendant of an unresolved polytomy shown in Fig. 84. Possible relationships presented in Fig. 86 show *Sutorectus* is hardly derived from the initial node except only one case (Fig. 86F), in which the remaining form a monophyly supported only by a single character with extremely low CI degree as 0.289. Therefore, the genus *Orectolobus* is regarded as a monophyletic group only when both *Eucrossorhinus* and *Sutorectus* are included.

VII. Classification based on cladistic results

1. Ranking

Based upon the cladistic analysis in the first and second steps, all OTU treated as the ingroup form a single monophyletic taxon. I give an ordinal rank, Orectolobiformes, to the clade A of Fig. 84, following Applegate (1972), Dingerkus (1986), Compagno (1984, 1988) and Nelson (1994). To provide a new classification based on the cladistic topology within this order, I follow the sequencing convention of Nelson (1972) formalized by Wiley (1981). I propose to give family rank to the five clades B, F, E1, J and N, respectively, to minimize taxonomic changes (Fig. 84). Although clade E1 includes only a single species, *Brachaelurus waddi*, I prefer to give separate family rank for this clade because it is supported by a number of apomorphies (eight) and recent taxonomic studies have accepted this family as valid (e.g., Compagno, 1984; Michael, 1993; Last and Stevens, 1994; Nelson, 1994).

Concerning clade N including *Ginglymostoma, Stegostoma* and *Rhincodon*, it forms a very stable monophyletic group in having a large number of synapomorphies. Applegate (1972) proposed the three families Ginglymostomatidae to *Ginglymostoma* and *Nebrius*, Stegostomatidae to *Stegostoma*, and Rhincodontidae to *Rhincodon*. However, Dingerkus (1986) erected a single family, Rhincodontidae, to include these taxa as a monophyletic group, because of the paraphyletic nature of *Pseudoginglymostoma, Ginglymostoma* and *Nebrius* that were included in Ginglymostomatidae by Applegate (1972). Subsequently, Compagno (1984, 1988), Last and Stevens (1994) and Nelson (1994) followed the taxonomy proposed by Dingerkus (1986) although Compagno (1988) suggested that *Pseudoginglymostoma, Ginglymostoma* and *Nebrius* are paraphyletic. Unfortunately, since I could dissect neither *Pseudoginglymostoma* nor *Nebrius*, interrelationships among them are still unresolved. Thus, I prefer to recognize the family Rhincodontidae for the clade N for the nomenclatural stability, especially concerning the probability of the non-monophyletic nature of *Ginglymostoma, Nebrius* and *Pseudoginglymostoma*. On the other hand, Applegate (1972) designated three suborders to accommodate these taxa : Rhincodontoidei to *Rhincodon*, Orectoloboidei to the taxa containing Brachaeluridae, Hemiscylliidae and Orectolobidae, and Parascylloidei to Parascylliidae, respectively, but his Orectoloboidei is found to be paraphyletic in the present cladogram. However, Parascylliidae (clade B) and the other clade (clade D) are stable monophyletic groups supported by 39 and 24 synapomorphies, respectively, and thus two suborders, Parascylloidei and Orectoloboidei, are proposed to those two clades in the present study.

Clade F forms a monophyletic group supported by 16 apomorphies. However, the genus *Orectolobus* is not monophyletic unless *Sutorectus* and *Eucrossorhinus* are included as discussed above. If the latter two genera are recognized as valid, then *Orectolobus* must be divided into several categories in the cladistic sense. Therefore, I propose that the genera *Sutorectus* and *Eucrossorhinus* should be synonymized into the genus *Orectolobus*.

The new classification of the order Orectolobiformes is summarized as follows. Two genera, *Nebrius* and *Pseudoginglymostoma*, which could not be treated in this study, are probably placed in the family Rhincodontidae by having some apomorphic features provided in the present study: presence of supraorbital blade, and a large number of radials in pectoral, pelvic, dorsal and anal fins (Dingerkus, 1986; Compagno, 1988). However, I propose these two genera as *incertae sedis* because the systematic positions are uncertain within this family. On the other hand, "*Heteroscyllium*" was originally designated as a monotypic genus by Regan (1908) to replace *Brachaelurus colcloughi*, and Compagno (1984) followed this category based on the presence of symphyseal groove; and long interspace between anal fin and lower caudal origin. However, Last and Stevens (1994) recommended that it is a junior synonym of the genus *Brachaelurus* because of the lack of the diagnostic characters shown by Regan (1908) and Compagno (1984) according to reexamination of a few additional specimens. Here, I follow Last and Stevens (1994) because of the external morphology and the part of skeletal condition on the basis of a single specimen (QMI27500).

Order Orectolobiformes Applegate, 1972
Suborder Parascylloidei Applegate, 1972
Family Parascylliidae Gill, 1862
Genus *Parascyllium* Gill, 1862
Genus *Cirrhoscyllium* Smith and Radcliffe, 1913
Suborder Orectoloboidei Applegate, 1972
Family Orectolobidae Gill, 1896
Genus *Orectolobus* Bonaparte, 1834
Family Brachaeluridae Applegate, 1972
Genus *Brachaelurus* Ogilby, 1907
Family Hemiscylliidae Gill, 1862
Genus *Hemiscyllium* Müller and Henle, 1838
Genus *Chiloscyllium* Müller and Henle, 1837
Family Rhincodontidae Müller and Henle, 1839
Genus *Rhincodon* Smith, 1829
Genus *Ginglymostoma* Müller and Henle, 1837
Genus *Stegostoma* Müller and Henle, 1837
Genus *Nebrius* Rüppell, 1837 *incertae sedis*
Genus *Pseudoginglymostoma* Dingerkus, 1986 *incertae sedis*

2. Key to suborders, families, and genera

2-1. Key to suborders

1a. Spiracle minute, without gill filaments nor dorsal spiracular caecum. Last gill opening very large, posterior hemibranch of last interbranchial septum without gill filaments. Origin of anal fin anterior to that of second dorsal fin. Hyoid group of ampullae of Lorenzini absent. Five or more vertebral ribs on diplospondylous vertebrae ·····Parascylloidei

1b. Spiracle moderate to large, with gill filaments and a dorsal spiracular caecum. Last gill opening moderate, posterior hemibranch of last interbranchial septum with gill filaments. Origin of anal fin below or posterior to that of second dorsal fin. Hyoid group of ampullae of Lorenzini present. Vertebral ribs usually absent on diplospondylous vertebrae (two or less, if present). ·····Orectoloboidei

2-2. Key to families

Parascylloidei

Parascylloidei includes only the single family Parascylliidae.

Orectoloboidei

1a. Head and trunk greatly depressed. Dermal lobes present on upper jaw and below eye. Teeth on medial region of both jaws large, erected, fang-like, without lateral cusps. Spiracle much larger than eye. ·····Orectolobidae

1b. Head and trunk cylindrical or fusiform. Dermal lobes absent. Teeth small, low, blunt, with or without lateral cusps. Spiracle same as or smaller than eye. ·····2

2a. Circumnarial fold absent. Spiracle posterior to eye. Precaudal tail much shorter than trunk. Supraorbital blade present. Radials of pectoral fin four or more, up to 10. ···Rhincodontidae

2b. Circumnarial fold present. Spiracle posteroventral to eye. Precaudal tail as long as or greater than trunk. Supraorbital blade absent. Radials of pectoral fin three or less. ·····3

3a. Symphyseal groove present. Teeth with well developed lateral cusps. Anal fin high, rounded, not overlapping lower caudal lobe. Tubules of buccal group of ampullae of Lorenzini not to pectoral girdle. Suprascapular cartilage absent. ·····Brachaeluridae

3b. Symphyseal groove absent. Teeth with indistinct lateral cusps. Anal fin low, overlapping lower caudal lobe. Tubules of buccal group of ampullae of Lorenzini extending over pectoral girdle. Suprascapular cartilage present. ·····Hemiscylliidae

2-3. Key to genera

Parascylliidae

1a. Throat barbel absent. Dorsal margin of interorbital wall opened. Ribs on diplospondylous vertebrae 10 or more. ·····*Parascyllium*

1b. Throat barbel present. Dorsal margin of interorbital wall closed. Ribs on diplospondylous vertebrae 9 or less. ·····*Cirrhoscyllium*

Hemiscylliidae

1a. Lower labial furrow completely continuous at symphyseal region. Nostrils subterminal on snout. Mandibular sensory canal continuous at symphyseal region. Epiphyseal foramen absent or, if present, completely isolated from prefrontal fontanelle. Muscle spiracularis inserting on mandibula. ·····*Chiloscyllium*

1b. Lower labial furrow separate. Nostrils terminal on snout. Mandibular sensory canal continuous at symphyseal region. Epiphyseal foramen fused with prefrontal fontanelle to form a large fenestra. Muscle spiracularis not inserting on mandibula. ·····*Hemiscyllium*

Rhincodontidae

1a. Caudal fin long, almost equal with precaudal length. Dorsal fins close. Epiphyseal foramen

absent. ..... *Stegostoma*

1b. Caudal fin considerably shorter than precaudal length. Dorsal fins well separated. Epiphyseal foramen fused with prefrontal fontanelle. ……2

2a. Lower caudal lobe extended, lunate-shaped. Mouth terminal. Dermal ridges present on lateral surface of body. ..... *Rhincodon*

2b. Lower caudal lobe indistinct. Mouth subterminal. Dermal ridges absent on lateral surface of body.……3

3a. Pectoral, dorsal and anal fins apically angular, pectoral fin narrow and falcated. ..... *Nebrius*

3b. Pectoral, dorsal and anal fins apically rounded, pectoral fins broad and not falcated.……4

4a. Second dorsal and anal fins about as large as first dorsal fin. Caudal fin short, less than 1/4 of total length. Foramina for internal carotid artery and orbital artery fused. ..... *Pseudoginglymostoma*

4b. Second dorsal and anal fins much smaller than first dorsal fin. Caudal fin longer, over 1/4 of total length. Foramina for internal carotid artery and orbital artery separated. ··· *Ginglymostoma*

3. Synonymies and diagnosis

Orectolobiformes Applegate, 1972

Orectolobiformes Applegate, 1972 : 743.

Diagnosis. Mouth nearly transverse, entirely in front of eye. Nasal barbel present. Oronasal groove present. Inner process prominent, located on medial region of ceratobranchial (except for *Rhincodon*). Rectus inferior with an extra bundle associated with eyestalk. Constrictor dorsalis with two muscle bundles. Levator pectoralis inferior present. Inclinator dorsalis originating from distal regions of basal cartilages in dorsal fins.

Parascylloidei Applegate, 1972

Parascylloidei Applegate, 1972 : 749.

Diagnosis. Body slender and elongated. Circumnarial fold present. Eye dorsolateral on head, with subocular pocket. Spiracle minute, without gill filaments nor dorsal spiracular caecum. Fifth gill opening large ; last interbranchial septum with no gill filaments on posterior surface. Anal fin far from lower caudal lobe, origin entirely anterior to that of second dorsal fin. Vertebral ribs present on diplospondylous vertebrae. Inner process of ceratobranchial γ triangular, inserted by isolated coraco-branchialisγ. Rostromandibularis, levator palpebrae anterodorsalis, rostronuchal and ethmonuchal muscles present. Hypaxial body muscle inserting on last branchial arch.

Parascylliidae Gill, 1862

Parascylliinae Gill, 1862 : 408.

Parascyllidae Dingerkus, 1986 : 241.

Diagnosis. See description of suborder.

Parascyllium Gill, 1862 (Fig. 87)

Parascyllium Gill, 1862 : 407-412 (type species *Hemiscyllium variolatum* Duméril, 1853 : 121, by original designation).

Neoparascyllium Whitley, 1939 : 227.

Diagnosis. Throat barbel absent. Precaudal vertebrae including monospondylous and diplospondylous 122 or more. Vertebral ribs on diplospondylous vertebrae 10 or more. Body with a dark collar band around gill region, or with dense small spots.

Five species are included with one species undescribed : *Parascyllium variolatum* (Dumerill, 1853) (Fig. 87) ; *P. collare* Ramsey and Ogilby, 1888 ; *P. ferrugineum* McCulloch, 1911 ; *P. multimaculatum* Scott,

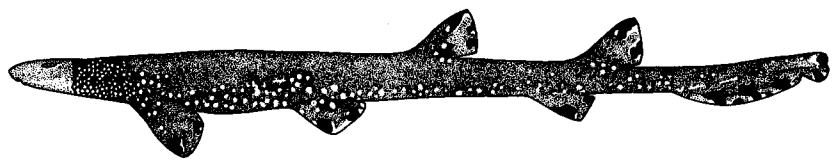

Fig. 87. Lateral view of *Parascyllium variolatum*, type species of this genus (from Compagno, 1984).

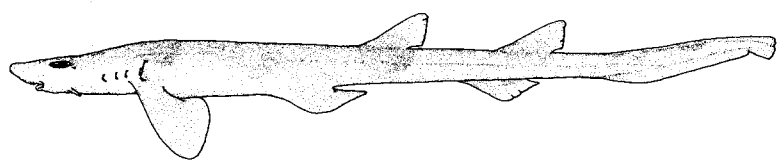

Fig. 88. Lateral view of *Cirrhoscyllium expolitum*, type species of this genus. Original drawing of the holotype USNM 4603, female, 330 mm TL (from Goto and Nakaya, 1996).

1935; *Parascyllium* sp. (after Last and Stevens, 1994).

Cirrhoscyllium Smith and Radcliffe, 1913 (Fig. 88)

Cirrhoscyllium Smith and Radcliffe *in* Smith, 1913: 568 (type species *Cirrhoscyllium expolitum* Smith and Radcliffe *in* Smith, 1913: 568, by original designation).

Zev Whitley, 1927: 290.

Diagnosis. Throat barbel present. Precaudal vertebrae usually 121 or less. Vertebral ribs on diplospondylous vertebrae 7 or less. Body with 6 to 10 dark saddles on back and sides.

Three species are included: *Cirrhoscyllium expolitum* Smith and Radcliffe, 1913 (Fig. 88); *C. japonicum* Kamohara, 1943; *C. formasanum* Teng, 1959.

Orectoloboidei Applegate, 1972

Orectoloboidei Applegate, 1972: 745

Diagnosis. Spiracle moderate to large, with gill filaments and a dorsal spiracular caecum. Last gill opening moderate, posterior hemibranch of last interbranchial septum with gill filaments. Origin of anal fin posterior to that of second dorsal fin. Hyoid group of ampullae of Lorenzini present. Vertebral ribs usually absent on diplospondylous vertebrae (two or less, if present).

Orectolobidae Gill, 1896

Orectolobidae Gill, 1896: 212.

Diagnosis. Head well depressed. Nostril terminal, with a long nasal barbel. Mouth very large, with large and fang-like teeth in anterior region in 2-3 rows. Symphyseal groove present. Eye dorsolateral on head. Spiracle very large, posteroventral to eye. Dermal lobes present around jaws and below eye and spiracle. Pectoral fin large, triangular-shaped. Anal fin small and high, close to origin of lower caudal lobe. Mandibular sensory canal continuous at symphyseal region, and separate from hyomandibular sensory canal distally. Nasal capsule supported by two depressed orbito-nasal processes. Pre-epibranchial cartilage present. Extra bundles of rectus inferior and r. internus inserting on stem of eyestalk.

Orectolobus Bonaparte, 1834 (Fig. 89)

Orectolobus Bonaparte, 1834: puntata 39 (type species *Squalus barbatus* Gmelin, 1789: 1493, by subsequent restriction of Gill, 1896: 211, junior synonym of *Squalus maculatus* Bonnaterre, 1788).

Crossorhinus Müller and Henle, 1837a: 113.

Crossorhinus Smith, 1837: 86 (type species *Squalus lobatus* Bloch and Schneider, 1801: 137 [= *Squalus barbatus* Gmelin, 1789], by original designation).

Eucrossorhinus Regan, 1908: 357 (type species *Crossorhinus dasypogon* Bleeker, 1867: 400, by original designation).

Sutorectus Whitley, 1939: 228 (type species *Crossorhinus tentaculatus* Peters, 1864: 123, by original designation).

Diagnosis. See diagnosis of family.

Six species are included with one species undescribed: *Orectolobus maculatus* (Bonnaterre, 1788) (Fig. 89); *O. ornatus*, (de Vis, 1883); *O. dasypogon* (Bleeker, 1867); *O. japonicus* Regan, 1906; *O. tentaculatus* (Peters, 1864); *Orectolobus* sp. (after Last and Stevens, 1994).

Brachaeluridae Applegate, 1972

Brachaeluridae Applegate, 1972: 745.

Diagnosis. Head broad and rounded. Symphyseal groove present. Spiracle as large as eye. Dermal lobes absent. Eye oval, with a weak subocular pocket. Anal fin high and rounded, close to origin of lower caudal lobe. A fenestra present on orbito-nasal process. Suprascapular cartilage absent. Propterygium of pectoral fin isolated. Suborbitalis originating from dorsal surface of neurocranium.

Brachaelurus Ogilby, 1907 (Fig. 90)

Brachaelurus Ogilby, 1907: 27 (type species *Chiloscyllium modestum* Günther, 1871: 654 by original designation, junior synonym of *Squalus waddi* Bloch and

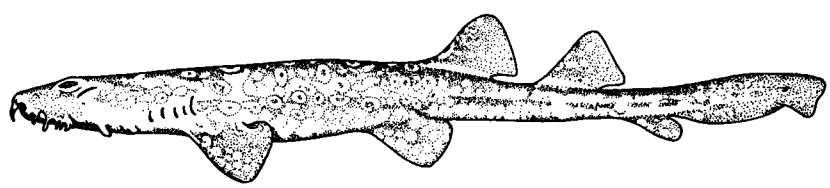

Fig. 89. Lateral view of *Orectolobus maculatus*, senior synonym of the type species, *Squalus barbatus*, of this genus (from Compagno, 1984).

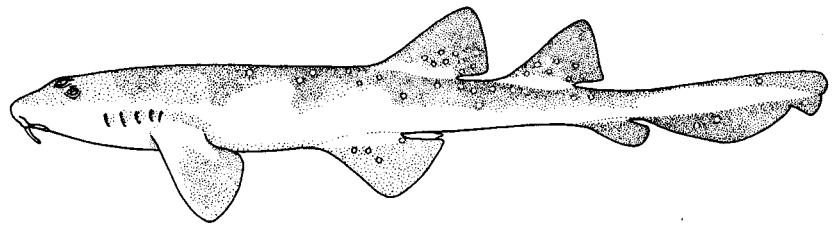

Fig. 90. Lateral view of *Brachaelurus waddi*, type species of this genus (from Compagno, 1984).

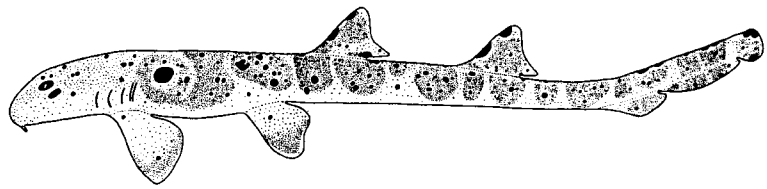

Fig. 91. Lateral view of *Hemiscyllium ocellatum*, type species of this genus (from Dingerkus and Defino, 1983).

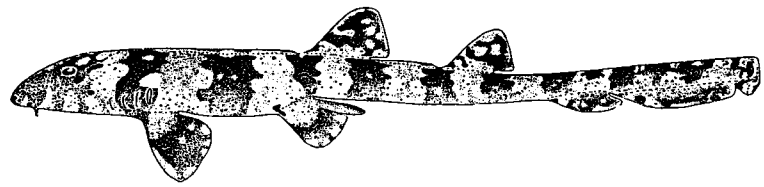

Fig. 92. Lateral view of *Chiloscyllium plagiosum*, type species of this genus (from Dingerkus and Defino, 1983).

Schneider, 1801).

Brachaelurus Ogilby, 1908 : 4 (type species *Brachaelurus colcloughi* Ogilby, 1908 : 4, by original designation ; not *Brachaelurus* Ogilby, 1907).

Cheloscyllium Maclay *in* Ramsey, 1880 : 97 (error for *Chiloscyllium* Müller and Henle, 1837a).

Cirriscyllium Ogilby 1908 : 4 (replacement for *Brachaelurus* Ogilby, 1907).

Heteroscyllium Regan, 1908 : 455 (type species *Brachaelurus colcloughi* Ogilby, 1908, replacement for *Brachaelurus* Ogilby, 1908 not *Brachaelurus* Ogilby, 1907).

Diagnosis. See diagnosis of family.

Two species are included : *Brachaelurus waddi* (Bloch and Schneider, 1801) (Fig. 90) ; *B. colcloughi* Ogilby, 1908.

Hemiscylliidae Gill, 1862

Subfamily Hemiscylliinae Gill, 1862 (Family Scyliorhinidae) : 408.

Hemiscylliidae Whitley, 1939 : 227.

Hemiscyllidae Dingerkus and Defino, 1983 : 7.

Diagnosis. Body slender and cylindrical. Head rounded. Symphyseal groove absent. Dermal lobes absent. Eye oval, with no subocular pocket. Spiracle as large as eye. Lower labial furrow well developed, forming thin and large dermal folds. Tubules of buccal group of ampullae of Lorenzini extending to over pelvic girdle. Interdorsal space more or less thicken, forming a dermal ridge. Anal fin low, overlapping lower caudal lobe. Rectus externus originating from behind foramen for ophthalmicus superficialis and profundus nerves. Foramen for brachial artery opening on anterior surface of coracoid.

Hemiscyllium Müller and Henle, 1838 (Fig. 91)

Hemiscyllium Müller and Henle, 1838 : 34 (type species *Squalus ocellatus* Bonnaterre 1788 : 8, by original designation).

Diagnosis. Nostrils terminal, tail long, distance between pelvic and anal fin greater than 38 percent of total length. Lower labial furrow separate. Mandibular sensory canal isolated at symphyseal region. Epiphyseal foramen fused with prefrontal fontanelle, forming a single large fenestra. Pectoral propterygium fused with mesopterygium. Muscle spiracularis not inserting on mandibula.

Four species are included : *Hemiscyllium ocellatum* (Bonnaterre, 1788) (Fig. 91) ; *H. freycineti* (Quoy and Gaimard, 1824) ; *H. trispeculare* Richardson, 1843 ; *H. strahani* Whitley, 1967.

Chiloscyllium Müller and Henle, 1837 (Fig. 92)

Chiloscyllium Müller and Henle 1837a : 112 (no species mentioned ; type species *Scyllium plagiosum* Bennett 1830 : 694, by subsequent monotypy of Müller and Henle *in* Smith, 1937 ; also by subsequent designation Gill, 1862 : 407).
Chyloscyllium Duméril, 1853 : 40.
Cheiloscyllium Hasse, 1878 : 146.
Synchismus Gill, 1862 : 408.

Diagnosis. Nostrils subterminal. Tail short, distance between pelvic and anal fins less than 38 percent of total length. Lower labial furrow continuous at symphyseal region. Mandibular canal continuous at symphyseal region. Epiphyseal foramen reduced or absent. Muscle spiracularis with a subdivision inserting on mandibula.

Eight species are probably valid : *Chiloscyllium plagiosum* (Bennett, 1830) (Fig. 92) ; *C. indicum* (Gmelin, 1789) ; *C. punctatum* Müller and Henle, 1838 ; *C. griseum* Müller and Henle, 1838 ; *C. hasselti* Bleeker, 1852 ; *C. arabicum* Gubanov, 1980 ; *C. burmensis* Dingerkus and Defino, 1983 ; *C. confusum* Dingerkus and Defino, 1983.

Rhincodontidae Müller and Henle, 1839

Rhincodontidae Müller and Henle, 1839 : 77.

Diagnosis. Body stout. Circumnarial fold absent. Eye oval, lateral on head, without subocular pocket. Spiracle posterior to eye, with a reduced dorsal spiracular caecum. Fifth gill opening as large as or smaller than others. Precaudal tail much shorter than trunk. Supraorbital blade present, providing insertions of obliquus muscles. Ventral extrabranchial articulating with ceratobranchial in arch β1-γ. Four or more radials present in pectoral fin. Dorsal, pelvic and anal fins with three radials.

Remarks. The family Rhincodontidae is originally designated for the monotypic species, *Rhiniodon typus* Smith, 1828, as the name *Rhiniodontes* in Müller and Henle (1839). Subsequently, Garman (1913) spelled it as Rhincodontidae for the generic name *Rhincodon*, which is a misspelling of *Rhiniodon* Smith, 1828. For a long time, two family names of Rhincodontidae and Rhiniodontidae have been used in various cases. Opinion 1278 of ICZN (1984) decided the familial name of this taxon should be spelled as Rhincodontidae Müller and Henle, 1839, and I follow this opinion.

Rhincodon Smith, 1829 (Fig. 93)

Rhincodon Smith, 1829 : 433 (type species *Rhincodon typus* Smith, 1828 : 2, monotypic, by original designation).
Rhiniodon Smith, 1828 : 2 (placed on Official Index of for purposes of priority : Opinion 1278 of ICZN, 1984).
Rhinchodon Smith, 1829 : 534 (used only in index).
Rhineodon Müller and Henle, 1837b : 84.
Rineodon Müller and Henle, 1838 : 37.
Rhinodon Müller and Henle, 1841 : 77.
Micristodus Gill, 1865 : 177 (type species *Micristodus punctatum* Gill, 1865 : 177, junior synonym of *Rhincodon typus* Smith, 1829 ; by original designation).

Diagnosis. Body fusiform ; head broad and depressed. Mouth large and terminal, with numerous, monocuspid teeth in over 300 rows. Gill openings large, internal gill aperture entirely covered with filter screen. First dorsal fin large, origin well anterior to pelvic fin. Second dorsal and anal fins considerably smaller than first dorsal, both located in midspace of precaudal tail. Caudal fin large, lunate, without distinct terminal lobe. Upper precaudal pit present. Dermal ridges present on lateral surface of body. Neural and hemal arches well developed ; hemal arches completely closed in tail vertebrae. Hypochordal processes greatly elongated and segmented into lower caudal lobe. Rectus muscles originating in a single tendon.

One species is included : *Rhincodon typus* Smith, 1929 (Fig. 93).

Remarks. The genus *Rhincodon typus* Smith, 1929 was originally designated as *Rhiniodon* Smith, 1828 a priori. Subsequently, a large number of generic names have been proposed such as *Rhineodon, Rhinodon* and

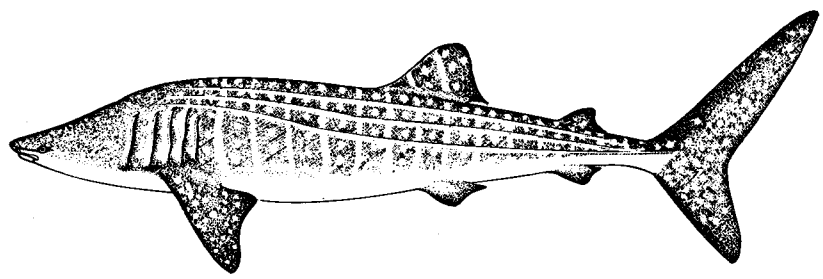

Fig. 93. Lateral view of *Rhincodon typus*, type species of this genus (from Compagno, 1984).

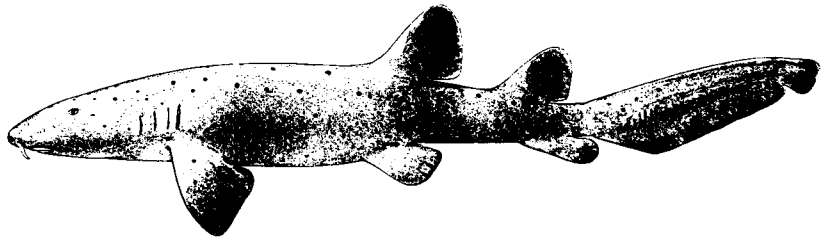

Fig. 94. Lateral view of *Ginglymostoma cirratum*, type species of this genus (from Garman, 1913).

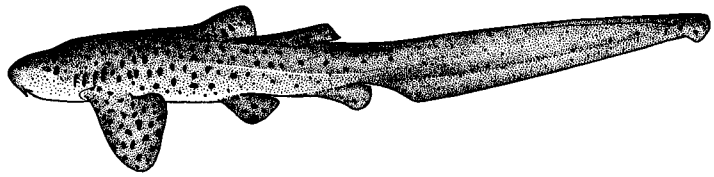

Fig. 95. Lateral view of *Stegostoma varium*, type species of this genus (from Compagno, 1984).

so on. Although the name *Rhiniodon* Smith, 1828 should be used for the valid generic name in the meaning of the principle of priority (Art. 23. of ICZN, 2000), opinion 1278 of ICZN (1984) decided to place *Rhincodon* Smith, 1829 on the Official Lists of Generic Names in Zoology with the Name Number 2219, and to place *Rhiniodon* Smith, 1828 on the Official Index of Rejected and Invalid Generic Names in Zoology with the Name Number 2141.

Ginglymostoma Müller and Henle, 1837 (Fig. 94)

Ginglymostoma Müller and Henle, 1837a : 113 (no species mentioned ; type species *Squalus cirratus* Bonnaterre, 1788 : 7, by subsequent designation by Jordan and Gilbert, 1883 : 18).

Diagnosis. Body thick ; head rounded. Mouth subterminal on head, with well developed labial furrows. Spiracle much smaller than eye. Pectoral and dorsal fins apically rounded. Second dorsal fin smaller than first dorsal. Anal fin rather high, rounded, weakly separated from origin of lower caudal lobe by a short distance. Lower caudal lobe indistinct ; subterminal notch distinct. A fenestra present on orbito-nasal process. Pharyngohyal present. Ventral extrabranchial cartilage present on hyoid arch. Suborbitalis with a subdivision inserting on palatobasal ridge.

One species is included : *Ginglymostoma cirratum* (Bonnaterre, 1788) (Fig. 94).

Stegostoma Müller and Henle, 1837 (Fig. 95)

Stegostoma Müller and Henle, 1837 : 112a (type species *Squalus fasciatus* Bloch, 1785 : 19 [=*Squalus fasciatus* Hermann, 1783 : 302], by original designation).

Diagnosis. Body short and stout ; with rounded head and compressed tail. Spiracle nearly as large as eye. Pectoral fin large, broad, triangular-shaped, not falcate. Dorsal fins small and low, closely located. Anal fin rounded, close to origin of lower caudal lobe. Upper caudal lobe extremely elongated, almost as long as precaudal body length. Subterminal notch distinct. Dermal ridges present on dorsal and lateral surfaces of body. Palatoquadrate tightly articulated with a prominent palatobasal ridge on neurocranium. Foramen for internal carotid artery single. Dorsal extrabranchial $\beta 2$-γ fused.

One species is included : *Stegostoma varium* (Seba, 1758) (Fig. 95).

Remarks. Various names have been used for this species including *Stegostoma varium* (Seba, 1758), *S. fasciatum* (Hermann, 1783), or *S. tigrinum* (Gmelin, 1789). Bigelow and Schroeder (1948) and Bass et al. (1975) used the earliest species name "*varium*" based on the rule of priority. Compagno (1984) pointed out that Seba (1758) showed the nomenclature haphazardly uninominal, binomial, and polynomial in the description, and thus he hesitated to use the name "*varium*" on the basis of the binomial rule (Art. 5 of ICZN, 2000). Compagno (1984) also pointed out that Seba (1758) apparently provided the binominal name *Squalus varius* with an accurate description, and a fine illustration for a juvenile of this shark. Although Compagno (1984) pended to judge the availability of the name *varium*, the binaminal nomenclature *S. varius* is acceptable according to the Application of Art. 11.4.3 of ICZN (2000) and the species name *varium* should be available.

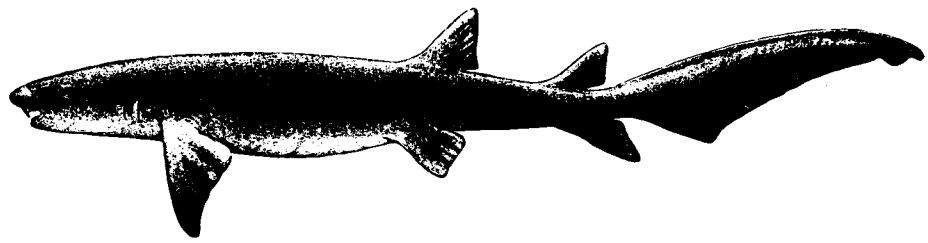

Fig. 96. Lateral view of *Nebrius ferrugineus*, type species of this genus (from Garman, 1913).

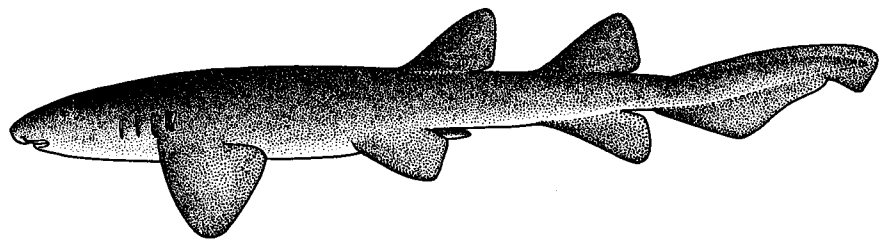

Fig. 97. Lateral view of *Pseudoginglymostoma brevicaudatum*, type species of this genus (from Compagno, 1984).

Incertae sedis of the family Rhincodontidae
Nebrius Rüppell, 1837 (Fig. 96)

Nebrius Rüppell, 1837: 62 (type species *Nebrius concolor* Rüppell, 1837: 62, by original designation).

Nebrodes Garman, 1913: 56 (replacement for *Nebrius* Rüppell, 1837).

Diagnosis. Head depressed. Teeth more or less compressed in sides of jaws. Mouth subterminal, with well developed labial furrows. Spiracle much smaller than eye. Nasal barbel long, extending near mouth gape. Pectoral fin apically angular, falcate. Dorsal and anal fins apically angular. Second dorsal fin slightly smaller than first dorsal. Anal fin as large as second dorsal, located below second dorsal, well separated from origin of lower caudal lobe. Caudal fin moderate, with distinct subterminal notch. Dermal ridges absent on back nor lateral surfaces of body.

One species is included: *Nebrius ferrugineus* (Lesson, 1830) (Fig. 96).

Pseudoginglymostoma Dingerkus, 1986 (Fig. 97)

Pseudoginglymostoma Dingerkus, 1986: 240 (type species *Ginglymostoma brevicaudatum* Günther *in* Playfair and Günther, 1866: 141, pl. 21, by original designation).

Diagnosis. Body stout, head rounded. Mouth with well developed labial furrows. Nasal barbel short, not extending to mouth gape. Spiracle much smaller than eye. Pectoral fin large, triangular, not falcate. Dorsal fins rounded, almost equal in size and shape. Anal fin large, rounded located below anal fin, and separated from origin of lower caudal lobe by a short distance. Caudal fin short, less than 1/4 of total length.

One species included: *Pseudoginglymostoma brevicaudatum* (Günther, 1866) (Fig. 97).

VIII. General discussion

1. Mode of reproduction

Mode of reproduction in orectolobiforms is known only by fragmentary descriptions of egg cases or juveniles, e.g., Smedley (1926), Deraniyagala (1934), Senta and Sarangdhar (1948), Compagno (1984), Michael (1993), Last and Stevens (1994), Miki (1994) and Masuda (1998), and detailed descriptions associated with behavior or evolution are still obscure. Thus, I review mode of reproduction and provide an evolutionary hypothesis based on the cladistic topology reconstructed in the present study in Orectolobiformes.

In elasmobranchs, mode of reproduction has been traditionally divided into oviparity, ovoviviparity and viviparity. Wourms (1977), Gilbert (1981-1982), and Dodd (1983) divided the mode into oviparity, aplacental viviparity and placental viviparity. Nakaya (1975) classified the oviparity into the single oviparity and multiple oviparity based on number of the offspring. Moreover, Compagno (1990b) classified these divisions into six categories, i.e., extended oviparity, retained oviparity, yolksac viviparity, cannibal viviparity, placental viviparity and uterine viviparity. Among orectolobiforms, three of the categories shown by Compagno (1990b) are recognized.

Parascylliidae and Hemiscylliidae represent the

extended oviparity, in which an egg is fertilized within each oviduct, enclosed in a keratinoid egg case secreted by the nidamental gland, and deposited on the substrate (Ogilby and McCulloch, 1908; Michael, 1993; Last and Stevens, 1994; Goto and Nakaya, 1996). Furthermore, the following differences are recognized. In Parascylliidae, at least some taxa, i.e., *Cirrhoscyllium expolitum, C. japonicum* and *Parascyllium multimaculatum*, are known to deposit two depressed, square-shaped egg cases with prominent vestibular horns on all corners simultaneously (Fig. 98A; Toda et al., 1991; Michael, 1993; Last and Stevens, 1994; Goto and Nakaya, 1996). Hemiscylliids deposit two depressed, rounded egg cases with greatly elongated, adhesive silky fibers extending from the alternate side, or sometimes from both sides of the egg case (Fig. 98C; Raj, 1914; Ogilby and McCulloch, 1908; Aiyar and Nalini, 1938; Senta and Sarangdhar, 1948; Masuda and Teshima, 1994; Miki, 1994; Masuda, 1998). In only one instance, a female of *Chiloscyllium griseum* had four egg cases in the oviducts (Senta and Sarangdhar, 1948).

Stegostoma is characterized by retained oviparity (Compagno, 1998, 1990b) in which more than two (usually four) eggs are enclosed by egg cases in the nidamental gland and deposited onto the substrate simultaneously (Smedley, 1926; Randall, 1990). The egg case is depressed and rounded, with short silky and adhesive fibers extending from the alternate side (Fig. 98D; Dotsu, 1972; Masuda et al., 1980).

The remaining taxa are classified into the yolksac viviparity, in which juveniles grow by absorbing yolksac in the oviducts, equivalent to the ovoviviparity in the traditional sense (Compagno, 1984; Michael, 1993; Last and Stevens, 1994). Among them, the following differences are recognized. The number of litters is seven to eight in *Brachaelurus* (Michael, 1993; Last and Stevens, 1994); about 20–30 in Orectolobidae (Randall, 1990; Michael, 1993; Last and Stevens, 1994); four to eight in *Nebrius* (Myers, 1989; Last and Stevens, 1994); 20–30 in *Ginglymostoma* (Compagno, 1984; Michael, 1993); and approximately 300 in *Rhincodon* (Joung et al., 1995). *Ginglymostoma, Nebrius* and *Rhincodon* produce well developed keratinoid egg cases in the oviducts during the early stage of development, and *Orectolobus* has rudimentary egg cases (Fig. 98C; Southwell, 1912–1913; Bigelow and Schroeder, 1948; Baughman, 1955; Quèro, 1984; Toda et al., 1991; Last and Stevens, 1994; Joung et al., 1995). However, no one has reported whether *Brachaelurus* makes such egg cases. In particular, *Rhincodon* has been believed to be oviparous, since a large egg case with a 355 mm TL of embryo was caught in the open sea off Texas by trawl net in 1953 (Baughman, 1955; Reid, 1957; Garrick, 1964). However, some authors believed that *Rhincodon* is viviparous because a juvenile obtained had a remnant of yolksac and the egg case had no tendrils on its surface (Gilbert, 1981–1982). Recently, an adult female of adult 8 m TL with approximately 300 individuals including both eggs and already hatched juveniles in the oviducts was caught off Taiwan in 1995 (Joung et al., 1995). They were variously developed from unfertilized eggs located in the proximal region of oviduct to fully developed juveniles located in near cloaca. Therefore, *Rhincodon* is viviparous and produces an egg case only during the early period of pregnancy. The egg case of the yolksac viviparous species is without tendrils or vestibular horns on the surface, except some unfertilized eggs of *Ginglymostoma* that have two feeble, vestigial tendrils (Baughmann, 1955; Gudger, 1940).

2. Comments on evolution of mode of reproduction.

The evolution of mode of reproduction within living elasmobranchs has been studied by some authors (White, 1937; Wourms, 1977; Compagno, 1988, 1990b). Based on their interpretations, oviparity is the most primitive system, and viviparity (yolksac viviparity) seems to be derived in some higher taxa with further divergence into cannibal viviparity, placental viviparity, and uterine viviparity. White (1937) pointed out that the oviparity is shared by primitive taxa, which were recorded from the Jurassic layer, while viviparous taxa did not appear until later than Cretaceous. Compagno (1990b) examined evolutionary trends of the mode of reproduction from his concepts of interrelationships of living elasmobranchs, but his results were merely based on traditional hypotheses. Furthermore, no one has dealt with the evolution of mode of reproduction within the orectolobiforms. Thus, I infer an evolutionary trend and immediate ancestral states of the reproduction mode of orectolobiforms based on the character optimization method. The character state of reproduction mode found in each terminal taxon is optimized on the cladogram reconstructed in the previous chapter, and the hypothetical ancestral state is inferred for each internode based on the most parsimony method (Carpenter, 1989; Brooks and McLennan, 1991; Swofford and Maddison, 1991; Wiley et al., 1991). Ancestral states within the clade are estimated by using the ACCTRAN option of PAUP ver. 3.0 (Swofford, 1990) and McClade ver. 3 (Maddison and Maddison, 1992). Depending on differences of the mode of reproduction in orectolobiforms described above, the following three characters are available.

A : Mode of reproduction (0) oviparity; (1) yolksac

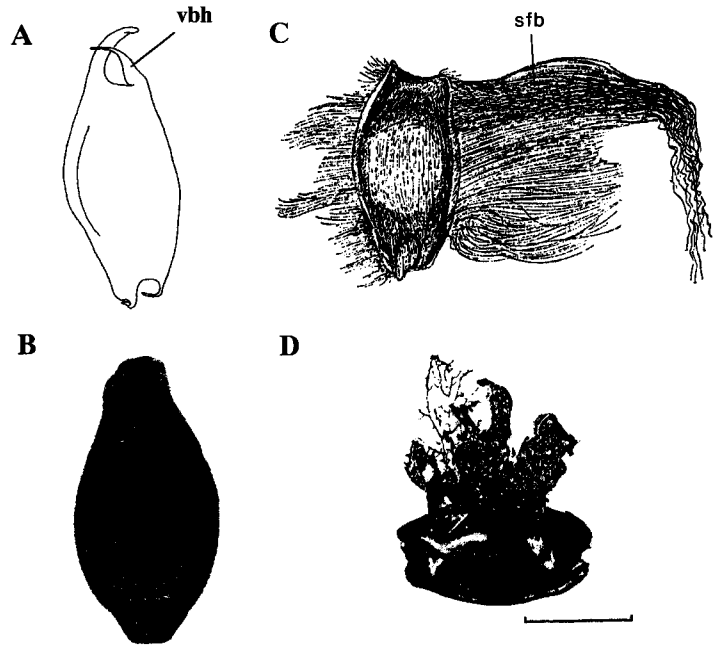

Fig. 98. Four types of egg cases in Orectolobiformes. (A) *Cirrhoscyllium japonicum* (original drawing of an 55 mm egg case in length removed from HUMZ 39399); (B) *Ginglymostoma cirratum* (from Gudger, 1942); (C) *Chiloscyllium griseum* (from Senta and Sarangdhar, 1948); (D) *Stegostoma varium* (from Dotsu, 1972).

viviparity. B: Maximum number of offspring (0) two; (1) four; (2) eight; (3) 20–30; (4) more than 100. C: Egg case (Fig. 98) (0) without tendrils nor vestibular horns (Fig. 98B); (1) with prominent vestibular horns (Fig. 98A); (2) with elongated and adhesive silky fibers (Fig. 98C-D).

According to this definition, each terminal taxon is assigned as follows: *Parascyllium* and *Cirrhoscyllium* A0B0C1; *Orectolobus* A1B3C ?; *Brachaelurus* A1B2C ?; *Hemiscyllium* and *Chiloscyllium* A0B1C2; *Stegostoma* A0B1C2; *Ginglymostoma* A1B3C0; *Rhincodon* A1B4C0. Concerning outgroups, several taxa represent placental viviparity, cannibal viviparity or uterine viviparity, all of which are absent in orectolobiforms. These categories are, however, restricted in the higher taxa within ordinal-ranked groups, and are apparently modified systems from the yolksac viviparity based on the structure (Lohberger, 1910; Shann, 1923; Bigelow and Schroeder, 1948; Springer, 1948; Amoroso, 1960; Schlernitzauer and Gilbert, 1966; Budker, 1971; Wourms, 1977; Yano, 1992). Therefore, it is most parsimonious that these modes were derived independently from yolksac viviparity. The remaining outgroups can be categorized into either oviparity or yolksac viviparity of Wourms (1977). Among oviparous species, extended oviparity, that primarily has two egg cases at once, is found in some scyliorhinids like *Halaelurus* (Nakaya, 1975). In scyliorhinids and rajids, the egg case is depressed and square-shaped, with a prominent vestibular horn extending from each corner (Bigelow and Schroeder, 1953; Cox, 1964; Nakaya, 1975), whereas *Heterodontus* possesses a thick and coiled egg case with no prominent tendrils nor vestibular horns (Smith, 1942). Yolksac viviparity, which makes a rudimentary egg case with no prominent tendrils nor vestibular horns, is found in a number of elasmobranchs (Daniel, 1934; Gudger, 1940; Breder and Rosen, 1966; Wourms, 1977). Among them, the number of litters is usually more than four to over 40 in most taxa (Gudger, 1940; Compagno, 1990b). On the other hand, chimaeroids are oviparous and make keratinous egg cases without tendrils (Wourms, 1977; Dodd, 1983; Didier, 1995), but the egg cases are different in their chemical structure from that of elasmobranchs (Wourms, 1977). Therefore, I attempt the ON state as an equivocal condition either retained oviparous, extended oviparous or yolksac viviparous, the number of offspring as ambiguous, and the shape of egg case as equivocal 0, 1. Therefore, ON state is assigned as A0,1B ? C0,1 *a priori*.

Three most parsimonious character optimizations are reconstructed on the cladogram inferred in the cladistic analysis based on ACCTRAN (Figs. 99–101). Concerning Fig. 99, it is inferred that the common ancestor of this order is primarily oviparous with acquisition of viviparity at Node E, the orectolobid-brachaelurid ancestor, and at Node O, the ancestor of *Rhincodon* and *Ginglymostoma*, respectively. Figure 100 reveals that the maximum number of offspring is primitively two, with increase to four in the ancestor of Orectoloboidei

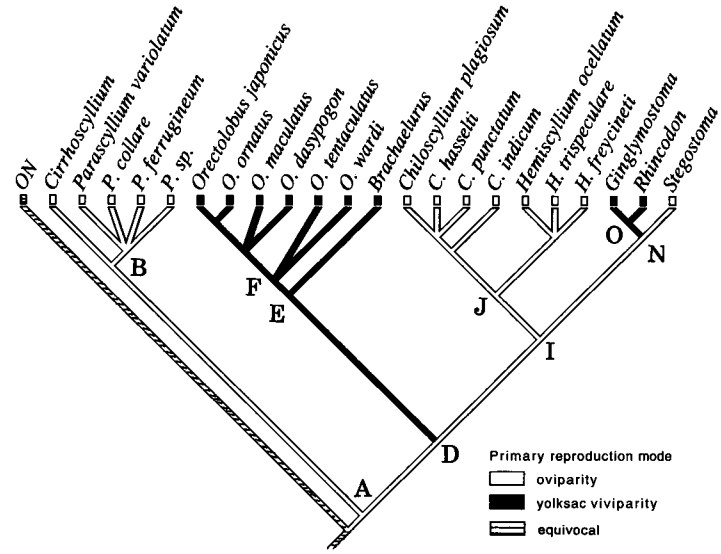

Fig. 99. Hypothesis of character optimization on the orectolobiform cladogram reconstructed by morphologucal synapomorphies in mode of reproduction.

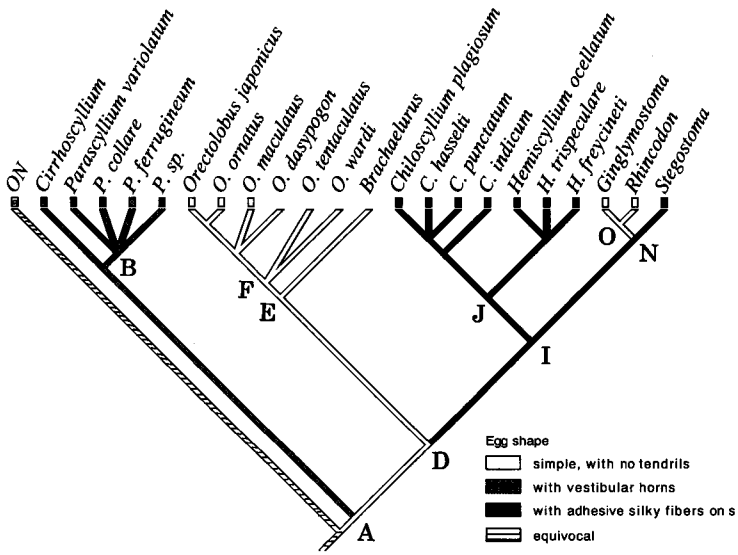

Fig. 100. Hypothesis of character optimization on the orectolobiform cladogram reconstructed by morphologucal synapomorphies in maximum number of offspring.

(Node D), and much larger number of offspring is subsequently acquired at the level of Node E and Node O, respectively. Two offspring appeared in the ancestor of Hemiscylliidae should be judged as a reversal from four offspring under the ACCTRAN. Figure 101 suggests that the egg case is primitively simple, without tendrils nor vestibular horns. The vestibular horns are acquired in the ancestor of Parascylloidei (Node B). The adhesive silky fibers occur at Node I containing Hemiscylliidae and Rhincodontidae, and are judged to be secondarily lost at Node O, the ancestor of *Rhincodon* and *Ginglymostoma*.

Primitively, the common ancestor of Orectolobiformes is estimated as an extended oviparous species, with a subsequent evolution to the retained oviparous nature in the common ancestor of Orectoloboidei. Parascylloidei primitively remains extended oviparity, with acquisition of vestibular horns to possibly anchor the egg cases on the substrate. From the retained oviparity, yolksac viviparity seems to have independently evolved in two different lineages accompanied with increasing number of offspring. One lineage is towards the Brachaeluridae and Orectolobidae, and the other towards the lineage containing *Ginglymostoma* and *Rhincodon*. Adhesive silky fibers on egg case are probably developed in the common ancestor of Hemiscylliidae and Rhin-

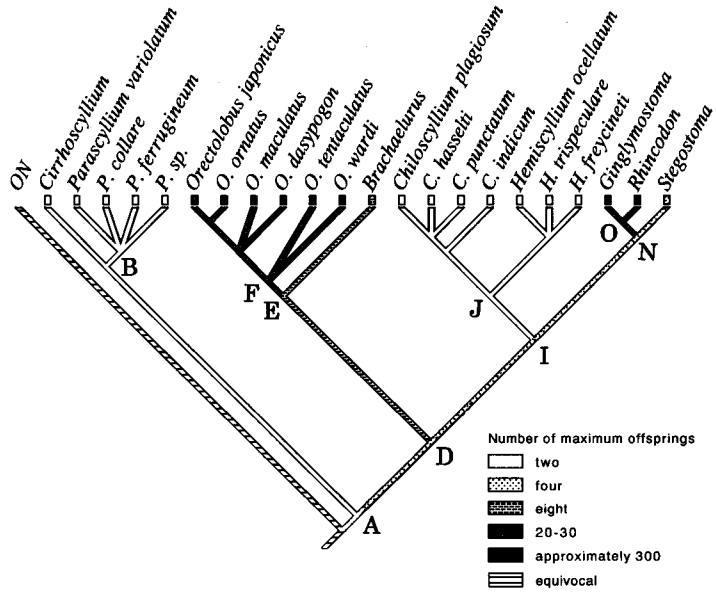

Fig. 101. Hypothesis of character optimization on the orectolobiform cladogram reconstructed by morphologucal synapomorphies in existences of vestibular horns or silky fibers on egg case.

codontidae in order to anchor the egg case tightly on the substrate. However those are secondarily lost in the ancestor of *Ginglymostoma* and *Rhincodon* because both genera swim actively rather than other orectolobiform taxa to acquire yolksac viviparity and thus did not have necessity for anchoring the egg on the substrate. On the other hand, the extended oviparity is acquired secondarily from the retained oviparous nature in the ancestor of Hemiscylliidae with the elongations of adhesive silky fibers to fix the egg case on the substrate tightly. Indeed, a fact which additional two egg cases were recorded from a female by Senta and Sarangdhar (1948) agrees with the hypothesis to reduce the number of eggs secondarily. The rhincodontid *incertae* genus *Nebrius* is yolksac viviparity with four to eight offspring, and seems to be closer to *Ginglymostoma* and/or *Rhincodon* than to *Stegostoma* based on the concept of parsimony. In addition, it is most parsimonious that *Nebrius* seems to be a sister group of the clade composed of *Rhincodon* and *Ginglymostoma* depending upon the number of offspring.

IX. Summary

The present study was made to provide an anatomical description of the order Orectolobiformes to determine the interrelationships within this order after the estimation of monophyly of this taxon, and develop a classification reflecting the genealogical relationships. Methodology of this study was based on the cladistic method using outgroup comparison. The two step procedure proposed by Maddison et al. (1984) was adopted in this study in order to estimate the outgroup-ingroup relationships of living elasmobranchs including all orectolobiforms in the first step and to elucidate the interrelationships within the re-defined orectolobiforms. Additionally, evolution of mode of reproduction was inferred on the basis of the interrelationships hypothesized in the cladistic analysis. Conclusion is summarized below.

(1) In the first step, 54 most parsimonious cladograms are reconstructed from 34 apomorphic characters adopted by the comparison with the fossil outgroups closely related with living elasmobranchs. The order Orectolobiformes is a well defined monophyletic taxon supported by two synapomorphies: foramen for ophthalmicus profundus fused with that for ophthalmicus superficialis and prominent inner process on medial margin of ceratobranchial.

(2) In the second step, the interrelationships within Orectolobiformes are reconstructed on the basis of 22 species and 136 anatomical characters including external morphology, skeleton, musculature, and sensory system. Six most parsimonious cladograms are provided from the branch-and bound algorithm of PAUP. Orectolobiformes is supported by 17 apomorphies in addition to two apomorphies supposed in the first step. *Cirrhoscyllium* and *Parascyllium* form a well defined monophyletic group sharing 41 apomorphies, and are initially derived from the orectolobiform clade. The remaining species form a clade supported by 24 apomorphies. *Orectolobus, Sutorectus, Eucrossorhinus* and *Brachaelurus* are a clade supported by 11 apomorphies, and species of *Orectolobus* are not monophyletic unless

Sutorectus and *Eucrossorhinus* are included. *Rhincodon* and *Ginglymostoma* form a clade supported by seven apomorphies to form a sister group of *Stegostoma* by having 25 synapomorphies. The cladistic result is equivalent to that of Compagno (1988), but is different from that of Dingerkus (1986) because of his misinterpretations of the synapomorphies.

(3) Depending upon the branching pattern, the suborders Parascylloidei and Orectoloboidei are proposed. Parascylloidei consists of only one family, Parascylliidae, containing two genera, *Parascyllium* and *Cirrhoscyllium*. Orectoloboidei consists of four families, viz. Orectolobidae, Brachaeluridae, Hemiscylliidae and Rhincodontidae. Orectolobidae contains only the genus *Orectolobus*, and the genera *Eucrossorhinus* and *Sutorectus* are synonymized. Brachaeluridae contains only the genus *Brachaelurus*. Hemiscylliidae contains two genera, *Chiloscyllium* and *Hemiscyllium*. The family Rhincodontidae is proposed for three genera examined, *Stegostoma, Ginglymostoma* and *Rhincodon* with additions of two incertae genera, *Nebrius* and *Pseudoginglymostoma*.

(4) Evolution of mode of reproduction within Orectolobiformes is inferred on the basis of the cladistic topology. The common ancestor had an extended oviparity, and the vestibular horns on the corners of egg case occurred in Parascylloidei. Orectoloboidei acquired retained oviparity with adhesive silky fibers on the egg case. Yolksac viviparity with additional increase of offspring was acquired in the brachaelurid-orectolobid clade and the *Rhincodon-Ginglymostoma* clade, respectively. Hemiscylliidae is judged to have acquired the extended oviparity secondarily with elongations of adhesive silky fibers.

X. Acknowledgments

I would like to express my sincere thanks to Dr. Kunio Amaoka (formerly Prof., Hokkaido University) and Prof. Kazuhiro Nakaya (HUMZ) for their guidance during this study and critical reading of the manuscript, and to Prof. Shigeru Nakao, Hokkaido University, for his critical reading and a lot of suggestions to the manuscript. I especially thank Dr. Shigeru Shirai (Japan Sea National Fisheries Research Institute) who kindly recommended me the theme of this study and a lot of guidance on systematic works of the fossil and living elasmobranchs, and who discussed phylogenetic methodology with me throughout this study. I also thank Assoc. Prof. Mamoru Yabe (HUMZ) for his useful suggestion on this study, and Dr. Kiyonori Nishida (Osaka Aquarium : *Kaiyu-kan*) for his guidance on systematic works of elasmobranchs and observation of locomotion in the aquarium and for his help to dissect the "largest material," whale shark. Additionally, I am grateful to Dr. Dominique A. Didier (ANSP) and Dr. Peter R. Last (CSIRO) who gave me useful suggestions to the draft manuscript.

I am deeply indebted to the followings for the permission of loan or gift of a large number of examined specimens deposited at their institutions : Dr. P.R. Last (CSIRO) ; Drs. G.J. Howes (who retired) and N.R. Merrett (BMNH) ; Drs. B. Sêret and G. Duhamel (MNHN) ; Dr. V.G. Springer (USNM) ; Drs. T. Iwamoto and W.N. Eschmeyer (CAS) ; Dr. K.E. Hartel (MCZ) ; Drs. J.R. Paxton and M. McGrouther (AMS) ; Dr. J.G. Nielsen (ZMUC) ; Dr. H.K. Larson (NTM) ; Dr. K. Smith (WAM) ; Dr. R. McKay (QM) ; Dr. H. Yang (TFRI) ; Dr. K. Matsuura (NSMT) ; Drs. O. Okamura and Y. Machida (BSKU) ; Dr. I. Nakamura (FAKU) ; Dr. S. Tanaka (MSM) ; Mr. S. Hagiwara (Shimoda Floating Aquarium) ; Mr. Fujino (Osaka Aquarium).

I also thank Dr. S. Gento (NSMT), Dr. T. Komai (Natural History Museum and Institute, Chiba), Dr. H. Endo (BSKU), Dr. H. Imamura (Museum of Hokkaido University), Dr. K. Sato (Okinawa Expo Aquarium), Mr. K. Yoshimura (Hokkaido Wakkanai Fisheries Experimental Station), Mr. E. Mihara (Hokkaido Hakodate Fisheries Experimental Station), and the following colleagues of HUMZ for their advice on my systematic works : F. Muto, K. Hoshino, H. Miyahara, T. Shimokawa, D. Tsutsui, M. Arai, T.J. Takahashi, T. Yamaguchi and R. Fujii. Furthermore, the following superiors and colleagues of the Fisheries Promotion Division, Governmental Office, Iwate Pref. and Iwate Fisheries Technology Center have given me time sufficient to finish this work : M. Takeichi, S. Kamimura, K. Kikuchi, K. Miyazawa, M. Omori, S. Watanabe, K. Nodaguchi and S. Itsukaichi. Finally, I could not finish this work without the help of my wife, Akiko.

XI. Literature cited

Aiyar, R.G. and K.P. Nalini. (1938). Observations on the reproductive system, egg case, embryos and breeding habits of *Chiloscyllium griseum* M. & H. *Proc. Indian Acad. Sci.(B)*, **7**, 252-269.

Allis, Jr., E.P. (1923). The cranial anatomy of *Chlamydoselachus anguineus*. *Acta Zool. (Stockholm)*, **4**, 123-221, pls. 1-23.

Amoroso, E.C. (1960). Viviparity in fishes. *Symp. Zool. Soc.*, **1**, 153-181.

Applegate, A.T. (1972). A revision of the higher taxa of orectolobids. *J. Mar. Biol. Ass. India*, **14**, 743-751.

Balfour, F.M. (1881). On the development of the skeleton of the paired fins of Elasmobranchii, considered in relation to its bearings on the nature of the limbs of the

Vertebrata. *Proc. Roy. Soc. London,* **1881**, 656-671, pls. 57-58.

Bass, A.J., D. D'Aubrey and N. Kistnasamy. (1975). Sharks of the east coast of southern Africa. IV. The families Odontaspididae, Scapanorhynchidae, Isuridae, Cetorhinidae, Alopiidae, Orectolobidae and Rhincodontidae. *Invest. Rep. oceanogr. Res. Inst.*, (**39**), 1-102.

Baughman, J.L. (1955). The oviparity of the whale shark *Rhincodon typus* with records of this and other fishes in Texas waters. *Copeia,* **1955**, 54-55.

Bennett, E.T. (1830). Catalogue of the fishes of Sumatra. *Memoir of the Life and Public Services of Sir Stamford Raffles*. 694 p. London.

Bigelow, H.B. and W.C. Schroeder. (1948). Sharks. p. 59-576, Tee-Van, J., Breder, C.M., Hildebrand, S.F., Parr, A.E. and Schroeder, W.C. (eds.). *Fishes of the Western North Atlantic. Part 1.* Sears Foundation for Marine Research, Yale Univ., New Haven.

Bigelow, H.B. and W.C. Schroeder. (1953). Sawfishes, guitarfishes, skates and rays. p. 1-514, Tee-Van, J., Breder, C.M., Hildebrand, S.F., Parr, A.E. and Schroeder, W.C. (eds.). *Fishes of the Western North Atlantic. Part 2.* Sears Foundation for Marine Research, Yale Univ., New Haven.

Bleeker, P. (1867). Description de trois espèces indédites de Crossorhinus de l'archipel des Moluques. *Arch. Néerl. Sci. Nat., Haarlem,* **2**, 400-402, pl. 21.

Bloch, M.E. (1785). *Naturgeschichte der ausl ndischen Fische*. Berlin, 1.

Bloch, M.E. and J.G. Schneider. (1801). *M.E. Blochii, Systema Ichthyologiae iconibus ex illustratum*. Post obitum auctoris opus inchoatum absolvit, correxit, interpolavit Jo. Gottlob Schneider, Saxo. Berolini. Sumtibus Austoris Impressum et Bibliopolio Sanderiano Commissum.

Bonaparte, C.L. (1834). Iconografia della fauna italica per le quatrtro classi degli animali vertebrati. Tomo III. *Pesci. Roma. Fasc.*, 6-11, puntate 29-58, 12 pls.

Bonnaterre, J.P. (1788). *Tabeau encyclop dique et méthodique des trois règnes de la nature. Ichthyologie*. Paris.

Braus, H. (1902). Ueber neuere Funde versteinerter Gliedmassen-Knorpel und Muskeln von Selachiern. *Verh. d. Phys., Med. Ges. Wuerzburg,* **34**, 177-192.

Breder, C.M., Jr. and D.E. Rosen. (1966). *Modes of reproduction in fishes*. The Natural History Press, New York.

Brooks, D.R. and D.A. McLennan. (1991). *Phylogeny, ecology, and behavior : A research program in comparative biology*. The University of Chicago Press, Chicago.

Brough, J. (1935). On the structure and relationships of the hybodont sharks. *Mem. Proc. Manchester Lit. Philo. Soc.,* **79**, 35-47.

Brown, C. (1900). Uebr das Genus *Hybodus* und seine systematische Stellung. *Palaeontographica,* **44**, 149-174.

Budker, P. (1971). *The life of sharks*. Columbia Univ. Press, New York.

Carpenter, J.M. (1989). Testing scenarios : Wasp social behavior. *Cladistics,* **5**, 131-144.

Carvalho, M.R. (1996). Higher-Level elasmobranch phylogeny, basal squaleans, and paraphyly. p. 35-62, Stiassny, M.L.J., Parenti, L.R. and Johnson, G.D. (eds.). *Interrelationships of fishes*. Academic Press.

Carvalho, M.R. and J. Maisey. (1996). Phylogenetic relationships of the Late Jurassic shark *Protospinax* Woodwad, 1919 (Chondrichthyes : Elasmobranchii). p. 9-46, Arratia, G. and Viohl, G. (eds.). *Mesozoic Fishes : Systematics and Paleoecology*. Verlag Dr. Friedrich Pfiel, Munich.

Chu, Y.T. and M.C. Wen. (1963). *A study of the lateral-line canals system and that of Lorenzini ampullae and tubules of Elasmobranchiate*. (In Chinese with English summary). Science and Technology Press, Shanghai, i-iv+132 pp., 64 pls.

Compagno, L.J.V. (1973). Interrelationships of living elasmobranchs. p. 15-61, pls. 1-2, Greenwood, P.H., Miles, R.S. and Patterson, C. (eds.). *Interrelationships of fishes*. Zool. J. Linn. Soc., 53 (Suppl. 1). Academic Press, London.

Compagno, L.J.V. (1977). Phyletic relationships of living sharks and rays. *Amer. Zool.,* **17**, 303-322.

Compagno, L.J.V. (1984). FAO species catalogue. Vol. 4. Sharks of the world. An annotated and illustrated catalogue of sharks species known to date. Part 1. Hexanchiformes to Lamniformes. *FAO Fish. Synop.*, (**125**) **4**, 1-249.

Compagno, L.J.V. (1988). *Sharks of the order Carcharhiniformes*. Princeton Univ. Press, Princeton.

Compagno, L.J.V. (1990). Relationships of the megamouth shark, *Megachasma pelagios* (Lamniformes ; Megachasmidae), with comments on its feeding habits. p. 357-379, Pratt, H.W., Jr., Gruber, S.H. and Taniuchi, T. (eds.). *Elasmobranchs as living resources : Advances in the biology, ecology, systematics, and the status of the fisheries*. NOAA Tech. Rep. NMFS 90.

Compagno, L.J.V. (1990b). Alternative life-history styles of cartilaginous fishes in time and space. *Env. Biol. Fish.,* **28**, 33-75.

Cox, K.W. (1964). Egg-cases of some elasmobranchs and a cyclostome from California waters. *Calif. Fish and Game,* **49**, 271-289.

Daniel, J.F. (1934). *The elasmobranch fishes, 3rd ed.* Univ. Calif. Press, Berkeley.

Davidson, P. (1918). The musculature of *Heptanchus maculatus. Univ. Calif. Pub. Zol.,* **18**, 151-170.

De Beer, G.R. (1937). *The development of the vertebrate skull*. Clarendon Press, London.

Denison, R.H. (1936). Anatomy of the head and pelvic fin of the whale shark, *Rhineodon. Bull. Amer. Mus. Nat. Hist.,* **73**, 477-515.

Deraniyagala, P.E.P. (1934). The embryo of the dogfish. *Chiloscyllium indicum. Spol. Zeyl.,* **18**, 249.

Didier, D. (1995). Phylogenetic systematics of extant chimaeroid fishes (Holocephali, Chimaeroidei). *Amer. Mus. Novit.,* **3119**, 1-86.

Dingerkus, G. (1986). Interrelationships of orectolobiform sharks (Chondrichthyes : Selachii). p. 227-245, Uyeno, T., Arai, R., Taniuchi, T. and Matsuura, K. (eds.). *Indo-Pacific fish biology : Proceedings of the Second International Conference on Indo-Pacific Fishes*. Ichthyological Society of Japan, Tokyo.

Dingerkus, G. and T.C. Defino. (1983). A revision of the orectolobiform shark family Hemiscyllidae (Chondrichthyes, Selachii). *Bull. Amer. Mus. Nat. Hist.,* **176**, 1-94.

Dodd, J.M. (1983). Reproduction in cartilaginous fishes (Chondrichthyes). p. 31-95, Rankin, J.C., Pitcher, T.J. and Duggan, R.T. (eds.). *Fish Physiology. Vol. 9.* Academic Press, San Diego.

Dotsu, Y. (1972). Collection of the T.S. Nagasaki Maru of Nagasaki University-I. Eggs of the tiger shark, *Stegostoma fasciatum. Bull. Fac. Fish. Nagasaki Univ.,* **33**, 1-6.

Duméril, A.M.C. (1853). Monographic de la tribu des scylliens ou roussettes (poissons plagiostomes) comprenant deux espéces nouvelles. *Rev. Mag. Zool. (Ser. 2),* **5**, 119-130.

Edgeworth, F.H. (1935). *The cranial muscles of vertebrates.* Cambridge Univ. Press, Cambridge, i-viii+493 pp., 841 figs.

Eldredge, N. and J. Cracraft. (1980). *Phylogenetic patterns and the evolutionary process. Method and theory in comparative biology.* Columbia Univ. Press, New York, i-x+349 pp.

Farris, J.A. (1970). Methods for computing Wagner trees. *Syst. Zool.,* **19**, 83-92.

Fitch, W.M. (1971). Toward defining the course of evolution : minimum change for a specific tree topology. *Syst. Zool.,* **20**, 406-416.

Fürbringer, K. (1904). Beiträge zur Morphologie des Skelettes der Dipnoer, nebst Bemerkungen über Pleuracanthiden, Holocephalen und Squaliden. Med.-Naturwiss. *Gesell. Jena,* **4**, 423-510.

Gardiner, B.G. (1984a). The relationships of the palaeoniscid fishes, a review based on new specimens of *Mimia* and *Moythomasia* from the Upper Devonian of Western Australia. *Bull. Brit. Mus. (Nat. Hist.), Geol.,* **37**, 173-428.

Gardiner, B.G. (1984b). The relationship of placoderms. *J. Vert. Paleont.,* **4**, 379-395.

Garman, S. (1885). *Chlamydoselachus anguineus* Garm. A living species of cladodont shark. *Bull. Mus. Comp. Zool., Harvard Coll.,* **12**, 1-35, pls. 1-20.

Garman, S. (1913). The Plagiostoma. *Mem. Mus. Comp. Zool., Harvard Coll.,* **36**, 1-515, 75 pls.

Garrick, J.A.F. (1964). Additional information on the morphology of an embryo whale shark. *Proc. U. S. Nat. Mus.,* **115**, 1-7.

Gaudin, T.J. (1991). A re-examination of elasmobranch monophyly and chondrichthyan phylogeny. *N. Jb. Geol. Palaeont. Abh.,* **182**, 133-160.

Gilbert, P.W. (1981-1982). Patterns of shark reproduction. *Oceanus,* **24**, 30-39.

Gill, T. (1862). Analytical synopsis of the order of Squali ; and revision of the nomenclature of the genera. *Ann. Lyc. Nat. Hist.,* **7**, 367-413.

Gill, T. (1865). On a new generic type of sharks. *Proc. Acad. Nat. Sci. Phila.,* **1865**, 177.

Gill, T. (1896). Notes on *Orectolobus* or *Crossorhinus*, genus of sharks. *Proc. U. S. Natl. Mus.,* **18**, 211-212.

Glickman, L.S. (1967). Subclass Elasmobranchii. p. 292-352, Orlov, Y.A. (ed.). *Fundamentals of paleontology, 11.* Israel Prog. Sci. Transl., Jerusalem.

Gmelin, J.F. (1789). Amphibia. Pisces. p. 1033-1816, Caroli a Linné. *Systema Naturae per regna tria naturae. 13th ed.* Vol. 1, Part 3. Lipsiae.

Goodrich, E.S. (1909). Vertebrata craniata (first fascicle : cyclostomes and fishes). p. i-xvii+1-513, Lankester, R. (ed.). *A treatise on Zoology, 9.* Adam and Charles Black, London.

Goto, T., K. Nakaya and K. Amaoka. (1992). Morphology of throat barbels of *Cirrhoscyllium japonicum* (Elasmobranchii, Parascylliidae), with comments on function and homology. *Japan. J. Ichthyol.,* **41**, 167-172.

Goto, T. and K. Nakaya. (1996). Revision of the genus *Cirrhoscyllium*, with a description of the neotype of *C. japonicum* (Elasmobranchii, Parascylliidae). *Ichthyol. Res.,* **43**, 199-209.

Goto, T. and K. Nishida. (2001). Internal morphology and phylogeny of whale shark. Nakabo, T. and Machida, Y. (eds.). *Fishes of Kuroshio Current, Japan.*

Gudger, E.W. (1940). The breeding habits, reproductive organs, and external embryonic development of *Chlamydoselachus* based on notes and drawings left by Bashford Dean. p. 521-646, Gudger, E.W. (ed.). *Bashford Dean Memorial Volume-Archaic Fishes, Art. 7.* American Museum of Natural History, New York.

Günther, A. (1871). Report on several collections of fishes recently obtained for the British museum. *Proc. Zool. Soc. London,* **1871**, 652-675, pl. 53-70.

Hasse, C. (1878). Das natürliche System der Elasmobranchier auf Grundlage des Baus und der Entwicklung der Wirbelsäule. *Zool. Anz.,* **1**, 144-148.

Hennig, W. (1966). *Phylogenetic systematics.* Univ. Illinois Press, Urbana, 263 pp.

Hermann, J. (1783). *Tabula affinitatum animalium, etc.* Argentorati.

Holmgren, N. (1940). Studies on the head in fishes. Embryological, morphological, and phylogenetical researches. Part I : Development of the skull in sharks and rays. *Acta Zool. (Stockholm),* **21**, 51-267.

Holmgren, N. (1941). Studies on the head in fishes. Embryological, morphological, and phylogenetical researches. Part II : Comparative anatomy of the adult selachian skull, with remarks on the dorsal fins in sharks. *Acta Zool. (Stockholm),* **22**, 1-100.

Holmgren, N. and T. Pehrson. (1949). Some remarks on the ontogenetical development of the sensory lines on the cheek in fishes and amphibians. *Acta Zool. (Stockholm),* **30**, 249-314.

Huber, O. (1901). Die kopulationsglieder der Selachier. *Z. Wiss. Zool.,* **70**, 1-87, 27-28 pls.

ICZN. (1984). International Commission on Zoological Nomenclature. Opinion1278. *Rhincodon* A. Smith, 1829 is conserved. *Bull. Zoo. Nom.,* **41**, 215-217.

ICZN. (2000). *International Code of Zoological Nomenclature, 4th edition, adopted by the International Union of Biological Sciences. Intern. Trust.* Zool. Nomencl., Brit. Mus. (Nat. Hist.), London. 339 pp.

Jaekel, O. (1906). Neue Rekonstruktionen von *Pleuracanthus sessilis* und von *Polyacrodus (Hybodus) hauffianus. Sitzberg. Gesellsch. Naturforsch. Freunde, Berlin,* **1906**, 155-159.

Jordan, D.S. and H.W. Fowler. (1903). A review of the elasmobranchiate fishes of Japan. *Proc. U. S. Natn. Mus.,* **26**, 593-674.

Jordan, D.S. and C.H. Gilbert. (1883). Synopsis of the fishes of North America. *Bull. U. S. Natn. Mus.,* **16**, 10-18.

Joung, S.J., C.T. Chen, K.M. Liu, Y.P. Hwang, T.C. Liu, E. Clark, T. Uchida, Y.Z. Chen and B.S. Lin. (1995).

Ovoviviparous whale shark. In Symposium on Taxonomy, Ecology, and Stocks of Elasmobranchs. *Japan. Soc. Elasmobranch Studies,* **32**, 32.

Koken, E. (1907). Ueber *Hybodus. Geol. Palaeont. Abh. n. s.,* **5**, 261-276.

Last P.R. and J.D. Stevens. (1994). *Sharks and rays of Australia.* CSIRO, Australia.

Leviton, A.E., R.H. Gibbs, Jr., E. Heal and C.E. Dawson. (1985). Standards in herpetology and ichthyology: Part 1. Standard symbolic codes for institutional resource collections in herpetology and ichthyology. *Copeia,* **1985**, 802-832.

Lohberger, J. (1910). Ueber Zwei Riesige Embryonen von *Lamna.* (Beiträge zur Naturgeschichte Ostasiens). *Abh. Bayer. Acad. Wiss.,* **4 (Suppl. 2)**, 1-45.

Luther, A.F. (1909a). Beiträe zur Kenntnis von Muskulatur und Skelett des Kopfes des Haies *Stegostoma tigrinum* Gm. und der Holocephalen mit einem Anhang über die Nasenrinne. *Acta Soc. Sci. Fenn.,* **37**, 1-60.

Luther, A.F. (1909b). untersuchungen über die vom N. trigeminus innervierte Muskulatur der Selachier (Haie und Rochen) unter Berücksichtigung ihrer Beziehungen zu benachbarten Organen. *Acta Soc. Sci. Fenn.,* **36**, 1-176, pls. 1-5.

Maddison, W.P., M.J. Donoghue and D.R. Maddison. (1984). Outgroup analysis and parsimony. *Syst. Zool.,* **33**, 83-103.

Maddison, W.P. and D.R. Maddison. (1992). *MacClade 3.0.* Interactive analysis of phylogeny and character evolution. Sinauer Associates, Sunderland, Massachusetts.

Maisey, J.G. (1977). The fossil selachian fishes *Palaeospinax* Egerton, 1872 and Nemacanthus Agassiz, 1837. *Zool. J. Linn. Soc.,* **60**, 259-273.

Maisey, J.G. (1978). Growth and form of finspines in hybodont sharks. *Palaeontol.,* **21**, 657-666.

Maisey, J.G. (1979). Finspine morphogenesis in squalid and heterodontid sharks. *Zool. J. Linn. Soc.,* **66**, 161-183.

Maisey, J.G. (1980). An evaluation of jaw suspension in sharks. *Amer. Mus. Novit.*, (**2706**), 1-17.

Maisey, J.G. (1982). The anatomy and interrelationships of Mesozoic hybodont sharks. *Amer. Mus. Novit.*, (**2724**), 1-48.

Maisey, J.G. (1984a). Higher elasmobranch phylogeny and biostrategraphy. *Zool. J. Linn. Soc.,* **82**, 33-54.

Maisey, J.G. (1984b). Chondrichthyan phylogeny: a look at the evidence. *J. Vert. Paleontol.,* **4**, 359-371.

Maisey, J.G. (1985). Cranial morphology of the fossil elasmobranch *Synechodus dubrisiensis. Amer. Mus. Novit.*, (**2804**), 1-28.

Maisey, J.G. (1986). Anatomical revision of the fossil shark *Hybodus fraasi* (Chondrichthyes: Elasmobranchii). *Amer. Mus. Novit.*, (**2857**), 1-16.

Maisey, J.G. (1987). Cranial anatomy of the Lower Jurassic shark *Hybodus reticulatus* (Chondrichthyes: Elasmobranchii), with comments on hybodontid systematics. *Amer. Mus. Novit.*, (**2878**), 1-39.

Masuda, H., C. Araga and T. Yoshino. (1980). *Coastal fishes of southern Japan.* Tokai Univ. Press, Japan.

Masuda, M. (1998). Mating spawning and hatching of the white spotted bamboo shark in an aquarium. *Japan. J. Ichthyol.,* **45**, 29-35.

Masuda, M. and M. Teshima. (1994). Reproduction of the white-spotted bamboo shark (*Chiloscyllium plagiosum*) in an aquarium. *J. Jpn. Assoc. Zool. Aqua.,* **36**, 20-23.

Michael, S.W. (1993). *Reef sharks and rays of the world: A guide to their identification, behavior, and ecology.* A Sea Challenger Publication, Monterey, California.

Miki, T. (1994). Spawning, hatching, and growth of the white spotted bamboo shark, *Chiloscyllium plagiosum. J. Japan. Ass. Zool. Aquarium,* **36**, 10-19. (In Japanese)

Miller, A.E. (1952). Note on the evolutionary history of the paired fins of elasmobranchs. *Proc. Roy. Soc. Edinberg,* **65**, 27-36.

Mivart, S.G. (1879). Notes on the fins of elasmobranchs, with considerations on the nature and homologues of vertebrate limbs. *Trans. Roy. Soc. London,* **10**, 439-484.

Moy-Thomas, J.A. (1936). The structures and affinities of the fossil elasmobranch fishes from the Lower Carboniferous rocks of Glencartholm, Eskdale. *Proc. Zool. Soc. London,* **1936**, 761-788.

Moy-Thomas, J.A. (1938). The early evolution and relationships of the elasmobranchs. *Biol. Rev.,* **14**, 1-26.

Moy-Thomas, J.A. and R.S. Miles. (1971). *Paleozoic fishes, 2nd ed.* Saunders, Philadelphia.

Müller, J. and F.G.J. Henle. (1837a). Gattungen der Haifische und Rochen, nach ihrer Arbeit: Ueber die Naturgeschichte der Knorpelfische. *Ber. K. Preuss. Akad. Wiss. Berlin,* **2**, 111-118.

Müller, J. and F.G.J. Henle. (1837b). Ueber die Gattungen der Plagiostomen. *Arch. Naturgesch.,* **3**, 394-401.

Müller, J. and F.G.J. Henle. (1838). On the generic characters of cartilaginous fishes, with descriptions of new genera. *Mag. Nat. Hist. (n. s.),* **2**, 33-37; 88-91.

Müller, J. and F.G.J. Henle. (1838-1841). *Systematische Beschreibung der Plagiostomen.* Berlin.

Myers, R.F. (1989). *Micronesian reef fishes: a practical guide to the identification of the coral reef fishes of the tropical central and western Pacific.* A Coral Graphics Production.

Nakaya, K. (1975). Taxonomy, comparative anatomy and phylogeny of Japanese catsharks, Scyliorhinidae. *Mem. Fac. Fish., Hokkaido Univ.,* **23**, 1-94.

Nelson, G.J. (1972). Phylogenetic relationships and classification. *Syst. Zool.,* **21**, 227-231.

Nelson, J.S. (1994). *Fishes of the world. 3rd ed.* John Wiley & Sons, New York.

Norris, H.W. and S.P. Hughes. (1920). The cranial, occipital, and anterior spinal nerves of the dogfish, *Squalus acanthias. J. Comp. Neur.,* **31**, 293-402.

Ogilby, J.D. (1907). Notes on exhibits. *Proc. R. Soc. Queensland,* **20**, 27-30.

Ogilby, J.D. (1908). On new genera and species of fishes. *Proc. Roy. Soc. Queensland,* **21**, 1-26.

Ogilby, J.D. and A.R. McCulloch. (1908). A revision of the Australian Orectolobidae. *Proc. Zool. Soc.,* **1908**, 264-299.

Patterson, C. (1967). Class Selachii and Holocephali. p. 666-675, Harland, W.B., House, M.R., Hughes, N.F., Reynolds, A.B., Rudwick, M.J.S., Satterthwaite, G.E., Tarlo, L.B.H. and Willey, E.C. (eds.). *The fossil record.* Geological Society, London.

Peyer, B. (1946). Die schweizerischen Funde von *Aster-*

acanthus (*Strophodus*). *Schweiz. Palaeont. Abh.*, **64**, 1-101.

Peters, W. (C.H.) (1864). Über eine Percoidengattung, *Plectroperca*, aus Japan und eine neue Art von Haifischen, *Crossorhinus tentaculatus*, aus Neuholland. *Monatsb. Acad. Wiss. Berlin,* **1864**, 121-126.

Playfair, R.L. and A.C. Günther. (1866). *The fishes of Zanzibar, with a list of the fishes of the whole east coast of Africa*. London.

Quêro, J.-C. (1984). Ginglymostomatidae. p. 93-94, Whitehead, P.J.P., Bauchot, M.-L., Hureau, J.-C., Nielsen, J. and Tortonese, E. (eds.). *Fishes of the North-eastern Atlantic and Mediterranean*. Unesco.

Raj, S.B. (1914). Note on the breeding of *Chiloscyllium griseum* M. & H. *Rec. Indian Mus.*, **16**, 215-240.

Ramsey, E.P. (1880). Notes on *Galeocerdo rayneri*, with a list of other sharks taken in Port Jackson. *Proc. Linn. Soc. New South Wales,* **5**, 95-97.

Randall, J.E. (1990). *Fishes of the Great Barrier Reef and Coral Sea*. Crawford House Press, Australia.

Regan, C.T. (1906). A classification of the selachian fishes. *Proc. Zool. So : 159. London,* **1906**, 722-758.

Regan, C.T. (1908). A revision of the sharks of the family Orectolobidae. *Proc. Zool. Soc.,* **1908**, 347-364.

Reid, G.K. (1957). External morphology of an embryo whale shark, *Rhincodon typus* Smith. *Copeia,* **1957**, 157-158.

Ridewood, W.G. (1895). On the spiracle and associated structures in elasmobranch fishes. *Anatomische Anzeiger,* **14**, 425-433.

Ridewood, W.G. (1921). On the calcification of the vertebral centra in sharks and rays. *Trans. Roy. Soc.* (*Ser. B*), **210**, 311-407.

Rosen, D.E., P.L. Forey, B.G. Gardiner and C. Patterson. (1981). Lungfishes, tetrapods, paleontology, and plesiomorphy. *Bull. Amer. Mus. Nat. Hist.*, 159-276.

Rüppell, W.P.E.S. (1835-1838). *Neuer Wirbelthiere zu der Fauna von Abyssinien gehörig. Fische, des Rothen Meeres*. Frankfurt-am-Main.

Schaeffer, B. (1967). Comments on elasmobranch evolution. p. 3-35, Gilbert, P.W., Mathewson, R.F. and Rall, D.P. (eds.). *Sharks, skates, and rays*. The Johns Hopkins Press, Baltimore.

Schaeffer, B. (1981). The xenacanth shark neurocranium, with comments on elasmobranch monophyly. *Bull. Amer. Mus. Nat. Hist.,* **169**, 1-66.

Schaeffer, B. and M. Williams. (1977). Relationships of fossil and living elasmobranchs. *Amer. Zool.,* **17**, 293-302.

Schlernitzauer, D.A. and P.W. Gilbert. (1966). Placentation and associated aspects of gestation in the bonnethead shark, *Sphyrna tibro*. *J. Morphol.,* **120**, 219-231.

Seba, A. (1758). *Locupletissimi rerum naturalium thesauri accurata descriptio*. Amsterdam, vol. 3.

Senta, S.B. and P.N. Sarangdhar. (1948). Observations on the development of *Chiloscyllium griseum* M. & H., *Pristis cuspidatus* Lath. and *Rhynchobatus djiddensis* (Forsk.). *Rec. Indian Mus.,* **96**, 1-23, 1 pl.

Shann, E.W. (1923). The embryonic development of the porbeagle shark, *Lamna cornubica. Proc. Zool. Soc.,* **11**, 161-171.

Shirai, S. (1992a). *Squalean phylogeny : a new framework of "squaloid" sharks and related taxa*. Hokkaido Univ. Press, iv+151, 58 pls.

Shirai, S. (1992b). Identity of extra branchial arches of Hexanchiformes (Pisces, Elasmobranchii). *Bull. Fac. Fish. Hokkaido Univ.,* **43**, 24-32.

Shirai, S. (1992c). Phylogenetic relationships of the angel sharks, with comments on elasmobranch phylogeny (Chondrichthyes, Squaliformes). *Copeia,* **1992**, 505-518.

Shirai, S. (1996). Phylogenetic interrelationships of neoselachians (Chondrichthyes : Euselachii). p. 9-34, Stiassny, M.L.J., Parenti, L.R. and Johnson, G.D. (eds.). *Interrelationships of fishes*. Academic Press.

Smedley, N. (1926). On a stage in the development of the tiger-shark, *Stegostoma tigrinum. J. Malayan Br. Roy. Asiat. Soc.,* **4**, 166.

Smith, A. (1828). Descriptions of new, or imperfectly known objects of the animal kingdom, found in the south of Africa. *So. Afr. Commercial Advertiser,* **3**, 2.

Smith, A. (1829). Contributions to the natural history of South Africa, etc. *Zool. J.,* **4**, 433-444.

Smith, A. (1937). On the necessity for a revision of the groups included in the Linnean genus *Squalus. Proc. Zool. Soc. London,* **5**, 85-86.

Smith, H.M. (1913). The hemiscylliid sharks of the Philippine Archipelago, with description of a new genus from the China Sea. *Proc. U. S. Natl. Mus.,* **45**, 567-569.

Smith, H.M. (1937). The anatomy of the frilled shark *Chlamydoselachus anguineus* Garman. p. 331-520, Gudger, E.D. (ed.). *Bashford Dean Memorial Volume : Archaic Fishes, Art. 6, Amer. Mus. Nat. Hist.*

Smith, B.G. (1942). The heterodontid sharks : Their natural history and the external development of *Heterodontus* (*Cestracion*) *japonicus* based on notes and drawings by Bashford Dean. p. 651-770, Gudger, E.W. (ed.). *Bashford Dean Memorial Volume : Archaic Fishes, Art. 6, Amer. Mus. Nat. Hist.*

Southwell, T. (1912-1913). Notes from the Bengal Fisheries Laboratory, No. 6. Embryological and developmental studies of Indian fishes. *Rec. Indian Mus.*, **16** : 215-240, pls. 16-19.

Springer, S. (1948). Oviphagus embryos of the sand shark, *Carcharias taurus. Copeia,* **1948**, 153-157.

Springer, S. (1966). A review of Western Atlantic cat sharks, Scyliorhinidae, with descriptions of a new genus and five new species. *U.S. Fish Wildl. Surv. Fish. Bull.,* **65**, 581-624.

Stensiö, E.A. (1937). Notes on the endocranium of a Devonian *Cladodus. Bul. Geol.,* **27**, 128-144.

Strasburg, D.W. (1963). The diet and dentition of *Isistius brasiliensis*, with remarks on tooth replacement in other sharks. *Copeia,* **1963**, 33-40.

Swofford, D.L. (1991). *Phylogenetic Analysis Using Parsimony* (*PAUP*), *version 3.0s*. Illinois Natural History Survey, Urbana.

Swofford, D.L. and W.P. Maddison. (1992). Parsimony, character-state reconstructions, and evolutionary inferences. p. 186-223, Mayden, R.L. (ed.). *Systematics, Historical Ecology, and North American Freshwater Fishes*. Stanford Univ. Press, Stanford, California.

Toda, M., S. Uchida, Y. Kamei and N. Tanaka. (1991). On reproduction of orectoloboid sharks. p. 17-23, the 35th Meeting of Aquarists of JAZGA. (In Japanese). Japanese Association of Zoological Gardens and Aquar-

iums.
Watrous, L.E. and Q.D. Wheeler. (1981). The out-group comparison method of character analysis. *Syst. Zool.*, **30**, 1-11.
White, E.G. (1930). The whale shark, *Rhineodon typus*. Description of the skeletal parts and classification based on the Marathon specimen captured in 1923. *Bull. Amer. Mus. Nat. Hist.*, **61**, 129-160.
White, E.G. (1937). Interrelationships of the elasmobranchs with a key to the order Galea. *Bull. Amer. Mus. Nat. Hist.*, **74**, 25-138, pls. 1-51.
Wiley, E.O. (1981). *Phylogenetics. The theory and practice of phylogenetic systematics*. John Wiley and Sons, New York, xv+439 pp.
Wiley, E.O., D. Siegel-Causey, D.R. Brooks and V.A. Funk. (1991). *The complete cladist : a primer of phylogenetic procedures*. Univ. Kansas Printing Service Lawrence, Kansas.
Whitley, G.P. (1927). Studies in ichthyology No. 1. *Rec. Australian Mus.*, **15**, 289-304
Whitley, G.P. (1939). Taxonomic notes on sharks and rays. *Aust. Zool.*, **9** : 227-262.
Woodward, A.S. (1886). On the relationships of the mandibular and hyoid arches in a Cretaceous shark (*Hybodus dubrisiensis*, Mackie). *Proc. Zool. Soc. London*, **1886**, 218-224.
Wourms, J. (1977). Reproduction and development in chondrichthyan fishes. *Amer. Zool.*, **17**, 379-410.
Wu, E.H. (1994). Kinematic analysis of jaw protrusion in orectolobiform sharks : a new mechanism for jaw protrusion in elasmobranchs. *J. Morphol.*, **222**, 175-190.
Yano, K. (1992). Comments on the reproductive mode of the false cat shark *Pseudotriakis microdon*. *Copeia*, **1992**, 460-468.
Young, G.C. (1982). Devonian sharks from South-eastern Australia and Antarctica. *Palaeontol.*, **25**, 817-843.
Zangerl, R. and M.E. Williams. (1975). New evidence on the nature of the jaw suspension in Paleozoic anacanthous sharks. *Palaeontol.* **18**, 333-341.

XII. Appendices

Appendix 1. Abbreviations used in the text figures.

aab : adductor arcuum branchialium
acc : accessory cartilage of basibranchial
acd : arcualis dorsalis
acm : accessory cartilage on mandibula
acp : accessory cartilage of palatoquadrate
acs : accessory cartilage on symphysis of mandibula
adv : adductor pelvicus
aim : anterior sheet of intermandibularis
alc : anterior upper labial cartilage
am : adductor mandibulae
amh : adductor mandibulae hyoideus
aop : antorbital process
apc : apron of coracoid
apr : apron of tooth
apv : anterior peivic basal
asp : ascending process of endolymphatic fossa
axs : stem cartilage
b : joint cartilage
ba : basal cartilage of anal fin
bb : basibranchial
bd : basal cartilage of dorsal fin
bdp : basidorsal process
bh : hasihyal
bp : basal plate
br : branchial ray
brh : branchial ray on hyoid arch
bua : buccal group of ampullae of Lorenzini
bvp : basiventral process
cb : ceratobranchial
cbs : constrctor branchiales superficiales
ccl : cucullaris
ced : cutting edge
ch : ceratohyal
chd : constrictor hyoideus dorsalis
chv : constrictor hyoideus ventralis
cnf : circumnarial fold
coa : coraco-arcualis
cob : coraco-branchialis
codI : constrictor dorsalis I
coh : coraco-hyoideus
cor : coracoid
cos : canal for orbital sinus
cpn : canal for pectoral nerves and brachial artery
cpv : condyle of pelvic basipterygium
db : dorsal bundle
dbc : double cone
dc : disc of eyestalk
dic : dorsal intercalary plate
dl : dilitator
dlb : dermal lobe
dmc : dorsal marginal cartilage
doa : deep ophthalmic group of ampullae of Lorenzini
dpc : depressor pectoralis
dpv : depressor pelvicus
dsc : dorsal spiracular caecum
dtc : dorsal terminal cartilage
eb : epibranchial
ech : extrabranchial cartilage on hyoid arch
ecr : epichordal radial
eld : endolyophatic duct
elf : endolymphatic fenestra
enc : extra cartilage of nasal cartilage

enm : ethmonuchal muscle
epf : epiphyseal foramen
epp : ethmopalatine process
epx : epaxial
es : eyestalk
esob : extra bundle of suborbitalis
etg : groove on orbitonasal proces
exd : dorsal extrabranchial cartilage
exe : expansion of epibranchial
exf : flexor externus
exh : expansion of hyomandibular facet
exp : fossa for depressor pectoralis
exv : ventral extrabranchial cartilage
fbr : foramen for brachial artery
fco : fenestra on apron of coracoid
fcpv : facet of pelvic basipterygium
fed : fenestra on orbitonasal process
feld : endolymphatic fossa
fhm : hyomandibular facet
foph : foramen for ophthalmicus superficialis and ophthalmicus profundus
fpv : foramen for pelvic nerves
fsn : slit like fenestrae on nasal capsule
fxc : flexor caudalis
gco : genio-coracoideus
gpx : gill pickax
hb : hypobranchial
hcp : hypochordal process
hda : hyoid group of ampullae of Lorenzini
hm : hyomandibula
hmc : articular condyle for cranio-hyomandibular articulation
hmVII : foramen for hyomandibularis VII
hor : horizontal myoseptum
hpx : hypaxial
hyc : hyomandibular sensory canal
ibm : subdivision of interbranchialis
ibr : interbranchialis
ica : foramen for internal carotid artery
ican : inclinator analis
icde : extra bundle of inclinator dorsalis
icd : inclinator dorsalis
im : intermandibularis
imd : intermedialia
inc : inner nasal cartilage
ins : inter-nasal septum
ioc : infraorbital sensory canal
iow : interorbital wall
ipb : interpharyngobranchialis
itf : flexor internus
lb : lateral bundle
lcm : ligamentum cranio-mandibularis
lcp : lateral cusp of tooth
lcp : ligamentum cranio-palatoquadrati
leth : ligamentum for articulation with palatobasal ridge of neurocranium
lhp : ligamentum hyomandibulo-palatoquadrati
lhy : ligamentum hyomandibulo-ceratohyal
ljs : ligamentous complex for articulation of mandibulo-hyomandibula
llc : lower labial cartilage
llf : lower labial furrow
lmd : ligamentum mandibulo-ceratohyal
lmp : ligamentum mandibulo-palatoquadrati
lpa : levator palpebrae anterodorsalis
lpd : levator pectoralis distalis
lpi : levator pectoralis inferior
lpq : levator palatoquadrati
lps : levator pectoralis superficialis
lpv : levator pelvicus
lrm : lateral rostral rod
maf : articular fossa of mandibula
mag : foramen magnum
mc : condyle of mandibula
mcp : medial cusp of tooth
md : mandibula
mda : mandibular group of ampullae of Lorenzini
mdc : mandibular sensory canal
mee : membrana elastica externa
mk : mandibular knob
msp : mesopterygium
mtp : metapterygium
mtx : metapterygial axis
nbl : nasal barbel
nc : nasal capsule
nsh : notochordal sheath
oa : foramen for orbital artery
occ : occipital condyle
ohc : occipital hemicentrum
ol : outer-lip muscle
onc : outer nasal cartilage
onp : orbito-nasal process
onv : opening for orbito-nasal vein
oprf : foramen for ophthalmicus profundus
oqi : obliquus inferior
oqs : obliquus superior
ospf : foramen for ophthalmicus superficialis
otc : otic capsule
ozc : outer zone
pac : condyle for anterior pelvic basal
par : muscle parietalis
pare : extra bundle of muscle parietalis
pba : foramen for pseudobranchial artery
pbb : pharyngobranchial blade
pbr : palatobasal ridge
pc : palatoquadrate concavity

pcc : articular condyle of coracoid
pcd : condyle of palatoquadrate
pcm : pericardial membrane
pcp : process for levator pectoralis
pcv : posterior canal vacuity
pec : pre-epibranchial cartilage
pff : prefrontal fontanelle
ph : pharyngobranchial
phc : prehypochordal cartilage
phy : pharyngohyal
pim : posterior sheet of intermandibularis
pit : foramen for pituitary vein
plc : posterior upper labial cartilage
plf : perilymphatic fenestra
plp : post-palatoquadrate process
poc : preorbital canal
pop : postorbital process
pq : palatoquadrate
pr : inner process of ceratobranchial
prf : profundus canal
prm : process of mandibula
pro : main foramen for trigeminal and facial nerves
prp : propterygium
pub : puboischiadic bar
pvb : pelvic basipterygium
pvc : articular condyle for pelvic basipterygium
pvf : facet for pelvic basipterygium
pvp : prepelvic process
rb : vertebral rib
rd : radial
rdc : pectoral radial
rdv : pelvic radial
rex : rectus externus
rgp : ridge of palatoquadrate for adductor mandibulae
rif : rectus inferior
rife : extra bundle of rectus inferior
rit : rectus internus
rite : extra bundle of rectus internus
rsp : rectus superior
rm : medial rostral rod
rmd : rostromandibularis
rnc : rostronuchal muscle
rt : tooth root
sbl : supraorbital blade
sc : scapular
scl : scondary calcified lamella
smsp : subdivision of spiracularis
soa : superficial ophthalmic group of ampullae of Lorenzini
sob : suborbitalis
soc : supraorbital crest
socn : supraorbital sensory canal
sok : supraocular knob
sos : suborbital shelf
spc : spur
spg : symphyseal groove
sp : spiracle
spcf : spiracular cleft
spm : spiracularis
spn : supraneural
spr : sphenopterotic ridge
ssc : suprascapular cartilage
ssp : subspinalis
stc : supratemporal sensory canal
vic : ventral intercalary plate
vmc : ventral marginal cartilage
vtc : ventral terminal cartilage
II : foramen opticum
III : foramen for oculomotor nerve
IV : foramen for trochlear nerve
VI : foramen for abducens nerve
IX : foramen for glossopharyngeal nerve
X : foramen for vagus nerve

Appendix 2. Input data matrix of living elasmobranchs for the first step.

Taxon	1111111111222222222233333 12345678901234567890123456789012345
ON	00000000000000000000000000000000000
	1
Squalea	01111000000100000000000101000001010
	1 1 1 1
Heterodontus	10000111100000001010000100010000110
Cirrhoscyllium	10000111111111121101101011101101001
Parascyllium	10000111111111121101101011101101001
Orectolobus	10000111111111201001000110011000010
Brachaelurus	10000111111111201011000120011000010
Hemiscyllium	10000111111111211011000110011110010
Chiloscylium	10000111111111211011000110011100010
	1
Ginglymostoma	10000111111111211001001110011110010
Stegostoma	10000111111111211011001100011111010
Rhincodon	10000111111111211000001110010111110
Scyrhiorhinus	10000111011111111101110000001000001
Cephaloscyllium	10000111011111111101110000001000001
Schroederichthys	10000111011111111101110000001000001
Apristurus	10000111011111111101111001001000101
Galeus	10000111011111111101111001001000101
Halaelurus	10000111011111111101111001001000001
Gollum	10000111011111011011100010010001010
Triakis	10000111011111111101110011001000001
Mustelus	10000111011111111101110011001000001
Hemitriakis	10000111011111111101110011001000001
Carcharhinus	10000111011111111101111011001000001
Lamna	10??011101111100001110010010000110
Alopias	10??011101111111111111001101000011O
Pseudocarcharias	10??011101111110011110010010000110
Mitsukurina	10??011101111110101111011000000111

Appendix 3. Input data matrix of Orectolobiformes for the second step.

```
                          1111111111222222222233333333334444444444555555555
Taxon                     1234567890123456789012345678901234567890123456789012345678
-------------------------------------------------------------------------------------
ON                        000000000000000000000000000000000?000000000000000000?000
                                 1
Cirrhoscyllium            1010001002100O1?1110010110001101101000000101101100100002l0
Parascyllium
P. variolatum             1010001002110O1?1110010110001101101000000101101100100002l0
P. collare                1010001002110O1?1110010110001101101000000101101100100002l0
P. ferrugineum            101?001002110O1?1110010110001101101000000101101100100002l0
P. sp.                    1010001002110O1?1110010110001101101000000101101100100002l0
Orectolobus
O. japonicus              0001112001000100000000000101101100012001001011201010100000
O. ornatus                0001112001000100000000000101101100012001001011201010100000
O. maculatus              0001112001000100000000000101101100012001001011201010100010
O. wardi                  0001112000000100000100200101101100012001001011201010100010
Sutorectus                0001112001000100000000000101101100012001001011201010100110
Eucrossorhinus            0001112000000100000000000101101100012001101011201010100010
Brachaelurus              0101100101000100000100200101101001001011000001200110000010
Chiloscyllium
C. Plagiosum              0101000010000100001000000011100001000011000001200111010010
C. hasselti               0101000010000100001000000011100001000011000001200111010010
C. punctatum              0101000010000100001000000011100001000011000001200111010010
C. indicum                0101000011000100001000000011100001000011000001200111010110
Hemiscyllium
H. ocellatum              0101000012000100001000000011100001000011000001200111010110
H. trispeculare           0101000012000100001000000011100001000011000001200111010110
H. freycineti             0101000012000100001001000011100001000011000001200111010110
Ginglymostoma             0000010112001101011010000001001000000101100001300011201111
Stegostoma                0001000010001100011010100001000000200101000001300111001111
Rhincodon                 0010010002001101011010000101001200010001000011322011201101
```

Input data matrix (continued).

```
                                                                    11111111111111111
                  56666666666777777777788888888899999999990000000000111111111
Taxon             90123456789012345678901234567890123456789012345678901234567890123456
-------------------------------------------------------------------------------------
ON                00000000000000??0??000000000000?00?0000000000000000??00000000000
                   1   1       1                        1
                       2
Cirrhoscyllium    10000001111000000??1111000001101010001111000111000011001100000000
Parascyllium
P. variolatum     10000001111000000??1111000001101010001111000111000011001100000000
P. collare        10000001111000000??1111000001101010001111000111000011001100000000
P. ferrugineum    10000001111000000??1111000001101010001111000111000011001100000000
P. sp.            1000000?111000000??1111000001101010001111000111000011001100000000
Orectolobus
O. japonicus      00000200101000001101010001021000010101010111100100010110100000000
O. ornatus        00000200101000001101010001021000010101010111100100010110100000000
O. maculatus      00000200101000001101010001021000010101010111100100010110100000000
O. wardi          00000200101000001101010001021000010101010111100100010110100000000
Sutorectus        00000200101000001101010001021000010101010111100100010110100000000
Eucrossorhinus    00000200101000001101010001021000010101010111100100010110100000000
Brachaelurus      00000200001000000100010001122000010101010121100200010120100000000
Chiloscyllium
C. plagiosum      00000100001000100100010011113001030111010101100000020100100000000
C. hasselti       00000100001000100100010011113001030111010101100000020100100000000
C. punctatum      00000100001000100100010011113001030111010101100000020100100000000
C. indicum        00000100001000100100010011113001030111010101100000020100100000000
Hemiscyllium
H. ocellatum      00000100001000100100010011113001030101010101100010020101100000000
H. trispeculare   00000100001000100100010011113001030101010101100010020101100000000
H. freycineti     00000100011000100100010011113001030101010101100010020101100000000
Ginglymostoma     01110110001101001101010011103000020101010121100001120101100000000
Stegostoma        01111111001111001101010011103000020101010121100001120100100000000
Rhincodon         01111312001112011111010011103000020101010101100001120100100000000
```

Input data matrix (continued).

	1111111111111111111
	1112222222223333333
Taxon	78901234567890123456
ON	000000000?0000000000
	1
Cirrhoscyllium	10000002101001020100
Parascyllium	
P. variolatum	10000002101001020100
P. collare	10000002101001020100
P. ferrugineum	10000002101001020100
P. sp.	10000002101001020100
Orectolobus	
O. Japonicus	00111101111101200001
O. ornatus	00111101111101200001
O. maculatus	00111101111101201001
O. wardi	00111101101101101001
Sutorectus	00111101101101101001
Eucrossorhinus	00111101111101301001
Brachaelurus	00111101101101000001
Chiloscyllium	
C. Plagiosum	01101111101020000012
C. hasselti	01101111101020000012
C. punctatum	01101111101020000012
C. indicum	01101111101020000012
Hemiscyllium	
H. Ocellatum	011001111010100000012
H. trispeculare	011001111010100000012
H. freycineti	011001111010100000012
Ginglymostoma	00101101100000010000
Stegostoma	00101101100000010011
Rhincodon	00101101100000010010